



## CONSTRUCTION INDUSTRY COUNCIL RESEARCH FUND

### FINAL REPORT

**Period covered (dd/mm/yy):** 24/July/ 2019 to 23/December/2021

#### PROJECT TITLE

*Promoting the Use of Recycled Aggregates Derived from Demolition Waste in Concrete*

#### INVESTIGATOR(S) AND DEPARTMENT/UNITS INVOLVED

Research Team	Name/Post	Unit/Department/Institution
Principal Investigator	Prof. C.S. Poon/Head	Department of Civil and Environmental Engineering, The Hong Kong Polytechnic University
Co-investigator(s)	Dr. D.X. Xuan/Lab Manager	Department of Civil and Environmental Engineering, The Hong Kong Polytechnic University

#### PROJECT DURATION

	Original	Revised (if applicable)	Date of CIC Approval (must be quoted)
Project Start Date	24 July 2019		
Project Completion Date	23 July 2021	23 Sept 2021	22/04/2020
		23 Dec 2021	08/10/2020
Duration (in month)	24 months	29 months	

# **CONTENTS**

<b>1. INTRODUCTION .....</b>	<b>3</b>
<b>2. RESEARCH OBJECTIVES.....</b>	<b>3</b>
<b>3. RESEARCH METHODOLOGY .....</b>	<b>4</b>
<b>4. RESEARCH ACTIVITIES FOR DEVELOPMENT OF DIFFERENT TREATMENT TECHNIQUES.....</b>	<b>6</b>
4.1 COLLECTION AND CRUSHING OF CONSTRUCTION AND DEMOLITION WASTE .....	6
4.2 PERFORMANCE OF RCA AND RAC TREATED BY CO <sub>2</sub> AND NANO- SILICA.....	7
4.3 PERFORMANCE OF MICROBIOLOGICAL-TREATED RCA AND RAC .....	14
4.4 APPLICATIONS OF RAC IN FINAL PRODUCTS.....	17
<b>5. MARKET DEMAND IN RELATION TO LOCAL CONSTRUCTION INDUSTRY...20</b>	
5.1 STRUCTURAL APPLICATIONS .....	21
5.2 NON-STRUCTURAL APPLICATIONS.....	22
5.3 SUMMARY OF THE POTENTIAL DEMAND OF RCA .....	24
<b>6. COST ANALYSIS AND QUALITY CONTROL OF RECYCLED AGGREGATE ...25</b>	
<b>7. CARBON EMISSION FACTOR OF RECYCLED PRODUCT BY CAT .....</b>	<b>30</b>
<b>8. SPECIFICATION RECOMMENDATION ON THE USE OF COARSE RECYCLED AGGREGATE IN CONCRETE .....</b>	<b>32</b>
<b>9. CONCLUSIONS AND WAY FORWARD .....</b>	<b>34</b>
9.1 CONCLUSIONS AND RECOMMENDATIONS .....	34
9.2 WAY FORWARD .....	35

## **APPENDICES — PUBLICATIONS**

## 1. **INTRODUCTION**

- CIC appointed the research team led by the Principal Investigator Prof. Chi-sun POON of the Hong Kong Polytechnic University (PolyU) to conduct the research, namely “Promoting the Use of Recycled Aggregates Derived from Demolition Waste in Concrete” in July 2019.
- The original project period was 24 months after the commencement date on 24 July 2019. Due to temporary closure of the PolyU in late 2019 and the COVID-19 outbreak, the Com-ENV approved a 2-month and a 3-month project extension respectively. The completion date is therefore extended to 23 December 2021.
- In this final report, the main findings of the research are briefly summarized.

## 2. **RESEARCH OBJECTIVES**

- Different novel enhancement techniques for treating recycled aggregates will be developed;
- The fundamental mechanisms of these enhancement techniques for optimization will be unraveled;
- Enhance the properties of precast/cast in-situ concrete prepared with treated recycled aggregates;
- Life cycle cost and quality of recycled aggregates and the new products will be compared with existing construction materials;
- The research end products (structural precast, non-structural precast or

ready mixed concrete and others) and their market demand and value in relation to local construction industry will be evaluated;

- The supply chain will be assessed with assistance of local companies and organizations in government, including production of good quality recycled aggregates, transportation and storage by manufacturers;
- Suggestions on amendment of the existing specifications will be given for implementation in public and private works in association with governmental partners.

### 3. RESEARCH METHODOLOGY

In the research application, the technical roadmap of the proposed project is illustrated in **Figure 1**.

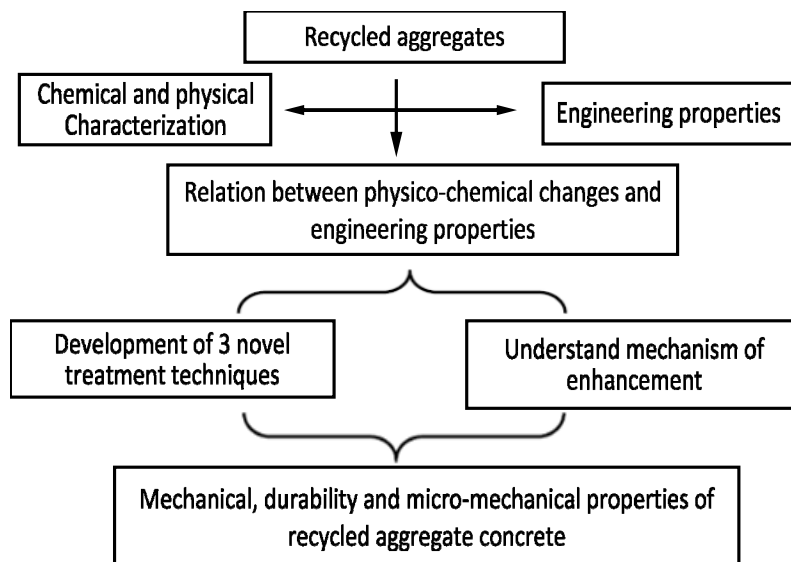


**Figure 1 Technical roadmap of the project**

## Part I: Developing accelerated CO<sub>2</sub>-curing coupled with lime-soaking technique

The aims of this part are to (1) study the influence of characteristics of recycle concrete aggregate (RCA) on carbonation efficiency when subjected to accelerated CO<sub>2</sub> curing coupled with limewater soaking process as shown in Figure 2, (2) investigate the microstructural evolution of RCA after this treatment for optimization.

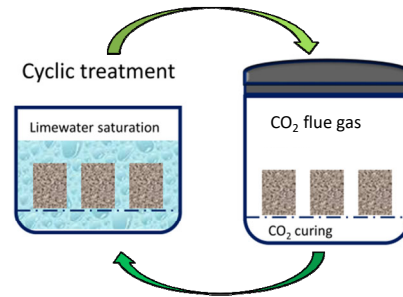


**Figure 2 CO<sub>2</sub>-curing coupled with lime-soaking technique**

## Part II: Developing modified nano-particle treatment technique

The aims of this part are to (1) develop a modified nano-particle material for the treatment of RCA as shown in Figure 3; (2) study the microstructure development of the treated recycled aggregates for optimization.

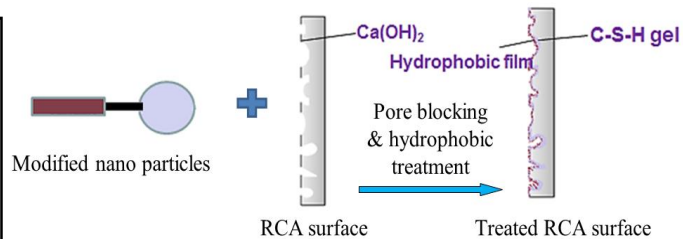


**Figure 3 Modified nano-particle materials for the treatment of RCA**

## Part III: Developing microbiological modification treatment technique

The aims of this part are to (1) optimize the microbial carbonate precipitation (MCP) method as shown in **Figure 4**, (2) enhance the properties of RCA by covering the surface of RCA and filling the pores in terms of efficient MCP.

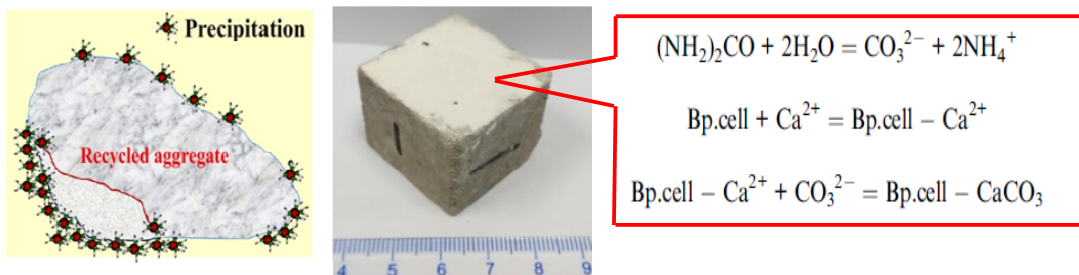


**Figure 4 Microbial carbonate precipitations in recycled aggregates**

## Part IV: Performance of recycled aggregate concrete and structural concrete

## elements

Batches of concrete mixtures are prepared with natural aggregates, RCA and the treated RCA by using the above techniques. Engineering properties of the concrete mixtures are determined in terms of mechanical and durability properties.

#### 4. RESEARCH ACTIVITIES FOR DEVELOPMENT OF DIFFERENT TREATMENT TECHNIQUES

##### 4.1 COLLECTION AND CRUSHING OF CONSTRUCTION AND DEMOLITION WASTE

The collection of construction and demolition waste for this project was carried out from a CEDD sorting plant, a local recycler and a real demolition site as shown in **Figure 5**. After crushing in **Figure 6**, recycled aggregates were obtained for preparing recycled aggregate concrete for this research.



**Figure 5 Collection of construction and demolition waste**

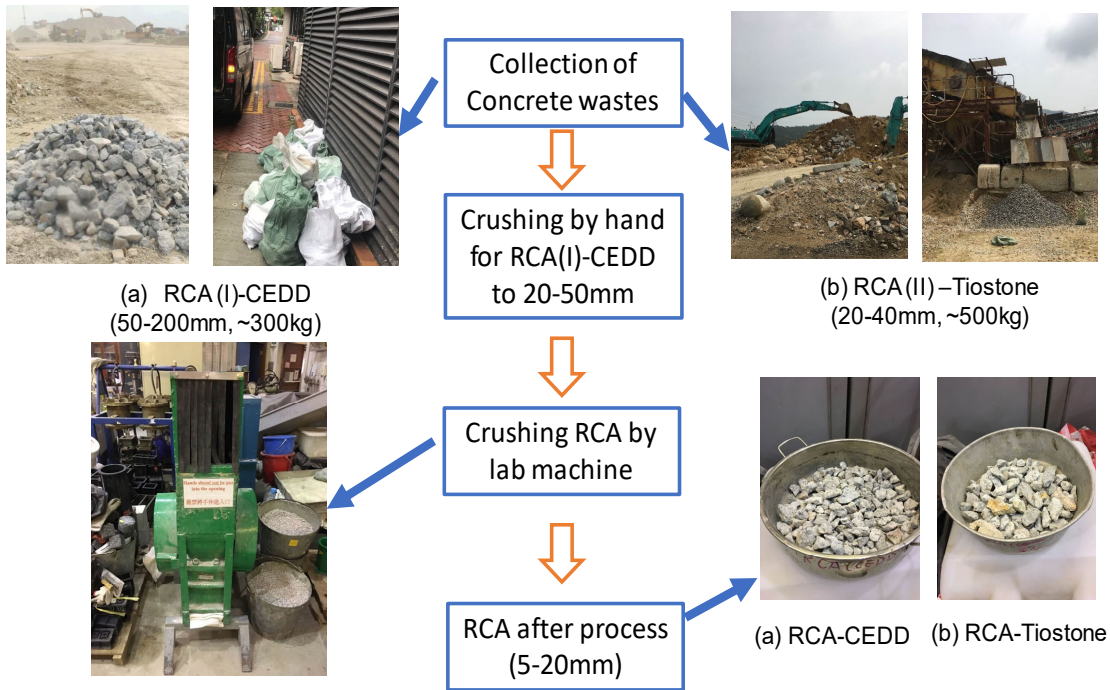


**Figure 6** Crushing of construction and demolition waste to recycled aggregates

#### 4.2 PERFORMANCE OF RCA AND RAC TREATED BY CO<sub>2</sub> AND NANO-SILICA

In this section, the major results are listed while more detailed experimental results can be found in the publications as appendices of this report.

##### 4.2.1 PHYSICAL PROPERTIES OF RCA AFTER TREATMENTS

The physical properties of RCA before and after five different treatment methods are shown in **Table 1**. The results showed that after using all these treatment methods, the water absorption decreased, the dry particle density increased. Moreover, the change of water absorption was more significant than that of dry particle density. Among three carbonation treatment method, using the pressurized carbonation caused the highest decrease in water absorption and increase in dry particle density. The use of nano-silica (NS) spraying method only gave rise to small decrease in water absorption. The combined pressurized carbonation with the NS spraying method brought about larger decrease in water absorption than the single

pressurized carbonation or NS spraying method.

**Table 1 Physical properties of RCA before and after treatments**

Treatment method	Size of RCA (mm)	Water absorption (%)			Dry particle density (g/cm <sup>3</sup> )		
		Before treatment	After treatment	Decreasing rate	Before treatment	After treatment	Increasing rate
Flow-through carbonation	5-10	7.71	7.02	8.9%	2.190	2.219	1.3%
	10-20	6.82	6.39	6.3%	2.216	2.233	0.8%
Pressurized carbonation	5-10	7.76	6.64	14.4%	2.207	2.257	2.3%
	10-20	6.40	5.64	11.9%	2.252	2.292	1.8%
Water carbonation	5-10	7.83	7.41	5.3%	2.192	2.203	0.5%
	10-20	6.99	6.70	4.1%	2.216	2.228	0.5%
NS spraying	5-10	7.83	7.54	3.6%	2.192	2.215	1.0%
	10-20	6.99	6.79	2.8%	2.215	2.234	0.9%
Microbiological modification treatment	5-20	8.22	7.39	10.1%	2.318	2.389	3.0%
Combined pressurized carbonation with NS spraying	5-10	7.76	6.45	16.8%	2.207	2.254	2.1%
	10-20	6.40	5.48	14.4%	2.252	2.293	1.8%

#### 4.2.2 COMPRESSIVE STRENGTH OF RAC

The 28 days compressive strength of the eight groups of concrete are shown in **Figure 7**. It showed that the compressive strength of NAC was 33.2% higher than that of RAC with non-treated RCA (RAC-non). After using the assessed treatments methods, the compressive strength of RAC can be increased by different extents. Among different types of carbonation treatment methods, the pressure carbonation method was the best one in enhancing the compressive strength. When using the pressure carbonation on RCA, the compressive strength of RAC was increased by 9.1%, while the increasing rate were 3.9% and 3.3% respectively for the use of flow-through carbonation and wet carbonation. After using the NS spraying treatment method, the compressive strength of RAC was enhanced by 10.2%, which was higher than using carbonation treatment methods. Especially, when using the method

of combined pressurized carbonation with NS spraying, the increasing rate of the compressive strength of RAC reached to 20.7%, which was much higher than that using PC-method or NS-method separately.

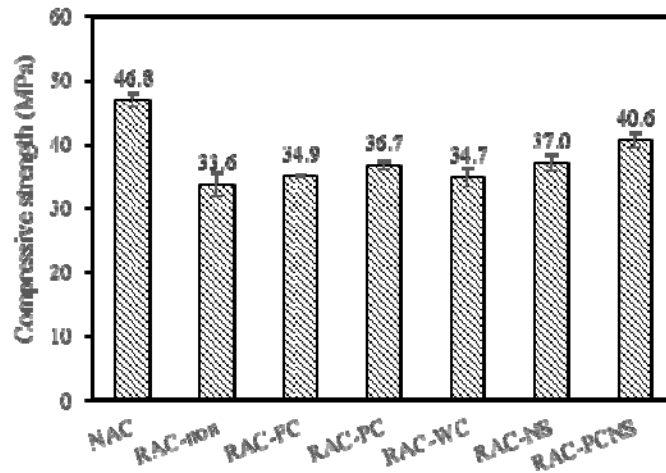


**Figure 7 Compressive strength of hardened concretes**

#### 4.2.3 ELASTIC MODULUS OF RAC

The elastic modulus of the seven groups of concrete is shown in **Figure 8**. It can be found that the elastic modulus of RAC was significantly reduced when compared with that of NAC. The reduction rate was even higher than that of compressive strength. Generally, the elastic modulus of RAC was increased after using the assessed carbonation treatment methods, but the magnitude of the increase was less than 3%. When using the NS spraying method, the elastic modulus of RAC was increased by 7.6%, which was higher than using the carbonation treatment methods. After using the method of combined pressurized carbonation with NS spraying, the elastic modulus of RAC was further increased and the increasing rate reached to 10.0%, which was higher than that using the pressurized carbonation or NS spraying separately. In addition, the magnitude of the increase in elastic modulus of RAC was much lower than that of compressive strength, indicating that the influence of the carbonation treatments and NS spraying treatments on elastic modulus of RAC was

less obvious than compressive strength.

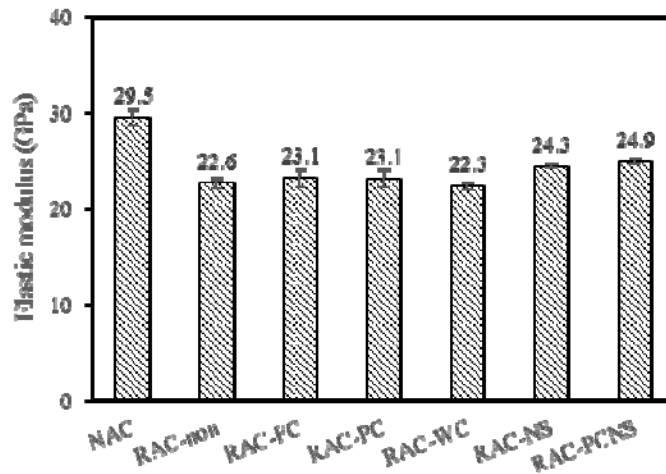


**Figure 8 Elastic modulus of hardened concretes**

#### **4.2.4 RATE OF WATER ABSORPTION OF HARDENED CONCRETE**

The rate of water absorption due to capillary force of the unsaturated concrete is an important index of concrete durability. Higher absorption rate means inferior durability. The initial and secondary absorption rates of the seven groups of concrete are shown in **Figure 9**. It showed that the initial and secondary absorption rate of NAC was 48.9% and 61.1% lower than that of RAC prepared with the untreated RA (RAC-non). The rate of water absorption reduced after using the studied treatment methods. Among three carbonation treatments, the pressurized carbonation method caused largest reduction, while the water carbonation led to the lowest reduction. After using the NS spraying, the absorption rate of RAC showed a similar reduction with the pressurized carbonation, but the magnitude of reduction was still much lower than that of NAC. Additionally, when adopting the method of combined pressurized carbonation with NS spraying, the absorption rate of the corresponding RAC (RAC-PCNS) was significantly reduced, which was even close to that of NAC.

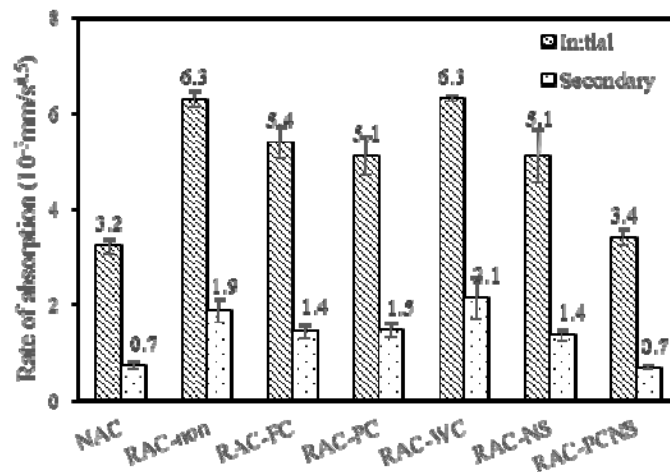


**Figure 9 Rate of water absorption of hardened concretes**

#### 4.2.5 CHLORIDE PENETRATION RESISTANCE OF HARDENED CONCRETE

The charge passed of the concrete is a parameter to reflect its chloride penetration resistance, which is another important index of concrete durability. Higher charge passed means lower chloride penetration resistance. The chloride penetration resistance of the seven groups of concrete is shown in **Figure 10**. It can be found that the charge passed of RAC with the untreated RCA (RAC-non) was much higher than that of NAC. After using RCA treatment methods, the charge passed of RAC can be reduced with different extents. Among the three carbonation treatment methods, the flow-through carbonation and pressurized carbonation were better in improving the chloride penetration resistance of RAC. When using the single NS spraying treatment method, the charge passed of RAC only decreased by 3.8%. However, when the combined pressurized carbonation with NS spraying method was used, the charge passed of RAC showed a much significantly reducing, the decreasing rate was reached to 24.4%.

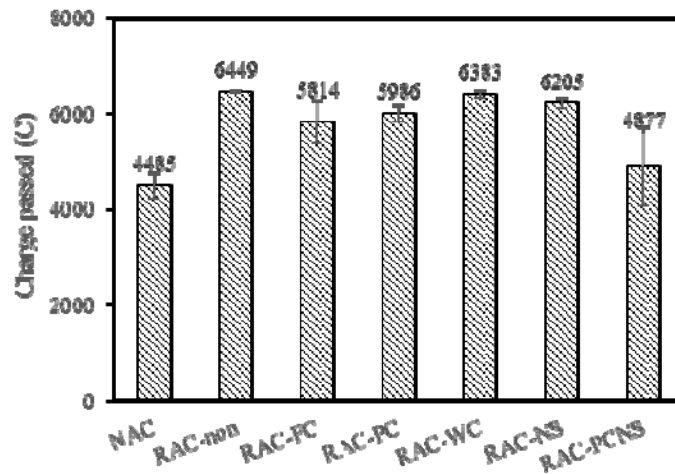


**Figure 10 Chloride penetration resistance of hardened concretes**

#### **4.2.6 CARBONATION RESISTANCE OF HARDENED CONCRETE**

The carbonation depth of concrete is an indicator to assess its carbonation resistance. Lower carbonation depth means better carbonation resistance. The photos of the seven groups of concrete subjected to 28 days carbonation after spraying phenolphthalein solution are shown in **Figure 11**. According to the color, it can be found that in the inner part of RACs which had not been carbonated, many carbonated RCA particles were observed when using flow-through carbonation, pressurized carbonation and combined pressurized carbonation with NS spraying. However, no obvious carbonated RCA particle was observed after using water carbonation.

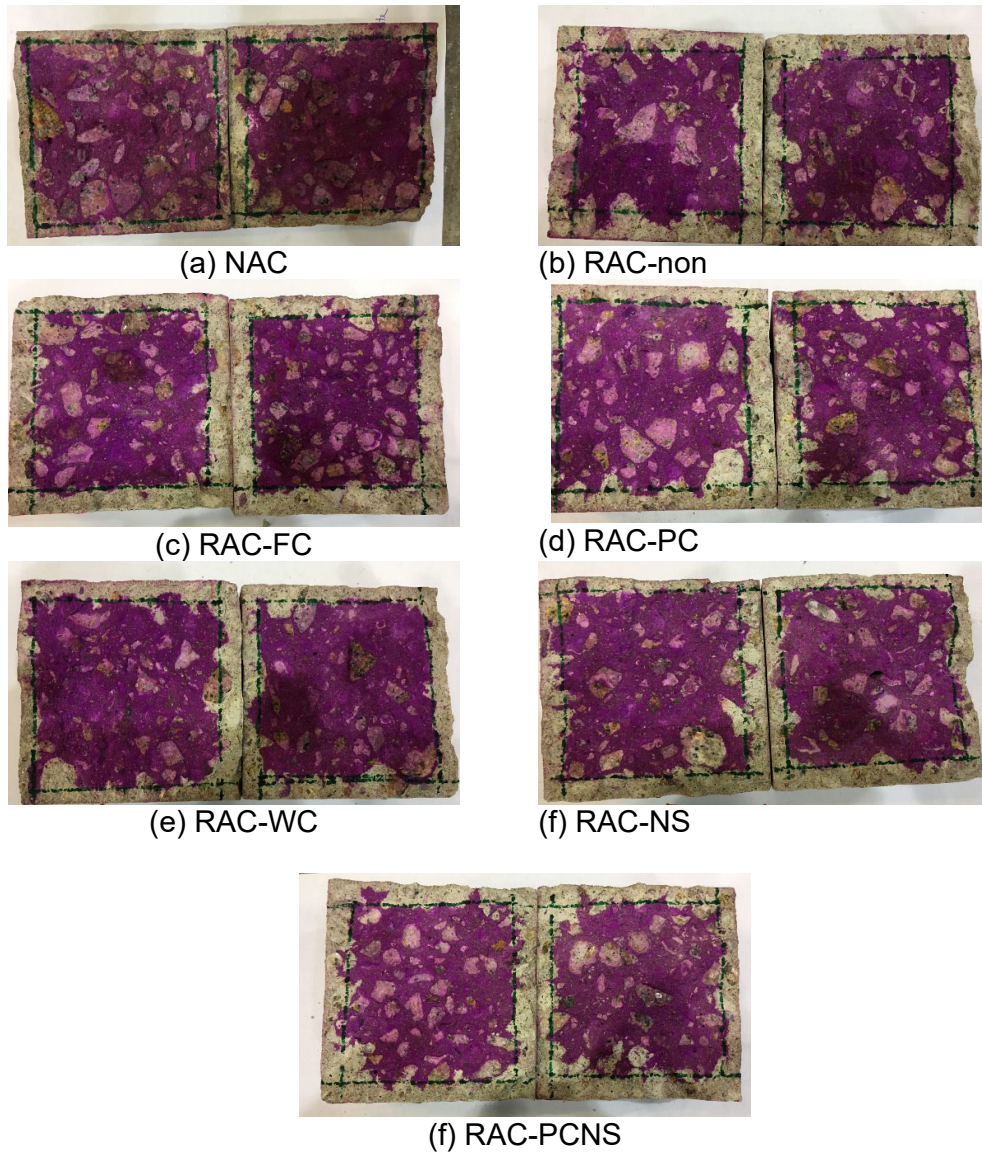


**Figure 11 Photos of concretes subjected to 28 days carbonation after spraying phenolphthalein solution.**

The 7 days and 28 days carbonation depths of the seven groups of concrete are shown in **Figure 12**. The results showed that the 7 days and 28 days carbonation depths of RAC-non were much higher than that of NAC. After using flow-through carbonation and pressurized carbonation, the 7 days carbonation depths of RACs were further increased. That is because the RCAs have been carbonated already, which increased the average carbonation depth when the carbonation depth was small. However, the 28 days carbonation depths of these RACs were lower than that

of RAC-non. That is because the RCAs were densified after carbonation, which reduced the penetration rate of CO<sub>2</sub>. In contrast, the 7 days and 28 days carbonation depths of RAC-WC were both reduced compared to RAC-non. That is because only the surface layer of the RCA was carbonated after using water carbonation. At the same time, a lot of nano-CaCO<sub>3</sub> particles were formed on the surface of RCA, which can densify the new ITZ. As a result, the penetration rate of CO<sub>2</sub> was reduced. In factor, it is similar to the NS spraying method, of which the new ITZ can be significantly enhanced by the NS particles. That is why the 7 days and 28 days carbonation depths of RAC-NS were similar to that of RAC-WC. For the PCNS-method, the 7 days carbonation depths of RAC-PCNS were higher than RAC-non because of the carbonated RCA, but the 28 days carbonation depths of RAC-PCNS were lower than RAC-non.

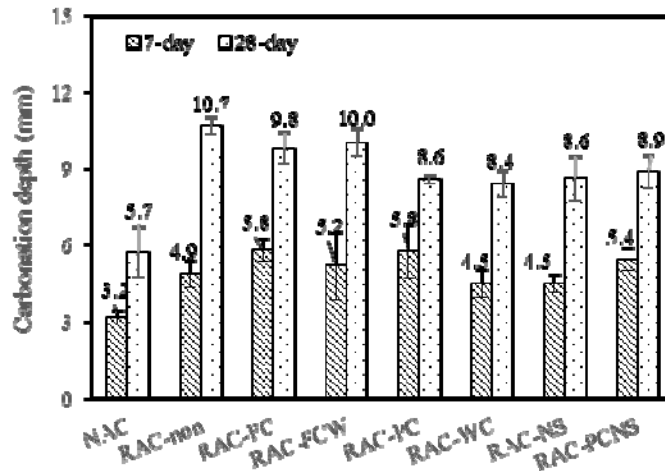
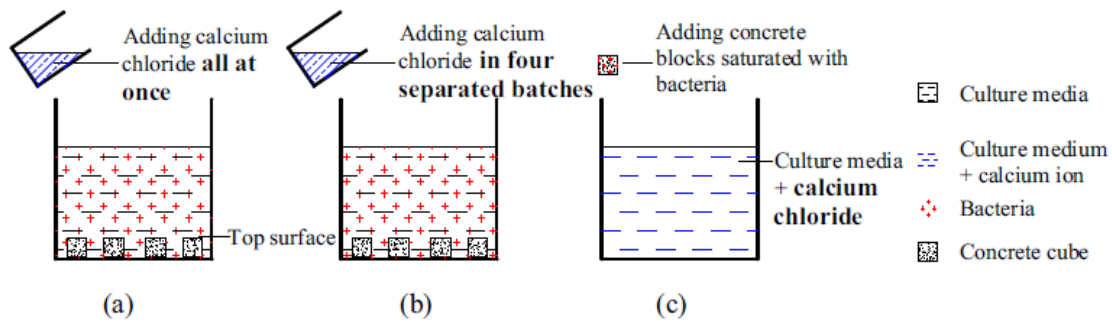


Figure 12 Carbonation resistance of hardened concrete

#### 4.3 PERFORMANCE OF MICROBIOLOGICAL-TREATED RCA AND RAC

*Sporosarcina pasteurii* (DSM No. 33) was chosen for the microbial induced carbonate precipitation (MICP) as shown in **Figure 13**. The culture media was composed of 20 g/L tryptone, 5 g/L NaCl, and 20 g/L urea. The experimental process

was conducted as follows: the prepared RCA was modified with different MICP precipitation methods; RAC was then cast using the modified RCA. The compressive strength and micro properties of RAC were experimentally tested to reveal the modification mechanism.



**Figure 13 Schematic diagrams of precipitation methods: (a) Precipitation method 1, (b) Precipitation method 2, (c) Precipitation method 3.**

#### 4.3.1 WATER ABSORPTION BEFORE AND AFTER MICP MODIFICATION

Figure 14 shows the water absorption of RCA by different MICP methods. It was found that the precipitation method 2 can reach a higher reduction in water absorption compared to other methods. Static and rotation modifications did not influence the water absorption obviously.

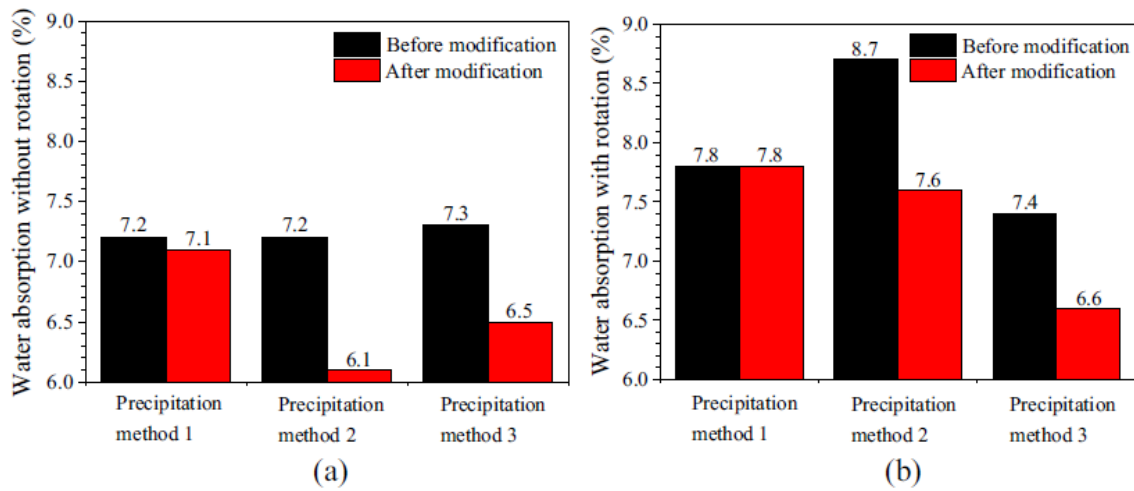


**Figure 14 Water absorption before and after modification (a) static; (b) Rotation**

### 4.3.2 COMPRESSIVE STRENGTH OF MRAC

**Figure 15** shows the compressive strength of RAC with untreated RCA (CRAC) and with the treated RCA by MICP (MRAC). It was found that after MICP treatment, the compressive strength of MRAC was increased from 49.3 MPa to 52.4 MPa. This was attributed to MICP filling the pores on the surface, which might enhance the properties of ITZ.

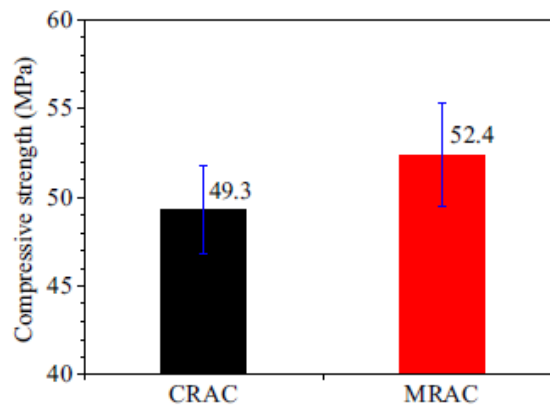


**Figure 15 Compressive strength of CRAC and MRAC**

### 4.3.3 ITZ PROPERTIES OF MRAC

Two different types of ITZs were measured, including ITZ 1 between the original natural aggregate and the new mortar, the ITZ 2 between the old mortar and the new mortar, as shown in **Figure 16**. Figure 17 shows the mean values of the microhardness of two types of ITZs. It can be noted that original ITZ 2 was lower than that of ITZ 1. After the MICP treatment, there was no obvious change, in which most bacteria were absorbed. These bacteria induced the formation of MICP, enhancing the properties of ITZ2. While for ITZ 1, little bacteria were absorbed in surface of the natural aggregate, therefore no obvious improvement was found.

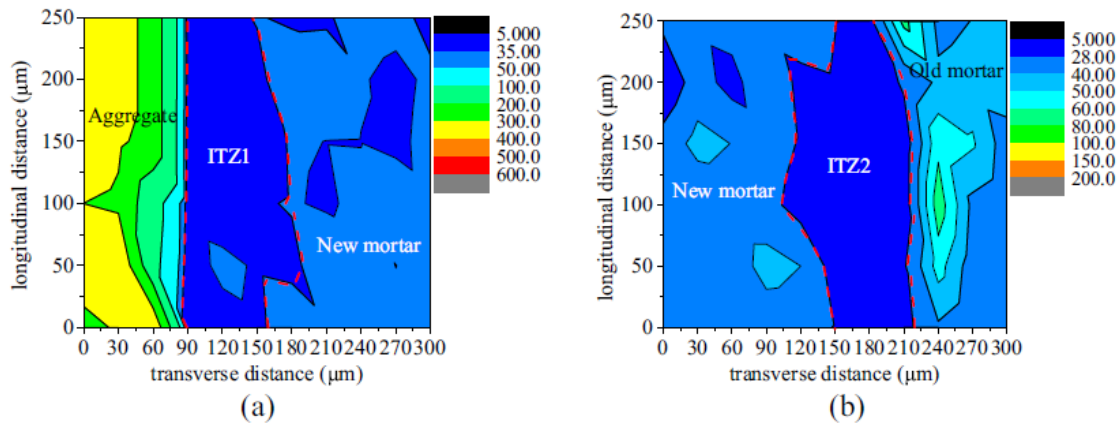


**Figure 16 Microhardness distribution map: (a) ITZ 1, (b) ITZ 2**

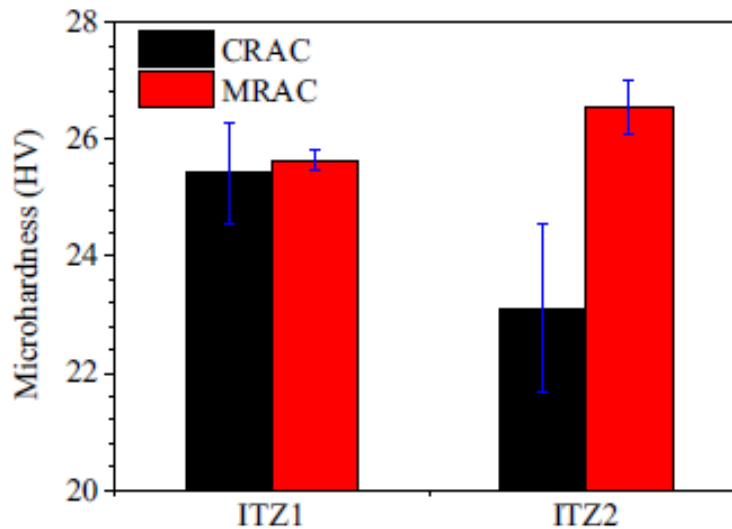


**Figure 17 Mean values of microhardness of two types of ITZs**

#### 4.4 APPLICATIONS OF RAC IN FINAL PRODUCTS

##### 4.4.1 Production of U-channels, road Kerbs and drain covers

Based on the above research results, the research team worked with a local precast company (Jetco Engineering (HK) Limited) to collect concrete debris a demolition site, produce recycled concrete aggregates and precast concrete products, including road kerbs and U-channels as shown in **Figure 18**. It was found that these products can be successfully produced by using the NS-treated RCA and they can also attain the required performance for application.

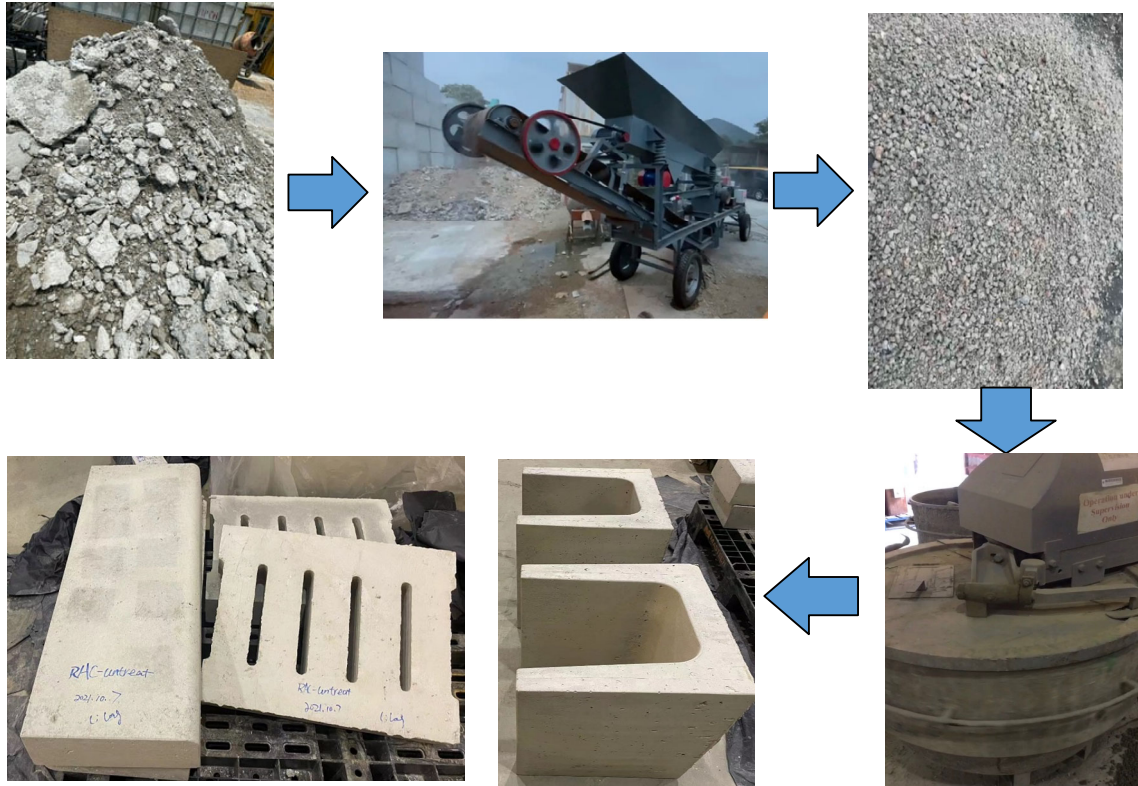


**Figure 18 Application of treated RCA in RAC products of road kerbs, drain covers and U-channels**

#### 4.4.2 Eco-shoreline seawater blocks (CEDD)

In order to further use RCA in real applications, **Figure 19** shows the production process of eco-shoreline seawater concrete blocks using recycled aggregates. It was found that using 100% of RCA, eco-shoreline seawater concrete can be designed with good properties and it can be eventually applied in real applications.



**Figure 19 Production process of eco-shoreline seawater blocks**

#### **4.4.3 Low-pH sea-sand seawater eco-engineered seawall panels (LCF)**

Liaised with SLO, CEDD, a type of low pH concrete has been designed in the laboratory and it will be used to produce rocky Eco-shoreline seasand block as shown below in **Figure 20**.



**Figure 20 Example of eco-shoreline concrete panel**

## 5. MARKET DEMAND IN RELATION TO LOCAL CONSTRUCTION INDUSTRY

Recycled coarse aggregates are categorized based on their properties. Recommendations are given for the use of different categories of recycled coarse aggregates in concrete for various concrete products and applications. Consideration for the use of recycled coarse aggregates in concrete and mortar is taken in two main streams: structural and non-structural; engineering and architectural.

For structural applications, recycled coarse aggregates with properties meeting the requirements stipulated in CS3: 2013 can be used for production of concrete for structural use with the limitations given in Works Bureau Technical Circular 12/2002: “Specifications Facilitating the Use of Recycled Aggregates” issued on 27 March 2002. In the designed mix proportions for concretes with strength grades C20 or below, 100% replacement of the coarse aggregates by recycled coarse aggregates is allowed. Whilst, for concretes with strength grades above C20 but not exceeding C35, 20% replacement is allowed. Although recycled concrete aggregates are allowed in some European countries for use up to concretes with strength grade C45, their use in concretes with strength grades over C35 is prohibited in Hong Kong at the moment. Following the growing trend of adopting medium to high strength concretes (C45 or above) in structural designs, recycled coarse aggregates are only confined to limited applications such as blinding or minor structures (e.g., planters) for ready mixed concretes and non-structural units (e.g., road kerbs, seawall blocks, etc.) for precast concrete fabrications. Based on the Works Bureau Technical Circular 12/2002 as mentioned above, recycled fine aggregate is prohibited for use in structural concrete. To broaden the applications of recycled aggregates, thoughts beyond structural concrete should be explored. Different nominal sizes of aggregate are used as filler materials in concretes, mortars, grouts for various structural and non-structural

applications including ready mixed concretes, precast concrete products, mortars for architectural use, grouting materials, etc. For products with structural applications, there may be more stringent requirements for mechanical strength and durability, but these properties are less important for products only for non-structural and architectural applications. In this regard, exploration for the use of recycled coarse and fine aggregates in non-structural and architectural applications, other than ordinary concrete, may be a way worth-considering to broaden their outlet channels. Possible applications of recycled coarse and fine aggregates are discussed in the following.

## **5.1 STRUCTURAL APPLICATIONS**

### **5.1.1 READY MIXED CONCRETE**

Ready mixed concrete is the main supply source for concrete used in building and construction works. In recent years, concretes of strength class at or below C45 become less and less and are only used for minor works or blinding use. Taking in account the average annual consumption of ready mixed concrete of around 6.5 million cubic meter and the portion of C20 or below is around 5% of the total consumption, the annual demand for concrete at strength class of C20 or below will be around 325,000 cubic meters and the demand for coarse aggregate is around 260,000 tonnes. Considering the fact that there is only about 20% of the ready mixed concrete batching plants have the storage and batching facilities to accommodate recycled coarse aggregate, about 52,000 tonnes of recycled coarse aggregate can be potentially consumed annually in this outlet. Since most of ready mixed concretes are required to follow the requirements in the General Specification, recycled fine aggregate cannot be used. Meanwhile, the portion of C35 to C45 is assumed about 10% of the total consumption.

## **5.1.2 STRUCTURAL PRECAST UNITS**

Structural precast concrete units include facades, staircase, slabs, cubical units, etc. for building works and bridge segments, tunnel segments, etc. for civil works. These precast concrete units do not only require medium to high strength class of concrete ( $\geq C45$ ), but also require relatively large piece of land space for production and storage. In addition, the required labour intensity is also very large. In this regard, basically all the precast factory manufacturing structural precast concrete units are set up in the Mainland. On the one hand, due to the relatively high strength class used in these precast concrete products, the use of recycled concrete aggregates is basically prohibited in the current specification. On the other hand, the requirements for large land space and labour intensity also do not allow the setting up of precast factories for these products in Hong Kong to consume the locally produced recycled aggregates.

## **5.2 NON-STRUCTURAL APPLICATIONS**

### **5.2.1 PRECAST CONCRETE UNIT FOR NON-STRUCTURAL USE OR FOR MINOR WORKS**

In building and constructions works, there are demands of various precast concrete units (e.g., road kerbs, paving blocks, lightweight blocks, dry walls, counterweights, etc.), with no or little requirements. In precast concrete fabrication, influence of the higher water absorption rate on workability loss of concrete is not as hazardous as ready mixed concrete due to relatively short haul distance within precast concrete fabrication factories. Although there is not any relevant official statistics, it is assumed that the portion of concretes having strength class of C20 or below is about 10,000 cubic meters. It is also assumed that most of all of the precast units with strength class of C20 or below are not for structural use, recycled fine aggregate can also be

used in the concrete mix. In this regard, considering that the total aggregates per cubic meter of concrete is in the order of 1.7 Tonnes, the potential consumption of recycled aggregate (100% replacement), both coarse & fine, is about  $10,000 \times 1.7 = 17,000$  tonnes while around 11,000 tonnes is for recycled coarse aggregate and 6,000 tonnes is for recycled fine aggregate. It is also assumed that the precast units with strength class above C20 is about 10,000 cubic meters, only recycled coarse aggregate can be used with 100% replacement as proposed. Taking that the average quantity of coarse aggregate in the concrete mix is in the order of 1.1 tonnes per cubic meter, the potential demand for recycled coarse aggregate in this portion is about  $10,000 \times 1.1 = 11,000$  tonnes.

Since most of the precast concrete units are fabricated in the Mainland, there are practical difficulties and economic concerns for transferring local recycled aggregates in Hong Kong to precast concrete factories in the Mainland for production. Nevertheless, for those minor precast units such as road kerbs, paving blocks, dry walls, etc., the land space required for production and storage of finished products is not as large as structural precast units (e.g., facades, staircases, etc.). In addition, automation can be largely introduced into the production process to reduce the requirement for labour intensity and land space. If this can be done and if the Hong Kong Government can offer some support to the recycling industry by providing suitable land space, some production operations of these kinds of small precast concrete units can be flowed back in Hong Kong and consume the locally produced recycled aggregates.

### **5.2.2 DRY MORTAR PRODUCTS**

Dry mortar is a collective name for various kinds of mortar products using cementitious binder, fine aggregates and some functional additives as the main ingredients developed and manufactured for different applications in building and

construction works. Since there is less structural and/or durability concern with dry mortar products, acceptance for incorporating recycled aggregates in lieu of virgin aggregates is much relaxed. In dry mortar products, render, plaster and screed materials have the least demand for mechanical strength, except the tensile adhesive strength for eliminating risk of detachment from substrates. In addition, these products require thixotropic properties that the viscosity of the mortar is able to increase within a short period of time in order to achieve anti-sagging properties for plaster/render materials and low consistency properties for screed materials for adjustment of fall directions. In this regard, the expected higher water absorption of recycled fine aggregate becomes a beneficial characteristic although it increases the water demand of the mortar for achieving the consistency suitable for machine spray, which is the commonest application method for plaster and render materials nowadays. Since mechanical strength is not the main concern for plaster, render and screed materials, higher cementitious content to cover the higher water content is not always required or at least not as demanding as concrete for structural use. Local consumption of plaster, render and screed materials for building and construction projects in Hong Kong, excluding those in the retail market for small renovation works, is in the order of around 300,000 tonnes (approximately 170,000 m<sup>3</sup>) per annum. This accounts for a potential demand for fine aggregate of approximately 210,000 tonnes per annum.

### **5.3 SUMMARY OF THE POTENTIAL DEMAND OF RCA**

Based on the statistics speculated above, the potential demands of recycled aggregates are summarized in **Table 2** below.

**Table 2 Estimated potential demand of recycled aggregates**

Item	Concrete Product	Market demand (m <sup>3</sup> )	Demand for recycled aggregates (Tonnes)	
			Coarse	Fine
1.	Ready mixed concrete ( $\leq$ C20)	325,000	52,000	--
2.	Ready mixed concrete (C35-C45)	650,000	104,000	--
3.	Non-structural precast concrete units ( $\leq$ C20)	10,000	11,000	6,000
4.	Non-structural precast concrete units ( $>$ C20)	10,000	11,000	--
5.	Dry Mortar (plasters & renders)	170,000	--	210,000
	Total:		178,000	216,000

**6. COST ANALYSIS AND QUALITY CONTROL OF RECYCLED AGGREGATE**

The manufacturing process for virgin aggregates is rather conventional and the processes involved is listed below in **Figure 21**.

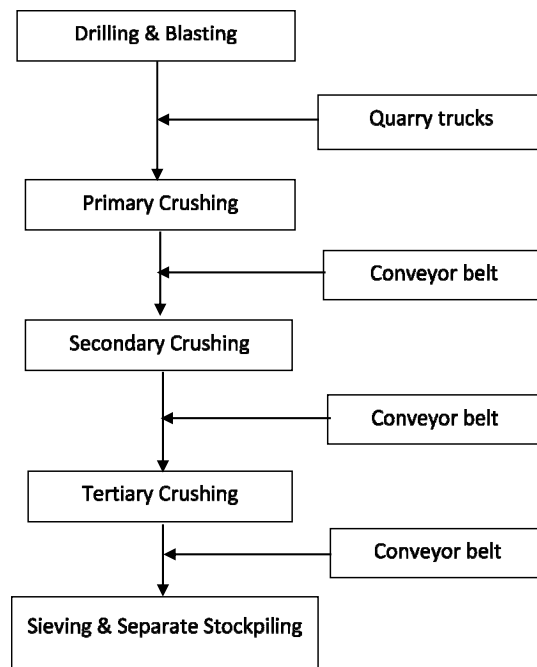


**Figure 21 Workflow in quarries for manufacturing virgin aggregates**

- **Cost of locally produced natural aggregate by considering quarrying, screening, crushing and sieving.**

After collection of relevant market information both in Hong Kong and the Zhujiang Delta, the main components and their cost in the production operations, including labour, equipment maintenance, power consumption, fuel, stockpiling, etc., of concrete aggregates are tabulated in **Table 3** below. The costs stated here include only the direct costs of the production operations and the costs for initial quarry formation, equipment set up and rock resources are not included.

**Table 3 Typical cost composition for production of aggregates from virgin rock in a quarry**

<b>Process</b>	<b>Approximate market cost</b>	<b>Cost converted to HK\$/T</b>	<b>Remark</b>
Drilling, blasting and breaking large explored boulders to < 0.8m in diameter	HK\$25/m <sup>3</sup>	HK\$10/T	Based on the price of explosives at ~HK\$40,000/T. Costs for formation of platforms & accesses are not included.
Chiseling large boulder after blasing to < 0.8m and loading to quarry truck by wheel loader/backhoe	HK\$10/m <sup>3</sup>	HK\$4/T	--
Transportation of boulders from quarry face to primary crusher by quarry trucks	HK\$10/T	HK\$10/T	Assuming the distance between the quarry face is about 2 km away from the primary crusher.
Primary, secondary & tertiary crushing	HK\$15/T	HK\$15/T	Power consumption cost in HK is taken into account. The maintenance cost for equipment is based on equipment set associated with the Primary Crusher Model: AVJ 912 manufactured by Guangzhou Municipality Hua Qian Quarry Heavy Machineries Co., Ltd.
Sieving	HK\$4/T	HK\$4/T	--
<b>Total:</b>		<b>HK\$43/T</b>	

Note: Source of information: Lotti Construction Materials Co., Ltd. (HK) & Hui Jin Quarry Products Co., Ltd. (Mainland)

- **Cost of the imported natural aggregate from mainland China.**

As a result of numerous factors, both economical and policy related, the price of aggregates in Guangdong Province and those exported to the Hong Kong market has risen by 80 – 100% in year 2021 up to the current price in the range of HKD180 – 200 per ton delivered to Hong Kong ports.

- **Cost of production of coarse recycled aggregate (different types proposed in specification) using the traditional processing method and cost of the treated recycled aggregate by spraying micro-silica suspension.**

A typical workflow for the production process of recycled concrete aggregate is exhibited in **Figure 22**. The workflow and the associated production cost are expected to be similar for Type I, II & III recycled coarse aggregates in the proposed specification.

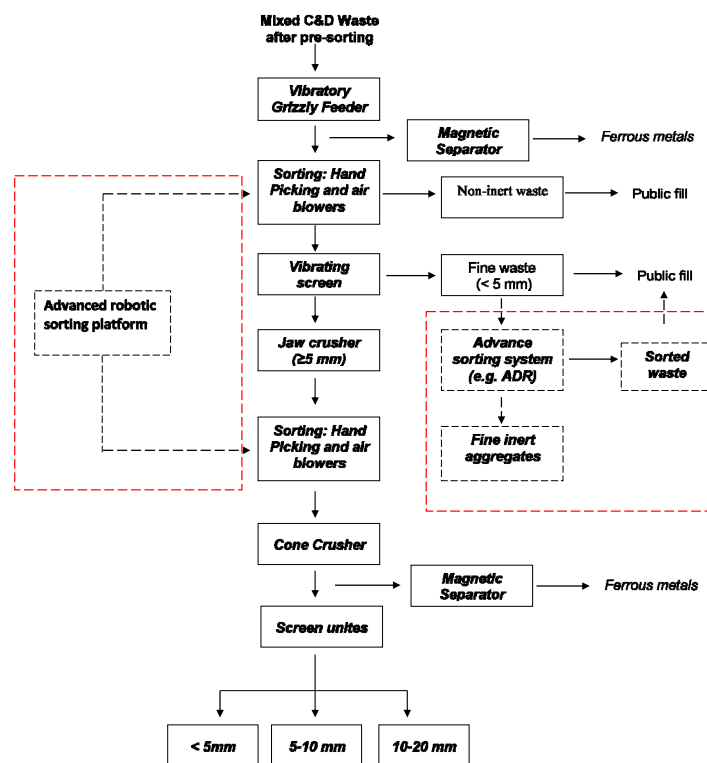


**Figure 22 Typical workflow for production of recycled aggregate**

Typical cost composition of turning the inert C & D materials to concrete aggregates is listed in **Table 4**.

**Table 4 Typical cost composition for production of recycled aggregates from C & D wastes**

Process	Estimated cost	Cost converted to HK\$/T	Remark
Sorting of hard cores from incoming inert C & D materials	HK\$10/T	HK\$10/T	C & D materials containing more than 50% by weight of inert construction waste
Secondary & tertiary crushing	HK\$10/T	HK\$10/T	Primary crushing is not required.
Sieving	HK\$4/T	HK\$4/T	--
Total:		<b>HK\$24/T</b>	Untreated recycled aggregate
		<b>HK\$34-44/T</b>	Treated recycled aggregate

Note: There is an estimated additional cost of HK\$10-20/T for treatment of recycled coarse aggregates for reducing its water absorption rate by using nano-silica suspension.

Source of information: Lotti Construction Materials Co., Ltd. (HK) & Hui Jin Quarry Products Co., Ltd. (Mainland)

- **Quality of Recycled Aggregates**

It is the conception of many engineers that recycled aggregates have poorer quality than virgin aggregates and will affect the durability of the resulted concrete, although the required strength is achieved. Most engineers are also lack of confidence whether the concretes using recycled aggregates can achieve the quality requirements including the prime parameter of compressive strength in a consistent manner. Albeit there had been a number of construction works in early 2000's completed with concretes using recycled aggregates including some schools and the prestigious Wetland Park project, most engineers are still not able to grasp the experience with concretes using recycled aggregates. By borrowing the experience in early 2000's, specifying in government contracts is the fastest way to promote and encourage the use recycled aggregates in concretes, at least in the initial stage.

The performance of concretes using recycled aggregates in more pilot projects will surely inspire confidence of engineers for more intensive use.

Recycled aggregates obtained from construction projects such as tunnel boring, site formation, etc. in which the raw material (rocks) is just similar to that of an ordinary quarry site have similar properties as virgin aggregates. However, recycled aggregates obtained from construction and demolition (C & D) wastes may contain hardened cement paste, broken bricks, tiles, etc., which may have higher absorption rate causing higher water demand than virgin aggregates for achieving the required workability or incurring faster workability loss after mixing but before casting. To combat this possible shortcoming of recycled aggregated obtained from C & D wastes, the conventional method is to increase mixing water in the concrete mix proportion, while the total quantity of binder materials is also increased to maintain the same or similar water/binder ratio, or to employ higher dosage of water reducing agent with better workability retention ability. The Hong Kong Polytechnic University has categorized recycled coarse aggregates into three types based on their properties and has also developed a treatment method (HKPU Method) for reducing the water absorptivity of recycled aggregates such that their increased water demand in the concrete mix and more rapid workability loss can be suppressed to a minimum without altering other mechanical and physical properties.

Conclusively, the quality of recycled aggregates depends on the origins from which the raw materials, mainly hard cores or hardened concrete and other contaminated building materials, are recycled. For hard cores obtained from sound rock excavation in some civil projects (e.g., tunnel boring operation through sound rock stratum), quality of the aggregates produced in the recycling process may not differ from that produced from quarries with virgin rocks. In contrast, for the C & D wastes obtained from building demolition works, there may complex combinations of the inert

materials for recycling leading to wider range of quality performance for being used as aggregates for concrete or mortar production. In this regard, it may be beneficial to separate and categorized collected waste materials from different sources with different congenital quality levels for the production of aggregates to be used in concretes/mortars for different applications.

## 7. CARBON EMISSION FACTOR OF RECYCLED PRODUCT BY CAT

The system boundary for recycled aggregates (both treated and untreated) was A1-A4 in accordance with the Carbon Assessment Tool (CAT) method. For recycled products (e.g. concretes), the system boundary was A1-A3 (which includes raw materials production and supply, transportation to Hong Kong and then to the batching plants, and the production of concrete at batching plants) according to the CAT method.

The functional unit of recycled aggregates (both treated and untreated) was considered as 1 tonne, whereas it was 1 m<sup>3</sup> for recycled product (e.g. concrete) production. **Table 5 and Table 6** list the mixture proportions of C40 and C20 concretes.

**Table 5 Mixture proportions of C40 concrete**

Materials	Materials (kg/ m <sup>3</sup> )		
	C40(RCA-T)	C40(RCA-U)	C40(Nor)
OPC	364	364	364
Recycled coarse aggregates (RCA) (5-20 mm)	1176	1176	1176
Natural fine aggregates (<5 mm)	661	661	661
Water	200	200	200
SP	4.93	4.93	2.00
Nano-silica	10.58	--	--

**Table 6 Mixture proportions of C20 concrete**

Materials	Materials (kg/ m <sup>3</sup> )		
	<i>C20(RCA-T)</i>	<i>C20(RCA-U)</i>	<i>C20(Nor)</i>
OPC	297	297	297
Recycled coarse aggregates (RCA) (5-20 mm)	1139	1139	1139
Natural fine aggregates (<5 mm)	759	759	759
Water	205	205	205
Nano-silica	10.25	--	--

**Table 7** therefore lists the carbon emission factor of recycled aggregate and recycled aggregate concrete by CAT. Some main findings are given below:

- The calculation found that the carbon emission factor of untreated and treated RCA was 0.011 kg CO<sub>2</sub> eq/kg and 0.013 kg CO<sub>2</sub> eq /kg, respectively.
- The LCA results show that about 439 kg CO<sub>2</sub> eq greenhouse gas emissions was associated with C40 normal concrete, which is about 5% higher than that of concrete produced with recycled concrete aggregates (RCA), for both C40(RCA-T) and C40 (RCA-U) production regardless of the use of treated or untreated RCA.
- The saving for C20 concrete produced with RCA is even higher (about 7%) compared to that of normal concrete. Both C20 (RCA-T) and C20 (RCA-U) saves about 20 kg CO<sub>2</sub> eq emission than the normal C20 concrete.
- The CO<sub>2</sub> eq emission saving was not that high as the aggregates only contribute to about 14% of the total emission, whereas about 84% by OPC (for normal C40 concrete). For C20 concrete, aggregates only contribute to about 17% of the total emission.

- In addition to CO<sub>2</sub> eq emission saving, both C40 and C20 concretes save huge amount of natural aggregates (e.g. resource saving) due to the use of high-volume RCA.

The results indicate that RCA treatment with nano-silica does not affect the carbon emission significantly, as only 2 kg CO<sub>2</sub> eq emission is induced by the RCA treatment process (with nano-silica) for producing per m<sup>3</sup> of concrete (for both C40 and C20).

**Table 7 Carbon emission factor of recycled product by CAT**

<b>Materials</b>	<b>Unit CO<sub>2</sub> eq</b>
Recycled coarse aggregates	0.011 kg CO <sub>2</sub> eq/kg
Treated recycled coarse aggregates by nano-silica	0.013 kg CO <sub>2</sub> eq /kg
C40 prepared with natural aggregates	439 kg CO <sub>2</sub> eq /m <sup>3</sup>
C40 prepared with recycled coarse aggregates	416 kg CO <sub>2</sub> eq /m <sup>3</sup>
C40 prepared with treated recycled coarse aggregates	418 kg CO <sub>2</sub> eq /m <sup>3</sup>
C20 prepared with natural aggregates	369 kg CO <sub>2</sub> eq /m <sup>3</sup>
C20 prepared with recycled coarse aggregates	343 kg CO <sub>2</sub> eq /m <sup>3</sup>
C20 prepared with treated recycled coarse aggregates	345 kg CO <sub>2</sub> eq /m <sup>3</sup>

8. **SPECIFICATION RECOMMENDATION ON THE USE OF COARSE RECYCLED AGGREGATE IN CONCRETE**

A meeting has been arranged with the Standing Committee on Concrete Technology of CEDD, with membership from all major government departments which uses aggregates and concrete on 30<sup>th</sup> Dec 2021 to discuss the findings of this research. The project team was actively preparing materials for this meeting so that the use of

recycled aggregates was explained to the government stakeholders. **Table 8** shows recommendations on coarse recycled aggregates for use in concrete and concrete products.

**Table 8 Specification Recommendation on the Use of Coarse Recycled Aggregate in Concrete**

		NA in CS3:2013	RA in CS3:2013****		RA					Testing method	
					Type I		Type II		Type III		
Requirement on composition	Rc+Ru	n.a.	n.a.	n.a.	≥95%	≥90%	≥70%			BS EN 933-11:2009	
	Rb	n.a.	n.a.	n.a.	≤5%	≤10%	≤30%				
	Ra	n.a.	n.a.	n.a.	≤1%	≤1%	≤1%				
	FL	n.a.	≤0.5%*		≤ 2cm <sup>3</sup> /kg	≤ 2cm <sup>3</sup> /kg	≤ 2cm <sup>3</sup> /kg				
	X+Rg	n.a.	≤1%**		≤1%	≤1%	≤1%				
Requirement on properties	Grading	Table 3.1 in CS3	Table 3.1 in CS3		Table 3.1 in CS3	Table 3.1 in CS3	Table 3.1 in CS3			CS3 Section 10	
	Max. content of Fines (<0.075mm)	4%	4%		2%	3%	4%			CS3 Section 10	
	Max. content of sand (<4mm)	n.a.	5%		5%	5%	5%			CS3 Section 10	
	Flakiness index	30%	40%		40%	40%	40%			CS3 Section 11	
	Min. Oven-dry Density (kg/m <sup>3</sup> )	2000	2000		2300	2000	2000			CS3 Section 17	
	Max. Water absorption	0.8%	10%		5%	10%	15%			CS3 Section 17	
	Max. Chloride content	0.01% <sup>a</sup> 0.03% <sup>b</sup> 0.05% <sup>c</sup> No limit <sup>d</sup>	0.01% <sup>a</sup> 0.03% <sup>b</sup> 0.05% <sup>c</sup> No limit <sup>d</sup>		0.01% <sup>a</sup> 0.03% <sup>b</sup> 0.05% <sup>c</sup> No limit <sup>d</sup>	0.01% <sup>a</sup> 0.03% <sup>b</sup> 0.05% <sup>c</sup> No limit <sup>d</sup>	0.01% <sup>a</sup> 0.03% <sup>b</sup> 0.05% <sup>c</sup> No limit <sup>d</sup>			CS3 Section 21	
	Max. Sulphate content	1%	1%		1%	1%	1%			CS3 Section 21	
Application field	Max. RA Replacement Ratio	n.a.	20%	100%	30%	100%	20%	100%	20%	100%	
	Use condition	No limit	Not for water retaining structure	Non-structure	Not for water retaining structure	Non-structure	Not for water retaining structure	Non-structure	Not for water retaining structure	Non-structure	
	Max. strength	No limit	35MPa	20MPa	45MPa	No Limit	45MPa	No Limit	35MPa	No Limit	

**Note:**

Rc- Concrete, concrete products, mortar, concrete masonry units.

Ru- Unbound aggregate, natural stone, Hydraulically bound aggregate.

Rb- Clay masonry units (i.e. bricks and tiles), Calcium silicate masonry units, Aerated non-floating concrete.

Ra- Bituminous materials.

FL-Floating material (less dense than water).

Rg- Glass.

X- Other: Cohesive (i.e. clay and soil), Miscellaneous: metals (ferrous and nonferrous), non-floating wood, plastic and rubber, Gypsum plaster.

\* It consists of wood and materials less dense than water.

\*\* Bituminous materials are included.

a: when used in prestressed concrete and heat-cured concrete containing embedded metal.

b: when used in concrete containing embedded metal and made with cement complying with BS 4027.

c: when used in concrete containing embedded metal and made with cement complying with BS EN 197-1 or combinations with ground granulated blast furnace slag (GGBS) or pulverized-fuel ash (PFA).

d: when used in other concrete.

## 9. **CONCLUSIONS AND WAY FORWARD**

### 9.1 CONCLUSIONS AND RECOMMENDATIONS

- Quality of recycled aggregates can be improved by the techniques developed in this study;
- Consideration for the use of recycled coarse aggregates in concrete and mortar is taken in two main streams: structural and non-structural. Estimated potential demand of recycled aggregates in the HK market is about 400,000 tonnes/year;
- The cost of locally produced and treated recycled aggregate is around HK\$34-44/T (excluding land, management and transport cost) which is lower than that of the imported natural aggregate (HK\$180 – 200/Tonnes);
- Concrete products such as road kerbs, drain covers and U-channels have been produced successfully by using the recycled aggregates in a small scale local precast concrete company;
- Carbon emission factors of recycled products based on the assessment method of CAT have been calculated;
- Proposals have been developed to revise current specifications on the Use of Coarse Recycled Aggregate in Concrete ;
- Specifying in government contracts is the fastest way to promote and encourage the use recycled aggregates in concretes, at least in the initial stage;
- The performance of concrete using recycled aggregates in more pilot projects will surely inspire confidence of engineers for more wider use;
- To broaden the applications of recycled aggregates, thoughts beyond structural concrete should be explored. For example, dry mortar products

cover a wide range of pre-packaged building products for various non-structural or mainly architectural applications such as render, plaster, patch-up mortar, floor screed and other higher caliber materials.

## 9.2 WAY FORWARD

**Figure 23** shows potential beneficiaries and potential benefits of the proposed project. The research had been conducted closely with collaboration with local recyclers (i.e. Tiostone Environmental Ltd., Government – Construction Ltd, CEDD’s Waste Sorting Facilities) and users of RCA (i.e.: precast concrete manufactures) for implementing the developed treatment techniques and reusing the treated RCA in precast concrete components. Meanwhile, compared with the existing specifications developed by Government, revision of the specifications on the Use of Coarse Recycled Aggregate in Concrete has been proposed.

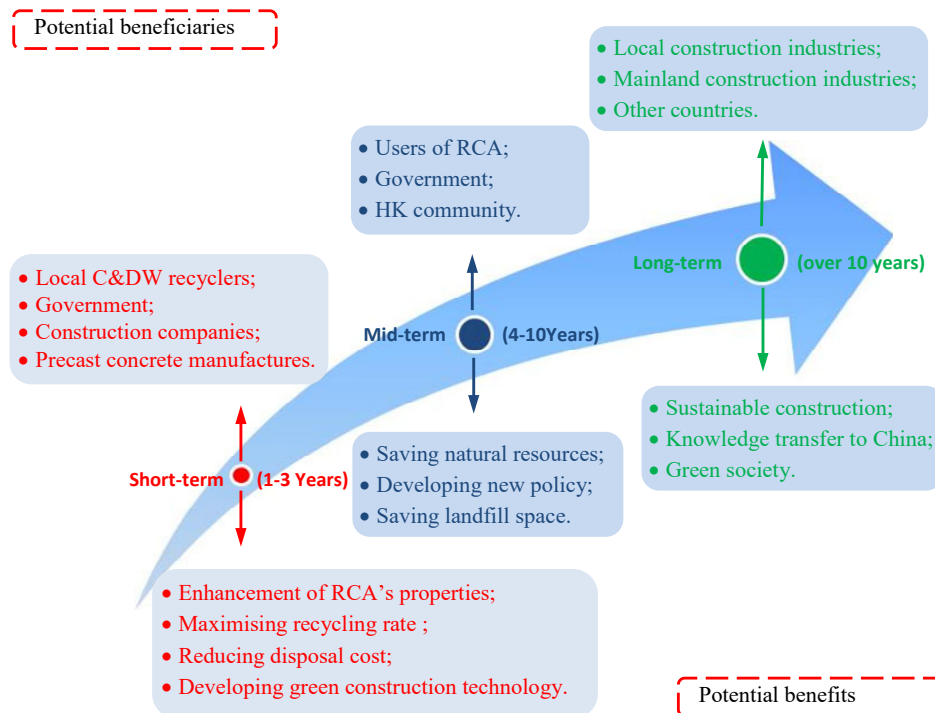


**Figure 23 Potential beneficiaries and potential benefits of the proposed project**

Other site trials can be further conducted after the completion of the project in collaboration with relevant Government Departments to demonstrate the feasibility of the developed techniques in real applications.

## **APPENDICES — PUBLICATIONS**

**In this research, more experimental results were reported in publications as shown below:**

1) Long Li, Dongxing Xuan, Adebayo Olatunbsoun Sojobi, Songhui Liu, Shaohua Chu, Chi Sun Poon. Development of nano-silica treatment methods of recycled aggregates to enhance recycled aggregate concrete. *Cement and Concrete Composites*. 2021, 118:103963.

2) Shaohua Chu, Chi Sun Poon, CS Lam, Long Li. Effect of natural and recycled aggregate packing on properties of concrete paving blocks. *Construction and Building Materials*. 2021, 278:122247.

3) Adebayo Olatunbsoun Sojobi, Dongxing Xuan, Long Li, Songhui Liu, Chi Sun Poon. Optimization of flow-through gas-solid carbonation conditions of recycled aggregates using a linear weighted sum method. *Developments in the Built Environment*. 2021, 7:100053.

4) Long Li, Dongxing Xuan, Chi Sun Poon. Stress-strain curve and carbonation resistance of recycled aggregate concrete after using different RCA treatment techniques. *Applied Science*, 2021, 11, 4283

5) Xiaoliang Fang, Dongxing Xuan, Peiliang Shen, and Chi Sun Poon. Fast Enhancement of Recycled Fine Aggregates Properties by Wet Carbonation. *Journal of Cleaner Production*. 2021, 313:127867.

6) Long Li, Dongxing Xuan, Adebayo Olatunbsoun Sojobi, Songhui Liu, Chi Sun Poon. Efficiencies of carbonation and nano silica treatment methods in enhancing the performance of recycled aggregate concrete. *Construction and Building Materials*, 2021, 208:125080.

7) Long Li, Dongxing Xuan, Chi Sun Poon. Modification of recycled aggregate by spraying colloidal nano silica and silica fume. *Materials and Structures*. 2021, 54:223.



# Development of nano-silica treatment methods to enhance recycled aggregate concrete

Long Li, Dongxing Xuan, Adebayo Olatunbsoun Sojobi, Songhui Liu, S.H. Chu, Chi Sun Poon\*

Department of Civil and Environmental Engineering, The Hong Kong Polytechnic University, Hong Kong

## ARTICLE INFO

### Keywords:

Recycled aggregate concrete  
Nano-silica  
Particle size  
Dosage  
Interface  
Microhardness

## ABSTRACT

The reuse of recycled aggregates (RA) for producing recycled aggregate concrete (RAC) is a promising way to alleviate the environmental impacts and improve construction sustainability. Because of the inferior properties of RA than natural aggregate, pre-treatments of RA are commonly considered to improve the performance of RAC. In this study, three nano-silica (NS) treatment methods, i.e., pre-spraying plus air-drying, pre-spraying without air-drying and pre-soaking plus air-drying, were adopted and evaluated systematically by varying the dosage and the particle size of NS suspension. The mechanical properties and durability of RAC such as compressive strength, elastic modulus, rate of water absorption and chloride penetration resistance were evaluated. For the microstructural assessment, the micro-hardness test was conducted to investigate the influence of these NS treatment methods on the old mortar and the new mortar near the interface. The experimental results showed that the NS pre-spraying treatments were superior to the NS pre-soaking method and the pre-spraying without air-drying was the best in terms of the enhancement in mechanical properties and durability. The optimum dosage of NS suspension for pre-spraying was 3% of RA by mass and a larger particle size of NS would be more effective. In addition, the microhardness of both the old mortar and the new mortar near the interface were enhanced after using the three NS treatment methods, and the microstructure enhancement of the latter played a more important role for the enhancement of the performance of RAC.

## 1. Introduction

In recent decades, the construction industry has developed rapidly especially in developing countries, resulting in the depletion of natural resources and the generation of large amounts of construction and demolition waste. The production of recycled aggregate concrete (RAC) that uses recycled aggregate (RA) to replace natural aggregate (NA) has been promoted as an effective way to utilize construction and demolition waste and conserve natural resources. But there are still drawbacks related to RAC when compared with natural aggregate concrete (NAC) such as poorer mechanical properties and durability. Thus, RAC has been mainly limited to non-structural uses at present [1]. In general, compared with NA, RA has a lower density, higher water absorption, higher porosity and more cracks [2–5]. As a result, RAC has relatively inferior properties to that of NAC [6–10].

In order to facilitate the large-scale application of RAC, many techniques have been developed to try to improve the properties of RA and RAC. According to the classification and the proposed treatment method in our previous study [11], these techniques can be classified into four

categories: (1) Removal of the adhered old mortar in RA; (2) Strengthening the adhered old mortar in RA; (3) Enhancement of the interface zone between RA and the new mortar of RAC; (4) Enhancement of the new mortar of RAC.

The removal of old adhered mortar can improve the quality of RA such as lower water absorption and higher density, leading to an improvement in performance of RA as well as RAC. A variety of techniques have been adopted to remove the adhered old mortar in RA, e.g., mechanical grinding [12,13], heat grinding [14,15], ultrasonic cleaning [16] and pre-soaking in acid solutions such as HCl, H<sub>2</sub>SO<sub>4</sub> and H<sub>3</sub>PO<sub>4</sub> [17]. However, the associated disadvantages are increased energy consumption, higher CO<sub>2</sub> emission, higher amount of waste fines produced, and the increased chloride and sulfate contents in RA due to acidic solutions [4].

For strengthening of the adhered old mortar in RA, the physical properties of RA can be improved. Currently, calcium carbonate precipitation in the old mortar of RA by acceleration carbonation method [18–21] is one of most promising old mortar strengthening techniques. By this method, calcium carbonate is precipitated in the pores where

\* Corresponding author.

E-mail address: [cecsphoon@polyu.edu.hk](mailto:cecsphoon@polyu.edu.hk) (C.S. Poon).

CO<sub>2</sub> reacts with main cement hydration products, i.e., Ca(OH)<sub>2</sub> and hydrated calcium silicate hydrate (C–S–H). Such calcium carbonate filling effect may be also realized through the microbial carbonate precipitation method [22]. Another method to strengthen the adhered old mortar in RA is by immersing RA in a sodium silicate solution which can significantly reduce the water absorption of RA [23], but this method might increase the risk of alkali silica reaction because of the introduced alkali.

The enhancement of the new interface zone between RA and the new cement mortar is another way to improve the properties of RAC. This can be realized by coating RA with a layer of polymer emulsion like polyvinyl alcohol [24,25], cement slurry, pozzolan slurries like fly ash and silica fume [26], and nano materials like nano-silica (NS) [27,28] by pre-mixing or pre-soaking. Polyvinyl alcohol strengthens the RA by filling the pores of RA and seals the surface of RA after solidified, and also reduces water-to-cement ratio of the new interface zone [29]. Cement slurry and pozzolan slurries could fill the pores and voids of the old adhered mortar and also react with Ca(OH)<sub>2</sub> to form C–S–H gel [29,30], leading to the enhancement of the adhered old mortar and the new interface zone. Similarly, nano materials also have a filling effect in RA and promote cement hydration process due to their high reactivity and small size [31].

Rather than pre-treatment of RA, another treatment method aims to improve the properties of new cement mortar with addition of a certain amount of supplementary cementitious materials [32,33] or nano materials like NS [31,34] in RAC. That is because the supplementary cementitious materials and nano materials could improve the pore structures of the new cement paste due to the filling effect and pozzolan reaction. It was reported the long-term mechanical properties and durability of RAC could be improved by incorporating fly ash [32], the compressive strength of RAC can be improved to equal or exceed that of NAC by adding fly ash or silica fume as a fine aggregate replacement [33], and the mechanical properties and durability of RAC could be improved by incorporating a certain amount of nano-materials [35].

As stated above, NS has been adopted as a surface treatment material or supplementary cementitious material to improve the properties of RAC. It was reported that these NS treatment methods can improve the mechanical properties and durability of RAC [31,34–38]. In some studies, the compressive strength of RAC after NS treatment can be similar to or even higher than that of NAC [31,34]. However, the addition of NS as a supplementary cementitious material in RAC will reduce the workability of the fresh concrete [34], and requires the addition of admixtures such as superplasticizer to improve concrete workability. Regarding the NS surface treatment of RA by pre-soaking, it needs a large amount of NS suspension for complete immersion of RA and the porous RA would also absorb a certain amount of NS suspension. This would be not an economic method. Comparing with the pre-soaking method, pre-spraying a layer of NS suspension on the surface of RA would consume a much smaller amount of NS suspension, and it is quite easy to build a pre-spraying treatment facility together with the crushing line. Therefore, the aim of this study is to explore the effect of pre-spraying NS suspension on the surface of RA on the mechanical properties and durability of RAC.

## 2. Materials and experimental program

### 2.1. Materials

The cement used in this study was an ordinary Portland cement CEM I 52.5 N. Its chemical composition is listed in Table 1. The fine aggregate

**Table 1**  
Chemical composition of the ordinary Portland cement determined by XRF.

Composition	MgO	Al <sub>2</sub> O <sub>3</sub>	SiO <sub>2</sub>	SO <sub>3</sub>	K <sub>2</sub> O	CaO	Fe <sub>2</sub> O <sub>3</sub>
Content (%)	1.28	4.11	19.06	4.96	0.96	66.87	2.76

used was a river sand, of which the fineness modulus was 2.6. The RA was collected from a local construction waste recycling company. The RA mainly consisted of old concrete and crush stone and their mass proportions were 87.5% and 12.5%, respectively. Almost no other impurities were found in RA. Crushed granite was used as the natural aggregate (NA). Both the RA and NA were sieved into two fractions: 10–20 mm and 5–10 mm. The physical properties of NA and RA are shown in Table 2. Two types of water base commercial NS suspensions from a chemical company in Zhejiang province of China were used, which were named as NS-1 and NS-2. The average particle sizes of the NS-1 and NS-2 were 12.2 nm and 106.0 nm, respectively as provided by the manufacturer. The particle size distributions of these two types of NS suspensions were determined by a Particle Size and Zeta Potential Analyzer (Zetasizer Nano ZS90) as shown in Fig. 1. According to the X-ray fluorescence (XRF) test results, the contents of SiO<sub>2</sub> in NS-1 and NS-2 were 31.2% and 34.3%, respectively.

### 2.2. Treatments of RA by NS suspensions

The air-dried RA was treated with NS suspensions according to the methods as shown in Table 3. The untreated RA was marked as RA-1. To study the effect of the NS dosage, the NS-1 was sprayed on the surface of RA with different NS suspension to aggregate (N/A) ratios by mass and then the treated RA was stored in an outdoor environment (T ≈ 20 °C, RH ≈ 75%) for 1 month for air-drying before casting concrete. Here, to achieve an evenly spraying, a batch of RA (5 kg per batch) was continuously rotated in an inclined mixer with a size of Φ500mm × 170 mm (as shown in Fig. 2) at a rotating speed of 10 rev/min. The NS suspension was sprayed on the rotating RA by a handheld liquid spraying device. The air-drying process was to simulate the real treatment condition for RA, which may be stored for a period in an air-drying state before use. This NS treatment methods was labeled as “pre-spraying plus air-drying”. When N/A ratio was 1%, 3% and 5%, the corresponding treated RA was marked as RA-2, RA-3 and RA-4, respectively. The amount of NS suspension sprayed on the RA was controlled based on the N/A ratio. For example, when the N/A ratio was 3%, 150 g of NS suspension was sprayed on 5 kg RA. To study the effect of NS particle size, a batch of RA (RA-5) was treated with a larger size of NS suspension (NS-2) using the same method of pre-spraying plus air-drying, and the N/A ratio was 3%.

Except for the pre-spraying plus air-drying method, other two NS treatment methods were used as well, including pre-soaking RA in NS suspension for 3 h and then storing the RA in outdoor environment for 1 month for air-drying before casting (hereinafter called “pre-soaking plus air-drying”), and pre-spraying NS on the surface of RA and casting concrete immediately (hereinafter called “pre-spraying without air-drying”). The corresponding two types of RA were marked as RA-6 and RA-7, respectively. For the pre-soaking plus air-drying method, the NS-1 suspension was diluted before RA pre-soaking by mixing the NS-1 suspension with twice extra water by mass.

The physical properties of RA before and after NS treatments are given in Table 4. It shows that after spraying NS with different sizes on the surface of RA or pre-soaking RA in NS suspension, the water absorption of RA only decreased slightly. It might be because the filling of NS particles into the porous RA and the reaction between the NS and the Ca(OH)<sub>2</sub> were only beneficial to densify the surface layer of RA. The inner part of the RA was not affected.

### 2.3. Mix proportions of new concrete

Eight concrete mixtures were casted, including the concrete prepared with NA, RA-1, RA-2, RA-3, RA-4, RA-5, RA-6 and RA-7. The corresponding concrete mixture was labeled as NAC, RAC-1, RAC-2, RAC-3, RAC-4, RAC-5, RAC-6 and RAC-7, respectively. The mix proportions are given in Table 5. Due to high water absorption of RA, additional amounts of water (additional water) were added to maintain

**Table 2**  
Physical properties of coarse aggregate.

Aggregate	Size (mm)	Water absorption (%)	Dry particle density (kg/m <sup>3</sup> )	Apparent density (kg/m <sup>3</sup> )	Crushing value	10% fine value (kN)
RA5-10	5-10	5.99%	2263	2619	–	–
RA10-20	10-20	4.85%	2312	2604	30.0%	107.2
NA5-10	5-10	0.69%	2634	2683	–	–
NA10-20	10-20	0.57%	2602	2641	24.1%	163.4

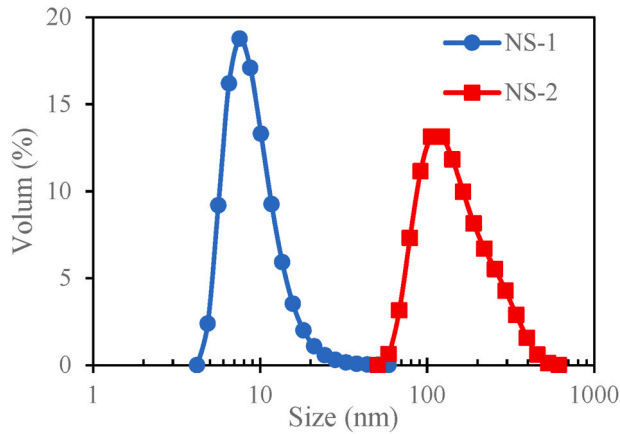


Fig. 1. Particle size distributions of NS suspensions.

**Table 3**  
NS suspension treatment program of RA.

No.	Treatment methods	N/A ratio	Size of NS particles (nm)	SiO <sub>2</sub> content in NS suspension
RA-1	Untreated	0	0	0
RA-2	Pre-spraying plus air-drying	1%	12.2	31.2%
RA-3	Pre-spraying plus air-drying	3%	12.2	31.2%
RA-4	Pre-spraying plus air-drying	5%	12.2	31.2%
RA-5	Pre-spraying plus air-drying	3%	106.0	34.3%
RA-6	Pre-soaking plus air-drying	–	12.2	10.4%
RA-7	Pre-spraying without air-drying	3%	12.2	31.2%

a consistent effective water to cement (W/C) ratio. As the water absorption of RA before and after treatment showed no significant differences, the same values were used for all types of RA. As the moisture content of all untreated and untreated RA were about 2.2%, and the same value was used for all of them. For RAC-7, as the NS-1 suspension was pre-sprayed on the surface of RA, the additional water was determined after the deduction of the water in the NS suspension involved.

For each mixture, the prepared concrete specimen included five cylinders with the dimension of  $\Phi 100 \times 200$  mm and three cubes with the dimension of  $100 \times 100 \times 100$  mm. After casting, the specimens were cured in the lab environment ( $T \approx 20$  °C,  $RH \approx 60\%$ ) for 24 h before demoulding and then cured in a water tank for 28 days in the laboratory environment.

2.4. Testing methods

2.4.1. Measurement of physical properties of aggregates

The physical properties of coarse aggregate including water absorption and density, aggregate crushing value and 10% fine value were determined in accordance with BS 812-2, BS 812-110 and BS812-111.



Fig. 2. Inclined mixer with handheld liquid spraying device.

**Table 4**  
Physical properties of RA before and after NS treatment.

Treatment method	State of RA	Water absorption of RA (10-20 mm) (%)	Dry particle density of RA (10-20 mm) (kg/m <sup>3</sup> )
Pre-spraying NS-1 plus air-drying (N/A ratio was 5%)	Before treatment	5.2	2288
	After treatment	5.1	2286
Pre-spraying NS-2 plus air-drying (N/A ratio was 5%)	Before treatment	5.4	2269
	After treatment	5.3	2266
Pre-soaking in the diluted NS-1 plus air-drying	Before treatment	5.2	2284
	After treatment	4.9	2293

The RA samples after testing the water absorption and density were treated with the NS suspensions and then the NS treated RA samples were used for testing the water absorption and density again to reduce variation due to sampling.

2.4.2. Measurement of slump

After mixing in a laboratory mixer, the slump of the fresh concrete was measured using the standard slump test apparatus according to ASTM C143.

**Table 5**  
Mix proportions of concrete (kg/m<sup>3</sup>).

Mixture number	Aggregate used	W/C ratio	Water	Additional water	Cement	Sand	Coarse aggregate (5–10 mm)	Coarse aggregate (10–20 mm)
NAC	NA	0.56	185	4.5	330	754	377	754
RAC-1	RA-1	0.56	185	39.7	330	754	377	754
RAC-2	RA-2	0.56	185	39.7	330	754	377	754
RAC-3	RA-3	0.56	185	39.7	330	754	377	754
RAC-4	RA-4	0.56	185	39.7	330	754	377	754
RAC-5	RA-5	0.56	185	39.7	330	754	377	754
RAC-6	RA-6	0.56	185	39.7	330	754	377	754
RAC-7	RA-7	0.56	185	16.3	330	754	377	754

#### 2.4.3. Measurement of compressive strength

The 28-day compressive strength of concrete specimens with the size of 100mm × 100mm × 100 mm was tested according to BS EN 12390-3. Three concrete specimens of each mixture were prepared for the measurement of compressive strength. The loading rate was fixed at 0.6 MPa/s.

#### 2.4.4. Measurement of elastic modulus

The stress-strain curve of concrete was determined using a stiff-framed servo-hydraulic testing machine MTS 815. Four concrete cylinders with the dimension of Φ100mm × 200 mm were tested. In this test, the loading speed was  $2 \times 10^{-3}$  mm/s, which was corresponded to the strain rates of  $10^{-5}$ /s. The loading was terminated when the force was decreased to around 20% of the peak force after failure. The applied compressive force was measured by an internal force transducer in the testing machine. The displacement of each concrete specimen was measured by two linear variable differential transformers. The average value was used to calculate the strain of the specimen. The elastic modulus  $E$  was determined from the stress-strain curve using the following equation:

$$E = (\sigma_1 - \sigma_2) / (\varepsilon_1 - \varepsilon_2) \quad (1)$$

Where,  $\sigma_1$  and  $\sigma_2$  are the stresses corresponding to 5% and 20% of the peak stress, respectively;  $\varepsilon_1$  and  $\varepsilon_2$  are the strain values at the stress level  $\sigma_1$  and  $\sigma_2$ , respectively. According to a previous study [39], the lower limit of this range was selected to remove the initial seating errors as a specimen was loaded, while the upper limit was selected at a value where the response was virtually linear.

#### 2.4.5. Measurement of rate of water absorption

The rate of water absorption of the prepared concrete was determined according to ASTM C1585-13. For each group of concrete, three cylinders with the dimension of Φ100 × 50 mm, which were cut from concrete cylinders with the dimension of Φ100 × 200 mm, were prepared. Before testing, the specimens were water saturated with the vacuum-saturation procedure in ASTM C1202-19 and then placed in an environmental chamber at a temperature of 50 °C and relative humidity of 80% for 3 days. After that, each specimen was placed inside a sealable container at  $23 \pm 2$  °C for 15 days. After conditioning, the side surface of each specimen was sealed with an epoxy resin adhesive, while one end of specimen which was not exposed to water was sealed with a loosely attached plastic sheet. Finally, the other end of each specimen was immersed in water with a water level of around 2 mm and the mass of the specimen at each specified testing time was recorded. According to the relationship between the time and the absorption ( $I$ ), which is the change in mass divided by the product of the cross-sectional area of the specimen and the density of water, the rate of water absorption can be determined. The initial and secondary rate of water absorption are defined as the slope of the line that is the best fit to  $I$  against the square root of time ( $s^{1/2}$ ) using all the points from 1 min to 6 h and 1 day to 7 days, respectively.

#### 2.4.6. Measurement of chloride penetration resistance

The chloride penetration resistance of concrete was determined according to the standard ASTM C1202-19 by using the same samples that used in the measurement of rate of water absorption. First, the epoxy side-sealed samples were water saturated with the vacuum-saturation procedure. They were then placed in applied voltage cells as described in the standard. One side of the test cell was filled with a 3% NaCl solution while another side was filled with 0.3 N NaOH solution. Next, the cells were connected to a data logger and a 60-volt potential difference was applied for 6 h. The charge passed was recorded every minute. The total charge passed in coulombs during 6 h was used to reflect the chloride penetration resistance. The test was carried out on three concrete specimens for each mixture at the age of 4 months.

#### 2.4.7. Measurement of microhardness

For the micro-hardness testing, two samples with dimension of around 20 × 20 × 15 mm were cut from a Φ100 × 200 mm cylinder at the age of 28 days from each group of concrete. Then, the samples were immersed in absolute ethyl alcohol for 24 h to stop the hydration of cement. Next, these samples were oven dried at 60 °C for 24 h and then impregnated in an epoxy resin in a Φ30 × 30 mm cylindrical rubber mould. After that, one surface of each sample was ground and polished by a polishing equipment (Buehler AutoMet 250) with grits of P180, P400, P1200 and MetaDi supreme diamond of 9 μm, 3 μm, 0.5 μm successively. Finally, these samples were cleaned, dried and stored in a vacuum chamber before further testing.

A digital Vickers micro-hardness tester (HVX-1000A, China) was used to measure the microhardness of the old mortar of RA and the new mortar near the interface. The testing loading was controlled as 10g. A typical indentation area near the interface is shown in Fig. 3. For each type of concrete mixture, the microhardness of at least four zones near the interface within the two samples was tested randomly. The method for selecting the indentation points are presented in Fig. 4. For the old mortar, the microhardness test was conducted at the distance of 20 μm from the exterior surface of RA. For the new mortar, the measured

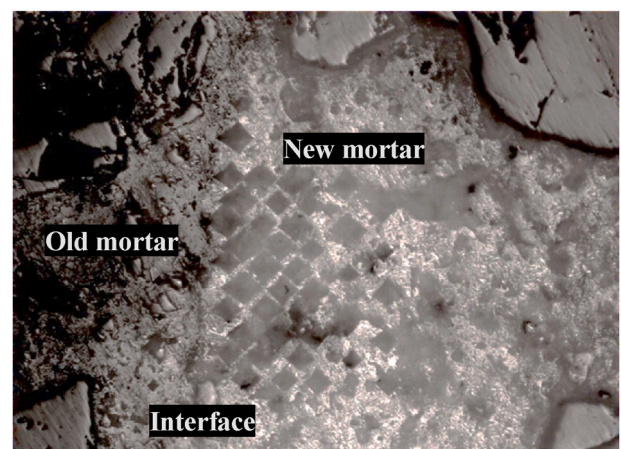


Fig. 3. A typical indentation area near the interface.

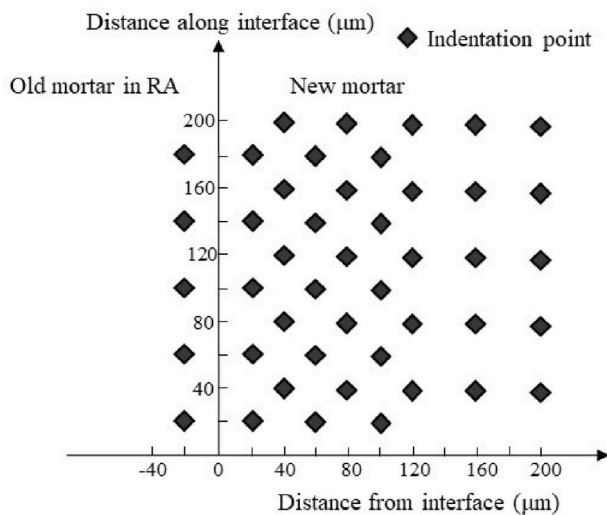


Fig. 4. Method for selecting the indentation points.

distance was from 20 μm to 200 μm from the interface. Five measurements were conducted at each distance with an interval of 40 μm.

### 3. Testing results and discussion

#### 3.1. Slump values of fresh concrete

The slump values of the eight groups of concrete are shown in Fig. 5. It can be seen that the slump values of different types of RACs had no significant difference except that RAC-2 and RAC-3 showed slightly higher slumps. It may be because after using the NS pre-spraying plus air-drying method, a silica gel layer was formed on the surface of RA, which decreases the rate of water absorption of RA, resulting in higher water contents in the new mortar when measuring slump. However, with further increasing the dosage of NS suspension, the increased number of NS particles would adsorb part of water in the new mortar, which might offset the effect of the silica gel layer. It indicates that the surface treatment of RA with NS by pre-spraying or pre-soaking has no obvious influence on the workability of concrete. Compared with the common method of pre-mixing NS with water and then the dry concrete mixture, which caused reduction of workability of concrete [34] due to the large surface area of nano-particles, the NS pre-spraying and pre-soaking treatments of RA had less influence on workability. In addition, it was observed that the slump values of RACs were slightly lower than that of NAC, which might be due to the higher water absorption value of the RA.

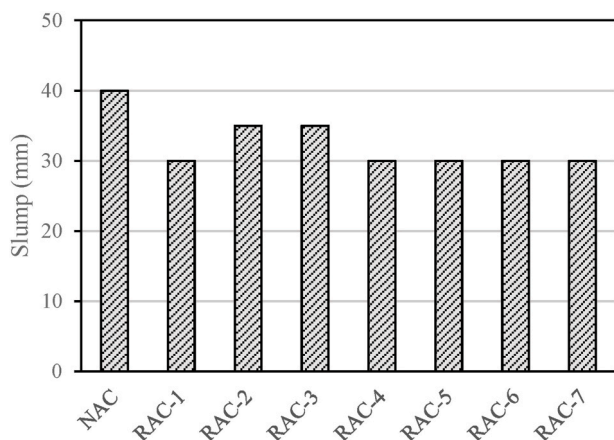


Fig. 5. Slump values of the fresh NAC and RACs.

#### 3.2. Compressive strength of hardened concrete

The compressive strength of the eight groups of concrete at age of 28 days are shown in Fig. 6. The compressive strength of NAC was 14.8% higher than that of RAC prepared with untreated RA (RAC-1). For the RAC-2, RAC-3 and RAC-4, which were treated by pre-spraying plus air-drying with N/A ratios of 1%, 3% and 5%, the compressive strengths were increased about 9.5%, 11.2%, 6.1%, respectively. It indicates that the compressive strength of RAC first increased and then decreased with the increase of the NS suspension dosage. Luo et al. [35] reported that there was an optimum NS dosage contributing to highest improvement in the compressive strength of RAC.

The compressive strength of RAC-5, which was treated by pre-spraying NS-2 with N/A ratio of 3%, increased by 13.9% when compared with RAC-1, and the increased magnitude was higher than that of RAC-3. This implies that the improvement could be more significant when the larger size of NS was used for pre-spraying. It may be because most of the pores in RA are below 100 nm in size [2], more NS particles were able to penetrate into the RA after spraying the smaller NS-1 on the surface of RA. In contrast, more NS particles remained on the surface of RA for the larger NS-2, leading to more obvious improvement of the interfacial zone.

Comparing the results of different NS treatment methods in Fig. 6, it can be found that the method of pre-spraying without air-drying attained the highest improvement of compressive strength, followed by the method of pre-spraying plus air-drying and the lowest was the method of pre-soaking plus air-drying.

#### 3.3. Elastic modulus of hardened concrete

The elastic modulus values of the eight groups of concrete are shown in Fig. 7. The elastic modulus of NAC was 21.2% higher than that of RAC without treatment. The difference in elastic modulus was larger than that of compressive strength. That means the elastic modulus of concrete was more sensitive to the porous old mortar adhered on RA than that of the compressive strength. When compared with RAC-1, the increasing rates of the elastic modulus of RAC-2, RAC-3, RAC-4, RAC-5, RAC-6 and RAC-7 were -5.1%, 1.2%, -0.1%, 6.2%, 3.9% and 3.9%, respectively. It indicates that the studied three NS treatment methods had no obvious influence on the elastic modulus of RAC. This phenomenon is similar to the treatment method of pre-mixing NS in concrete as reported by Mukharjee and Barai [36].

#### 3.4. Rate of water absorption

The rate of water absorption due to capillary force of the unsaturated concrete is an important index of concrete durability. The initial and

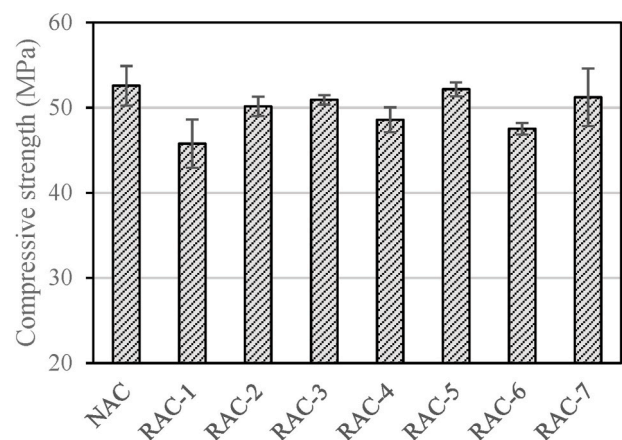


Fig. 6. Compressive strength of NAC and RACs.

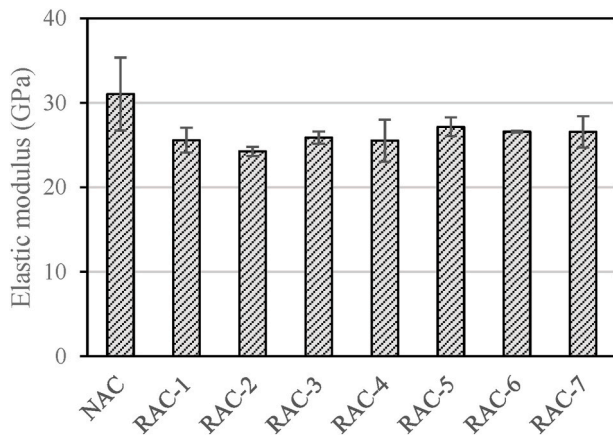


Fig. 7. Elastic modulus of NAC and RACs.

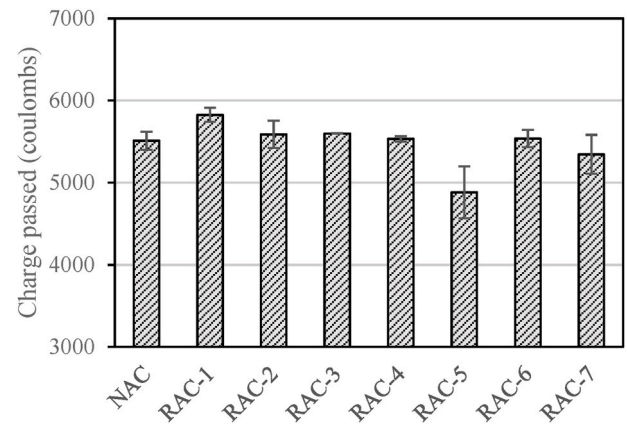


Fig. 9. Chloride penetration resistance of NAC and RAC.

secondary rates of water absorption of the 8 groups of concrete are shown in Fig. 8. It is found that the initial and secondary rates of water absorption of NAC were 37.0% and 31.3% respectively lower than that of RAC prepared with the untreated RA (RAC-1). However, the initial and secondary rates of water absorption of RAC could be reduced significantly by using the three NS treatments methods. With the dosage of the pre-sprayed NS increasing, the initial and secondary rates of water absorption of RAC did not show a clear increasing or decreasing tendency. When incorporating RA treated by pre-spraying larger size of NS, the initial and secondary water absorption rates of the correspond RAC (RAC-5) were reduced by 35.9% and 38.4% respectively, which were even comparable to that of NAC. When compared with different NS treatment methods, using the method of pre-spraying without air-drying had a lower water absorption rate than using the methods of pre-soaking plus air-drying and pre-spraying plus air-drying.

3.5. Chloride penetration resistance

The charge passed is a parameter to reflect the chloride penetration resistance of concrete, which is another important index of concrete durability. Higher charge passed means lower chloride penetration resistance. The charge passed values of the 8 groups of concrete are shown in Fig. 9. The charge passed value of RAC-1 which was prepared with the untreated RA was higher than that of NAC, while the charge passed values of RACs using the NS-treated RAs were reduced significantly. When using RA treated by pre-spraying different dosages of NS suspension, the charge passed values of the corresponding RACs did not show a significant change. When RA was treated by pre-spraying the larger size of NS, the charge passed value of the corresponding RAC

(RAC-5) showed a reduction of 16.2%, which was even lower than that of NAC. In addition, the method of pre-spraying without air-drying caused a larger reduction in charge passed compared to the other two methods.

3.6. Microhardness

The microhardness of the old mortar and the new mortar near the interface in the 8 groups of concrete are shown in Fig. 10. It could be found the microhardness of the new mortar near the interface in RAC-1 prepared with the untreated RA was lower than that of NAC. However, after RA was treated by NS suspension, the microhardness of the new mortar near the interface was generally improved although some variations were found. Both the heterogeneity of the material and NS treatment might be responsible for the large variation of the microhardness results. On one hand, both the RA and the new mortar which were consisted of cement paste and sand/aggregates were inhomogeneous materials. Especially for the surface layer of RA, part of them was carbonated while some others were not, which can be verified by spraying Phenolphthalein solution on RA, as shown in Fig. 11. The pink color means it was not carbonated. The varying material characteristics probably affected the microhardness results of the old mortar and new mortar at different zones. On the other hand, from Fig. 10, the variation of microhardness at four different areas seemed to be larger after NS treatments. It may be because the number of NS particles on the surface of RA varied at different zones although the spraying process was controlled as uniformly as possible, leading to different enhancement levels. In addition, Fig. 10 shows that the microhardness of the old mortar was higher than that of the new mortar near the interface for all types of RACs.

The average microhardness values of the old mortar at the surface layer of RA in different types of RACs are shown in Fig. 12. It shows that the average microhardness of the old mortar at the surface layer of RA was enhanced after using the NS treatments. Moreover, the enhancement was higher with the larger dosage of NS, using the smaller size NS and by using the method of pre-spraying plus air-drying. That is because the NS particles penetrated into the near-surface layer of RA [28], filled the pores and reacted with the Ca(OH)<sub>2</sub> to form additional C-S-H. Comparatively, it was more difficult for the larger size (100 nm) of NS to penetrate into RA, leading to a lower enhancement in microhardness of old mortar. With the use of the method of pre-spraying plus air-drying, more NS particles were reacted, leading to a higher enhancement of the RA.

The average microhardness values of the new mortar near the interface in NAC and different types of RACs are shown in Fig. 13. It shows that the average microhardness of the new mortar near the interface in RAC with the untreated RA (RAC-1) was significantly lower than that of NAC because the RA absorbed more water and caused a

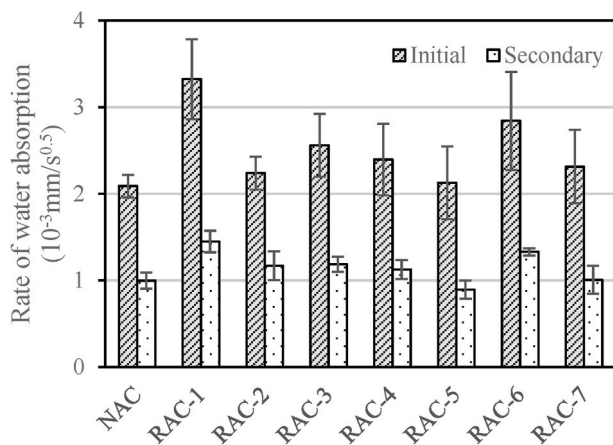


Fig. 8. Rate of water absorption of NAC and RACs.

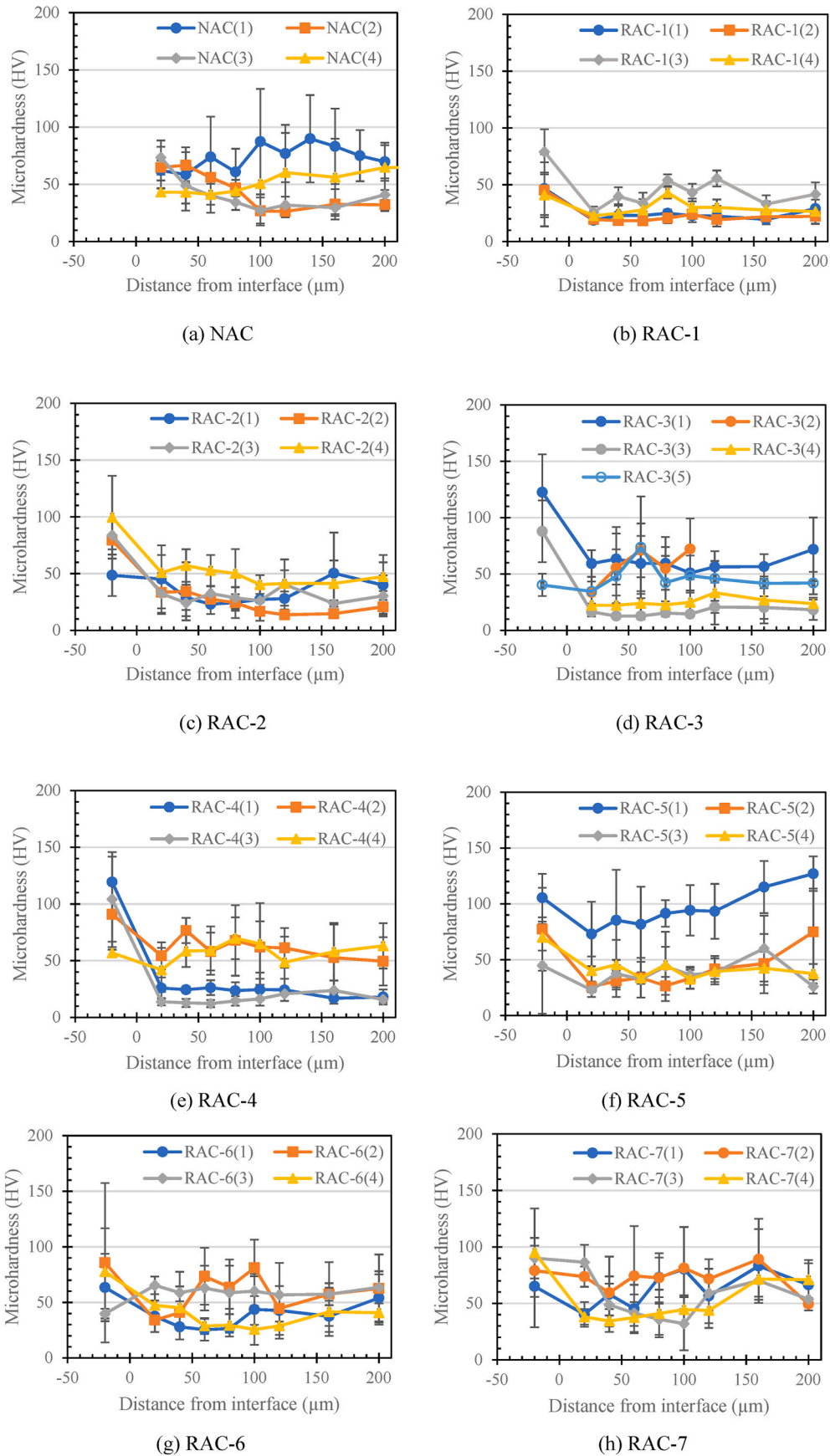


Fig. 10. Microhardness of the old and new mortar near the interface.



Fig. 11. Image of RA after spraying Phenolphthalein solution.

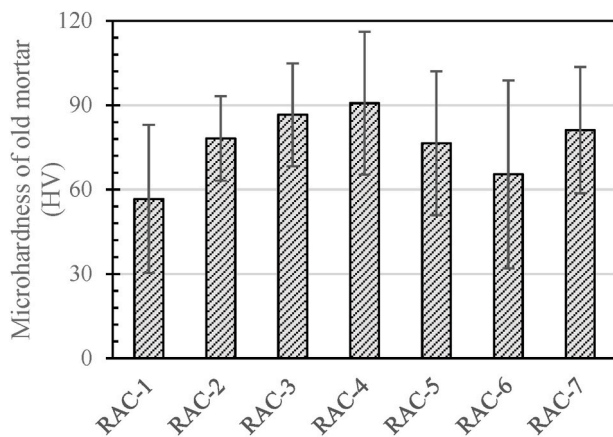


Fig. 12. Microhardness of the old mortar at the surface layer of RA.

higher localized W/C ratio of near the interface [2]. In contrast, the average microhardness of the new mortar near the interface was enhanced after using the NS treatments because NS particles on the surface of RA promoted the hydration of cement near the interface. Referring to the use of different dosages of NS suspension, it had the highest improvement when the N/A ratio was 3%. When using the larger size (100 nm) NS, the average microhardness of the new mortar near the interface was further improved and it was even close to that of NAC. That is because more NS particles with larger size left on the surface of RA and was incorporated into the new mortar. When comparing the three NS treatment methods, the method of pre-spraying without air-drying caused a higher improvement in the microhardness of the new mortar near the interface.

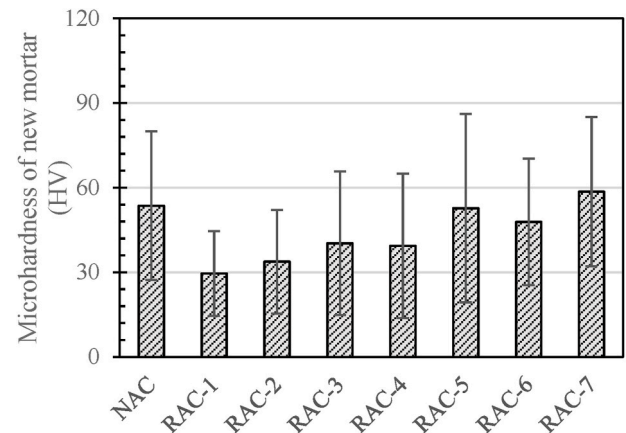


Fig. 13. Microhardness of the new mortar near the interface.

#### 4. Discussion

The microstructures of the untreated RA and the RA treated by NS pre-spraying plus air-drying method by scanning electron microscopy (SEM) are shown in Fig. 14. It shows that the surface of untreated RA was porous and the main phase composition was C-S-H, as shown in Fig. 14(a). After using the NS pre-spraying plus air-drying treatment method, the surface of RA was covered by a layer of silica gel of which the thickness was about 10  $\mu\text{m}$ , and there were a lot of agglomerated NS particles attached on the surface of silica gel layer, as shown in Fig. 14(b) and (c).

Based on the microstructures of RAs and the microhardness results of RACs, the improvement mechanism of the NS pre-spraying plus air-drying method is discussed below. The schematics of RACs before and after using the NS pre-spraying plus air-drying method are shown in Fig. 15. After spraying NS suspension on the surface of RA, part of the NS suspension penetrated into the porous surface layer of RA, of which the thickness was about 200  $\mu\text{m}$  [28]. These NS particles densified the microstructure of the surface layer of RA because of the pozzolanic reaction between NS particles and  $\text{Ca}(\text{OH})_2$  in RA and the filling effect of NS particles [28,40]. At the same time, a layer of silica gel was produced on the surface of RA by dehydration of the attached NS suspension, while some agglomerated NS particles remained on the surface of the silica gel layer. These NS particles were able to react with the cement in the new mortar, promoting the hydration of the cement because of pozzolanic and nucleation effects to produce additional C-S-H [41]. Moreover, the silica gel layer was able to absorb water from the new mortar, leading to a lower w/c of new mortar near the interface. As a result, the new mortar near the interface could be also enhanced. These microscale effects could cause the increase in microhardness of the surface layer of RA and the new mortar near the interface.

It was also observed that the microstructure enhancement effects of the new mortar near the interface using the different treatment methods and NS dosages correlated well with those on compressive strength and durability properties. But the enhancement effects on the old mortar at the surface layer of RA were varied. This demonstrates that the enhancement of the new mortar near the interface played a more important role in improving the compressive strength and durability of RAC when using the NS treatment methods.

In addition, the elastic modulus of RAC showed no significant changes after using the NS treatments. That is because the NS particles only penetrated into the near-surface layer of RA and enhanced the properties of the near-surface layer, while the NS particles that remained on the surface of RA only improved the properties of the new mortar near the interface. This implies that the volume of the enhanced old and new mortar was only a small percentage of the total volume of new and old mortar in RAC. It was reported that the elastic modulus of concrete

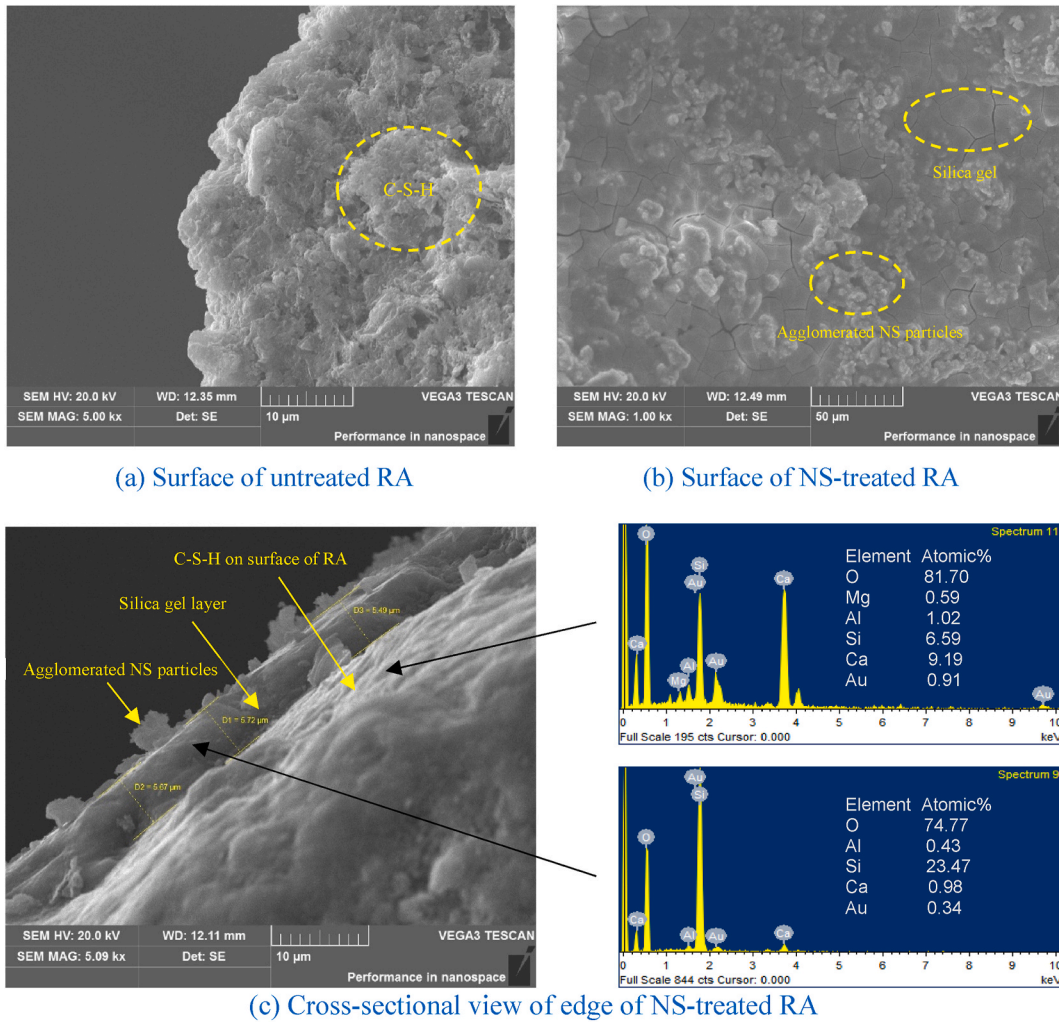


Fig. 14. SEM microstructures of untreated RA and treated RA by NS spraying plus air-drying method.

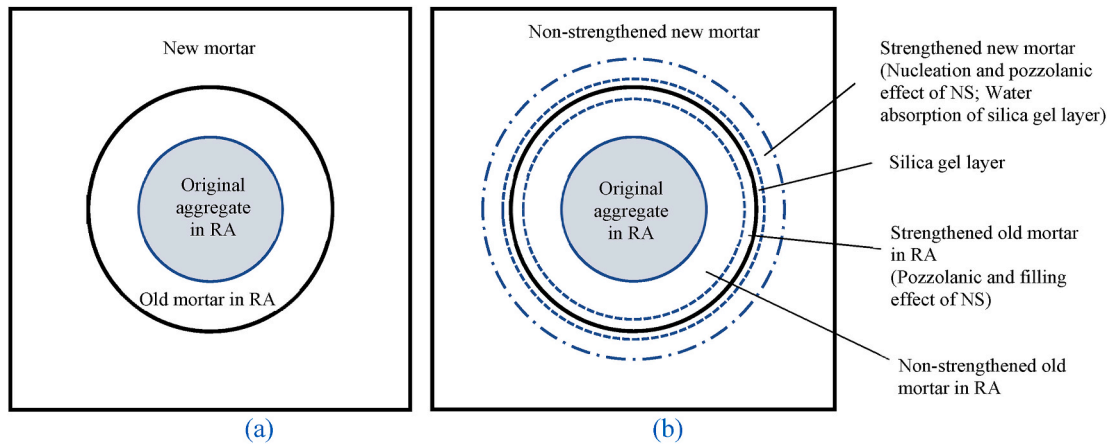


Fig. 15. Schematics of RACs before (a) and after (b) using the NS pre-spraying plus air-drying method.

could be predicted with a series model or a parallel model [42], which is shown as follows.

Series

$$\text{model: } \frac{1}{E} = \sum_{i=1}^n \frac{V_i}{E_i} \quad (2)$$

Parallel

$$\text{model: } E = \sum_{i=1}^n E_i \cdot V_i \quad (3)$$

Where  $E_i$  and  $V_i$  represent the Young's modulus and the volume fraction of concrete constituents (e.g., mortar, coarse aggregate, etc.),  $n$  is the number of constituents. The elastic modulus of concrete is governed by

the elastic modulus of the constituents and their volume fractions. When using the three NS treatment methods, although the surface layer of RA and the new mortar near the interface were enhanced, their volume fractions were quite small. As a result, the elastic modulus of RAC did not show a significant change.

## 5. Conclusions

In this study, three types of nano-silica (NS) treatment methods of recycled aggregates (RA) namely pre-spraying plus air-drying, pre-spraying without air-drying and pre-soaking plus air-drying were adopted to evaluate their impacts on the mechanical properties and durability of recycled aggregate concrete (RAC). Based on the tests results and discussion, the main findings can be summarized:

- (1) No obvious slump reduction was observed in RAC after using the three NS treatment methods, which was different from the traditional method of pre-mixing the NS particles with the mixing water that triggers a reduction in workability.
- (2) The compressive strength, rate of water absorption and chloride penetration resistance of RAC were improved for all three NS treatment methods assessed. However, these NS treatment methods had no significant influence on the elastic modulus of RAC.
- (3) An optimum dosage of 3% NS suspension by mass of RA is recommended for the NS pre-spraying plus air-drying treatment method. Pre-spraying NS suspension with a larger particle size on RA yielded a higher effectiveness in improving the mechanical and durability of RAC. The method of pre-spraying without air-drying was demonstrated to be superior to the other two methods.
- (4) Both the microhardness of the old mortar at the surface layer of RA, and the new mortar near the interface of RAC were improved after using the three NS treatment methods. The microstructure enhancement of the new mortar near the interface played a more important role for the enhancement of the performance of RAC.

## Declaration of competing interest

The authors declare that they have no known competing financial interests or personal relationships that could have appeared to influence the work reported in this paper.

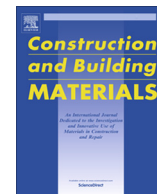
## Acknowledgements

The authors wish to thank the Hong Kong Construction Industry Council (CIC) for financial support.

## References

- [1] X. Ke, D. Xu, M. Cai, Experimental and numerical study on the eccentric compressive performance of RAC-encased RACFST composite columns, *Eng. Struct.* 224 (2020) 111227.
- [2] C.S. Poon, Z.H. Shui, L. Lam, Effect of microstructure of ITZ on compressive strength of concrete prepared with recycled aggregates, *Construct. Build. Mater.* 18 (6) (2004) 461–468.
- [3] A. Akbarnezhad, K.C.G. Ong, M.H. Zhang, C.T. Tam, T.W.J. Foo, Microwave assisted beneficiation of recycled concrete aggregates, *Construct. Build. Mater.* 25 (8) (2011) 3469–3479.
- [4] D.X. Xuan, A.A.A. Molenaar, L.J. M. Houben, Shrinkage cracking of cement treated demolition waste as a road base, *Mater. Struct.* 49 (2016) 631–640.
- [5] L. Li, J.Z. Xiao, D.X. Xuan, C.S. Poon, Effect of carbonation of modeled recycled coarse aggregate on the mechanical properties of modeled recycled aggregate concrete, *Cement Concr. Compos.* 89 (2018) 169–180.
- [6] J.Z. Xiao, J.B. Li, Ch Zhang, Mechanical properties of recycled aggregate concrete under uniaxial loading, *Cement Concr. Res.* 35 (6) (2005) 1187–1194.
- [7] D.X. Xuan, A.A.A. Molenaar, L.J.M. Houben, Compressive and indirect tensile strengths of cement-treated mix granulates with recycled masonry and concrete aggregates, *J. Mater. Civ. Eng.* 24 (5) (2012) 577–585.
- [8] J.S. Ryu, An experimental study on the effect of recycled aggregate on concrete properties, *Mag. Concr. Res.* 54 (1) (2002) 7–12.
- [9] I.B. Topçu, S. Sengel, Properties of concretes produced with waste concrete aggregate, *Cement Concr. Res.* 34 (8) (2004) 1307–1312.
- [10] M. Etxeberria, E. Vázquez, A. Mari, M. Barra, Influence of amount of recycled coarse aggregates and production process on properties of recycled aggregate concrete, *Cement Concr. Res.* 37 (5) (2007) 735–742.
- [11] D.X. Xuan, B.J. Zhan, C.S. Poon, Assessment of mechanical properties of concrete incorporating carbonated recycled concrete aggregates, *Cement Concr. Compos.* 65 (2016) 67–74.
- [12] M. Quattrone, S.C. Angulo, V.M. John, Energy and CO<sub>2</sub> from high performance recycled aggregate production, *Resour. Conserv. Recycl.* 90 (2014) 21–33.
- [13] S. Nagataki, A. Gokce, T. Saeki, M. Hisada, Assessment of recycling process induced damage sensitivity of recycled concrete aggregates, *Cement Concr. Res.* 34 (6) (2004) 965–971.
- [14] K. Bru, S. Touze, F. Bourgeois, N. Lippiatt, Y. Menard, Assessment of a microwave-assisted recycling process for the recovery of high-quality aggregates from concrete waste, *Int. J. Miner. Process.* 126 (2014) 90–98.
- [15] A. Akbarnezhad, K.C.G. Ong, M.H. Zhang, C.T. Tam, T.W.J. Foo, Microwave assisted beneficiation of recycled concrete aggregates, *Construct. Build. Mater.* 25 (8) (2011) 3469–3479.
- [16] A. Katz, Treatments for the improvement of recycled aggregate, *J. Mater. Civ. Eng.* 16 (6) (2004) 597–603.
- [17] V.W.Y. Tam, C.M. Tam, K.N. Le, Removal of cement mortar remains from recycled aggregate using pre-soaking approaches, *Resour. Conserv. Recycl.* 50 (1) (2007) 82–101.
- [18] B.J. Zhan, C.S. Poon, Q. Liu, S.C. Kou, C.J. Shi, Experimental study on CO<sub>2</sub> curing for enhancement of recycled aggregate properties, *Construct. Build. Mater.* 67 (2014) 3–7.
- [19] J.K. Zhang, C.J. Shi, Y.K. Li, X.Y. Pan, C.S. Poon, Performance enhancement of recycled concrete aggregates through carbonation, *J. Mater. Civ. Eng.* 27 (11) (2015), 04015029.
- [20] X.L. Fang, D.X. Xuan, C.S. Poon, Empirical modelling of CO<sub>2</sub> uptake by recycled concrete aggregates under accelerated carbonation conditions, *Mater. Struct.* 50 (2017) 200.
- [21] L. Li, C.S. Poon, J.Z. Xiao, D.X. Xuan, Effect of carbonated recycled coarse aggregate on the dynamic compressive behavior of recycled aggregate concrete, *Construct. Build. Mater.* 151 (2017) 52–62.
- [22] A.M. Grabiec, J. Klama, D. Zawal, D. Krupa, Modification of recycled concrete aggregate by calcium carbonate bio deposition, *Construct. Build. Mater.* 34 (2012) 145–150.
- [23] E. Güneş, M. Gesoğlu, Z. Algin, H. Yazıcı, Effect of surface treatment methods on the properties of self-compacting concrete with recycled aggregates, *Construct. Build. Mater.* 64 (2014) 172–183.
- [24] S.C. Kou, C.S. Poon, Properties of concrete prepared with PVA-impregnated recycled concrete aggregates, *Cement Concr. Compos.* 32 (8) (2010) 649–654.
- [25] A. Mansur, D. Santos, H. Mansur, A microstructural approach to adherence mechanism of poly (vinyl alcohol) modified cement systems to ceramic tiles, *Cement Concr. Res.* 37 (2) (2007) 270–282.
- [26] J. Li, H. Xiao, Y. Zhou, Influence of coating recycled aggregate surface with pozzolanic powder on properties of recycled aggregate concrete, *Construct. Build. Mater.* 23 (3) (2009) 1287–1291.
- [27] H. Zhang, Y. Zhao, T. Meng T, S.P. Shah, Surface treatment on recycled coarse aggregates with nanomaterials, *J. Mater. Civ. Eng.* 28 (2) (2015), 04015094.
- [28] W. Zeng, Y. Zhao, H. Zheng, C.S. Poon, Improvement in corrosion resistance of recycled aggregate concrete by nano silica suspension modification on recycled aggregates, *Cement Concr. Compos.* 106 (2020) 103476.
- [29] C. Shi, Y. Li, J. Zhang, W. Li, L. Chong, Z. Xie, Performance enhancement of recycled concrete aggregate – a review, *J. Clean. Prod.* 112 (2016) 466–472.
- [30] V.W.Y. Tam, X.F. Gao, C.M. Tam, Microstructural analysis of recycled aggregate concrete produced from two-stage mixing approach, *Cement Concr. Res.* 35 (6) (2005) 1195–1203.
- [31] W. Li, C. Long, V.W.Y. Tam, C.S. Poon, W.H. Duan, Effects of nano-particles on failure process and microstructural properties of recycled aggregate concrete, *Construct. Build. Mater.* 142 (2017) 42–50.
- [32] S.C. Kou, C.S. Poon, Long-term mechanical and durability properties of recycle aggregate concrete prepared with the incorporation of fly ash, *Cement Concr. Compos.* 37 (2013) 12–19.
- [33] V. Corinaldesi, G. Moriconi, Influence of mineral additions on the performance of 100% recycled aggregate concrete, *Construct. Build. Mater.* 23 (2009) 2869–2876.
- [34] B.B. Mukharjee, S.V. Barai, Influence of Nano-Silica on the properties of recycled aggregate concrete, *Construct. Build. Mater.* 55 (2014) 29–37.
- [35] Z. Luo, W. Li, V.W.Y. Tam, J. Xiao, S.P. Shah, Current progress on nanotechnology application in recycled aggregate concrete, *J. Sustain. Cement Base Mater.* 8 (2) (2019) 79–96.
- [36] B.B. Mukharjee, S.V. Barai, Development of construction materials using nano-silica and aggregates recycled from construction and demolition waste, *Waste Manag. Res.* 33 (6) (2015) 515–523.
- [37] K.H. Younis, S.M. Mustafa, Feasibility of using nanoparticles of SiO<sub>2</sub> to improve the performance of recycled aggregate concrete, *Adv. Mater.Sci. Eng.* (2018) 1–11, 2018.
- [38] F. Shaikh, V. Chavda, N. Minhaj, H.S. Arel, Effect of mixing methods of nano silica on properties of recycled aggregate concrete, *Struct. Concr.* (19) (2018) 387–399.
- [39] S. Harsh, Z. Shen, D. Darwin, Strain-rate sensitive behavior of cement past and mortar in compression, *ACI Mater. J.* 87 (5) (1990) 508–516.

- [40] J.-X. Lu, C.S. Poon, Improvement of early-age properties for glass-cement mortar by adding nanosilica, *Cement Concr. Compos.* 89 (2018) 18–30.
- [41] L.P. Singh, S.R. Karade, S.K. Bhattacharyya, M.M. Yousuf, S. Ahalawat, Beneficial role of nanosilica in cement based materials – a review, *Construct. Build. Mater.* 47 (2013) 1069–1077.
- [42] I. Yoshitake, F. Rajabipour, Y. Mimura, A. Scanlon A, Prediction method of tensile young's modulus of concrete at early age, *Adv. Civ. Eng.* (2012) 1–10.



# Effect of natural and recycled aggregate packing on properties of concrete blocks



S.H. Chu, Chi Sun Poon\*, C.S. Lam, L. Li

Department of Civil and Environmental Engineering, The Hong Kong Polytechnic University, Hong Kong

## HIGHLIGHTS

- Particle packing was identified as the key factor affecting concrete block performance.
- Packing optimization yielded 31% increase in packing and 156% increase in strength.
- The strength of recycled aggregate concrete is 94% of that of natural aggregate concrete.
- Empirical prediction equations for properties of concrete paving blocks were developed.

## ARTICLE INFO

### Article history:

Received 27 October 2020  
Received in revised form 1 January 2021  
Accepted 3 January 2021  
Available online 29 January 2021

### Keywords:

Recycled aggregate  
Concrete paving blocks  
Skid and abrasion  
Particle packing  
Strength

## ABSTRACT

Recycled aggregate (RA) could be re-utilized in concrete paving blocks. However, the use of RA in concrete might lead to inferior performance, which constitutes a major barrier in the wider application of recycled aggregate concrete (RAC). To tackle this issue, one promising solution might be the tailoring of aggregate packing without increasing the cement content, carbon footprint and cost. In this study, an experimental program was carried out to systematically investigate the effect of packing density on the properties of concrete blocks. Tests results showed that appropriate proportioning of RA increased the packing density and thus the compressive strength to approach that of natural aggregate (NA) mixtures. Such increased packing density was conducive to the performance of concrete blocks. After packing optimization, RAC exhibited comparable strength to that of NA concrete. Lastly, prediction equations were derived for various performance attributes of concrete paving blocks based on particle packing.

© 2021 Elsevier Ltd. All rights reserved.

## 1. Introduction

A huge amount of construction and demolition (C&D) waste is being generated in the process of the rapid urbanization worldwide [1,2]. In China, a total of approximately 2 billion tons of C&D waste is produced annually and largely disposed of in landfills, causing serious environmental problems [3,4]. Meanwhile, the excessive exploitation of resources during urbanization process has exacerbated the shortage of materials, such as sand and aggregate. As such, the key to tackle the above problems might lie in the reuse of C&D waste, particularly the portion that could be processed into recycled aggregate (RA) for concrete production [5–8]. In fact, abundant pioneering works exist in the literature that explored the feasibility of producing recycled aggregate concrete (RCA) [9–13]. Quite often, the use of RA as partial or full replacement of natural aggregate (NA) might bring about the prob-

lems of lower strength and lower dimensional stability compared to the use of NA in concrete [14,15].

Various attempts have been made to alleviate such negative influences of RA on concrete strength performance, such as decreasing the aggregate to cement (A/C) ratio and increasing the cement content [10,16]. Unfortunately, these attempts are prone to elevate the production cost and decrease the sustainability. A better method might be the tailoring of aggregate from the perspective of particle packing [17–20]. After decades of research, a consensus has been reached that the aggregate packing would exert significant influences on concrete performance [21–23]. In other words, a better aggregate packing allows the minimization of the volume of voids to be filled by paste [23]. Subsequently, a large amount of cement could be saved with the workability and strength properties little sacrificed or even improved [24,25]. Such design philosophy is believed to be also applicable to concrete paving blocks made with RA.

Pioneering works on the investigation of beneficial effects of aggregate packing on concrete properties have been abundant in the literature [26–29]. For instance, Fuller and Thompson [26]

\* Corresponding author.

E-mail addresses: [shchu@polyu.hk](mailto:shchu@polyu.hk) (S.H. Chu), [cecspoon@polyu.edu.hk](mailto:cecspoon@polyu.edu.hk) (C.S. Poon), [zinc\\_lam@cohl.com](mailto:zinc_lam@cohl.com) (C.S. Lam), [li.long@connect.polyu.hk](mailto:li.long@connect.polyu.hk) (L. Li).

studied the influences of graded particles on concrete strength and density and proposed an empirical equation for calculating the optimum grading curve of a batch of aggregates exhibiting the highest packing density:  $p = (\frac{d}{d_{max}})^q$ , in which  $p$  denotes the percentage of aggregate passing each sieve,  $d$  denotes the sieve size (aggregate size),  $d_{max}$  denotes the maximum aggregate size, and  $q$  is an empirical parameter.

Lee [27] studied the factors affecting the packing density of aggregate and proposed a method for designing dense asphaltic compositions based on aggregate grading. Kronlof [28] investigated the role of very fine aggregate in improving the particle packing of the concrete mixture incorporating silica fume and concluded that the strength of concrete can be increased by improving the packing, with the explanation that the water/binder ratio could be decreased and the strength of the interfacial transition zone (ITZ) increased. However, Lee et al. [29] pointed out that the packing density decreased sharply when the amount of particles finer than 0.6 mm exceeded 50% and recommended a higher water to cement (W/C) ratio for concrete made with high fine contents to achieve desirable cohesiveness. Despite the valuable efforts, these studies failed to present a comprehensive design philosophy for RAC based on particle packing.

Recently, the evolution of the advanced computer technology has boosted the development of various models such as Aim's model, Toufar's model and compressive packing model (CPM) for estimating the packing density of aggregates [30,31]. For instance, Fu and Dekelbab [30] used a computer program to simulate a random aggregate packing with the assumption that the aggregates were spherical in shape and due consideration has been given to the kinematics and dynamic conditions. Concrete mixes were designed utilizing the packing results generated from the computer and it was demonstrated that computational simulation results agreed well with experimental tests. Kwan and Fung [31] developed a new wet packing method and applied it to measure the packing densities of blended fine aggregates and mortars under the wet condition, with or without superplasticizer added, and with or without compaction applied. Based on the test results, a packing model was proposed and good agreement was achieved between the measured packing densities and the predicted packing densities based on two existing packing models [32,33], for both blended fine aggregates and mortars. These previous works laid a solid foundation for the use of particle packing theory in concrete production.

Nonetheless, few studies can be found in the literature that deal with the performance improvement of concrete paving blocks made with RA based on the optimization of particle packing systematically and the adoption of packing optimization as a tool to increase the performance of concrete paving blocks made with RA has been even rarer. To fill such research gap, the concept of particle packing was introduced into RAC with the aim of improving the performance of concrete paving blocks made with RAC to a higher level. Overall, in the present work, the key innovations lie in: (a) introducing the progressive packing optimization method into RAC for enhanced performance without increasing the cost and carbon footprint; (b) identifying the key influencing factor of particle packing in concrete paving blocks made with both RA and NA; and (c) establishing quantitative relations between the packing density and various performance attributes.

## 2. Method to determine the optimum packing

### 2.1. Packing determination

The experimental packing density of the blended aggregates was determined using an improved method based on previous

studies [30]. Details are presented below: first, the aggregates were oven dried for 24 h and cooled down to room temperature before the packing measurement and sieve analysis; second, 3 kg of blended aggregates were prepared and poured into a steel cylinder mold with an internal diameter of 150 mm and a height of 260 mm; third, the cylinder was placed horizontally and agitated by a rolling action for 30 s to ensure a uniform particle distribution; fourth, the steel cylinder was fixed on a shaking table and a 10 kPa load was applied onto the mixture for a 2-minute vibration, during which the volume reduction of the aggregate mixture was recorded by the settlement in height; fifth, the above procedure was repeated until the differences between the three maximum settlements were less than 0.5 mm (at least 3 times). For clearer illustration, the elevation and top views of the setup are presented in Fig. 1. After the measurement, the experimental packing density, denoted as  $\phi_{max}$ , could be determined as per Eq. (1),

$$\phi_{max} = \frac{\sum \frac{M_i}{\rho_{di}}}{(H - T)\pi(\frac{D}{2})^2} \quad (1)$$

where  $H$  is the total internal height of the cylinder (260 mm),  $T$  is the height from the top of the aggregate mixture to the top of the cylinder (mm),  $D$  is the internal diameter of the cylinder (150 mm),  $\rho_{di}$  is the particle density of each aggregate ( $\text{kg}/\text{m}^3$ ), and  $M_i$  is the mass of each aggregate mixture (kg). It should be noted that the packing density  $\phi_{max}$  is dimensionless.

### 2.2. Packing optimization

In order to optimize the packing density of the mixture, the aggregates were sieved and classified into six classes (labelled as A, B, C, D, E and F) according to their size ranges (5–10 mm, 2.36–5 mm, 1.18–2.36 mm, 0.6–1.18 mm, 0.3–0.6 mm and 0–0.3 mm). The aggregates of size class from the coarsest to the finest were sequentially introduced into the mix. The detailed procedure for progressive packing optimization is illustrated in Fig. 2: first, aggregates A and B were incorporated into the concrete mix and the proportions of aggregates A and B were varied by increasing the aggregate B contents to until the highest packing density was determined; second, the immediate next finer class of aggregate, aggregate C, was incorporated to the dry mixture, followed by the determination of the optimum proportions of each aggregate class; third, such process was repeated until the aggregate F was incorporated.

The above packing optimization process of introducing finer particles to a given particle system is based on the assumption that the finer particles could fill the voids that could not be filled by the coarse aggregate particle. It also implies that the coarse particles are dominant in content for the given particle system. In fact, there might be a second scenario: when the fine particles are dominant in content in the particle system, the incorporation of coarse particles might also increase the packing density, though the increase in packing density is less obvious compared to first scenario of the coarse particles are dominant in content [33,34]. Among the above two scenarios, the first one was selected for the packing optimization process. This is because that the total surface area of the particles in a particle system dominated by fine particles would be dramatically increased even though the overall packing density is high. Then, it would increase the water demand or superplasticizer dosage for acquiring a certain workability or decrease the workability at a certain water content and superplasticizer dosage.

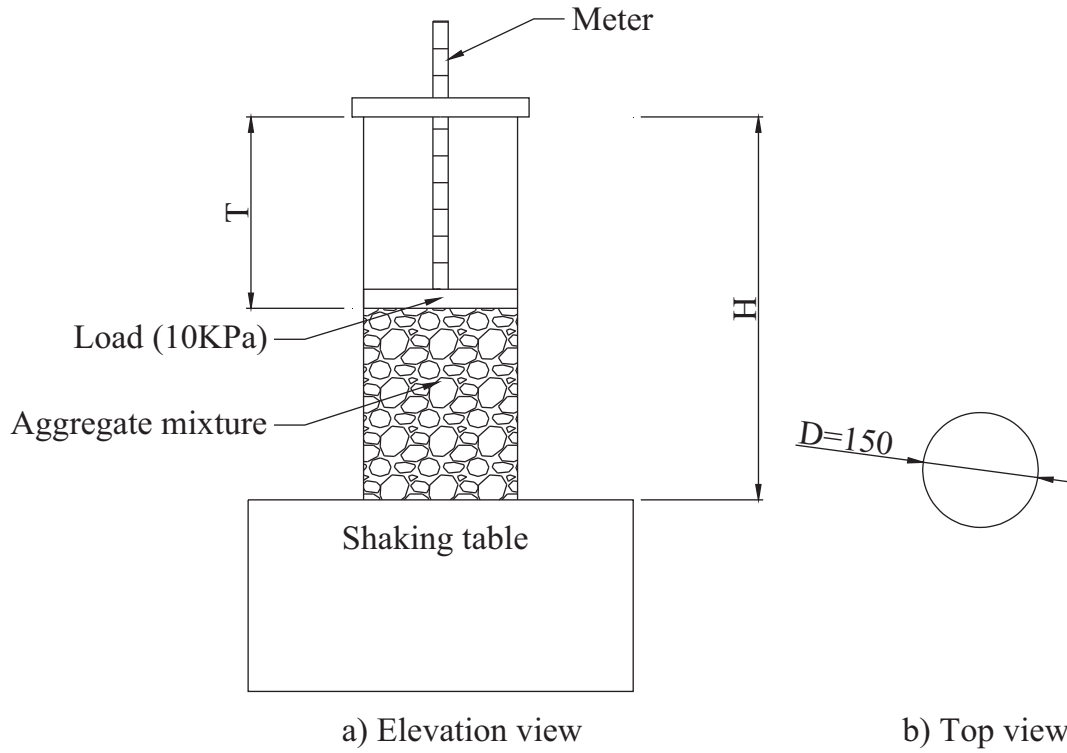


Fig. 1. Elevation and top views of the setup for packing density measurement.

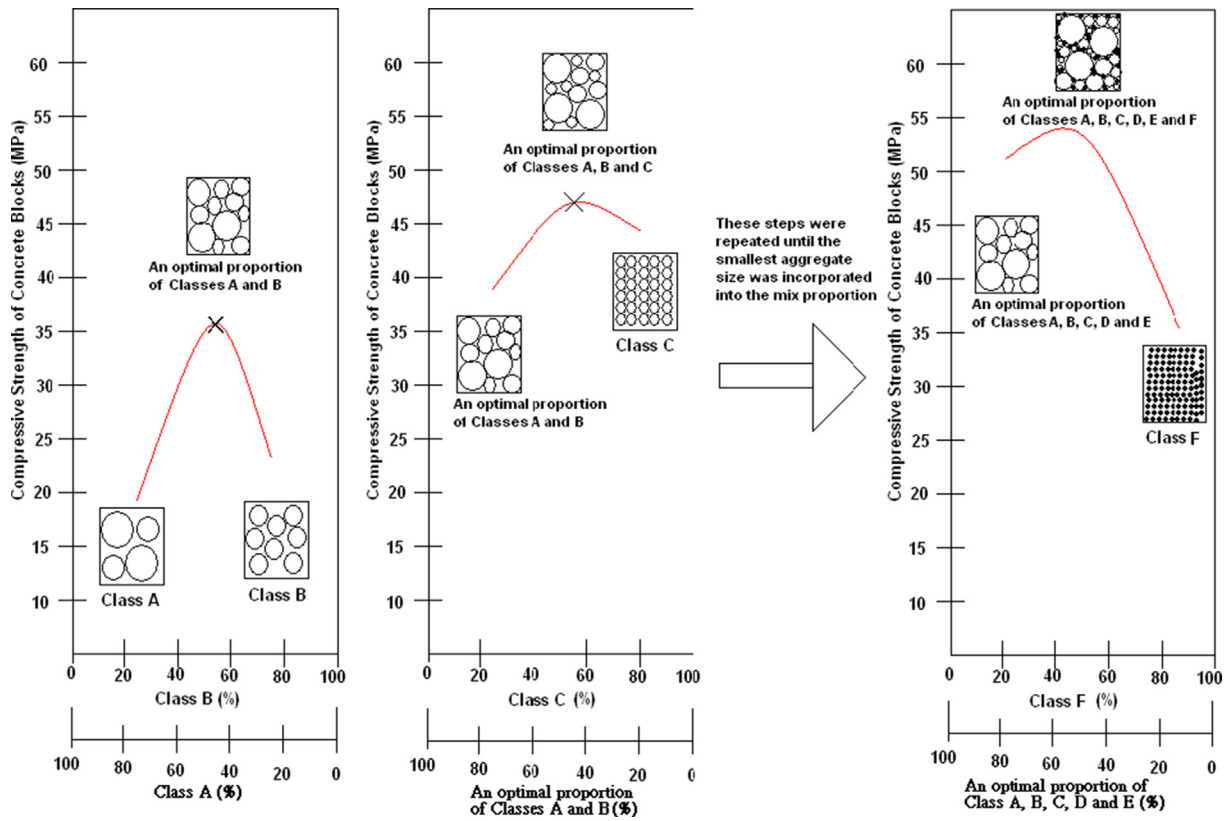


Fig. 2. Approach for progressive packing optimization.

### 3. Experimental program

#### 3.1. Materials

Type CEM I 52.5N ordinary Portland cement (OPC) complying with ASTM-C150 [35] was adopted in this study. The cement is commercially available in Hong Kong. Table 1 reports the properties of the cement. River sand aggregate (RSA) was used as the fine aggregate. The properties of RSA were tabulated in the second row of Table 2. Regarding the NA, crushed granite aggregates with maximum sizes of 5 mm and 10 mm were adopted and referred to as natural fine aggregate (NFA) and natural coarse aggregate (NCA), respectively. The physical properties of NA are shown in the third and fourth rows of the Table 2, respectively.

Regarding the RA, crushed concrete rubbles were obtained from a C&D waste recycling plant in Hong Kong. To be consistent, RA with maximum sizes of 5 mm and 10 mm were used and referred to as recycled fine aggregate (RFA) and recycled coarse aggregate (RCA), respectively. The physical properties of the recycled aggregates are reported in the last two rows of the Table 2, respectively. To determine the particle size distribution (PSD) curves of the RSA, NFA, NCA, RFA and FCA, sieve analysis was performed according to ASTM-C136. The measured PSD curves of RSA, NFA, NCA, RFA and FCA are presented in Fig. 3. As shown in the figure, the RSA has a median particle size of around 1.5 mm. The NFA and RFA have similar PSD curves with median particle sizes of around 1.8 mm and 1.6 mm, respectively. Likewise, the NCA and RCA have similar PSD curves with median particle sizes of around 7.5 mm and 8.0 mm, respectively.

#### 3.2. Experimental design

An experimental program, consisting of two phases, was carried out to evaluate the effect of aggregate packing and aggregate type on the properties of concrete paving blocks. More specifically, the optimization of aggregate packing and its influence on the properties of concrete paving blocks were investigated in Phase I. The influence of various combinations of coarse aggregate and fine

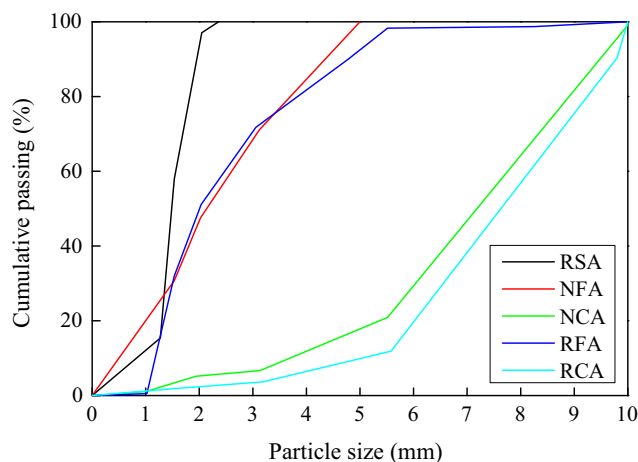


Fig. 3. PSD curves of RSA and aggregates.

aggregate on properties of concrete paving blocks were investigated in Phase II.

In Phase I, a total of 16 dry mixtures made with various sizes of RA were prepared. According to the procedure prescribed in Section 2.1, the packing densities of the aggregate mixtures were determined. As a comparison, the packing density of the quasi mono-sized aggregates, which were the aggregates A (5.0–10.0 mm), aggregate B (2.36–5.0 mm), aggregate C (1.18–2.36 mm), aggregate D (0.6–1.18 mm), aggregate E (0.3–0.6 mm) and aggregate F (0–0.3 mm) were also measured. The proportions of various sizes of RA are reported in Table 3. Then, the dry aggregate mixtures were utilized for producing concrete paving blocks at a fixed aggregate to cement (A/C) ratio of 5.00. A dry mix casting method was adopted which utilized concrete mixes with zero slump value and compaction was done by a compaction force immediately after casting [9]. This was to simulate the real production method in industry to allow immediate demoulding after casting and compaction to improve production efficiency. For easy identification, each mix was assigned a labelled in the form of i-j-X, where i-j denotes the mixture with blended aggregates from classes i to class j as mentioned in Section 2.2 and the X denotes the sample number (each number represents different aggregate proportioning) during the successive packing optimization process of adding the next class finer aggregate particles into the dry aggregate mixtures. For instance, A-F-1 denotes the mixture made with aggregate A (5.0–10.0 mm), aggregate B (2.36–5.0 mm), aggregate C (1.18–2.36 mm), aggregate D (0.6–1.18 mm), aggregate E (0.3–0.6 mm) and aggregate F (0–0.3 mm). A-F-2 denotes the mixture made with aggregate types same as A-F-1, but at different proportions of each type of aggregate (more amount of aggregate F).

In Phase II, concrete paving blocks were prepared with different types of aggregates, such as NFA, NCA, RCA and RSA. The volumet-

Table 1  
Properties of cement.

Composition/properties	Result
SiO <sub>2</sub> (%)	19.61
Fe <sub>2</sub> O <sub>3</sub> (%)	3.32
Al <sub>2</sub> O <sub>3</sub> (%)	7.33
CaO (%)	63.15
MgO (%)	2.54
SO <sub>3</sub> (%)	2.13
Loss on ignition (%)	2.97
Specific gravity	3.16
Specific surface area (cm <sup>2</sup> /g)	3520

Table 2  
Properties of aggregate.

Materials	Size range (mm)	Particle density (kg/m <sup>3</sup> )	Water absorption (%)	10% Fines value (crushing strength) (kN)
RSA	0–2.36	2620	1.0	–
NFA	0–5.0	2630	3.0	150
NCA	5.0–10.0	2650	1.2	157
RFA	0–5.0	2530	10.3	120
RCA	5.0–10.0	2550	3.0	120

**Table 3**  
Optimization of aggregate packing.

Mix no.	Cumulative passing (%)					
	0.3 mm	0.6 mm	1.18 mm	2.36 mm	5.0 mm	10.0 mm
A-B-1	0.0	0.0	0.0	0.0	0.0	100.0
A-B-2	0.0	0.0	0.0	0.0	40.0	100.0
A-B-3	0.0	0.0	0.0	0.0	60.0	100.0
A-B-4	0.0	0.0	0.0	0.0	80.0	100.0
A-C-1	0.0	0.0	0.0	20.0	52.0	100.0
A-C-2	0.0	0.0	0.0	40.0	64.0	100.0
A-C-3	0.0	0.0	0.0	50.0	70.0	100.0
A-C-4	0.0	0.0	0.0	62.5	77.5	100.0
A-D-1	0.0	0.0	20.0	52.0	71.2	100.0
A-D-2	0.0	0.0	40.0	64.0	78.4	100.0
A-D-3	0.0	0.0	60.0	80.0	88.0	100.0
A-E-1	0.0	20.0	52.0	71.0	83.0	100.0
A-E-2	0.0	40.0	64.0	78.0	87.0	100.0
A-E-3	0.0	10.0	46.0	67.6	80.6	100.0
A-F-1	10.0	19.0	51.4	70.8	82.5	100.0
A-F-2	19.9	27.9	56.7	74.0	84.4	100.0

**Table 4**  
Volumetric mix proportions of concrete paving blocks made with NA and RA.

Mix no.	Cement (kg/m <sup>3</sup> )	Water (kg/m <sup>3</sup> )	NCA (kg/m <sup>3</sup> )	RCA (kg/m <sup>3</sup> )	NFA (kg/m <sup>3</sup> )	RSA (kg/m <sup>3</sup> )	A/C ratio
NCA0NFA100	380	165	0	0	1898	0	5.00
NCA20NFA80	383	158	385	0	1530	0	5.00
NCA35NFA65	380	165	763	0	1138	0	5.00
NCA50NFA50	380	165	1144	0	758	0	5.00
NCA80NFA20	390	144	1564	0	389	0	5.00
NCA100NFA0	394	137	1971	0	0	0	5.00
NCA0RSA100	390	153	0	0	0	1949	5.00
NCA20RSA80	389	152	387	0	0	1560	5.00
NCA35RSA65	392	145	780	0	0	1180	5.00
NCA50RSA50	389	152	1161	0	0	780	5.00
NCA60RSA40	391	145	1562	0	0	394	5.00
NCA100RSA0	391	144	1954	0	0	0	5.00
RCA0RSA100	397	138	0	0	0	1983	5.00
RCA20RSA80	388	152	0	380	0	1562	5.00
RCA35RSA65	384	159	0	754	0	1163	5.00
RCA50RSA50	393	137	0	1162	0	796	5.00
RCA80RSA20	390	136	0	1553	0	399	5.00
RCA100RSA0	392	128	0	1960	0	0	5.00

ric mix proportions in Phase II are reported in Table 4. For easy identification, each mix was assigned a label. For instance, the NCA0NFA100 denotes the mixture made with 0% NCA and 100% NFA, and NCA80NFA20 denotes the mixture made with 80% NCA and 20% NFA. To be consistent, the aggregate to cement (A/C) ratio was fixed at 5.00, leaving the air voids to be filled by varying amounts of water. In actual mixing, 4.6 kg of cement and 23.0 kg of aggregate (all types) were consistently weighted for each concrete paving block mix. Note that the water content of the fresh mixture was adjusted with visual inspection to achieve a suitable workability for producing concrete paving blocks.

### 3.3. Block fabrication

Steel moulds were adopted for the fabrication of concrete paving blocks. The steel moulds had internal dimensions of 200 × 100 × 60 mm (length × width × depth) [36]. The concrete materials were cast into each mould in three layers and manual compaction was applied to each layer. Then, a machine-driven compaction was applied on each of the concrete paving blocks with a loading rate of 10 kN/s until the load of 500 kN for all the samples. After compaction, the samples were covered by a thin layer of plastic sheet to avoid water evaporation. One day after that,

the concrete paving blocks were demoulded and cured in water for 28 days at a temperature of 27 ± 3 °C.

### 3.4. Block testing

Compressive strength tests on the paving blocks were conducted in accordance with BS EN 1338 [37]. The equipment for skid resistance (SR) and abrasion resistance (AR) test are shown in Fig. 4. The skid resistance was determined using a British Pendulum Skid Resistance Tester and expressed as the measured British Pendulum Number (BPN) as per BS EN 1338 [37]. In the SR test, the mechanism is based on the energy dissipation from the rubber piece while sliding over the sample upon the free fall of the pendulum arm. The SR is an important consideration during pavement design as an inadequate SR would lead to higher risk of accidents both for moving vehicles and pedestrians. The AR test simulated the wearing and rutting characteristics and was determined by abrading the surface of the block specimen with an abrasive material under controlled conditions as specified by BS EN 1338 [37]. The density of hardened concrete block was determined according to BS EN 12390-7 [38]. The water absorption (WA) of concrete paving blocks was measured in accordance with AS/NZS 4456 [39].

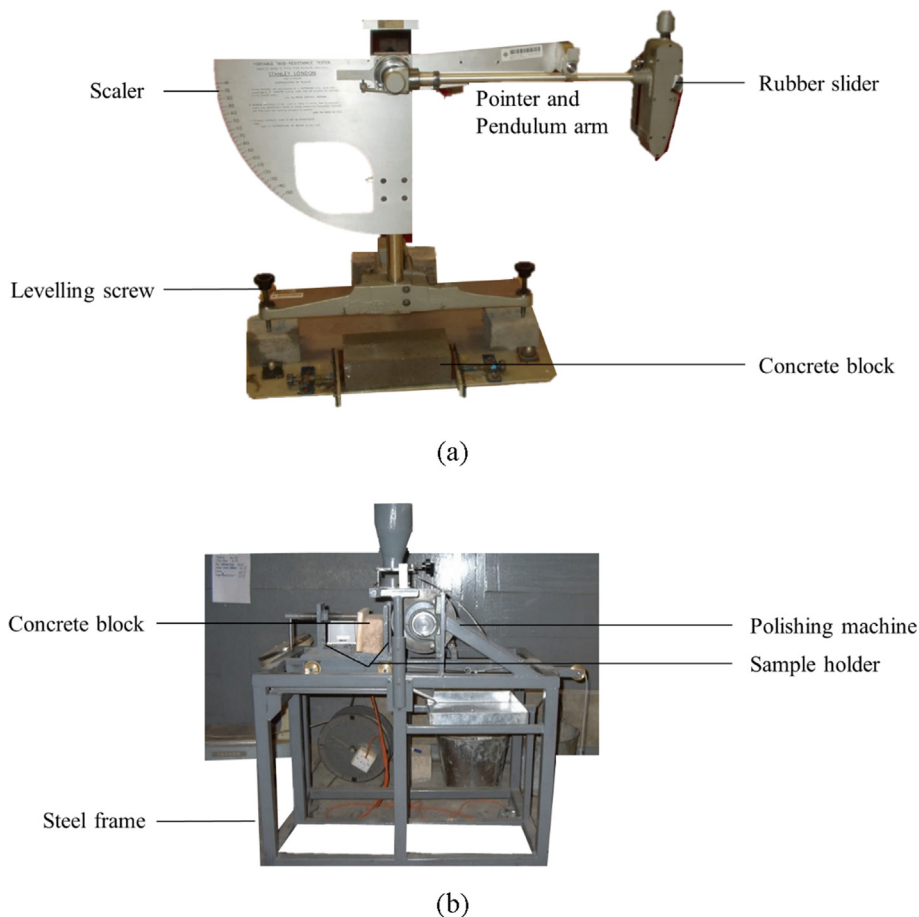


Fig. 4. Apparatus for (a) SR; (b) AR test.

#### 4. Results and discussion

A summary of the test results in Phase I and Phase II is presented in Table 5, with the results on packing density, strength, density, water absorption, SR and AR tabulated in the third to the last column sequentially. Detailed illustrations and discussions will be presented in the following parts.

##### 4.1. Phase I

The aggregate proportioning for higher packing density and the influence of packing density are discussed in this section. First, the sieve analysis results of 16 dry RA mixtures are reported in Table 3. In the table, RA of finer class were sequentially added from the first to the last row. For vivid illustration, the PSD curves of each mixture are depicted in Fig. 5(a). For each mixture, the packing density has been determined. The packing densities so determined were reported in the third column of the Table 5. From the table, it was found that the mixture A-F-1 exhibited the highest packing density of 0.738. The PSD curve corresponding to the mixture with the highest packing density was highlighted in Fig. 5(a) with a thicker dark grey line. To further evaluate the PSD curve of the mixture exhibiting the highest packing density, a comparison was made, as shown in Fig. 5(b), between the optimum PSD curve identified in the present study and the PSD curves generated from the formula by Fuller & Thompson [26]. Apparently, the optimum PSD curve identified in the present study largely lies between the PSD curves by Fuller & Thompson, demonstrating that good agree-

ment and a reliable PSD curve for the optimum packing have been achieved.

To demonstrate the effectiveness of the aggregate proportioning in improving the packing density, the packing densities of the mono-sized particle systems, A, B, C, D, E and F, are plotted in Fig. 6 as black square data points. Meanwhile, the maximum packing density results of the multi-sized particle systems after aggregate proportioning, consisting of aggregates from A to B, aggregates from A to C, aggregates from A to D, aggregates from A to E and aggregates from A to F, are plotted in Fig. 6 as red circle points sequentially from left to right. Apparently, as shown in the figure, the packing densities of multi-sized particle system are much higher than that of the quasi mono-sized particle systems, demonstrating that the proportioning of particles of various sizes could give rise to a much-improved packing density [40–43]. It should be noted that the percentage increase in the packing density could be up to 31% from 0.564 to 0.738 after the aggregate proportioning.

Apart from the packing density, the compressive strengths of the concrete paving blocks made with such aggregate mixtures are tabulated in the fourth column of the Table 5. To evaluate the progressive process of the packing optimization and its effect of the compressive strength of the concrete paving blocks, the compressive strengths at the maximum packing density of each scenario in Phase I are plotted against the six aggregate combinations, which are aggregates blended with A and B, aggregate blended with A, B and C, aggregate blended with A, B, C and D, aggregates blended with A, B, C, D and E, and aggregates blended with A, B, C, D, E and F, in Fig. 7(a). From the figure, it could be

**Table 5**  
Tests results of concrete paving blocks.

Phase	Mix no.	Packing density	Strength (MPa)	Density (kg/m <sup>3</sup> )	WA (%)	SR (BPN <sup>^</sup> )	AR (mm)
I	A-B-1	0.580	30.5	2200	12.1	109	25
	A-B-2	0.634	44.6	2225	8.9	102	24
	A-B-3	0.622	40.9	2206	9.8	105	24
	A-B-4	0.600	32.2	2176	12.7	103	25
	A-C-1	0.668	45.2	2222	9.2	100	24
	A-C-2	0.665	47.3	2219	8.2	102	23
	A-C-3	0.650	60.3	2220	8.3	103	25
	A-C-4	0.627	44.9	2223	9.1	102	25
	A-D-1	0.688	59.2	2268	8.4	98	23
	A-D-2	0.672	67.3	2270	7.2	100	24
	A-D-3	0.629	56.8	2189	8.2	99	25
	A-E-1	0.691	67.2	2282	7.3	95	24
	A-E-2	0.674	54.8	2237	6.8	96	24
	A-E-3	0.684	54.1	2216	7.1	97	23
	A-F-1	0.738	79.2	2305	6.4	95	22
	A-F-2	0.700	55.8	2235	6.6	96	23
II	NCA0NFA100	0.751	72.8	1943	3.16	90	25
	NCA20NFA80	0.764	77.5	2180	3.17	96	22
	NCA35NFA65	0.770	79.4	2145	3.16	95	22
	NCA50NFA50	0.764	84.8	2268	3.95	95	20
	NCA80NFA20	0.713	62.5	2032	4.06	102	22
	NCA100NFA0	0.633	31.1	317	10.05	110	24
	NCA0RSA100	0.659	21.2	655	3.45	92	24
	NCA20RSA80	0.699	44.4	1295	3.42	95	21
	NCA35RSA65	0.727	80.8	1985	3.40	94	20
	NCA50RSA50	0.755	94.4	2280	3.79	95	20
	NCA60RSA40	0.736	84.6	2340	3.40	98	20
	NCA100RSA0	0.633	31.1	317	10.05	110	24
	RCA0RSA100	0.659	21.2	655	3.45	92	24
	RCA20RSA80	0.690	47.8	1215	3.91	90	20
	RCA35RSA65	0.712	62.8	1845	4.05	94	21
	RCA50RSA50	0.722	69.5	1885	4.11	95	20
RCA80RSA20	0.645	19.9	650	6.11	110	26	
RCA100RSA0	0.633	7.1	365	7.85	115	25	

<sup>^</sup>British pendulum number.

observed that the compressive increased as the mixture changed from A-B to A-F. In addition, the concrete paving blocks made with aggregate with the highest packing density were demonstrated to exhibit the maximum compressive strengths. The compressive strength was increased by about 156% from 30.9 MPa to 79.2 MPa after appropriate aggregate proportioning, during which the cement content, aggregate content and A/C ratio remained the same.

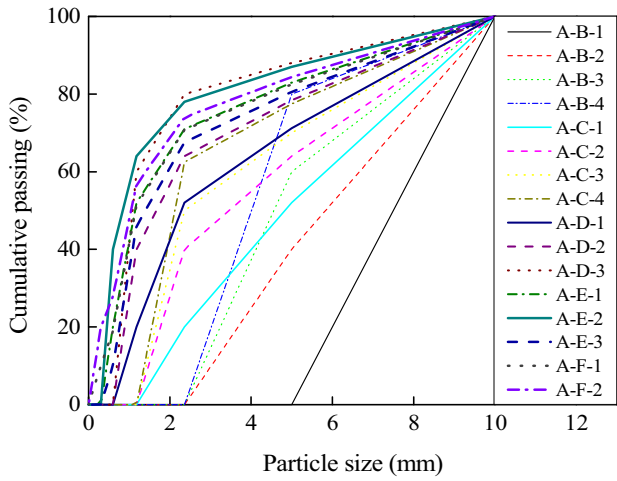
To quantitatively evaluate the influence of packing density on the compressive strength of the concrete paving blocks, correlations were made between the strength and the packing density, as shown in Fig. 7(b). Regression analysis was carried out to find out the best-fit curve for the data points and a reasonably high  $R^2$  value of 0.720 has been achieved, indicating that the packing density is a governing factor for the strength of concrete paving blocks [44–46]. The prediction equation is presented in the figure to show the goodness of fit. Overall, an important implication from the above observation and quantitative analysis is that the packing density of an aggregate mixture could be increased by introducing finer particles into the mixture. Subsequently, the improved packing density of the mixture would contribute to the compressive strength of the concrete paving blocks. Concrete paving blocks made with the optimized aggregate mixtures exhibited the maximum compressive strength, indicating that the mixture made with aggregates with a wider size range is likely to yield a better packing density of the dry mixture and a higher compressive strength of the concrete than the mixture with less-graded aggregates. This is due to the decreased volume of voids between the aggregate particles [47].

Apart from the strength, a better aggregate packing would also exert significant influence on the density and WA of the concrete

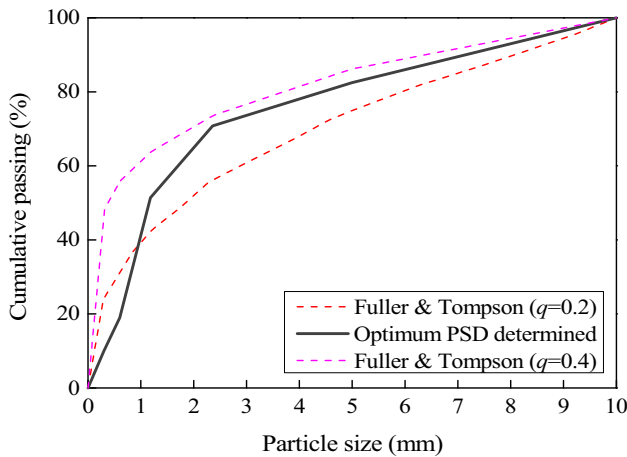
paving blocks. For vivid illustration, test results on the density, WA, SR and AR of the concrete paving blocks made with aggregates at the optimal packing are shown in Fig. 8(a–d), respectively. The figures revealed that the density of the concrete paving blocks increased with the packing density, while the WA, the SR and the AR of the concrete paving blocks decreased slightly with the increasing content of fine aggregate. The reason is that finer aggregates could successfully fill into the voids between the coarser particles [33,48], thus increasing the compressive strength and block density while decreasing the WA. Meanwhile, a higher packing density, which generally implies an appropriately higher content of fine particles, could enable a smoother surface which affected the SR and AR [42].

#### 4.2. Phase II

The influence of aggregate packing on the properties of concrete paving blocks made with various types of aggregates is discussed in this section. In Phase II, the compressive strength, density and WA of the concrete paving blocks are plotted against the aggregate combinations and the packing density in Figs. 9–11, respectively. As shown in Fig. 9, the compressive strength increased with the packing density, regardless of the aggregate type, echoing that a higher packing density could give rise to a higher compressive strength of the concrete paving blocks. From the Fig. 10, it can be observed that the block density also increased with the packing density. In other words, the optimization of packing density could lead to the maximum compressive strength and block density could be obtained. From Fig. 11, a general trend could be observed that, in general, the WA decreased with the packing density. The above phenomena revealed that the optimal packing could be



(a)



(b)

Fig. 5. (a) Optimization; and (b) comparison of PSD curves.

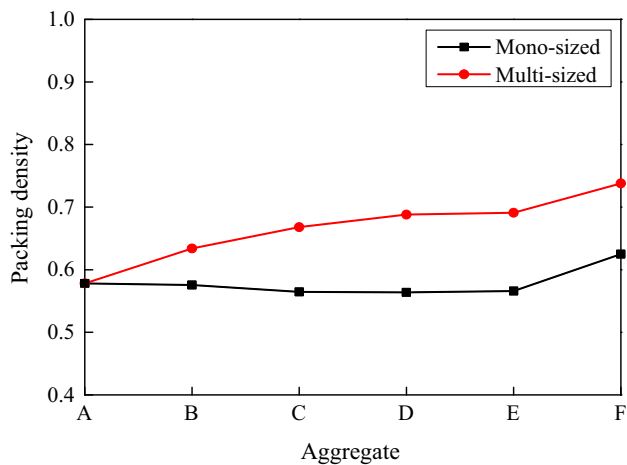


Fig. 6. Comparison between packing density of mono-sized and multi-sized particles.

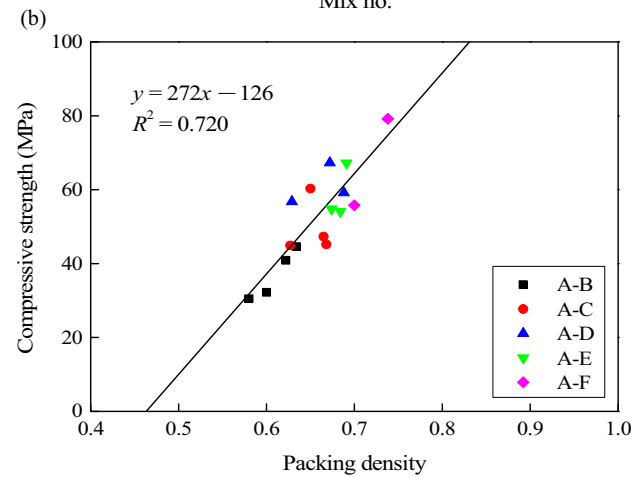
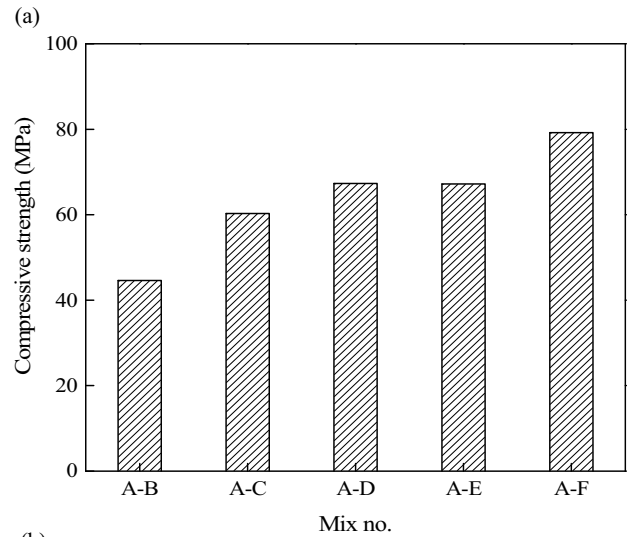


Fig. 7. Compressive strength results in Phase I.

attained by appropriate aggregate proportioning. In addition to that, the test results in the present study revealed that, at certain packing density, there exist no distinct differences in the properties of concrete paving blocks among the use of different types of aggregates. In other words, the packing density is the key factor that governs the properties of concrete paving blocks, which provides a new perspective to develop RAC exhibiting comparable performance to that of NAC.

To quantitatively evaluate the influences of packing density on the compressive strength, density and WA, correlations between the packing density and the various attributes of the concrete paving blocks were performed and the trend equations are indicated in Figs. 9–11, respectively. From Fig. 9, it could be found that a reasonably high  $R^2$  value of 0.879 has been achieved for the compressive strength and the packing density, indicating that the packing density did exert significant influence on the strength of the concrete paving blocks. Likewise, from Fig. 10, it was found that a very high  $R^2$  value of 0.928 has been reached for the linear prediction equation between the block density and the packing density, echoing the above findings. Lastly, a quite high  $R^2$  value of 0.917 has also been achieved for the prediction equation delineating the relation between WA and packing density, as shown in Fig. 11. The coefficients  $a$  and  $b$  were determined as  $1.44 \times 10^{22}$  and

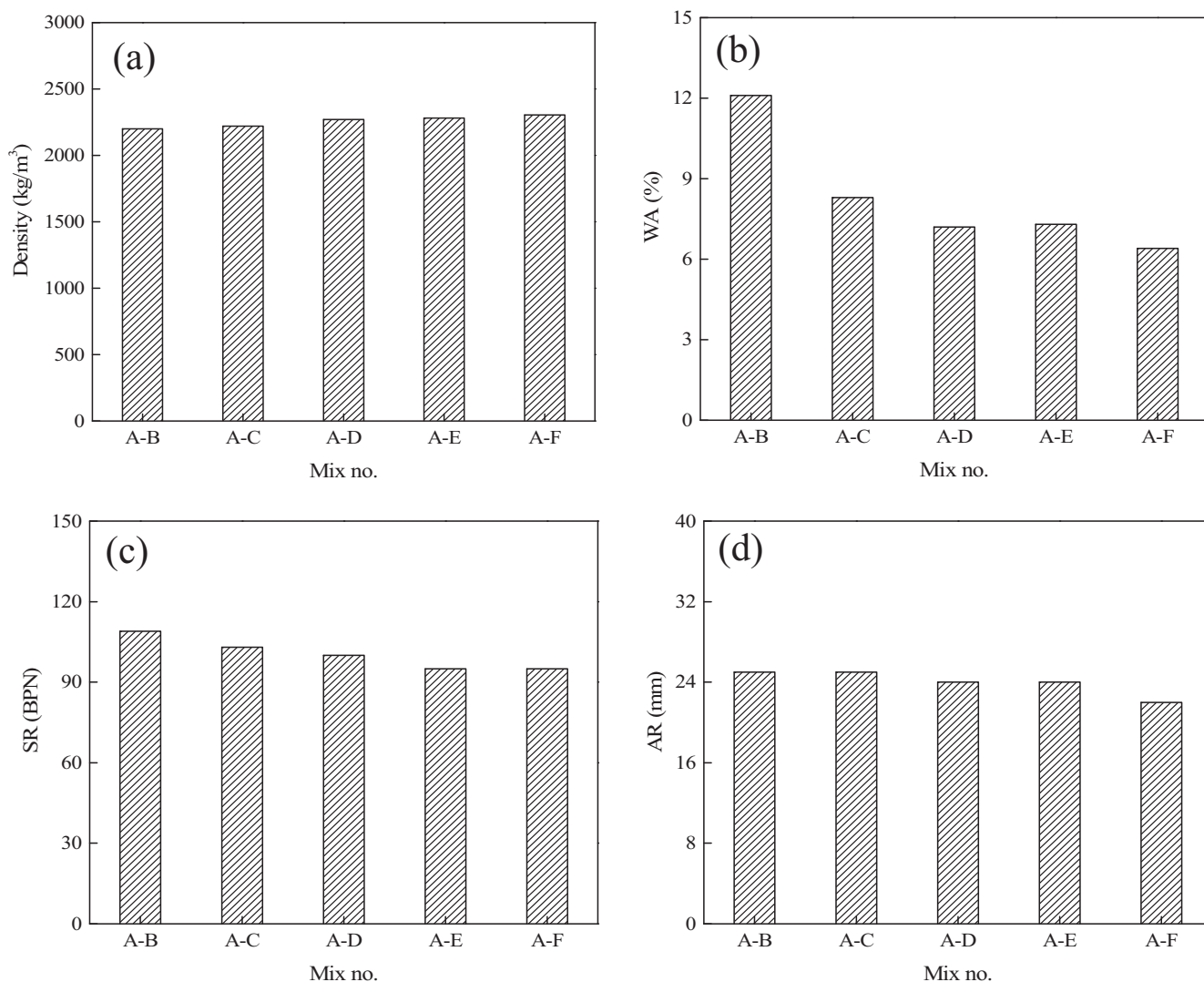


Fig. 8. Results in Phase I: (a) block density; (b) WA; (c) SR; and (d) AR.

$1.57 \times 10^{-34}$ , respectively, which are dependent on the other mix parameters.

## 5. Further discussion

Theoretically, the packing density, i.e., the maximum solid concentration, of a particle system consisting of mono-sized spherical particles is a constant. Due to variations in particle shape and particle size, the particle density of a dry aggregate mixture may be diverted from the above constant packing density. In the present work, the same type of aggregate with different sizes are classified into six classes and the aggregate of each size class was regarded as quasi mono sized. The packing density of such quasi-mono-sized particle system varied between 0.564 and 0.625. However, when appropriate proportioning was applied to such quasi mono-sized particle system by broadening the size range, the packing density could be elevated to up to 0.738. The percentage increase due to aggregate proportioning could be up to 31%.

However, when various types of aggregate were incorporated into the particle system, the packing density varied. For instance, the packing density of a particle system consisting only of NA was ranged between 0.633 and 0.770, the packing density of a particle system consisting only of NA and RSA was ranged between

0.633 and 0.755, and the packing density of a particle system consisting only of RA and RSA was ranged between 0.633 and 0.722. The above values indicated that the packing density of NA was generally larger than of RA and this was probably due to the fact some porous old paste or mortar might be inevitably adhered to the RA and adversely affected the packing. Overall, the packing density of a dry aggregate mixture could be significantly elevated by aggregate proportioning, although the packing density of RA was intrinsically lower than that of NA due to the presence of adhered old paste or mortar. It has been demonstrated that by appropriate aggregate proportioning, the packing density of a particle system consisting only of RA could approach the packing density of a particle system consisting only of NA, as evidenced by the relatively small difference in the maximum packing density of 0.738 for RA and 0.770 for NA [49].

In practical production, the findings from the present research could serve as important guidelines. For instance, it provides a new perspective that, by appropriate packing optimization, the performance of RAC could approach that of NAC, thus resolving the major hurdles in the wider application of RA. More specifically, the use of packing optimization could liberate the need of various RA treatment methods in the absence of the demanding conditions. Apart from it, the cement consumption has not been increased dur-

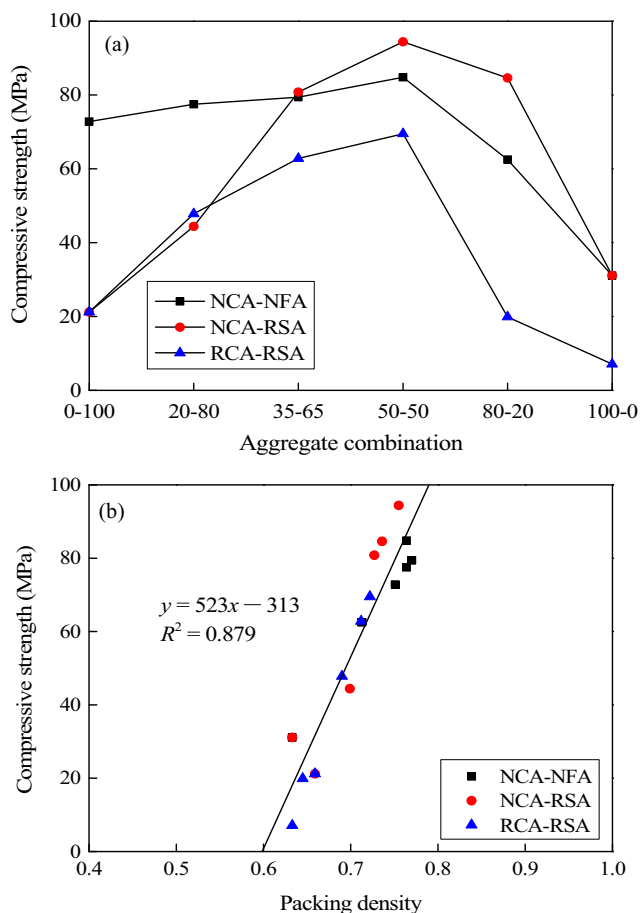


Fig. 9. Compressive strength results in Phase II.

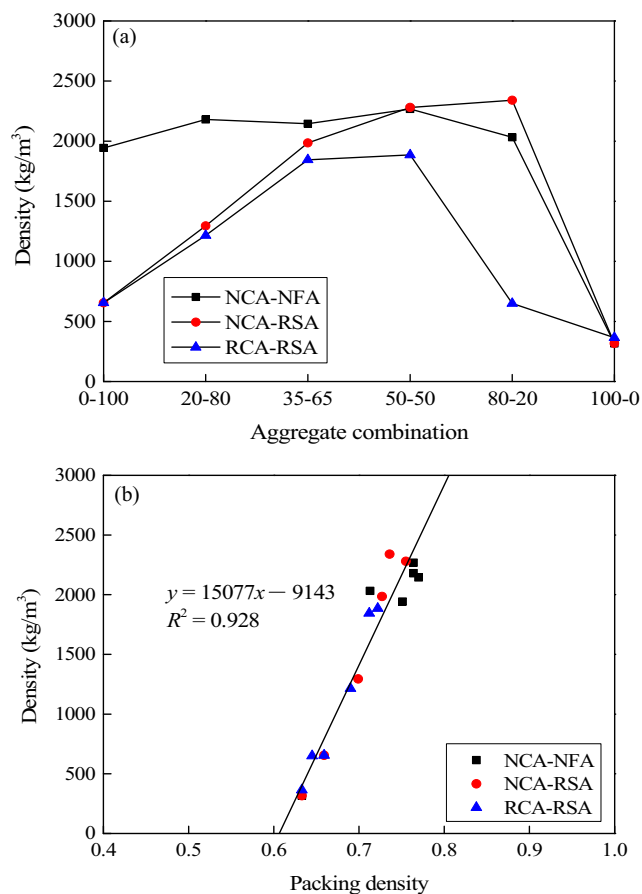


Fig. 10. Density results in Phase II.

ing the packing optimization process, while a possible decrease in cement consumption could even provide a higher sustainability. Second, it enables the prediction of the properties of RAC based on the key factor of packing density during the production of concrete paving blocks. Nevertheless, further studies on investigating the role of particle packing in properties and durability of general concrete production are recommended [50].

6. Conclusions

In this paper, an experimental program, consisting of two phases, was conducted with the aim of investigating the effects of aggregates packing on the properties of concrete paving blocks systematically. Based on the tests results and discussion, the following conclusions could be drawn,

1. The packing density of the RA particle system could be significantly increased by up to 31% after appropriate aggregate proportioning. In addition, the packing density of an RA particle system could be optimized to approach that of an NA particle system, despite the presence of adhered old paste or mortar for RA.
2. With appropriate packing optimization, the compressive strength of concrete paving blocks made with only RA could be increased by 156% from 30.9 MPa to 79.2 MPa, approaching the maximum compressive strength of 84.8 MPa obtained for concrete paving blocks made with only NA. Meanwhile, the cement content (converted to volumetric mix design) was below 400 kg/m<sup>3</sup> for all mixtures, without incorporating any supplementary cementitious materials.

3. The packing density was found to be a key factor that governs the properties of concrete paving blocks, regardless of the aggregate type, which provides a new perspective to understand and enhance the properties of RAC. In addition, the compressive strength and density increased with the packing density, while the WA decreased with the packing density.
4. Empirical equations for the prediction of the compressive strength and other properties have been derived with reasonably high R<sup>2</sup> values ranging between 0.720 and 0.928 based on the key factor of packing density. The quantitative relations between the compressive strength and packing density of concrete paving blocks made with both NA and RA have been revealed. Though empirical, these formulas do provide guidelines for future mixture design of concrete paving blocks.

CRediT authorship contribution statement

**S.H. Chu:** Methodology, Formal analysis, Visualization, Writing - original draft, Writing - review & editing. **Chi Sun Poon:** Conceptualization, Visualization, Methodology, Formal analysis, Supervision, Funding acquisition, Writing - review & editing. **C.S. Lam:** Conceptualization, Investigation, Formal analysis. **L. Li:** Formal analysis, Writing - review & editing.

Declaration of Competing Interest

The authors declare that they have no known competing financial interests or personal relationships that could have appeared to influence the work reported in this paper.

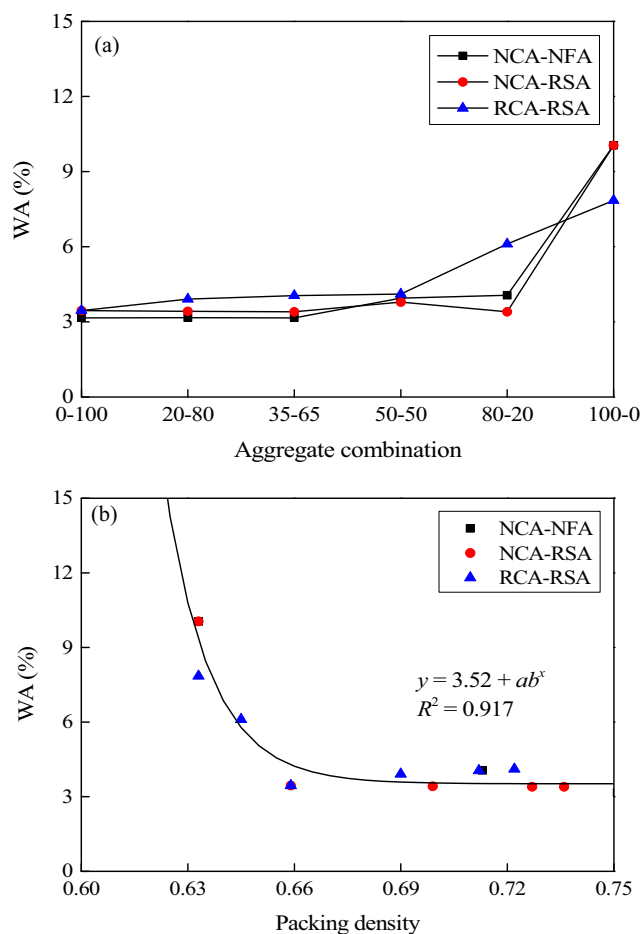


Fig. 11. WA results in Phase II.

## Acknowledgements

The authors would like to thank the Strategic Public Policy Research (SPPR) Funding Scheme, the Construction Industry Council, and The Hong Kong Polytechnic University for financial supports.

## References

- V.W.Y. Tam, A. Butera, K.N. Le, W. Li, Utilising CO2 technologies for recycled aggregate concrete: A critical review, *Constr. Build. Mater.* 250 (2020) 118903.
- H. Duan, T.R. Miller, G. Liu, V.W.Y. Tam, Construction debris becomes growing concern of growing cities, *J. Waste Manag.* 83 (2019) 1–5.
- P. Ghisellini, M. Ripa, S. Ulgiati, Exploring environmental and economic costs and benefits of a circular economy approach to the construction and demolition sector. A literature review, *J. Clean. Prod.* 178 (2018) 618–643.
- Z. Duan, S. Hou, J. Xiao, B. Li, Study on the essential properties of recycled powders from construction and demolition waste, *J. Clean. Prod.* 253 (2020) 119865.
- P. Pereira, L. Evangelista, J. De Brito, The effect of superplasticizers on the mechanical performance of concrete made with fine recycled concrete aggregates, *Cem. Concr. Compos.* 34 (9) (2012) 1044–1052.
- C. Thomas, J. De Brito, A.I. Cimentada, J.A. Sainz-Aja, Macro-and micro-properties of multi-recycled aggregate concrete, *J. Clean. Prod.* 245 (2020) 118843.
- B.J. Zhan, D.X. Xuan, C.S. Poon, K.L. Scrivener, Characterization of interfacial transition zone in concrete prepared with carbonated modeled recycled concrete aggregates, *Cem. Concr. Res.* 136 (2020) 106175.
- Z. Feng, Y. Zhao, W. Zeng, Z. Lu, S.P. Shah, Using microbial carbonate precipitation to improve the properties of recycled fine aggregate and mortar, *Constr. Build. Mater.* 230 (2020) 116949.
- Z. Tang, W. Li, V.W.Y. Tam, Z. Luo, Investigation on dynamic mechanical properties of fly ash/slag-based geopolymeric recycled aggregate concrete, *Compos. Part B Eng.* 185 (2020) 107776.
- Z. Ma, M. Liu, Q. Tang, C. Liang, Z. Duan, Chloride permeability of recycled aggregate concrete under the coupling effect of freezing-thawing, elevated temperature or mechanical damage, *Constr. Build. Mater.* 237 (2020) 117648.
- R. Mi, G. Pan, K.M. Liew, T. Kuang, Utilizing recycled aggregate concrete in sustainable construction for a required compressive strength ratio, *J. Clean. Prod.* 124249 (2020).
- Z. Peng, C. Shi, Z. Shi, B. Lu, S. Wan, Z. Zhang, J. Chang, T. Zhang, Alkali-aggregate reaction in recycled aggregate concrete, *J. Clean. Prod.* 255 (2020) 120238.
- S. Pradhan, S. Kumar, S.V. Barai, Multi-scale characterisation of recycled aggregate concrete and prediction of its performance, *Cem. Concr. Compos.* 106 (2020) 103480.
- A.K. Padmini, K. Ramamurthy, M.S. Mathews, Influence of parent concrete on the properties of recycled aggregate concrete, *Constr. Build. Mater.* 23 (2) (2009) 829–836.
- Y. Wang, J. Chen, Y. Geng, Testing and analysis of axially loaded normal-strength recycled aggregate concrete filled steel tubular stub columns, *Eng. Struct.* 86 (2015) 192–212.
- M.B. Leite, V.M. Santana, Evaluation of an experimental mix proportion study and production of concrete using fine recycled aggregate, *J. Build. Eng.* 21 (2019) 243–253.
- P. Gao, T.S. Zhang, J.X. Wei, Q.J. Yu, Evaluation of RRSB distribution and lognormal distribution for describing the particle size distribution of graded cementitious materials, *Powder Tech.* 331 (2018) 137–145.
- X. Wang, R. Yu, Q. Song, Z. Shui, Z. Liu, S. Wu, D. Hou, Optimized design of ultra-high performance concrete (UHPC) with a high wet packing density, *Cem. Concr. Res.* 126 (2019) 105921.
- J.J. Chen, P.L. Ng, S.H. Chu, G.X. Guan, A.K.H. Kwan, Ternary blending with metakaolin and silica fume to improve packing density and performance of binder paste, *Constr. Build. Mater.* 252 (2020) 119031.
- M.H. Lai, S.A.M. Binhowimal, L. Hanzic, Q. Wang, J.C.M. Ho, Dilatancy mitigation of cement powder paste by pozzolanic and inert fillers, *Struct. Concr.* 21 (2020) 1164–1180.
- L.G. Li, C.J. Lin, G.M. Chen, A.K.H. Kwan, T. Jiang, Effects of packing on compressive behaviour of recycled aggregate concrete, *Constr. Build. Mater.* 157 (2017) 757–777.
- S.H. Chu, Y. Jiang, A.K.H. Kwan, Effect of rigid fibres on aggregate packing, *Constr. Build. Mater.* 224 (2019) 326–335.
- S.H. Chu, J.J. Yao, A strength model for concrete made with marine dredged sediment, *J. Clean. Prod.* 274 (2020) 122673.
- Z.H. Duan, C.S. Poon, Properties of recycled aggregate concrete made with recycled aggregates with different amounts of old adhered mortars, *Mater. Design* 58 (2014) 19–29.
- Q. Wang, J. Zhang, J.C.M. Ho, Zeolite to improve strength-shrinkage performance of high-strength engineered cementitious composite, *Constr. Build. Mater.* 234 (2020) 117335.
- W.B. Fuller, S.E. Thompson, The laws of proportioning concrete, *Trans. Am. Soc. Civil Eng.* 59 (1907) 67–143.
- G. Lees, The rational design of aggregate gradings for dense asphaltic compositions, *Association of Asphalt Paving Technologists Proc.* 1970.
- A. Kronlöf, Effect of very fine aggregate on concrete strength, *Mater. Struct.* 27 (1994) 15–25.
- G. Lee, C.S. Poon, Y.L. Wong, T.C. Ling, Effects of recycled fine glass aggregates on the properties of dry-mixed concrete blocks, *Constr. Build. Mater.* 38 (2013) 638–643.
- G. Fu, W. Dekelbab, 3-D random packing of polydisperse particles and concrete aggregate grading, *Powder Technol.* 133 (2013) 147–155.
- A.K.H. Kwan, W.W.S. Fung, Packing density measurement and modelling of fine aggregate and mortar, *Cem. Concr. Compos.* 31 (2009) 349–357.
- A.B. Yu, R.P. Zou, N. Standish, Modifying the linear packing model for predicting the porosity of nonspherical particle mixtures, *Indus. Eng. Chem. Res.* 35 (10) (1996) 3730–3741.
- F. de Larrard, *Concrete mixture proportioning: a scientific approach*, CRC Press, 1999.
- L.G. Li, J.J. Feng, J. Zhu, S.H. Chu, A.K.H. Kwan, Pervious concrete: effects of porosity on permeability and strength, *Mag. Concr. Res.* 73 (2) (2021) 69–79.
- American Society for Testing and Materials, *ASTM C150/C150M-20 Standard Specification for Portland Cement*, ASTM International, PA, USA, 2020.
- C.S. Poon, D. Chan, Paving blocks made with recycled concrete aggregate and crushed clay brick, *Constr. Build. Mater.* 20 (8) (2006) 569–577.
- British Standard Institution. *BS EN 1338:2003. Concrete paving blocks. Requirements and test methods*, London, UK, 2003.
- British Standard Institution. *BS EN 12390-7:2000 Testing hardened concrete. Density of hardened concrete*, British Standards Institution, London, UK, 2000.
- Standards Australia. *AS/NZS 4456:2003. Masonry units, segmental pavers and flags - Methods of test*, Australia, 2003.
- R.P. Zou, J.Q. Xu, C.L. Feng, A.B. Yu, S. Johnston, N. Standish, Packing of multi-sized mixtures of wet coarse spheres, *Powder Tech.* 130 (1–3) (2003) 77–83.
- S.H. Chu, A.K.H. Kwan, Co-addition of metakaolin and silica fume in mortar: effects and advantages, *Constr. Build. Mater.* 197 (2019) 716–724.
- C. Hettiarachchi, W.K. Mamparachchi, Effect of surface texture, size ratio and large particle volume fraction on packing density of binary spherical mixtures, *Granul. Matter* 22 (1) (2020) 8.
- S.H. Chu, L.G. Li, A.K.H. Kwan, Development of extrudable high strength fiber reinforced concrete incorporating nano calcium carbonate, *Addit. Manuf.* (2020) 101617.

- [44] S.K. Ling, A.K.H. Kwan, Filler technology for low-carbon high-dimensional stability concrete, *Constr. Build. Mater.* 163 (2018) 87–96.
- [45] P.P. Li, Q.L. Yu, H.J.H. Brouwers, Effect of coarse basalt aggregates on the properties of Ultra-high Performance Concrete (UHPC), *Constr. Build. Mater.* 170 (2018) 649–659.
- [46] B. Li, S. Hou, Z. Duan, L. Li, W. Guo, Rheological behavior and compressive strength of concrete made with recycled fine aggregate of different size range, *Constr. Build. Mater.* (2020) 121172.
- [47] S.H. Chu, Effect of paste volume on fresh and hardened properties of concrete, *Constr. Build. Mater.* 218 (2019) 284–294.
- [48] S. Shen, H. Yu, Characterize packing of aggregate particles for paving materials: Particle size impact, *Constr. Build. Mater.* 25 (3) (2011) 1362–1368.
- [49] J.M. Kanema, J. Eid, S. Taibi, Shrinkage of earth concrete amended with recycled aggregates and superplasticizer: Impact on mechanical properties and cracks, *Mater. Design* 109 (2016) 378–389.
- [50] S. Yerazunis, J. Bartlett, A. Nissan, Packing of binary mixtures of spheres and irregular particles, *Nature* 195 (4836) (1962) 33–35.



## Optimization of gas-solid carbonation conditions of recycled aggregates using a linear weighted sum method



Adebayo Olatunbsoun Sojobi<sup>a,b,c</sup>, Dongxing Xuan<sup>a</sup>, Long Li<sup>a</sup>, Songhui Liu<sup>a,d</sup>, Chi Sun Poon<sup>a,\*</sup>

<sup>a</sup> Department of Civil and Environmental Engineering, The Hong Kong Polytechnic University, Hong Kong

<sup>b</sup> Department of Building and Real Estate, The Hong Kong Polytechnic University, Hong Kong

<sup>c</sup> Department of Architecture and Civil Engineering, City University of Hong Kong, Hong Kong

<sup>d</sup> Henan Key Laboratory of Materials on Deep-Earth Engineering, School of Materials Science and Engineering, Henan Polytechnic University, Jiaozuo, China

### ARTICLE INFO

#### Keywords:

Recycled concrete aggregates  
Gas-solid carbonation  
Pretreatment  
Temperature  
Optimization  
Wastewater  
Durability

### ABSTRACT

Optimization of pretreatment and various gas-solid interaction conditions is necessary for effective carbonation of recycled coarse aggregates derived from concrete wastes (RCA). This study demonstrated the use of linear weighted sum method to simultaneously optimize the pretreatment and carbonation test conditions. The optimization of the test conditions produced simplified, and eco-friendly pretreatments and drastically reduced the carbonation duration of RCA from 72 h to 3 weeks in previous studies to 18 h in this study. In addition, the optimum experimental conditions were validated by casting concrete using the carbonated RCAs. The optimized pretreatment and carbonation conditions were spraying  $\text{Ca}^{2+}$ -rich wastewater at a level of 60% of the 24 h water absorption of RCA, 12 h air drying and 6 h carbonation at 60 °C. This study also demonstrated that wastewater derived from ready-mix concrete batching plants can be utilized for spraying the RCAs to improve carbonation efficiency. Also, the mechanical and durability properties of concrete prepared with RCAs produced from the optimized conventional carbonation and pressurized carbonation were similar. Therefore, optimized conventional carbonation can be utilized as an alternative to pressurized carbonation. The improved mechanical and durability properties of concrete prepared with carbonated RCAs were attributed to the improved physical properties of carbonated RCAs and improved microhardness of the interfacial transition zone of the new mortar. The simplified, faster, ecofriendly, optimized pretreatment and carbonation conditions opens a new vista for industrial carbonation applications and optimization of gas-solid interactions.

### 1. Introduction

Much interests are now being paid on recycling recycled aggregates derived from construction and demolition wastes (CDW) due to sustainability concerns (Bao et al., 2020a; Silva et al., 2019; Xuan and Shui, 2011). Environmental sustainability concerns with respect to CDW includes leaching of hazardous chemicals from CDW, rapid natural

resource depletion, land depletion due to landfill-based waste management, greenhouse gas emission and risk of landslides of landfilled CDW by rainfall (Bao et al., 2020b; Behera et al., 2014; Bonoli et al., 2021; Lu et al., 2017). The economic sustainability concerns includes increased production costs and time, creation of new jobs and industries, increased landfilling operation and maintenance costs as well as increased government expenditure on new landfills (Alsheyab, 2021; Zhang et al.,

**Abbreviations:** RCA, Recycled coarse aggregates; RAC, Concrete prepared with recycled coarse aggregates; CDW, Construction and demolition wastes; NA, Natural aggregates; NAC, Concrete prepared with natural aggregates; RMA, Regular mortar aggregates; CS, Compressive strength; PC, Pressurized carbonation; FCSE, Optimized conventional carbonation; FC, Conventional carbonation; RAC-FC, Concrete prepared with 24-h carbonated recycled coarse aggregates (RCA); RAC-PC, Concrete prepared with pressurized carbonated RCA; RAC-FCSE, Concrete prepared with optimized carbonated RCA; NSC24-25, Regular mortar aggregates non-sprayed and carbonated for 24 h @ 25 °C; SC24-40, Regular mortar aggregates wastewater-sprayed, non-dried and carbonated for 24 h @ 40 °C; SC12-60, Regular mortar aggregates wastewater-sprayed, non-dried and carbonated for 12 h @ 60 °C; SA12C6-60, Regular mortar aggregates wastewater sprayed 12-h air dried and carbonated for 6 h @ 60 °C; SE6C6-60, Regular mortar aggregates wastewater sprayed, 6 h dried in environmental chamber and carbonated for 6 h @ 60 °C;  $\text{MH}_{\text{new mortar}}$ , Microhardness of new mortar surrounding the regular mortar aggregate;  $\text{MH}_{\text{RMA}}$ , Microhardness of the carbonated and uncarbonated regular mortar aggregate; BD, Bulk density; WA, Water absorption; BEC, Bulk electrical conductivity.

\* Corresponding author.

E-mail address: [cecspon@polyu.edu.hk](mailto:cecspon@polyu.edu.hk) (C.S. Poon).

<https://doi.org/10.1016/j.dibe.2021.100053>

Received 23 March 2021; Received in revised form 31 May 2021; Accepted 4 June 2021

Available online 17 June 2021

2666-1659/© 2021 The Authors. Published by Elsevier Ltd. This is an open access article under the CC BY-NC-ND license (<http://creativecommons.org/licenses/by-nc-nd/4.0/>).

**Table 1**  
Pre-treatment and carbonation conditions of RCA in previous researches.

References	Pre-treatment	Carbonation conditions	Benefits and drawbacks
Li et al. (2019)	<ul style="list-style-type: none"> <li>Drying in a chamber to obtain appropriate moisture content</li> </ul>	<ul style="list-style-type: none"> <li>20% CO<sub>2</sub></li> <li>70±5% RH</li> <li>23 ± 2 °C</li> <li>3 days</li> </ul>	<ul style="list-style-type: none"> <li>Drying to enhance carbonation.</li> <li>Long carbonation time.</li> </ul>
Kazmi et al. (2020)	<ul style="list-style-type: none"> <li>C Lime-treated, acid-treated and direct carbonation.</li> <li>Drying at 25 °C and 50% RH for 3 days.</li> </ul>	<ul style="list-style-type: none"> <li>100% CO<sub>2</sub></li> <li>+0.8 bar</li> <li>24 h</li> </ul>	<ul style="list-style-type: none"> <li>Lime-treatment before carbonation resulted in lowest WA and porosity of RCA.</li> </ul>
Wang et al. (2020a)	<ul style="list-style-type: none"> <li>Air-dried before direct carbonation.</li> <li>Impregnation with hydrated lime for 1 h.</li> <li>Dried at 50 °C.</li> </ul>	<ul style="list-style-type: none"> <li>20±3% CO<sub>2</sub></li> <li>20±2 °C</li> <li>70 ± 5% RH</li> <li>No pressure.</li> </ul>	<ul style="list-style-type: none"> <li>RAC exhibited good properties.</li> </ul>
Zhan et al. (2018)	<ul style="list-style-type: none"> <li>Presoaking in a saturated limewater for 3 days.</li> <li>Pre-drying for 3 days at 26 °C &amp; 50% RH.</li> </ul>	<ul style="list-style-type: none"> <li>100% CO<sub>2</sub></li> <li>+0.1 bar</li> <li>24 h</li> <li>Room temperature</li> </ul>	<ul style="list-style-type: none"> <li>Lower WA, higher CO<sub>2</sub> uptake.</li> <li>Increased microhardness recorded by lime-soaked RCA.</li> <li>High carbonation pressure and long time</li> </ul>
Zhan et al. (2020)	<ul style="list-style-type: none"> <li>Soaking in limewater for 56 days.</li> <li>Drying at 25 °C &amp; 50±2% RH for 14 days.</li> </ul>	<ul style="list-style-type: none"> <li>100% CO<sub>2</sub></li> <li>+1 bar</li> <li>25 °C</li> <li>7 days</li> </ul>	<ul style="list-style-type: none"> <li>Improvement in microhardness of RCA</li> <li>Improvement of their interfacial bonding (ITZ) of RAC</li> <li>High carbonation pressure and long time.</li> </ul>

2019a, 2019b). Beside these, the other major issues of CDW management are attributed to rapid urbanization, low recovery and recycling rates, ineffective government policies, management deficiencies and inadequate capacity to manage the wastes (Zhang et al., 2019b; Aslam et al., 2020; Bao and Lu, 2020; Kabirifar et al., 2020; Ruiz et al., 2020). Recycled concrete aggregates from CDW (RCA) has thus been identified as an alternative source of aggregates to mitigate the negative impact of natural aggregate (NA) exploitation, as well as the waste management and environmental issues arising from CDW disposal (Muduli and Mukharjee, 2020).

Recycling of CDW offers potential opportunities for waste reduction, resource efficiency and resource conservation, aversion of environmental pollution and risks, reduction of government expenditure on landfill operations and management and creation of new jobs and industries (Silva et al., 2019; Zhang et al., 2019b; Bao and Lu, 2020; Agrela et al., 2021; Liu et al., 2021; Yazdani et al., 2021). To reap the benefits of environmental and economic benefits of CDW recycling, governments of various countries have increased landfilling costs and set up environmental programmes and policies to encourage recycling (Ghaffar et al., 2020; Jain et al., 2015; Kurniawan et al., 2021; Li et al., 2020a; Turkylmaz et al., 2019; Wang et al., 2021). In addition, several companies have embraced in-house recycling/upcycling to achieve project efficiency, sustainable construction and improve their profits (Wang et al., 2021).

Despite numerous studies confirming the feasibility of using RCA in concrete for applications (Ceia et al., 2016; Majhi et al., 2018; Pereira-De-Oliveira et al., 2014; Rao et al., 2011), its use is largely limited owing to its inferior properties compared to NA, leading to reduction in mechanical and durability properties of recycled aggregate concrete (RAC) compared to natural aggregate concrete (NAC). Even though some studies reported that RCA application rate can reach up to 100% depending on the quality (Le and Bui, 2020; Rockson et al., 2020; Xuan

et al., 2012), most standards limit RCA utilization in different civil engineering works.

In recent years, carbonation treatment has attracted much interest to enhance the properties of RCA as shown in Table 1. It generally involves two steps, namely pre-treatment by using other foreign admixtures (i.e. Ca-rich foreign admixture, Ca(OH)<sub>2</sub> solution) and adjustment of proper carbonation conditions (i.e. temperature, pressure, duration, drying condition) to enhance carbonation. Recent studies have revealed that pre-treatment prior to carbonation had beneficial effects such as reduction of water absorption of the carbonated RCA, improved their strength and CO<sub>2</sub> uptake (Ouyang et al., 2020; Zhan et al., 2018). The significant improvement of RAC was attributed to the enhancement of the interfacial transition zone (ITZ) between the new and old mortar (Zhan et al., 2018; Shaban et al., 2019). This is due to the formation of a dense and compacted ITZ (Zhan et al., 2018; Hanif et al., 2020; Kim et al., 2018). Since the total aggregates occupy 55–80% of concrete by volume (Mindess et al., 2002; Saxena and Pofale, 2017; Tufail et al., 2017; Wang et al., 2018) and coarse aggregates occupy between 40 and 50% of concrete by volume (Saxena and Pofale, 2017; Li et al., 2016), therefore, utilization of the optimized carbonated RCA is a low-cost and eco-friendly alternative to improve the mechanical performance and durability of recycled concrete products.

Previous studies reported that the efficiency of the gas-solid carbonation of RCA is influenced by various experimental conditions, including pre-treatment (spraying/soaking) methods, temperature, carbonation duration, and type of pre-drying conditions (Fang et al., 2020). In most of the studies, the pressurized carbonation of RCA resulted in effective carbonation and improved strength development of RAC (Xuan et al., 2016). Several processing variables including carbonation pressure, moisture contents of samples, CO<sub>2</sub> concentrations were also reported to affect carbonation efficiency (Bao et al., 2017; Huijgen et al., 2005; Zhan et al., 2016; Zhao et al., 2015). In addition, porosity and permeability reduction alongside strength development of concrete have been linked to pressurized carbonation (Bao et al., 2017; Hay et al., 2021; Hyvert et al., 2010). However, the industrial operations of pressurized carbonation is more challenging compared to conventional carbonation by applying a CO<sub>2</sub> gas stream flowing through the recycled aggregates continuously under ambient pressure conditions.

Furthermore, recent studies have also identified moderate elevated temperature carbonation as an effective means to accelerate the rate of carbonation reaction, increase CO<sub>2</sub> uptake and promote the formation of carbonation products both on the surface and interior layers of RCA (Wang et al., 2019, 2020b). Moderate elevated temperature carbonation promotes the formation of CaCO<sub>3</sub> (calcite), enhances CO<sub>2</sub> molecular mobility and prevents pore blockage by a dense protective carbonated layer (Liang et al., 2020; Liu et al., 2018). In contrast, excessive elevated temperature carbonation promotes leaching of Ca<sup>2+</sup> ions, reduces CO<sub>2</sub> solubility leading to high pH of the water and lowers dissolution rate of Ca<sup>2+</sup> (Liang et al., 2020). In addition, there is lack of consensus on the optimum elevated temperature to be utilized to carbonate recycled aggregates (Azdarpour et al., 2017; Qian et al., 2016).

Therefore, this study aims to optimize the conventional carbonation process as stated above for effective carbonation of RCA using regular mortar aggregates (RMA) prepared in the laboratory and validated the optimal conditions by casting concrete using RCA collected from a local recycling plant concrete. The objectives of this study are:

- To investigate the influence of carbonation conditions on the physical properties of regular mortar aggregates
- To optimize the carbonation conditions including pretreatment by using wastewater sourced from concrete batching plants as a calcium-rich additive (Fang et al., 2020) and carbonation conditions using a linear weighted sum method
- To investigate the mechanical and durability properties of RAC containing the optimally treated RCA collected from a local recycling plant.

**Table 2**  
Chemical compositions of conventional and white OPC (% by mass).

Type	CaO	SiO <sub>2</sub>	Al <sub>2</sub> O <sub>3</sub>	Fe <sub>2</sub> O <sub>3</sub>	MgO	Na <sub>2</sub> O	K <sub>2</sub> O	SO <sub>3</sub>
Conventional OPC	63.15	19.61	7.52	3.32	2.14	0.13	0.32	2.03
White OPC	67.60	20.20	4.78	0.21	1.48	–	0.73	4.90

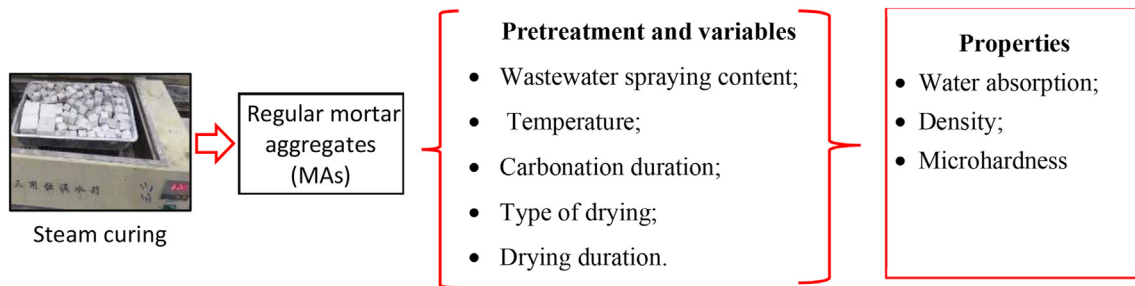


**Fig. 1.** Conventional gas-solid carbonation conditions of RMAs and properties tested.

This study is significant by revealing the optimum carbonation conditions for improving the properties of RCA using the linear weighted sum method. The optimized pretreatment and carbonation time were reduced significantly which makes it attractive to the construction industry. This study also demonstrated the usefulness of Ca-rich wastewater from ready-mixed concrete batching plant for improving the properties of RCA. This study also revealed the correlations between the mechanical and durability properties of concrete prepared with carbonated RCA and conventional coarse aggregates.

## 2. Materials and methodology

### 2.1. Materials and preparation of specimens

Regular mortar aggregates (RMAs) prepared in the laboratory were used in this study to investigate the influence of various pretreatment conditions and gas-solid carbonation test conditions in order to overcome inherent variability of recycled concrete aggregates (RCA) collected from recycling plants (Ouyang et al., 2020). White Ordinary Portland cements (OPC) provided by Green Island Cement Limited complying with ASTM Type 1 were used for preparing RMAs in combination with a siliceous river sand and water, while conventional OPC was used for preparing the new mortar. The white cement helped to easily delineate/differentiate the interface between the old mortar (RMAs) and the new mortar in RAC. The chemical compositions of the conventional and white cements are listed in Table 2. The mix proportion for producing RMAs was 0.5:1:2 (water: cement: sand). After homogeneously mixing the proportioned constituents in a mixer, casting of RMA was done in 20 × 20 × 20 mm steel moulds. The fresh RMAs were demoulded after 24 h and then steam cured for 7 days at 60 °C using a steam bath. White OPC was used in casting the regular mortar aggregates while conventional OPC was used in casting the mortar surrounding the regular mortar aggregates to easily delineate the regular mortar aggregate (representing the old mortar) from the surrounding new mortar. The OPC is called white because of its white colour and it is white because of its negligible ferric oxide content. In addition, conventional OPC was used in the concrete mix designs. The chemical compositions of both conventional OPC and white OPC were presented to show their similarity/differences, calcium oxide (CaO) content and the potential major ions contributing to carbonation. As shown in Table 2, the main difference is that conventional OPC has ferric oxide (Fe<sub>2</sub>O<sub>3</sub>) while white OPC has negligible ferric oxide. The similarity is that both conventional OPC and white OPC have similar CaO and SiO<sub>2</sub> contents, both of which enhance carbonation and also have similar pozzolanic content. Likewise, the major oxide in both conventional OPC and white OPC is CaO. Therefore, white OPC can be utilized to replace

**Table 3**  
Chemical compositions of wastewater (ppm).

Items	Ca <sup>2+</sup>	K <sup>+</sup>	pH
Wastewater	1211.8 ± 69.3	606 ± 59.6	12.8 ± 0.1

conventional OPC to simulate carbonation experiments similar to conventional OPC.

Meanwhile, the specimens for testing the microhardness of the carbonated RMAs and the new mortar were prepared by casting the mortars into 40 × 40 × 40 mm plastic moulds in two layers. First, the fresh new mortar prepared with the conventional OPC was cast into the moulds to reach approximately one-quarter of the height and vibrated for 10 s. Afterwards, respective RMAs (simulating the old mortars) were placed into the middle part of the moulds. Then, the fresh new mortar was further cast to fully cover the RMAs and vibrated again for 10–20 s. These specimens were demoulded after 24 h and steam cured at 60 °C for 7 days in a steam bath as shown in Fig. 1.

The chemical compositions of wastewater collected from a local ready-mixed concrete plant for pretreating the RMA and RCA are shown in Table 3. It was an alkaline wastewater with a rich Ca<sup>2+</sup> content. The precondition and carbonation treatments optimized for the regular mortar aggregates were: (i) amount of wastewater sprayed on the mortar aggregates, (ii) the temperature of carbonation, (iii) drying duration and drying type as shown in Fig. 1. The properties of the regular mortar aggregates investigated were water absorption, density and microhardness as shown in Fig. 1.

### 2.2. Conventional gas-solid carbonation conditions of RMAs and preparation of recycled aggregate concrete (RAC)

#### 2.2.1. Conventional gas-solid carbonation conditions of RMAs

The RMAs were placed in one layer inside a flat container as shown in Fig. 2 (a) and sprayed with wastewater with an inclined hand-held spraying device similar to previous studies (Fang et al., 2020, 2021). Before commencement of spraying, the container with the RMAs was placed on the weighing balance and the balance was zeroed. The RMAs were manually sprayed from the top and to ensure even spraying, the RMAs were turned manually after spraying a quarter of wastewater mass required for spraying. The wastewater quantities sprayed were 20%, 40%, 60% and 80% of total water absorption of RMAs while another RMA was soaked for 5s for comparison. The wastewater used was obtained from a local ready-mixed batching plant in Hong Kong, which was used to wash the returned concrete or concrete trucks (Xuan et al., 2018).

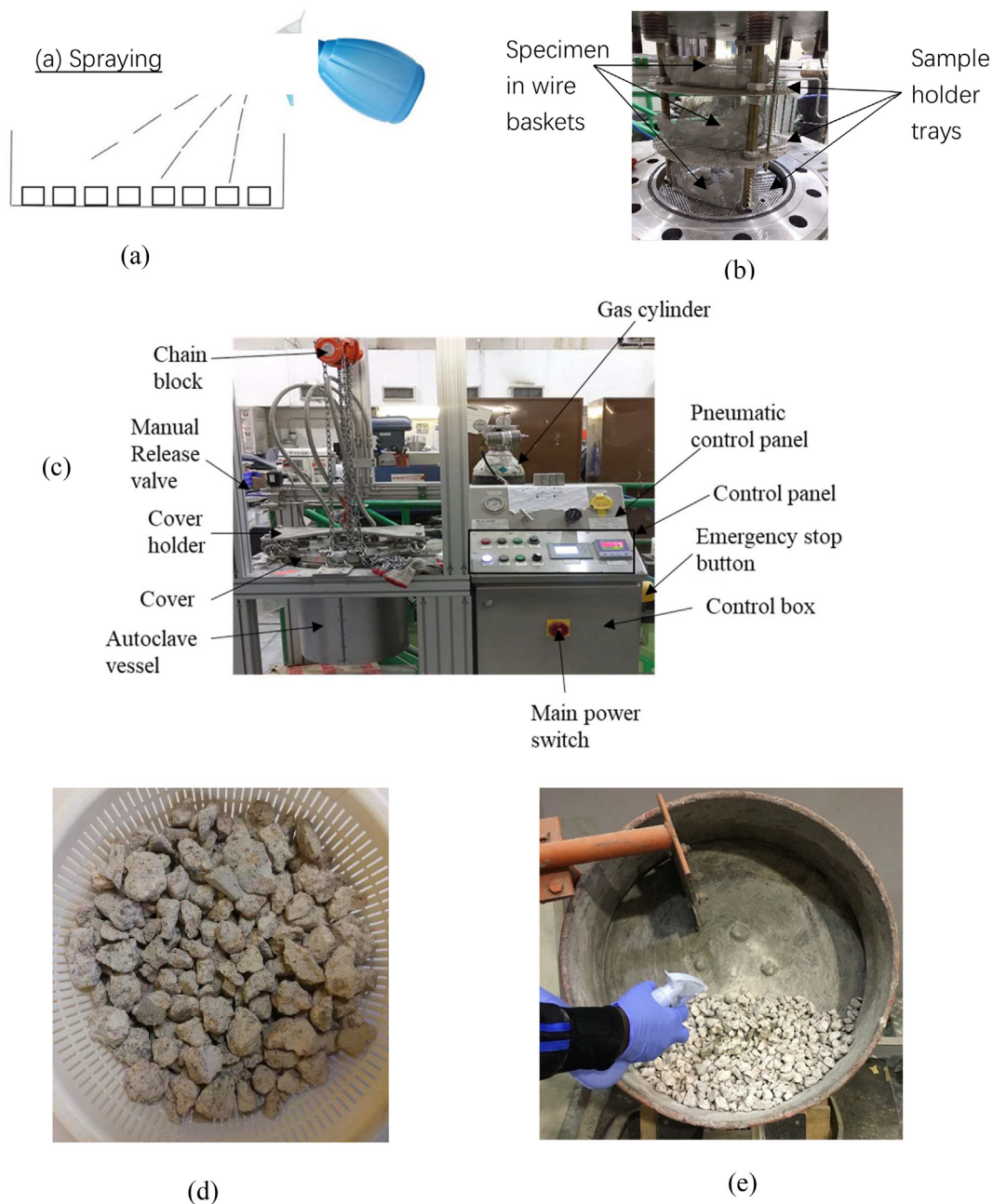


**Fig. 2.** (a) Spraying of regular mortar aggregates (b) Placement of regular mortar aggregates in layered autoclave chamber (c) Autoclave chamber for conventional and pressurized carbonation (d) RCA from pure demolished waste (e) Spraying of RCA with wastewater in inclined mixer using hand-held spraying device.

The wastewater is alkaline with a rich  $\text{Ca}^{2+}$  content. An industrial grade  $\text{CO}_2$  source (>99% purity  $\text{CO}_2$  gas) was used for carbonation of RMAs and RCA in this study. Before placement of RMAs and RCAs into the autoclave chamber, the manual release valve was opened to make sure there is zero pressure in the autoclave. Thereafter, the cover of the autoclave was opened first by loosening the nuts with the torque wrench followed by lifting the autoclave cover with the chain block in combination with the cover holder. To ensure uniform carbonation, the sprayed RMAs were placed in three wire baskets and each basket was placed in each of the three layers of the autoclave as displayed in Fig. 2(b).

With the aid of the chain block and cover holder, the specimens were lowered into the autoclave chamber as shown in Fig. 2 (c). The cover holder was removed and the nuts were tightened with the torque wrench. For conventional carbonation, the manual release valve was opened and there was no need to set pressure while for pressurized carbonation the

valve was closed and the pressure of 1 bar was utilized for pressurized carbonation which is below the 14 bar pressurized capacity of the autoclave equipment. The main power was switched on and with the aid of the temperature and pressure regulators on the control panel, the experimental condition was set and  $\text{CO}_2$  gas was injected into the chamber at a flow rate of  $1 \pm 0.5$  lit/min. The specimen for air drying conditions were air dried at ambient temperature of  $25^\circ\text{C}$  before carbonation inside the laboratory while the specimen for environmental chamber drying were dried at ambient temperature of  $25^\circ\text{C}$  and 50% relative humidity in the environmental chamber and the specimen for direct carbonation were immediately placed in the autoclave after wastewater spraying. The experimental carbonation conditions of RMAs as well as study framework are shown in Fig. 1. The temperature investigated were  $25^\circ\text{C}$ ,  $40^\circ\text{C}$ ,  $60^\circ\text{C}$  and  $80^\circ\text{C}$  while the carbonation duration investigated were 3 h, 6 h, 12 h, and 24 h. In addition, the type

**Table 4**

Water absorption and bulk density of RCAs after subsection to different carbonation conditions.

Test conditions	Water absorption (%)		Bulk density (kg/m <sup>3</sup> )	
	5–10 mm	10–20 mm	5–10 mm	10–20 mm
Uncarbonated	7.73	6.66	2193	2223
FC	7.02	6.39	2220	2330
PC	6.64	5.64	2260	2290
FCSE	6.53	5.90	2250	2270

of drying investigated were air drying before carbonation, environmental chamber drying before carbonation and direct carbonation (no drying). In addition, the effects of drying durations of 3 h, 6 h, 12 h and 24 h for both air drying and environmental chamber drying were investigated.

### 2.2.2. Preparation of recycled aggregate concrete (RAC)

Construction waste materials were collected from a local construction waste recycling company in Hong Kong. The pure concrete waste materials, without stone, were crushed in the laboratory with the aid of automated crusher to produce the RCAs utilized in this study, displayed in Fig. 2 (d). After crushing, the RCAs were sieved into two size ranges namely 5–10 mm and 10–20 mm in line with the mix design. To achieve an even spraying, the RCAs were sprayed in an inclined mixer at a rotating speed of 10 rev/min for every 5 kg batch as shown in Fig. 2 (e). The RCAs were stored in plastic bags and sealed prior to carbonation. After carbonation, they were stored again in plastic bags prior to concrete casting. The RCAs were carbonated using the optimized conditions obtained in RMA experiments. For comparison, the same batch of RCAs were carbonated at different conditions, namely: conventional carbonation at ambient temperature for 24 h (FC), pressurized carbonation at ambient temperature for 24 h (PC) and the optimized elevated temperature carbonation (FCSE) shown in Table 5. Table 4 lists the water absorption and bulk density values of RCAs after subjecting to different carbonation conditions.

Based on dry bulk densities for uncarbonated and carbonated RCAs displayed in Table 4, the RCAs can be described as normal weight aggregates (NWA) since the apparent bulk density range of 2193–2260 kg/m<sup>3</sup> for 5–10 mm RCA and 2223–2330 kg/m<sup>3</sup> for 10–20 mm RCA were within 2100–3000 kg/m<sup>3</sup> required for NWA (BS-EN-206-1, 2000). In addition, it was observed that similar bulk densities were obtained by both optimized conventional carbonation and pressurized carbonation.

Also, it was observed that RAC prepared at optimized conventional carbonation conditions (RAC-FCSE) recorded lower water absorption compared to conventional carbonation (RAC-FC) and achieved comparable water absorption with RCA subjected to pressurized carbonation (RAC-PC). The water absorption obtained in our study was comparable to results from a previous study (Xuan et al., 2017). This implies improvement in RCA properties by conventional carbonation was limited due to the rapid densification of the surface (Fang et al., 2021) and limited supply of moisture. Therefore, optimized carbonation is preferable owing to reduced water absorption of carbonated RCAs and slightly improved

bulk densities. Recent studies also reported similar improvements in RCA properties due to carbonation and wastewater pretreatment (Li et al., 2019; Fang et al., 2020, 2021). However, pre-treatment with wastewater prior to optimized conventional and pressurized carbonations supplied extra Ca<sup>2+</sup> ions in the pore solution which provided extra carbonation products resulting in improved and comparable bulk density and lower water absorption of RC (Fang et al., 2021). Therefore, optimized conventional carbonation and pressurized carbonation have similar carbonation efficiency.

For validation purposes, NAC and four types of RACs prepared with real RCAs from a local recycling plant were cast and the mix proportions are shown in Table 5. The four types of RACs were prepared using 100% replacement of NAs with the carbonated RCAs. Based on their respective water absorptions, water adjustments were made for each batch to ensure the same effective water to cement ratio of 0.6. For each mix, four concrete cylinders with dimensions of  $\Phi 100 \times 200$  mm and four cubes with the dimensions of  $100 \times 100 \times 100$  mm were prepared. After casting, the specimens were covered with a plastic sheet and cured in the laboratory environment for 24 h before demoulding and then cured by full immersion in a water tank at ambient temperature for 7 day and 28 days in the laboratory. The mechanical and durability properties of NAC and RACs, including compressive strength, elastic modulus, sorptivity and bulk electricity conductivity, were tested on specific days and evaluated for comparison.

### 2.2.3. Linear weighted sum method to optimize testing conditions

Optimization studies have attracted a lot of interest in diverse disciplines to reduce production cost, improve production process efficiency and product quality and thereby reduce maintenance expenses. Two commonly utilized optimization techniques in concrete design are Taguchi and Response Surface Methodology. Recent Taguchi optimization studies have shown that processing of concrete materials/concrete at optimized conditions is crucial to achieve best mechanical and durability properties (Chen et al., 2017; Mubina et al., 2019; Onoue et al., 2019). Taguchi design of experiment utilizes fractional factorial design approach to accomplish single, dual and multi-objective optimization of concrete composition and processing conditions in an efficient and systematic manner. Though Taguchi has the potential to reduce experimental runs with L<sup>9</sup> orthogonal arrays, the time and cost-effectiveness of Taguchi approach depends on the array type selected which can range between L9 to L36. Taguchi optimization method utilizes the control factors to eliminate the noise caused by the uncontrollable factors to achieve desired target performance while minimizing the associated loss. Based on desired response, optimum control factors are identified and selected from consideration of the interactive effects of the signal-to-noise ratios.

Taguchi optimization applications are diverse and has been utilized in composition optimization of alternative binders, tertiary blended cements, artificial fly ash aggregates, fly-ash based geopolymer mortar, sandcrete block and lightweight aggregates to mention a few (Chen et al., 2017; Onoue et al., 2019; Ikeagwuani et al., 2020; Peyronnaard and Benzaazoua, 2012; Shivaprasad and Das, 2018; Teirmotashlu et al.,

**Table 5**

Mix proportions for natural/recycled aggregate concrete (kg/m<sup>3</sup>).

Items	Treatment methods of RCAs	Cement	Sand	Agg. 5–10 mm	Agg. 10–20 mm	Effective W/C
Control	Natural aggregates	325	752	282	846	0.6
RAC	No carbonation treatment					
RAC-FC	Conventional carbonation for 24 h <sup>a</sup>					
RAC-PC	Pressurized carbonation for 24 h at 1 bar					
RAC-FCSE	<ul style="list-style-type: none"> <li>•Spray wastewater (60% of water absorption)</li> <li>•Conventional carbonation</li> <li>•Temperature: 60 °C</li> <li>•Duration: 6 h</li> </ul>					

<sup>a</sup> carbonation by applying a CO<sub>2</sub> gas stream flowing through the recycled aggregates continuously under ambient pressure conditions.

2018). Specifically, Taguchi optimization method has been utilized in reduction of production duration of concrete pavement, reduction of production temperature of asphalt mix, eco-friendly and economic design of self-compacting cement composite through 64% cement replacement with supplementary cementitious materials (SCM), improve corrosion durability of RC structures, composition optimization of pervious concrete pavement, permeable asphalt concrete, lightweight concrete, alkali-activated fly ash binders and identify the optimum processing temperature for binders (Cabrera-Luna et al., 2018; Ghanei et al., ; Hinislioglu and Bayrak, 2004; Hoseinpour-Lonbar et al., 2020; Jalal et al., 2019; Joshaghani et al., 2015; Panagiotopoulou et al., 2015; Slebi-Acevedo et al., 2020; Suttaphakdee et al., 2016). The major disadvantages of Taguchi optimization approach are limited visualization of multiple interactive effects of input factors on desired product properties, pre-screening requirement of variables to select the most important factors and their suitable ranges as well as accurate interpretation of results to select optimum conditions.

RSM (response surface methodology) is a mathematical and statistical technique for experimental design, which utilizes desirability optimization approach to select the optimum process conditions or composition (Chelladurai et al., 2020). Most RSM optimization studies focused mainly on material composition optimization and was applied to plastic fibre-reinforced recycled concrete with improved cracking properties and strength, hybrid fibre-reinforced concrete, clay-based self-compacting rigid concrete pavement, mortar, steel fibre reinforced ultra-high performance concrete, rapid-repair cement mortar, blended concrete, design eco-efficient UHPC and pervious recycled concrete (Ahmed et al., 2020; Bankir and Sevim, 2020; Busari et al., 2019; Delarami et al., 2021; Dingqiang et al., 2020; Hassan et al., 2020; Rivera et al., 2019; Zhang et al., 2020). By specifying the desirable minimum and maximum ranges of output properties (quality ranges), the composition or process conditions that gives the highest desirability value is selected as the optimum (Chelladurai et al., 2020; Bankir and Sevim, 2020; Dingqiang et al., 2020). With the aid of in-built ANOVA, input parameters that have significant effect on specified product qualities are found while regression model equations are generated for the responses (Zhao et al., 2015; Bankir and Sevim, 2020). With the aid of the 2D and 3D visualization graphs it generates, RSM aids understanding of the effects of the input parameters on the output responses (product quality) (Delarami et al., 2021; Hassan et al., 2020; Aydemir and Ozkul, 2020; Carrion et al., 2020; Usman et al., 2020).

RSM has enormous capabilities and has been applied to identify significant parameters to optimize both fresh and hardened properties of concrete and varied composition of concrete mixtures to achieve different target slumps and different target strengths (Fardin and dos Santos, 2021; Li et al., 2020b; Mohammed et al., 2018). In addition, RSM can assess the suitability of alternative fine aggregates, SCMs and fibres in concrete, and rank their effectiveness for different construction applications (Rivera et al., 2019; Mohammed et al., 2019a, 2019b; Noroozi et al., 2019; Pinheiro et al., 2020; Qi et al., 2020). RSM has also been applied to study the effect of porous aggregate properties on autogenous shrinkage reduction (Sun et al., 2019) and Los Angeles value of aggregates on concrete strength (Tunc and Alyamac, 2020). In summary, RSM can be utilized in both material selection and process configuration to replace conventional construction materials with new eco-friendly materials without sacrificing desired product qualities. Based on literature review, multi-stage optimization using RSM is scarce as well as its application to concrete durability. The major disadvantage of RSM is large experimental runs requirements which is time-consuming and expensive. To minimize the drawbacks of both optimization methods, a recent study advocated coupling both RSM and Taguchi optimization methods to maximize their benefits (Zhang et al., 2019b).

In this study, linear weighted sum optimization method was applied because it is suitable for one-factor at a time (OFAT) experiments utilized in this research. Linear weighted sum is a simplified optimization method

recommended by some researchers (Sojobi, 2019; Sojobi and Liew, 2020) and has several advantages such as simplified computation and elimination of bias, allows consideration of several properties concurrently and facilitates ranking of the outcome of experimental conditions to determine the optimized experimental condition. In addition, it can also be utilized to rank the effectiveness of the various pretreatment conditions on the physical properties of the aggregates. Optimizing the pretreatment conditions of RCA before usage has the potential to effectively carbonate RCA, shorten the accelerated carbonation process and improve durability of recycled concrete (Xuan et al., 2018; Lin et al., 2015; Zhan et al., 2019). The testing condition with the highest rank is selected as the optimum testing condition which can be utilized in RAC production.

### 2.3. Determination of physical properties of RMAs

The water absorption and bulk density of RMAs before and after carbonation treatments were determined in accordance to BS-EN-1097-6 (BS-EN-1097-6, 2013) as well as the microhardness. The water absorption and bulk density were determined using the wire basket method because it gave more consistent results compared to the pycnometer method, it is less prone to experimental errors, faster and more convenient. Based on previous study (Fang et al., 2020), improvements from carbonation and spraying with wastewater are reflected in reduction of water absorption, increase in bulk density and improvement in microhardness of the RMAs. The variables tested for RMAs were wastewater spraying content, temperature, carbonation duration, type of drying and drying duration.

### 2.4. Determination of mechanical and durability properties of RACs

#### 2.4.1. Compressive strength and elastic modulus

The compressive strength test of RAC was conducted using  $100 \times 100 \times 100$  mm cubes at a loading rate of 0.6 MPa/s at 7 and 28 days. The elastic modulus was determined in accordance with BS-EN-12390 (BS-EN-12390, 2013). The stress-strain curve of concrete was firstly determined at the loading speed of 0.6 MPa/s. The displacement of each concrete specimen was measured by two linear variable differential transformers (LVDTs). The average value was used to calculate the strain of the specimen. The elastic modulus  $E$  was then determined as the secant modulus of the stress-strain curve at the range of 5% to 1/3 peak stress.

#### 2.4.2. Sorptivity (Capillary water absorption)

The sorptivity test of RAC was carried out by using three concrete discs ( $\emptyset 100 \times 50$  mm) in accordance with ASTM-C1585 (ASTM-C1585, 2013). The sorptivity was calculated by using the increase in mass due to water uptake, divided by the cross-sectional area of the specimen exposed to the water. The weight variations of the specimens were measured at 0, 1, 5, 10, 20, 30 min and 1, 2, 3, 4, 5, 6 h for the first stage and 1, 2, 3, 4, 5, 6 and 7 days for the second stage. A recent study reported reduction in sorptivity of carbonated and wastewater-sprayed RCA compared to carbonated and uncarbonated RCA (Fang et al., 2021).

#### 2.4.3. Bulk electrical conductivity

Measurement of bulk electrical conductivity of RAC was performed on three concrete discs ( $\emptyset 100 \times 50$  mm) according to the procedures described in ASTM-C1760 (ASTM-C1760, 2012). This test measured the electrical current through a saturated specimen with a potential (U) of 60 V DC across the ends of the specimen. The current (I) was measured at 1 min after the voltage was first applied. The electrical conductivity ( $\sigma$ , S/m) was then calculated by an equation described in a publication (Xuan et al., 2017). A recent study reported 15.1% reduction in bulk electrical conductivity of concrete with carbonated RCAs (Xuan et al., 2017).

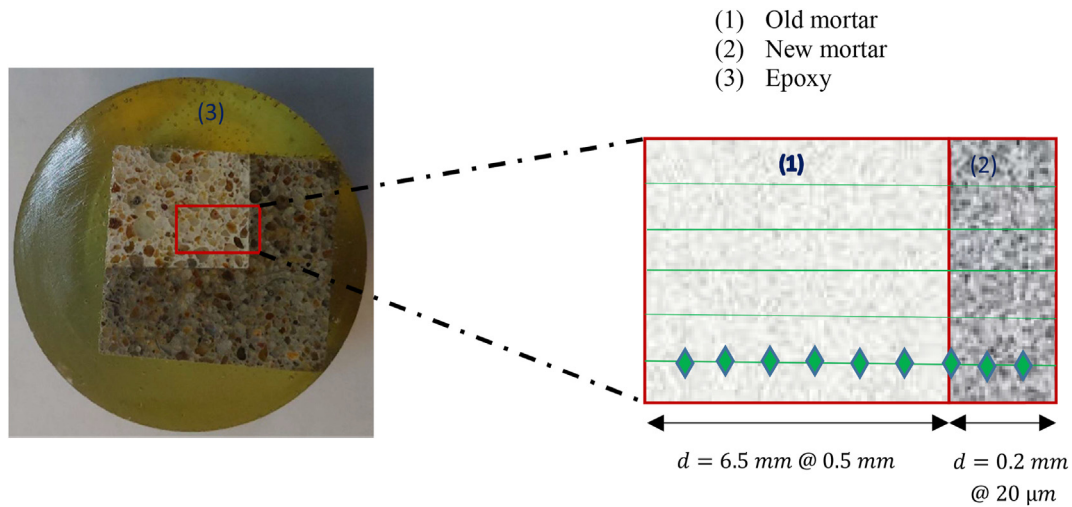


Fig. 3. Test protocol of microhardness indentation around the interface between carbonated RCA (old mortar) and new mortar. Green diamonds represent the testing points.

Table 6  
Experimental conditions and physical properties of RMA.

Items	Conditions	Bulk density (kg/m <sup>3</sup> )	Water absorption (%)
NSC 24-25	-Non-sprayed -Carbonation: Conventional -Carbonation duration: 24 h -Temperature: 25 °C	2108 ± 5.00	6.86±0.15
SC24-40	-Wastewater-sprayed -No drying (Direct carbonation) -Carbonation: Conventional -Carbonation duration: 24 h - Temperature: 40 °C	2089 ±5.95	6.27±0.02
SC12-60	-Wastewater-sprayed -No drying (Direct carbonation) -Carbonation: Conventional -Carbonation duration: 12 h - Temperature: 60 °C	2220±21.92	5.12±0.50
SA12C6-60	-Wastewater-sprayed -Drying type: Air drying at 25 °C -Drying duration: 12 h -Carbonation: Conventional -Carbonation duration: 6 h - Temperature: 60 °C	2167 ±14.13	4.89±0.68
SE6C6-60	-Wastewater sprayed -Drying duration: 6 h -Drying type: Environmental chamber at RH: 50% -Carbonation duration: 6 h - Temperature: 60 °C	2199±14.00	5.06±0.72

2.4.4. Microhardness measurement of ITZ between carbonated aggregates and new mortar

The carbonated RMA and the new mortar were polished by a grinding and polishing equipment (Buehler AutoMet 250) after fixing in an epoxy resin according to the previous established procedures (Zhan et al., 2018). The samples were stored in a vacuum chamber for 24 h before testing the microhardness. The microhardness measurements were performed by using a digital optical Vickers microhardness tester (HVX-1000A, China) equipped with 40 x measurement lens and 10 x objective lens. For the new mortar, the microhardness was conducted up to 160 μm away from the surface of RMA at an interval of 40 μm. For the carbonated RMA, microhardness test was conducted up to 6.5 mm inside the surface of RMA at an interval of 0.5 mm. The microhardness test

protocol is shown in Fig. 3. The number of microhardness measurements at one point is between 6 and 8 and the standard deviation was determined using excel spreadsheet. A recent study reported increase in ITZ of RCA by carbonation treatment (Zhan et al., 2020).

RCA is covered by old mortar and during carbonation of RCA, it is the old mortar that is carbonated. When RCA is used in production of new concrete, a new interfacial zone is formed between the old mortar and the new mortar. Our experiment simulates the old mortar and the new mortar using the carbonated regular mortar aggregates that was surrounded with new mortar. Therefore, the microhardness results of RMA and the surrounding new mortar represents the microhardness of the real RCAs and the new mortar. The advantage of this method is that it avoids the variability of attached mortar of RCAs (Jayasuriya et al., 2018).

3. Results and discussion

3.1. Influence of test conditions on properties of RMAs

3.1.1. Bulk density and water absorption

Table 6 shows the experimental conditions and physical properties of the carbonated RMAs. The 12-h direct carbonation of the wastewater-sprayed RMAs at 60 °C (SC 12-60) exhibited the highest bulk density, followed by the wastewater-sprayed RMAs dried in an environmental chamber for 6 h, and carbonated for 6 h at 60 °C (SE6C6-60). The wastewater-sprayed RMA air-dried for 12 h and carbonated for 6 h at 60 °C (SA12C6-60) had the third highest bulk density. All the three RMAs mentioned above recorded higher bulk densities than that of the non-sprayed RMAs prepared using the conventional carbonation at the ambient temperature (control) (NSC24-25). However, the wastewater-sprayed RMAs carbonated at 40 °C (SC24-40) recorded the lowest bulk density compared to the control (NSC24-25). This implies the wastewater spraying combined with an appropriate elevated temperature and drying condition is beneficial and crucial to improve the density of RMA and carbonation efficiency.

It was also found that the wastewater-sprayed RMAs air-dried for 12 h prior to carbonation (SA12C6-60) recorded the lowest water absorption of 4.89%, which represented a reduction of 28.7% in the water absorption when compared to the control (NSC24-25). This implies that the pre-drying process of the wastewater-sprayed RMAs prior to carbonation is essential to reduce the water absorption of the carbonated RMAs. A low water absorption is desirable for RCA to achieve significant improvement in the mechanical and durability properties of RAC.

**Table 7**  
Optimization of wastewater spraying quantity for the carbonated RMA.

Spray quantity	Final sum	Ranking
20%	1.08	2
40%	0.77	4
60%	1.39	1
80%	1.00	3
Soaking	0.75	5

**Table 8**  
Optimization of temperature for the carbonated RMA.

Temperature (°C)	Final sum	Ranking
40	0.57	2
60	1.94	1
80	0.49	3

**Table 9**  
Optimization of drying condition for the carbonated RMA.

Test conditions	Normalized Final sum	Ranking
3 h direct carbonation	0.81	11
6 h direct carbonation	0.86	10
12 h direct carbonation	0.87	9
24 h direct carbonation	0.89	8
3 h air drying before carbonation	1.08	4
6 h air drying before carbonation	1.07	5
12 h air drying before carbonation	1.11	3
24 h air drying before carbonation	1.05	6
3 h environmental chamber drying before carbonation	0.97	7
6 h environmental chamber drying before carbonation	1.14	2
24 h environmental chamber drying before carbonation	1.15	1

### 3.2. Optimization of test conditions to enhance the properties of RMA

#### 3.2.1. Optimization of test variables using the linear weighted sum method

The test variables (amount of wastewater spraying; temperature; carbonation durations; pre-drying method) were optimized using the linear weighted sum method to optimize the testing conditions. The amount of wastewater sprayed on the surface ranged from 20% to 80% of the water absorption value of the RMA while a soaking treatment in wastewater for 5 s was also used for comparison. The elevated temperature investigated ranged from 40 °C to 80 °C. The optimization results are shown in Table 7. Similarly, for the optimization of the temperature, the results are displayed in Table 8. Subsequently, based on the results, the optimum wastewater spraying amount of 60% and the optimum temperature of 60 °C were recommended to improve the quality of the recycled aggregates.

Table 9 shows the optimization of carbonation durations and drying methods (namely direct carbonation, pre-air drying before carbonation, and pre-environmental-chamber drying before carbonation). It was found that the 24-h pre-environmental-chamber drying attained the best results, followed by the 6 h pre-environmental-chamber drying and the

**Table 10**  
Ranking of influence of test conditions on the physical properties and overall physical properties.

Test conditions	Bulk density	Ranking	WA	Ranking	Overall properties	Ranking
Wastewater spraying	0.95	3	1.07	1	2.82	3
Carbonation temperature	0.64	4	0.97	3	2.90	4
Carbonation duration	1.18	2	1.03	2	3.04	2
Drying process	1.23	1	0.93	4	3.24	1

12 h air drying before carbonation. Since the difference between the 24 h and 6 h pre-environmental-chamber drying (228.25 and 227.81) is insignificant, the 6 h pre-environmental-chamber drying process was preferable to save time and energy costs. Furthermore, to improve the efficiency of the carbonation process, the air-drying processes can also be utilized. Therefore, in this study, a 12-h air drying period, and the 6 h elevated temperature carbonation was selected for treatment of wastewater-sprayed recycled aggregates.

#### 3.2.2. Ranking of various test conditions

The relative importance of all the tested conditions listed in Table 6 was also investigated using the linear weighted sum method and the normalized results are displayed in Table 10. The pre-drying process recorded the highest impact on the bulk density, followed by carbonation duration. In addition, wastewater spraying recorded the highest influence on the water absorption, followed by carbonation duration alone. In terms of the overall physical properties of RCA, a combination of pre-drying and carbonation duration recorded the highest influence, followed by carbonation duration alone and wastewater spraying.

In summary, the optimized carbonation conditions are: (i) spraying with wastewater containing additional  $\text{Ca}^{2+}$  at the level of 60% of the 24-h water absorption of recycled aggregates, (ii) followed by a 12-h air drying period and (iii) 6-h elevated temperature carbonation at 60 °C.

## 4. Mechanical properties and durability of RAC prepared with the optimized carbonated RCA

### 4.1. Mechanical properties of NAC and RACs

After finding the optimized carbonation conditions, and by using the carbonated RCAs listed in Table 4, different types of RACs were prepared as shown in mixture proportions displayed in Table 5. Table 11 lists the mechanical properties of RACs. The optimized RAC-FCSE recorded the highest 7-day compressive strength ( $\text{CS}_7$ ) of 29.1 MPa, while RAC-PC (pressurized carbonation) recorded the highest 28-day compressive strength ( $\text{CS}_{28}$ ), followed by RAC-FCSE with  $\text{CS}_{28}$  of 35.6 MPa. The increase in 28-th day compressive strength ( $\text{CS}_{28}$ ) was 9.1%, 5.8% and 3.9% for RAC-PC, RAC-FCSE and RAC-FC, respectively, compared with the uncarbonated counterpart (RAC). Also, utilization of 100% RCA in concrete resulted in 23.4% reduction in elastic modulus. However, a slight improvement in elastic modulus of concrete with carbonated RCA was observed. The elastic modulus was higher than elastic modulus of 19.9–21.9 GPa obtained in another study with 0% and 3% steel fibre at 100% RCA (Kachouh et al., 2019). Although the mechanical properties in terms of compressive strength and E values did not differ much, higher improvements were noticed in the durability properties.

**Table 11**  
Mechanical properties of RAC prepared with different carbonated RCAs.

Label	$\text{CS}_7$ (MPa)	$\text{CS}_{28}$ (MPa)	Elastic modulus (GPa)
NAC (control)	36.9±1.1	46.8 ±0.9	29.5±0.7
RAC	27.7 ± 0.7	33.6±1.6	22.6± 0.4
RAC-FC	27.2 ± 0.3	34.9 ± 0.1	23.1 ± 0.8
RAC-PC	28.6± 0.4	36.7±0.1	23.1± 0.8
RAC-FCSE	29.1± 0.4	35.6±0.6	23.2± 0.4

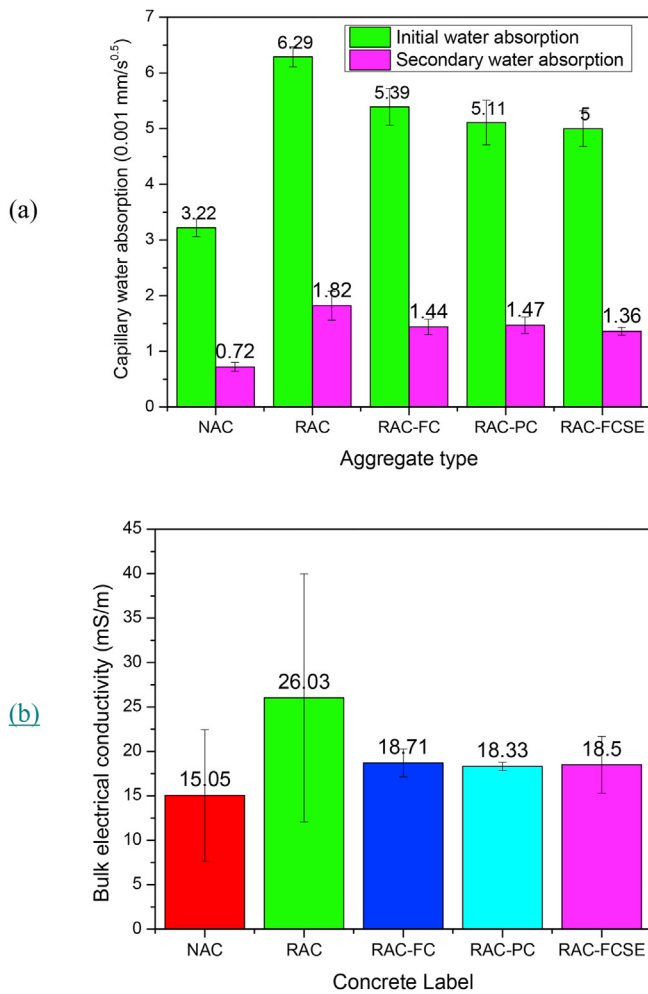


**Fig. 4.** Durability properties of different types of concrete (a) capillary water absorption (b) bulk electrical conductivity. NAC = concrete prepared with natural coarse aggregates; RAC = uncarbonated RCAs; RAC-FC = concrete prepared with conventional carbonated RCAs; RAC-PC = concrete prepared with pressurized carbonated RCAs; RAC-FCSE = concrete prepared with optimized wastewater sprayed and carbonated RCAs.

4.2. Sorptivity and bulk electrical conductivity of RAC

Sorptivity is the ability of concrete to absorb and transmit water and other liquids by capillary suction and provides an engineering measure of microstructure, total porosity and pore diameter which affect the durability properties of concrete (Bao et al., 2020a; Alexandridou et al., 2018; Bravo et al., 2015; Uzoegbo et al., 2016). Sorptivity is a function of the permeability of the pore system of concrete and is a useful durability indicator (Shaikh et al., 2018). On the other hand, bulk electrical conductivity (BEC) provides rapid indication of resistance of concrete to chloride ion penetration and indirectly measures the interconnected porosity of concrete (Habibi et al., 2021; Kurda et al., 2019). Increasing RCA beyond 30% content in concrete tend to accelerate steel corrosion due to the porous nature of RCA (Arredondo-Rea et al., 2019). This situation makes measuring bulk electrical conductivity very important especially where 100% RCA applications is used. Therefore, to avert the accelerated corrosion problem, strengthening the RCA prior to usage in concrete is important.

The durability of concrete was investigated using sorptivity and bulk electrical conductivity and the results are displayed in Fig. 4 (a) and (b). Sorptivity was divided into two types namely initial water absorption (IWA) and secondary water absorption (SWA). As shown in Fig. 4 (a), initial water absorption is higher than secondary water absorption because it measures capillary water absorption within the first 6 h of the experiment and the pores are not yet filled up. But as the experiment progresses, the pores get filled up and the capillary water absorption reduced drastically. Compared to uncarbonated RAC, concrete prepared with optimized carbonation (RAC-FCSE) exhibited 20.5% reduction and 25.3% reduction in initial and secondary water absorption respectively. In addition, concrete prepared with optimized carbonated RCAs and pressurized carbonated RCAs (RAC-PC) recorded similar initial and secondary water absorption. These results demonstrated that the optimized conventional carbonation was as effective as the pressurized carbonation to enhance the properties of RAC. In addition, similar reduction trend was observed in both the initial and secondary capillary water absorption. Surface pre-treatment of RCA increases surface homogeneity, improves ITZ microstructure, and reduces porosity (Al-Bayati et al., 2016). Another study also reported that both capillary water absorption and chloride diffusion were sensitive to the quality of RCA and water-binder ratio and were closely related to the ITZ microstructure (Bao et al., 2020a).

Furthermore, the bulk electrical conductivities of RAC-FC, RAC-PC and RAC-FCSE were similar as shown in Fig. 4 (b), indicating that RAC-

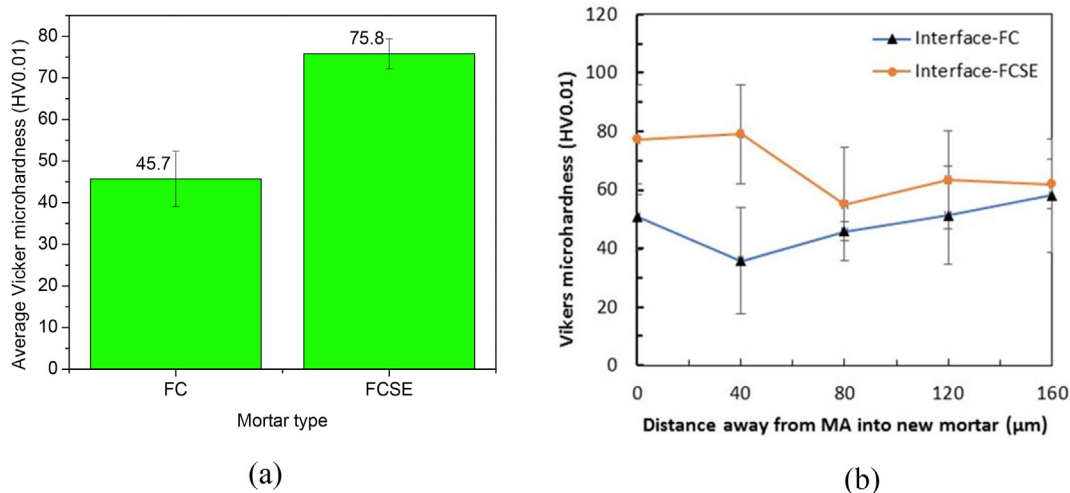


**Fig. 5.** Microhardness comparison of (a) conventionally carbonated (FC) and optimized wastewater-sprayed and carbonated RMA (FCSE) (b) interfacial zone of the new mortar surrounding the RMAs produced by conventional carbonation (FC) and optimized wastewater-sprayed and carbonated RMA (FCSE).

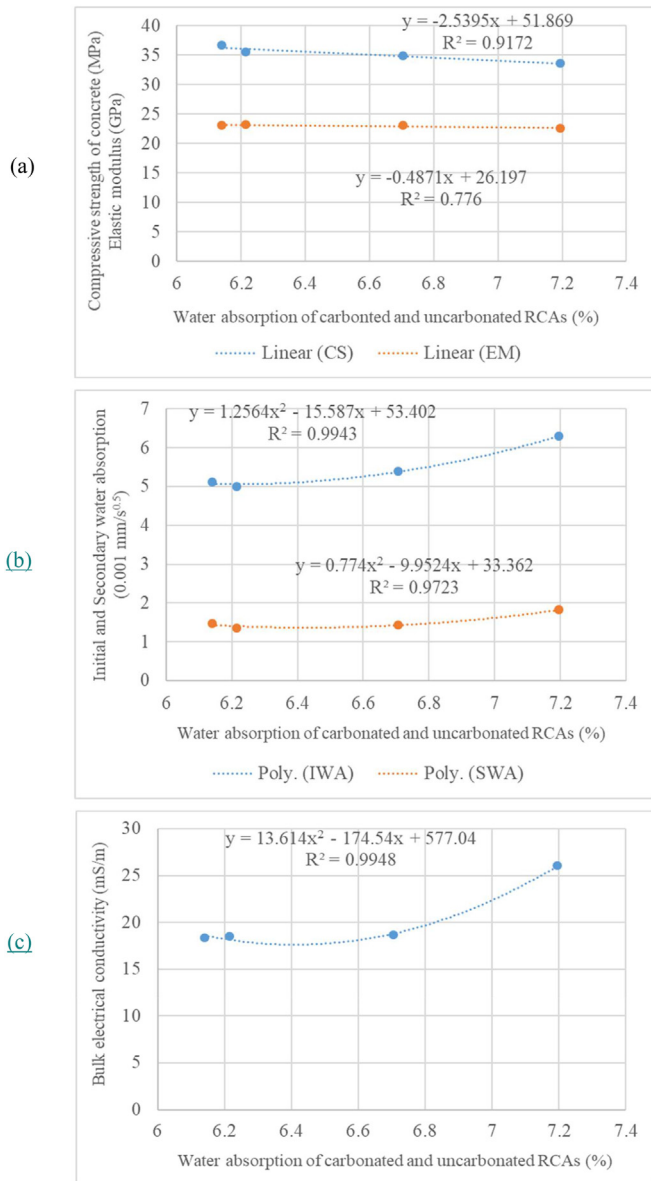


**Fig. 6.** Relationships between water absorption of carbonated and uncarbonated RCAs and (a) compressive strength and elastic modulus (b) initial and secondary water absorption (c) bulk electrical conductivity of concrete prepared with carbonated and uncarbonated RCAs.

FCSE achieved similar bulk electrical conductivity compared with RAC-PC. Bulk electrical conductivity of concrete tended to increase with increase in both initial and secondary water absorption. Conversely, compressive strength tended to decrease with increase in bulk electrical conductivity. Therefore, bulk electrical conductivity is related to the compressive strength and sorptivity of concrete prepared with natural and carbonated RCAs.

#### 4.3. Microhardness of carbonated RMA and new mortar

Microhardness testing is the hardness of a material surface at the microscopic level. Microhardness of aggregate is important because it gives a measure of the strength of the aggregate and the quality improvement derived from different pretreatment methods. Knowledge of the microhardness gives valuable information on the optimum pretreatment conditions in production of high-quality RCA. Microhardness can also reveal the mechanism governing the durability and mechanical

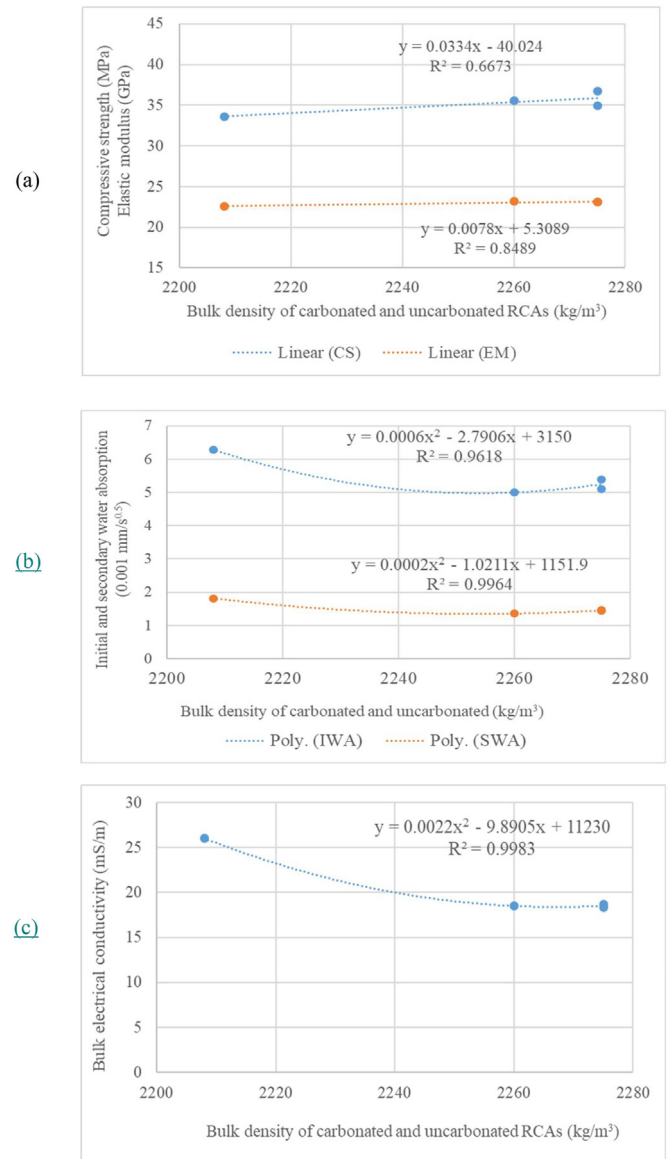


**Fig. 7.** Relationships between bulk density of carbonated and uncarbonated RCAs and (a) compressive strength and elastic modulus (b) initial and secondary water absorption (c) bulk electrical conductivity of concrete prepared with carbonated and uncarbonated RCAs.

properties of the aggregates. RMAs were utilized because their properties were more consistent compared to RCA (Jayasuriya et al., 2018).

Fig. 5 showed the microhardness of the interfacial area of the specimen prepared with the carbonated RMA and new mortar. As shown in Fig. 5 (a), it was observed that adopting the optimized conventional carbonation (FCSE) can enhance the microhardness of RMA itself. Fig. 5(b) showed the improvement of the interface can be up to 160 μm away from the carbonated RMA into the new mortar. A recent study corroborated the microhardness findings reported in (Fang et al., 2020), where the authors attributed the improved microhardness at the ITZ to both porosity reduction and the growth of C-S-H gel due to calcite grains serving as nucleation sites (Zhan et al., 2020).

#### 4.4. Correlation between properties of carbonated RCAs and the mechanical and durability properties of resulting concrete

As shown in Fig. 6 (a), linear decreasing relationship was observed between water absorption of carbonated and uncarbonated RCAs and

**Table 12**  
Correlation coefficients between RCA properties and resulting concrete.

Properties of RCA	Properties of concrete prepared with carbonated and uncarbonated RCAs				
	Compressive strength	Elastic modulus	Initial water absorption	Secondary water absorption	Bulk electrical conductivity
WA	-0.96	-0.88	0.96	0.85	0.88
BD	0.82	0.92	-0.89	-0.9	-0.97

**Table 13**  
Comparison of pretreatment and carbonation effects on RCA in previous research and current study.

Treatment method	RCA type	Water absorption (%)			Reference
		Untreated	After treatment	Reduction (%)	
Direct carbonation	5–20 mm	6.85	5.65	17.5	Kazmi et al. (2020)
Acid-treated & carbonated	5–20 mm		6.43	6.1	
Lime-treated & carbonated	5–20 mm		5.47	20.1	Wang et al. (2020a)
Direct carbonation	2.25–6.25 mm	4.93	4.25	13.8	
Air-dried, lime-treated and carbonated	2.25–6.25 mm		3.91	20.7	Li et al. (2019)
Environmental-chamber dried & carbonated for 3 days	20–30 mm	4.62	3.14	32.0	
Optimized ww spray & carbonation	5–10 mm	7.73	6.53	15.5	Current study
	10–20 mm	6.66	5.90	11.4	

compressive strength and elastic modulus of concrete prepared with carbonated and uncarbonated RCAs. This implies reduction of water absorption of carbonated RCAs leads to improvement in compressive strength and elastic modulus of resulting concrete. However, much better relationship was observed between water absorption of RCAs and compressive strength than elastic modulus (EM). In contrast, a positive polynomial relationship was observed between water absorption of RCAs and concrete prepared with carbonated and uncarbonated RCAs and both initial and secondary water absorption as shown in Fig. 6 (b). This implies reduction in water absorption of carbonated RCAs results in reduction of both initial and secondary water absorption of resulting concrete as well. However, slightly better relationship was observed between water absorption of RCAs and initial water absorption than secondary water absorption of resulting concrete. Likewise, a positive polynomial relationship was observed between WA of carbonated and uncarbonated RCAs and bulk electrical conductivity of concrete prepared with carbonated and uncarbonated RCAs as shown in Fig. 6 (c). This implies reduction in water absorption of carbonated RCAs results in reduction in bulk electrical conductivity of concrete prepared with carbonated and RCAs. Positive polynomial relationship was also observed between bulk electrical conductivity and water absorption of concrete prepared with carbonated and uncarbonated RCAs by another study (Xuan et al., 2017).

With respect to the bulk density of RCAs, a positive linear relationship was observed with both compressive strength and elastic modulus of concrete prepared with carbonated and uncarbonated RCAs as shown in Fig. 7 (a). However, a better relationship was observed between bulk density of RCAs and elastic modulus than compressive strength. Furthermore, a negative polynomial relationship was observed between bulk density of RCAs and both initial and secondary water absorption of concrete prepared with carbonated and uncarbonated RCAs as depicted in Fig. 7 (b). A slightly better relationship was observed with secondary water absorption compared to initial water absorption. Also, a negative polynomial relation was observed between bulk density of RCAs and concrete prepared with carbonated RCAs as shown in Fig. 7 (c). This implies carbonation of RCAs results in increased bulk density of RCAs and reduction in bulk electrical conductivity of concrete prepared with carbonated RCAs. The result of the regression coefficients was also corroborated by the correlation coefficients shown in Table 12. While negative correlation was recorded between water absorption of RCAs and both compressive strength and elastic modulus of concrete, a positive correlation was obtained with initial and secondary water absorption and bulk electrical conductivity of concrete prepared with carbonated RCAs as shown in Table 12. Furthermore, a positive correlation was observed

between bulk density of RCAs and both compressive strength and elastic modulus of concrete prepared with carbonated and uncarbonated RCAs while a negative correlation was observed with initial and secondary water absorption and bulk electrical conductivity. These results imply water absorption and bulk density of carbonated and uncarbonated RCAs have opposite effects on mechanical and durability properties of concrete.

Table 13 shows the comparison of water absorption reductions of RCAs from previous studies which utilized different pretreatment methods. It was observed that water absorption reductions from current study is better than acid-treated, carbonated RCAs. However, it seems less effective comparable to air dried, lime-treated carbonation and those carbonated for longer h and treated with highly concentrated lime. Compared to current study, those methods are more energy demanding and utilizes chemical agents which is not required in wastewater spraying. Therefore, optimized wastewater spraying is an environmentally friendly method for enhancing the carbonation of RACs and improving the mechanical and durability properties of concrete prepared with carbonated RACs.

## 5. Conclusions

Optimization of conventional gas-solid carbonation conditions is important for effective carbonation of RCA. A linear weighted sum method was used to optimize the carbonation conditions of recycled aggregates in this study. The following conclusions can be drawn:

- The adopted linear weighted average sum method was helpful in simultaneously optimizing both the pretreatment and carbonation test conditions involving several input factors and corresponding output responses.
- The optimized pretreatment and gas-solid carbonation conditions: spraying  $\text{Ca}^{2+}$ -rich wastewater at a level of 60% of the 24-h water absorption of the recycled aggregates, followed by a 12-h air drying and 6-h carbonation at 60 °C.
- Concrete prepared by using the optimized conventional carbonated RCAs exhibited improved mechanical and durability properties similar to concrete prepared with pressurized carbonated RCAs.
- The improvement in the mechanical and durability properties of concrete prepared with carbonated RCAs is attributed to the improvement in the microhardness of both the wastewater-sprayed RCAs and the interfacial zones (ITZ) of the new mortar facilitated by optimized pretreatment and carbonation conditions. The

improvement in the microhardness of the new mortar was observed up to 160  $\mu\text{m}$  in the new mortar.

- Although the mechanical properties in terms of compressive strength and E values did not differ much, higher improvements were noticed in the durability properties compared to mechanical properties. For instance with the use of the optimized carbonation conditions, 20.5% reduction in initial water absorption, 25.3% reduction in secondary water absorption and 28.9% reduction in bulk electrical conductivity were recorded for the concrete prepared with the carbonated RCAs compared to uncarbonated RCAs.

### Novelty of this study

This study demonstrated the use of a linear weighted sum method to simultaneously optimize the pretreatment and carbonation test conditions. The optimization of the test conditions produced simplified, and eco-friendly pretreatments and drastically reduced the carbonation duration of RCA from 72 h in previous study (Zhan et al., 2020) to 18 h in this study. In addition, the optimum experimental conditions were validated by casting new concrete using the carbonated RCAs. This study also demonstrated that wastewater derived from ready-mix concrete batching plants can be utilized for spraying the RCAs to improve the carbonation efficiency. Also, the mechanical and durability properties of concrete prepared with RCAs produced from the optimized conventional carbonation and pressurized carbonation were similar. Therefore, optimized conventional carbonation can be utilized as an alternative to pressurized carbonation.

### Funding

This work was supported by CIC (Construction Industry Council) of Hong Kong.

### CRediT author contribution statement

Adebayo Sojobi: Investigation, Validation, Data curation, Formal Analysis, Writing - original draft. Dongxing Xuan: Conceptualization, Methodology, Supervision, Writing - review & editing. Long Li: Resources, Validation. Songhui Liu: Resources, Methodology. Chi Sun Poon: Project administration, Resources, Writing - review & editing.

### Declaration of competing interest

The authors declare that they have no known competing financial interests or personal relationships that could have appeared to influence the work reported in this paper.

### Acknowledgements

The authors appreciate financial support received from the Construction Industry Council, Hong Kong (CIC) (CICR/03/19).

### References

BS-EN-1097-6, 2013. Test for Mechanical and Physical Properties of Aggregates Part 6: Determination of Particle Density and Water Absorption. BSI Standards.  
 BS-EN-12390, 2013. Testing Hardened Concrete Part 13: Determination of Secant Modulus of Elasticity in Compression. British Standards Institution, United Kingdom.  
 BS-EN-206-1, 2000. European Standard. Specification, Performance, Production and Conformity. British Standards Institution, United Kingdom.  
 ASTM-C1585, 2013. Standard Test Method for Measurement of Rate of Absorption of Water by Hydraulic-Cement Concretes. ASTM International.  
 ASTM-C1760, 2012. Standard Test Method for Bulk Electrical Conductivity of Hardened Concrete. ASTM International.  
 Agrela, F., Diaz-Lopez, J., Rosales, J., Cuenca-Moyano, G., Cano, H., Cabrera, M., 2021. Environmental assessment, mechanical behavior and new leaching impact proposal of mixed recycled aggregates to be used in road construction. *J. Clean. Prod.* 280, 1–17.

Ahmed, T.W., Ali, A.A.M., Zidan, R.S., 2020. Properties of high strength polypropylene fiber concrete containing recycled aggregate. *Construct. Build. Mater.* 241, 1–12.  
 Al-Bayati, H., Das, P., Tighe, S., Baaj, H., 2016. Evaluation of various treatment methods for enhancing the physical and morphological properties of coarse recycled concrete aggregate. *Construct. Build. Mater.* 112, 284–298.  
 Alexandridou, C., Angelopoulos, G.N., Coutelieri, F.A., 2018. Mechanical and durability performance of concrete produced with recycled aggregates from Greek construction and demolition waste plants. *J. Clean. Prod.* 176, 745–757.  
 Alsheyab, M., 2021. Recycling of construction and demolition waste and its impact on climate change and sustainable development. *Int. J. Env. Sci. Technol.* 1–10.  
 Arredondo-Rea, S., Coral-Higuera, R., Gomez-Soberon, J., Gamez-Garcia, D., Bernal-Camacho, J., Rosas-Casarez, C., Ungsson-Nieblas, M., 2019. Durability parameters of reinforced recycled aggregate concrete: case study. *Appl. Sci.* 9 (617), 1–13.  
 Aslam, M., Huang, B., Cui, L., 2020. Review of construction and demolition waste management in China and USA. *J. Environ. Manag.* 264, 1–13.  
 Aydemir, E.B., Ozkul, M.H., 2020. Investigation of effect of bitumen chemical composition, elastomeric polymer and paraffin wax additives on the properties of bitumen by using response surface method. *Construct. Build. Mater.* 234, 1–12.  
 Azdarpour, A., Karaei, M.A., Hamidi, H., Mohammadian, E., Barati, M., Honarvar, B., 2017. CO<sub>2</sub> sequestration using red gypsum via pH-swing process: effect of carbonation temperature and NH<sub>4</sub>HCO<sub>3</sub> on the process efficiency. *Int. J. Miner. Process.* 169, 27–34.  
 Bankir, M.B., Sevim, U.K., 2020. Performance optimization of hybrid fiber concrete according to mechanical properties. *Construct. Build. Mater.* 261, 1–18.  
 Bao, Z., Lu, W., 2020. Developing efficient circularity for construction and demolition waste management in fast emerging economies: lessons learned from Shenzhen, China. *Sci. Total Environ.* 724, 1–9.  
 Bao, W., Zhao, H., Li, H., Li, S., Lin, W., 2017. Process simulation of mineral carbonation of phosphogypsum with ammonia under increased CO<sub>2</sub> pressure. *J. CO<sub>2</sub> Util.* 17, 125–136.  
 Bao, Z., Lee, W., Lu, W., 2020a. Implementing on-site construction waste recycling in Hong Kong: barriers and facilitators. *Sci. Total Environ.* 747, 1–11.  
 Bao, J., Li, S., Zhang, P., Ding, X., Xue, S., Cui, Y., Zhao, T., 2020b. Influence of the incorporation of recycled coarse aggregate on water absorption and chloride penetration into concrete. *Construct. Build. Mater.* 239, 1–9.  
 Behera, M., Bhattacharyya, S., Minocha, A., Deoliya, R., Maiti, S., 2014. Recycled aggregate from C&D waste and its use in concrete—A breakthrough towards sustainability in the construction sector: a review. *Construct. Build. Mater.* 68, 501–516.  
 Bonoli, A., Zanni, S., Serrano-Bernado, F., 2021. Sustainability in building and construction within the framework of circular cities and European new green deal. *The contribution of concrete recycling. Sustainability* 13, 1–16.  
 Bravo, M., de Brito, J., Pontes, J., Evangelista, L., 2015. Durability performance of concrete with recycled aggregates from construction and demolition waste plants. *Construct. Build. Mater.* 77, 357–369.  
 Busari, A., Dahunsi, B., Akinmusuru, J., 2019. Sustainable concrete for rigid pavement construction using de-hydroxylated kaolinic clay: mechanical and microstructural properties. *Construct. Build. Mater.* 211, 408–415.  
 Cabrera-Luna, K., Maldonado-Bandala, E.E., Nieves-Mendoza, E.E., 2018. Supersulfated binders based on volcanic raw material: optimization, microstructure and reaction products. *Construct. Build. Mater.* 176, 145–155.  
 Carrion, A.J.D.B., Subhy, A., Rodriguez, M.A.L., Presti, D.L., 2020. Optimisation of liquid rubber modified bitumen for road pavements and roofing applications. *Construct. Build. Mater.* 249, 1–15.  
 Ceia, F., Raposo, J., Guerra, M., Júlio, E., De Brito, J., 2016. Shear strength of recycled aggregate concrete to natural aggregate concrete interfaces. *Construct. Build. Mater.* 109, 139–145.  
 Chelladurai, S.J.S., Murugan, K., Ray, A.P., Upadhyaya, M., Narasimharaj, V., Gnanasikaran, S., 2020. Optimization of process parameters using response surface methodology: a review. *Mater. Today Proc.* 1–4.  
 Chen, H.J., Chang, S.N., Tang, C.W., 2017. Application of the Taguchi method for optimizing the process parameters of producing lightweight Aggregates by incorporating tile grinding sludge with reservoir sediments. *Materials* 10, 1–16.  
 Delarami, A., Moghaddam, A.M., Yazadani, M.R., Najjar, S., 2021. Investigation of the main and interactive effects of mix design factors on the properties of cement emulsified asphalt mortars using mixture design of experiment. *Construct. Build. Mater.* 266, 1–18.  
 Dingqiang, F., Yu, R., Kangning, L., Junhui, T., Zhonghe, S., Chunfeng, W., Shuo, W., Zhenfeng, G., Zhengdong, H., Qiqi, S., 2020. Optimized design of steel fibres reinforced ultra-high performance concrete (UHPC) composites: towards to dense structure and efficient fibre application. *Construct. Build. Mater.* 1–13.  
 Fang, X., Zhan, B., Poon, C.S., 2020. Enhancing the accelerated carbonation of recycled concrete aggregates by using reclaimed wastewater from concrete batching plants. *Construct. Build. Mater.* 239, 1–10.  
 Fang, X., Zhan, B., Poon, C., 2021. Enhancement of recycled aggregates and concrete by combined treatment of spraying Ca<sup>2+</sup> rich wastewater and flow-through carbonation. *Construct. Build. Mater.* 277, 1–9.  
 Fardin, H.E., dos Santos, A.G., 2021. Predicted responses of fatigue cracking and rutting on Roller Compacted Concrete base composite pavements. *Construct. Build. Mater.* 272, 1–11.  
 Ghaffar, S., Burman, M., Braimoh, N., 2020. Pathways to circular construction: an integrated management of construction and demolition waste for resource recovery. *J. Clean. Prod.* 244, 1–9.  
 A. Ghanei, H. Eskandari-Naddaf, A. Davoodi, Corrosion behavior and optimization of air-entrained reinforced concrete, incorporating microsilica, *Struct. Concr.* 19 1472–1480.

- Habibi, A., Ramezani-pour, A., Mahdikhani, M., Bamshad, O., 2021. RSM-based evaluation of mechanical and durability properties of recycled aggregate concrete containing GGBFS and silica fume. *Construct. Build. Mater.* 270, 1–13.
- A. Hanif, Influence of the pretreatment of recycled aggregates, in: F. Pacheco-Torgal, Y. Ding, F. Colangelo, R. Tuladhar, A. Koutamanis (Eds.), *Advances in Construction and Demolition Waste Recycling*, Woodhead Publishing 2020.
- Hassan, W.N.F.W., Ismail, M.A., Lee, H.S., Meddah, M.S., Singh, J.K., Hussin, M.W., Ismail, M., 2020. Mixture optimization of high-strength blended concrete using central composite design. *Construct. Build. Mater.* 243, 1–13.
- Hay, R., Kashwani, G., Celik, K., 2021. Carbonation, strength development, and characterization of calcined limestone as a potential construction material. *Cement Concr. Res.* 139, 1–15.
- Hinislioglu, S., Bayrak, O.U., 2004. Optimization of early flexural strength of pavement concrete with silica fume and fly ash by the Taguchi method. *Civ. Eng. Environ. Syst.* 21 (2), 79–90.
- Hoseinipour-Lonbar, M., Alavi, M.Z., Palassi, M., 2020. Selection of asphalt mix with optimal fracture properties at intermediate temperature using Taguchi method for design of experiment. *Construct. Build. Mater.* 262, 1–10.
- Huijgen, W.J., Witkamp, G.J., Comans, R.N.J., 2005. Mineral CO<sub>2</sub> sequestration by steel slag carbonation. *Environ. Sci. Technol.* 39, 9676–9682.
- Hyvert, N., Sellier, A., Duorat, F., Rougeau, P., Francisco, P., 2010. Dependency of C–S–H carbonation rate on CO<sub>2</sub> pressure to explain transition from accelerated tests to natural carbonation. *Cem. Concr. Res.* 40, 1582–1589.
- Ikeagwuani, C.C., Nwonu, D.C., Ugwu, C.K., Agu, C.C., 2020. Process parameters optimization for eco-friendly high strength sandcrete block using Taguchi method, *Heliyon*, 6, 1–14.
- Jain, N., Garg, M., Minocha, A.K., 2015. Green concrete from sustainable recycled coarse aggregates: mechanical and durability properties. *J. Waste Manage.* 1–8.
- Jalal, M., Teimortashlu, E., Grasley, Z., 2019. Performance-based design and optimization of rheological and strength properties of self-compacting cement composite incorporating micro/nano admixtures. *Compos. B Eng.* 163, 497–510.
- Jayasuriya, A., Adams, M., Bandelt, M., 2018. Understanding variability in recycled aggregate concrete mechanical properties through numerical simulation and statistical evaluation. *Construct. Build. Mater.* 178, 301–312.
- Joshaghani, A., Ramezani-pour, A.A., Golroo, A., 2015. Optimizing pervious concrete pavement mixture design by using the Taguchi method. *Construct. Build. Mater.* 101, 317–325.
- Kabirifar, K., Mojtahedir, M., Wang, C., 2020. Construction and demolition waste management contributing factors coupled with reduce, reuse, and recycle strategies for effective waste management: a review. *J. Clean. Prod.* 263, 1–16.
- Kachouh, N., El-Hassan, H., El-Maaddawy, T., 2019. Effect of steel fibers on the performance of concrete made with recycled concrete aggregates and dune sand. *Construct. Build. Mater.* 213, 348–359.
- Kazmi, S.M.S., Munir, M.J., Wu, Y.F., Patnaikuni, I., Zhou, Y., Xing, F., 2020. Effect of recycled aggregate treatment techniques on the durability of concrete: a comparative evaluation. *Construct. Build. Mater.* 264, 1–13.
- Kim, Y., Yanif, A., Kazmi, S.M.S., Munir, M.J., Park, C., 2018. Properties enhancement of recycled aggregate concrete through pretreatment of coarse aggregates-Comparative assessment of assorted techniques. *J. Clean. Prod.* 191, 339–349.
- Kurda, R., de Brito, J., Silvestre, J., 2019. Water absorption and electrical resistivity of concrete with recycled concrete aggregates and fly ash. *Cement Concr. Compos.* 95, 169–182.
- Kurniawan, T., Lo, W., Singh, D., Othman, M., Avtar, R., Hwang, G., Albadarin, A., Kern, A., Shirazian, S., 2021. A societal transition of MSW management in Xiamen (China) toward a circular economy through integrated waste recycling and technological digitization. *Environ. Pollut.* 277, 1–18.
- Le, H.B., Bui, Q.B., 2020. Recycled aggregate concretes – a state-of-the-art from the microstructure to the structural performance. *Construct. Build. Mater.* 257, 1–15.
- Li, X., Xu, Y., Chen, S., 2016. Computational homogenization of effective permeability in three-phase mesoscale concrete. *Construct. Build. Mater.* 121, 100–111.
- Li, Y., Zhang, S., Wang, R., Zhao, Y., Men, C., 2019. Effects of carbonation treatment on the crushing characteristics of recycled coarse aggregates. *Construct. Build. Mater.* 201, 408–420.
- Li, J., Zuo, J., Wang, G., He, G., Tam, V., 2020a. Stakeholders' willingness to pay for the new construction and demolition waste landfill charge scheme in Shenzhen: a contingent valuation approach. *Sustain. Cities. Soc.* 52, 1–8.
- Li, Z., Lu, D., Gao, X., 2020b. Multi-objective optimization of gap-graded cement paste blended with supplementary cementitious materials using response surface methodology. *Construct. Build. Mater.* 248, 1–11.
- Liang, C., Pan, B., Ma, Z., He, Z., Duan, Z., 2020. Utilization of CO<sub>2</sub> curing to enhance the properties of recycled aggregate and prepared concrete: a review. *Cement Concr. Compos.* 105, 1–14.
- Lin, W.Y., Heng, K.S., Sun, X., Wang, J.Y., 2015. Influence of moisture content and temperature on degree of carbonation and the effect on Cu and Cr leaching from incineration bottom ash. *Waste Manag.* 43, 264–272.
- Liu, W., Su, S., Xu, K., Chen, Q., Xu, J., Sun, Z., Wang, Y., Hu, S., Wang, X., Xue, Y., Xiang, J., 2018. CO<sub>2</sub> sequestration by direct gas-solid carbonation of fly ash with steam addition. *J. Clean. Prod.* 178, 98–107.
- Liu, H., Zhang, J., Li, B., Zhou, N., Li, D., Zhang, L., Xiao, X., 2021. Long term leaching behavior of arsenic from cemented paste backfill made of construction and demolition waste: experimental and numerical simulation studies. *J. Hazard Mater.* 416, 1–13.
- Lu, W., Webster, C., Peng, Y., Chen, X., Zhang, X., 2017. Estimating and calibrating the amount of building-related construction and demolition waste in urban China. *Int. J. Constr. Manag.* 1, 13–24.
- Majhi, R.K., Nayak, A.N., Mukharjee, B.B., 2018. Development of sustainable concrete using recycled coarse aggregate and ground granulated blast furnace slag. *Construct. Build. Mater.* 159, 417–430.
- Mindess, S., Young, J., Darwin, D., 2002. *Concrete*. Pearson Education, London.
- Mohammed, B.S., Khed, V.C., Nuruddin, M.F., 2018. Rubbercrete mixture optimization using response surface methodology. *J. Clean. Prod.* 171, 1605–1621.
- Mohammed, B.S., Al-Hadithi, A.L., Mohammed, M.H., 2019a. Production and optimization of eco-efficient self compacting concrete SCC with limestone and PET. *Construct. Build. Mater.* 197, 734–746.
- Mohammed, B.S., Haruna, S., Wahab, M.M.B.A., Liew, M.S., 2019b. Optimization and characterization of cast in-situ alkali-activated pastes by response surface methodology. *Construct. Build. Mater.* 255, 776–787.
- Mubina, S., Khanra, A.K., Saha, B.P., 2019. Optimization of processing parameters, physical and mechanical properties of SiC – CNF composites using Taguchi approach. *Mater. Today Proc.* 18, 5300–5308.
- Muduli, R., Mukharjee, B.B., 2020. Performance assessment of concrete incorporating recycled coarse aggregates and metakaolin: a systematic approach. *Construct. Build. Mater.* 233, 1–22.
- Noroozi, R., Shafabakhsh, G., Kheyroddin, A., Moghaddam, A.M., 2019. Investigating the effects of recycled PET particles, shredded recycled steel fibers and Metakaolin powder on the properties of RCCP. *Construct. Build. Mater.* 224, 173–187.
- Onoue, K., Iwamoto, T., Sagawa, Y., 2019. Optimization of the design parameters of fly ash-based geopolymer using the dynamic approach of the Taguchi method. *Construct. Build. Mater.* 219, 1–10.
- Ouyang, K., Shi, C., Chu, H., Guo, H., Song, B., Ding, Y., Guan, X., Zhu, J., Zhang, H., Wang, Y., Zheng, J., 2020. An overview on the efficiency of different pretreatment techniques for recycled concrete aggregate. *J. Clean. Prod.* 263, 1–17.
- Panagiotopoulou, C., Tsvilis, S., Kakali, G., 2015. Application of the Taguchi method for the composition optimization of alkali activated fly ash binders. *Construct. Build. Mater.* 91, 17–22.
- Pereira-De-Oliveira, L.A., Nepomuceno, M.C.S., Castro-Gomes, J.P., Vila, M.F.C., 2014. Permeability properties of self-Compacting concrete with coarse recycled aggregates. *Construct. Build. Mater.* 51, 113–120.
- Peyronnaard, O., Benzaazoua, M., 2012. Alternative by-product based binders for cemented mine backfill: recipes optimisation using Taguchi method. *Miner. Eng.* 29, 28–38.
- Pinheiro, C., Rios, S., da Fonseca, A.V., Fernandez-Jimenez, A., Cristelo, N., 2020. Application of the response surface method to optimize alkali activated cements based on low-reactivity ladle furnace slag. *Construct. Build. Mater.* 264, 1–10.
- Qi, Z., Chen, W., Zhang, L., Huang, Z., 2020. An integrated design method for functional cementitious composites (FCC). *Construct. Build. Mater.* 249, 1–14.
- Qian, L., Jiaxiang, L., Liqian, Q., 2016. Effects of temperature and carbonation curing on the mechanical properties of steel slag-cement binding materials. *Construct. Build. Mater.* 124, 999–1006.
- Rao, M.C., Bhattacharyya, S.K., Barai, S.V., 2011. Influence of field recycled coarse aggregate on properties of concrete. *Mater. Struct. Constr.* 44, 205–220.
- Rivera, J.F., Cristelo, N., Fernandez-Jimenez, A., de Gutierrez, R.M., 2019. Synthesis of alkaline cements based on fly ash and metallurgical slag: optimisation of the SiO<sub>2</sub>/Al<sub>2</sub>O<sub>3</sub> and Na<sub>2</sub>O/SiO<sub>2</sub> molar ratios using the response surface methodology. *Construct. Build. Mater.* 213, 424–433.
- Rockson, C., Tamanna, K., Alam, M.S., Rteil, A., 2020. Effect of cover on bond strength of structural concrete using commercially produced recycled coarse and fine aggregates. *Construct. Build. Mater.* 255, 1–16.
- Ruiz, L.A.L., Ramon, X.R., Domingo, S.G., 2020. The circular economy in the construction and demolition waste sector - a review and an integrative model approach. *J. Clean. Prod.* 248, 1–15.
- Saxena, S., Pofale, A., 2017. Effective utilization of fly ash and waste gravel in green concrete by replacing natural sand and crushed coarse aggregate. *Mater. Today Proc.* 4, 9777–9783.
- Shaban, W.M., Yang, J., Su, H., Liu, Q.F., Tsang, D.C.W., Wang, L., Xie, J., Li, J., 2019. Properties of recycled concrete aggregates strengthened by different types of pozzolan slurry. *Construct. Build. Mater.* 216, 632–647.
- Shaikh, F., Chavda, V., Minhaj, N., Arel, H., 2018. Effect of mixing methods of nano silica on properties of recycled aggregate concrete. *Struct. Concr.* 19, 387–399.
- Shivaprasad, K.N., Das, B.B., 2018. Determination of optimized geopolymerization factors on the properties of pelletized fly ash aggregates. *Construct. Build. Mater.* 163, 428–437.
- Silva, R., de Brito, J., Dhir, R., 2019. Use of recycled aggregates arising from construction and demolition waste in new construction applications. *J. Clean. Prod.* 236, 1–16.
- Slebi-Acevedo, C.J., Silva-Rojas, I.M., Lastra-Gonzalez, P., Pascual-Munoz, P., Castro-Fresno, D., 2020. Multiple-response optimization of open graded friction course reinforced with fibers through CRITIC-WASPAS based on Taguchi methodology. *Construct. Build. Mater.* 233, 1–17.
- Sojobi, A.O., 2019. *Experimental Studies on Mechanical Properties of Recycled Concrete*. Department of Architecture and Civil Engineering, City University of Hong Kong, Hong Kong.
- Sojobi, A.O., Liew, K.M., 2020. Flexural behaviour and efficiency of CFRP-laminate reinforced recycled concrete beams. *Compos. Struct.* 260, 1–16.
- Sun, Y., Yu, R., Shui, Z., Wang, X., Qian, D., Rao, B., Huang, J., He, Y., 2019. Understanding the porous aggregates carrier effect on reducing autogenous shrinkage of Ultra-High Performance Concrete (UHPC) based on response surface method. *Construct. Build. Mater.* 222, 130–141.
- Suttaphakdee, P., Dulsang, N., Lorwanishpaisarn, N., Kasemsiri, P., Posi, P., Chindaprasit, P., 2016. Optimizing mix proportion and properties of lightweight concrete incorporated phase change material paraffin/recycled concrete block composite. *Construct. Build. Mater.* 127, 475–483.

- Teirmotashlu, E., Dehestani, M., Jalal, M., 2018. Application of Taguchi method for compressive strength optimization of tertiary blended self-compacting mortar. *Construct. Build. Mater.* 190, 1182–1191.
- Tufail, M., Shahzada, K., Gencturk, B., Wei, J., 2017. Effect of elevated temperature on mechanical properties of limestone, quartzite and granite concrete. *Int. J. Concr. Struct. Mater.* 11 (1), 17–28.
- Tunc, E.T., Alyamac, K.E., 2020. Determination of the relationship between the Los Angeles abrasion values of aggregates and concrete strength using the Response Surface Methodology. *Construct. Build. Mater.* 260, 1–13.
- Turkyilmaz, A., Guney, M., Karaca, F., Bagdatkyzy, Z., Sandybayeva, A., Sirenova, G., 2019. A comprehensive construction and demolition waste management model using PESTEL and 3R for construction companies operating in central Asia. *Sustainability* 11, 1–16.
- Usman, A., Sutanto, M.H., Napiyah, M., Zoorob, S.E., Abdulrahman, S., Saeed, S.M., 2020. Irradiated polyethylene terephthalate fiber and binder contents optimization for fiber-reinforced asphalt mix using response surface methodology. *Ain Shams Eng. J.* 1–12.
- H. Uzoegbo, Dry-stack and compressed stabilized earth-block construction, in: K. Harries, B. Sharma (Eds.), *Nonconventional and Vernacular Construction Materials. Characterisation, Properties and Applications*, Woodhead Publishing 2016, pp. 205–249.
- Wang, Y., Wu, L., Wang, Y., Liu, C., Li, Q., 2018. Effects of coarse aggregates on chloride diffusion coefficients of concrete and interfacial transition zone under experimental drying-wetting cycles. *Construct. Build. Mater.* 185, 230–245.
- Wang, D., Noguchi, T., Nozaki, T., 2019. Increasing efficiency of carbon dioxide sequestration through high temperature carbonation of cement-based materials. *J. Clean. Prod.* 238, 1–10.
- Wang, J., Zhang, J., Cao, D., Dang, H., Ding, B., 2020a. Comparison of recycled aggregate treatment methods on the performance for recycled concrete. *Construct. Build. Mater.* 234, 1–13.
- Wang, N., Feng, Y., Guo, X., 2020b. Atomistic mechanisms study of the carbonation reaction of CaO for high temperature CO<sub>2</sub> capture. *Appl. Surf. Sci.* 532, 1–9.
- Wang, Z., Zhang, Z., Jin, X., 2021. A study on the spatial network characteristics and effects of CDW generation in China. *Waste Manag.* 128, 179–188.
- Xuan, D.X., Shui, Z.H., 2011. Rehydration activity of hydrated cement paste exposed to high temperature. *Fire Mater.* 35 (7), 481–490.
- Xuan, D.X., Molenaar, A.A.A., Houben, L.J.M., 2012. Compressive and indirect tensile strengths of cement-treated mix granulates with recycled masonry and concrete aggregates. *J. Mater. Civ. Eng.* 24 (5), 577–585.
- Xuan, D., Zhan, B., Poon, C.S., 2016. Development of a new generation of eco-friendly concrete blocks by accelerated mineral carbonation. *J. Clean. Prod.* 133, 1235–1241.
- Xuan, D., Zhan, B., Poon, C.S., 2017. Durability of recycled aggregate concrete prepared with carbonated recycled concrete aggregates. *Cement Concr. Compos.* 84, 214–221.
- Xuan, D., Poon, C.S., Zheng, W., 2018. Management and sustainable utilization of processing wastes from readymixed concrete plants in construction: a review. *Resour. Conserv. Recycl.* 136, 238–247.
- Yazdani, M., Kabirifar, K., Frimpong, B., Shariati, M., Mirmozaffari, M., Boskabadi, A., 2021. Improving construction and demolition waste collection service in an urban area using a simheuristic approach: a case study in Sydney, Australia. *J. Clean. Prod.* 280, 1–17.
- Zhan, B.J., Xuan, D.X., Poon, C.S., Shi, C.J., 2016. Effect of curing parameters on CO<sub>2</sub> curing of concrete blocks containing recycled aggregates. *Cem. Concr. Compos.* 71, 122–130.
- Zhan, B.J., Xuan, D.X., Poon, C.S., 2018. Enhancement of recycled aggregate properties by accelerated CO<sub>2</sub> curing coupled with limewater soaking process. *Cement Concr. Compos.* 89, 230–237.
- Zhan, B.J., Xuan, D.X., Zeng, W., Poon, C.S., 2019. Carbonation treatment of recycled concrete aggregate: effect on transport properties and steel corrosion of recycled aggregate concrete. *Cement Concr. Compos.* 104, 1–8.
- Zhan, B.J., Xuan, D.X., Poon, C.S., Scrivener, K.L., 2020. Characterization of interfacial transition zone in concrete prepared with carbonated modeled recycled concrete aggregates. *Cement Concr. Res.* 136, 1–14.
- Zhang, L., Sojobi, A., Liew, K., 2019a. Sustainable CFRP-reinforced recycled concrete for cleaner eco-friendly construction. *J. Clean. Prod.* 233, 56–75.
- Zhang, L.W., Sojobi, A.O., Kodur, V.K.R., Liew, K.M., 2019b. Effective utilization and recycling of mixed recycled aggregates for a greener environment. *J. Clean. Prod.* 236, 1–27.
- Zhang, Q., Feng, X., Chen, X., Lu, K., 2020. Mix design for recycled aggregate pervious concrete based on response surface methodology. *Construct. Build. Mater.* 259, 1–11.
- Zhao, H., Li, H., Bao, W., Wang, C., Li, S., Lin, W., 2015. Experimental study of enhanced phosphogypsum carbonation with ammonia under increased CO<sub>2</sub> pressure. *J. CO<sub>2</sub> Util.* 11, 10–19.

Article

# Stress–Strain Curve and Carbonation Resistance of Recycled Aggregate Concrete after Using Different RCA Treatment Techniques

Long Li, Dongxing Xuan and Chi Sun Poon \*

Department of Civil and Environmental Engineering, The Hong Kong Polytechnic University, Hung Hom, Hong Kong; li.long@connect.polyu.hk (L.L.); d.x.xuan@polyu.edu.hk (D.X.)

\* Correspondence: cecspoon@polyu.edu.hk

**Abstract:** Five recycled coarse aggregate (RCA) treatment techniques including flow-through carbonation, pressurized carbonation, wet carbonation, nano silica (NS) pre-spraying and combined pressurized carbonation with NS pre-spraying, were utilized to improve the performance of recycled aggregate concrete (RAC). The characteristics of the stress–strain curves of RACs including peak stress, peak strain, elastic modulus, ultimate strain and toughness were evaluated after using the above RCA treatment techniques. A theoretical model for natural aggregate concrete was used to analyse the stress–strain curve of RAC. Additionally, the carbonation resistance of RAC after using different RCA treatment techniques were investigated. The results showed that the calculated stress–strain curve of RAC based on the theoretical model matched well with the experimental results. Among the three types of carbonation techniques, pressurized carbonation caused the highest improvement in peak stress and elastic modulus of RAC, followed by flow-through carbonation, the last was wet carbonation. The NS pre-spraying method contributed to even higher improvement in peak stress and elastic modulus of RAC than the pressurized carbonation method. The combined pressurized carbonation with NS pre-spraying exhibited the highest enhancement of RAC because both the RCA and the new interface transition zone (ITZ) were improved. The carbonation resistance of RAC was improved after using all the studied RCA treatment techniques.

**Keywords:** recycled aggregate concrete; nano silica; carbonation treatment; carbonation resistance; stress–strain curve



**Citation:** Li, L.; Xuan, D.; Poon, C.S. Stress–Strain Curve and Carbonation Resistance of Recycled Aggregate Concrete after Using Different RCA Treatment Techniques. *Appl. Sci.* **2021**, *11*, 4283. <https://doi.org/10.3390/app11094283>

Academic Editor: Doo-Yeol Yoo

Received: 2 April 2021

Accepted: 27 April 2021

Published: 9 May 2021

**Publisher's Note:** MDPI stays neutral with regard to jurisdictional claims in published maps and institutional affiliations.



**Copyright:** © 2021 by the authors. Licensee MDPI, Basel, Switzerland. This article is an open access article distributed under the terms and conditions of the Creative Commons Attribution (CC BY) license (<https://creativecommons.org/licenses/by/4.0/>).

## 1. Introduction

A huge amount of construction and demolition waste is being produced globally, which brings in many environmental problems and induces a heavy burden to the limited landfill capacity especially in populated areas such as Hong Kong. In the past decades, much research has been conducted to utilize waste concrete as recycled coarse aggregate (RCA) as partial or whole replacement of natural coarse aggregate (NCA) to produce recycled aggregate concrete (RAC). It can not only reduce the amount of waste concrete, but also decrease the consumption of the natural resources to produce NCA. Nevertheless, because of the inferior physical properties of RCA when compared to NCA, such as higher water absorption, higher porosity, lower density and the presence of initial cracks [1–4], the mechanical properties and durability of RAC are lower than that of natural aggregate concrete (NAC) [5–9]. As a result, the use of RAC is currently still limited, and most of the applications are in non-structural uses [10].

To broaden the application of RAC, many RCA treatment techniques have been proposed to enhance the performance of RAC in the past few decades. In general, there are three categories of RCA treatment techniques in terms of their enhancement mechanisms. The first type is to remove the old mortar that is attached on RCA by mechanical grinding [11,12], heat grinding [13,14], ultrasonic cleaning in water [15], soaking in acid

solutions [16], etc. However, these techniques have obvious disadvantages such as high energy consumption, high CO<sub>2</sub> emission, large amount of waste fines produced and the increased chloride and sulfate contents [3]. The second type is to enhance the old mortar of RCA and the old interface transition zone (ITZ) with methods such as accelerated carbonation [17–20], microbial carbonate precipitation [21], pre-soaking in sodium silicate solution [22] or polyvinyl alcohol [23,24], etc. The third type is to enhance the new ITZ between RCA and new mortar and many surface treatment techniques have been proposed to realize this purpose such as coating RCA with cement slurry [25], pozzolan slurries [26], nano materials [27,28].

Among these RCA treatment techniques, accelerated carbonation has attracted much research interest. According to the review study by Liang et.al [29], four types of acceleration carbonation methods have been utilized to pretreat RCA, which includes standard carbonation [30], pressurized carbonation [17–19], flow-through CO<sub>2</sub> curing (or flow-through carbonation) [31], and water-CO<sub>2</sub> cooperative curing (or wet carbonation) [32]. By using acceleration carbonation, CO<sub>2</sub> reacts with the hydration product of cement such as Ca(OH)<sub>2</sub> and C-S-H and un-hydrated cement clinkers to produce calcium carbonate and silica gel, which densifies the microstructures of RCA [29,33]. As a result, the physical properties of RCA and the performance of RAC could be improved. However, different carbonation treatment methods vary a lot in terms of efficiency and operation easiness. It is necessary to compare the efficiencies of different carbonation treatment methods.

The use of nano silica (NS) to pretreat RCA has also attracted many researchers' interests. Currently, the commonly used technique is by pre-soaking RCA in colloidal NS [27,28,34]. This technique not only improves the physical properties of RCA, but also enhances the new ITZ between RCA and new mortar. However, this technique may have low economic feasibility because it consumes a large amount of NS due to high water absorption of RCA. Recently, a new NS treatment method, namely pre-spraying NS on the surface of RCA, was proposed by the authors [35]. It consumes much less NS than using the NS pre-soaking method. Moreover, it causes better improvement in the performance of RAC than using the pre-soaking method. However, considering the high price of NS, it is necessary to compare the efficiency of the NS pre-spraying treatment with other RCA treatment techniques before using it in real applications.

As mentioned above, the carbonation treatments could enhance the physical properties of RCA while the NS pre-spraying could improve the properties of the new ITZ between RCA and the new mortar. As a result, the performance of RAC could be improved. However, it is not clear which treatment contributes to better. As known, stress–strain curve and carbonation resistance are very important properties for structural concrete. Therefore, the objective of this study is to compare the characteristics of stress–strain curve and carbonation resistance of RAC after using NS pre-spraying and three types of carbonation treatments, namely flow-through carbonation, pressurized carbonation and wet carbonation. Moreover, a combined method with pressurized carbonation and NS-spraying was first adopted in this study. Considering that pressurized carbonation could enhance RCA while the NS pre-spraying method mainly enhance the new ITZ of RAC, it is expected that the combined pressurized carbonation with NS pre-spraying may give rise to an overall better enhancement of RAC.

## 2. Materials and Experimental Program

### 2.1. Materials

The cement used was an ordinary Portland cement CEM I 52.5N. The fine aggregate was a river sand with a fineness modulus of 2.6. The RCA was produced in the laboratory by crushing a batch of waste concrete block collected from a construction site in Hong Kong. The RCA was then sieved into two fractions, namely 10–20 mm and 5–10 mm. Crushed granite with sizes of 10–20 mm and 5–10 mm were used as NCA. The water absorption and particle density of NCA and RCA are shown in Table 1. A commercial colloidal nano silica (NS) with an average size of 106 nm was used. The pH value was 9.5. The density

was 1.206 kg/m<sup>3</sup>. According to the X-ray fluorescence results, the contents of SiO<sub>2</sub> in the colloidal NS was 34.3%, the content of Na<sub>2</sub>O was 0.2% and the rest was water.

**Table 1.** Water absorption and particle density of coarse aggregates.

Aggregate	Size (mm)	Water Absorption (%)	Particle Density (kg/m <sup>3</sup> )
RCA5–10	5–10	6.72%	2229
RCA10–20	10–20	7.77%	2196
NCA5–10	5–10	0.69%	2634
NCA10–20	10–20	0.57%	2602

## 2.2. Different RCA Treatment Techniques

In this study, five RCA treatment techniques, which includes flow-through carbonation, pressurized carbonation, wet carbonation, NS pre-spraying, and the combined pressurized carbonation with NS pre-spraying, were adopted to enhance the performance of RAC. The details of them are given as follows.

### 2.2.1. Flow-Through Carbonation

Before the flow-through carbonation, RCA was pre-conditioned by storing in a chamber (T = 25 °C, RH = 50%) for 24 h, because this is the optimum moisture content for acceleration carbonation [29]. Next, RCA was spread out with one layer in a cylindrical chamber, in which pure CO<sub>2</sub> (>99% purity) was injected from one side and emitted from the other side. The flow rate of CO<sub>2</sub> was 1.0 L/min. After carbonation for 24 h at room temperature (25 °C), RCA was stored in a chamber (T = 25 °C, RH = 50%) for air-drying before using it for casting concrete.

### 2.2.2. Pressurized Carbonation

A carbonation chamber, which was introduced in our previous study [19], was used for the pressurized carbonation. Similar to the flow-through carbonation, RCA was also pre-conditioned by storing in a chamber (T = 25 °C, RH = 50%). Then, RCA was placed inside the carbonation device and CO<sub>2</sub> was injected. The pressure in the chamber was control at +1.0 Bar. The duration of the pressurized carbonation was 24 h. Finally, the treated RCA was air-dried in a chamber (T = 25 °C, RH = 50%) before preparing the concrete.

### 2.2.3. Wet Carbonation

A batch of RCA was placed in layers in porous baskets and soaked in tap water, and the water was stirred by a mechanical device at 200 rpm at 25 °C. Then, CO<sub>2</sub> was injected into the water by using a flow rate controller and a fine-bubble generating diffuser. The water to RCA ratio was controlled at 10:1, and the CO<sub>2</sub> gas flow rate was 0.2 L/min/(100 g RCA). The duration of wet carbonation was 6 h. Finally, RCA was removed from the container and air-dried in a chamber (T = 25 °C, RH = 50%) before preparing the concrete.

### 2.2.4. NS Pre-Spraying

The colloidal NS was pre-sprayed evenly on the surface of air-dried untreated RCA by a liquid spraying device when each batch of 5.0 kg RCA was rotated in an inclined mixer with a rotation speed of 10 rev/min. The amount of colloidal NS was control at 3% of RCA by mass. After that, the treated RCA was stored in a chamber (T = 25 °C, RH = 50%) for air-drying before casting the concrete.

### 2.2.5. Combined Pressurized Carbonation with NS Pre-Spraying

First, a batch of untreated RCA was carbonated by following the procedure of the pressurized carbonation technique above. Then, the colloidal NS was pre-sprayed on the surface of carbonated RCA with the same procedure of NS pre-spraying technique

described above. Finally, the treated RCA was also air-dried in the chamber ( $T = 25\text{ }^{\circ}\text{C}$ ,  $\text{RH} = 50\%$ ) before preparing the concrete.

### 2.3. New Concrete Mix Proportions

Seven new concrete mixtures were prepared with the NCA, untreated RCA, and the RCA treated by five RCA treatment techniques above. The corresponding concrete mixtures were labeled as NAC, RAC-non, RAC-FC, RAC-PC, RAC-WC, RAC-NS and RAC-PCNS, respectively. The control mix proportion is given in Table 2. Considering the water absorption and moisture content of each type of coarse aggregate, extra amounts of water were added to maintain a consistent effective water to cement (W/C) ratio.

**Table 2.** Mix proportions of the control concrete ( $\text{kg}/\text{m}^3$ ).

W/C Ratio	Water	Cement	Sand	Coarse Aggregate (5–10 mm)	Coarse Aggregate (10–20 mm)
0.60	195	325	752	282	846

### 2.4. Testing Methods

#### 2.4.1. Measurement of Water Absorption and Particle Density of RCA

The water absorption and particle density of NCA and RCA were determined in accordance with BS 812-2. The particle density on an oven-dried basis was used in this study. To reduce the variation of sampling, the same batch of RCA was used to testing the water absorption and particle density before and after each type of RCA treatment technique.

#### 2.4.2. Measurement of Density of Hardened Concrete

The density of hardened concrete was measured according to BS EN 12390-7. In this study, the mass of the hardened concrete in water-saturated state was measured. The volume of the hardened concrete was obtained by water displacement. The density of the hardened concrete was determined as the mass divided by the volume.

#### 2.4.3. Measurement of Stress–Strain Curve of Concrete

Three concrete cylinders with the dimension of  $\Phi 100\text{ mm} \times 200\text{ mm}$  were tested for each mixture. The stress–strain curve of concrete was determined according to the loading procedure prescribed in BS EN-12390. The loading rate was  $0.6\text{ MPa/s}$ . The loading was terminated when the force was decreased to around 20% of the peak force after failure. The applied compressive force was measured by an internal force transducer in the testing machine. The displacement of each concrete specimen was measured by two linear variable differential transformers. The stress–strain curve of concrete could be obtained based on the force and average displacement.

#### 2.4.4. Measurement of Carbonation Resistance of Concrete

The carbonation depth of concrete was determined according to an accelerating carbonation method described in BS EN 12390-12 using  $100\text{ mm} \times 100\text{ mm} \times 100\text{ mm}$  cubes. First, the concrete cubes were preconditioned in the indoor laboratory environment for 14 days after curing in water for 28 days. Then, these samples were placed in a storage chamber, in which the  $\text{CO}_2$  concentration was 3.5% by volume with the storage chamber was at a temperature of  $20\text{ }^{\circ}\text{C}$  and relative humidity of 57%, for periods of up to 28 days. After 7 days and 28 days of carbonation test, 2 concrete cubes were split in halves and the fractured surfaces were sprayed with a phenolphthalein indicator, which caused the uncarbonated zone to have pink color and uncarbonated zone the original concrete grey color. The edge of the pink color zone was marked and the distance to the sample surface at 4 points on each of the 4 faces was measured. The average value was calculated as the carbonation depth of each sample.

### 3. Results and Discussion

#### 3.1. Water Absorption and Particle Density of RCA

Compared with that of the original RCA, the percentage of the decrease in water absorption of RCA and the increase in particle density of RCA after using different treatment techniques are shown in Figures 1 and 2, respectively. In the figures, FC, PC, WC, NS and PCNS represent flow-through carbonation, pressurized carbonation, wet carbonation, NS pre-spraying, and the combined pressurized carbonation with NS pre-spraying, respectively. It can be observed that the decrease in water absorption of the smaller size aggregate (RCA5–10) was larger than that the larger aggregate (RCA10–20). Among the three types of carbonation techniques, pressurized carbonation caused the largest reduction (14.4% for RCA5–10 and 11.9% for RCA10–20) in the water absorption value, followed by flow-through carbonation, and the last one was wet carbonation. After using the NS pre-spraying technique, the water absorption of RCA was only slightly decreased (3.6% for RCA5–10 and 2.8% for RCA10–20) which was even less than that of the wet carbonation. When using the combined pressurized carbonation with NS pre-spraying method, the water absorption exhibited the highest decrease (16.8% for RCA5–10 and 14.4% for RCA10–20) suggesting that these two methods can work effectively to enhance RCA. Generally, the increasing trend of the particle density corresponded to the decreasing trend of water absorption after the RCA was subjected to the different treatment methods. However, the magnitude of the increase in the particle density was much lower than that of the decrease in water absorption.

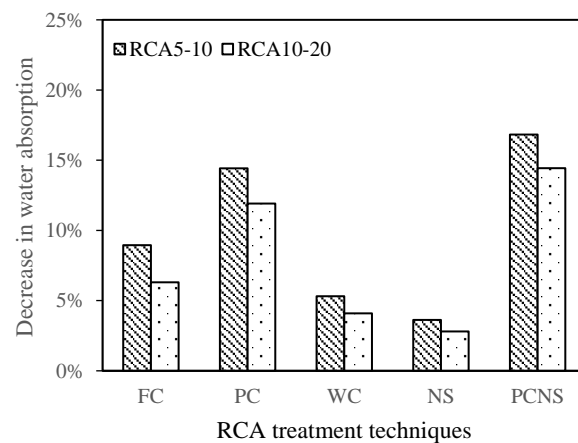


Figure 1. Decreasing rate of water absorption of RCA.

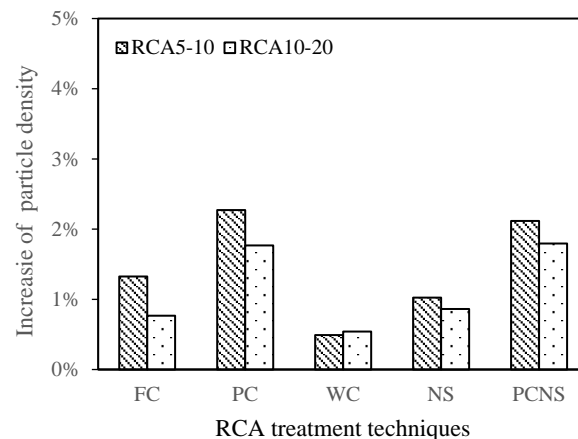


Figure 2. Increasing rate of particle density of RCA.

The images of the un-treated RCA and RCAs treated by three types of carbonation methods after spraying phenolphthalein solution are shown in Figure 3. A pink color

(within dotted line in Figure 3) represents that the area was not carbonated. Some of untreated RCA was shown to have been carbonated on the surface because it was placed in air for a long time. However, the interior of the RCA was not carbonated. After using the pressurized carbonation technique, most of the interior of the RCA was carbonated. When using the flow-through carbonation, the carbonation degree was lower than using the pressurized carbonation. The carbonation depth of RCA was very small after subjecting to the wet carbonation. The results indicate that the water absorption and particle density of RCA are dependent on the carbonation degree of RCA.

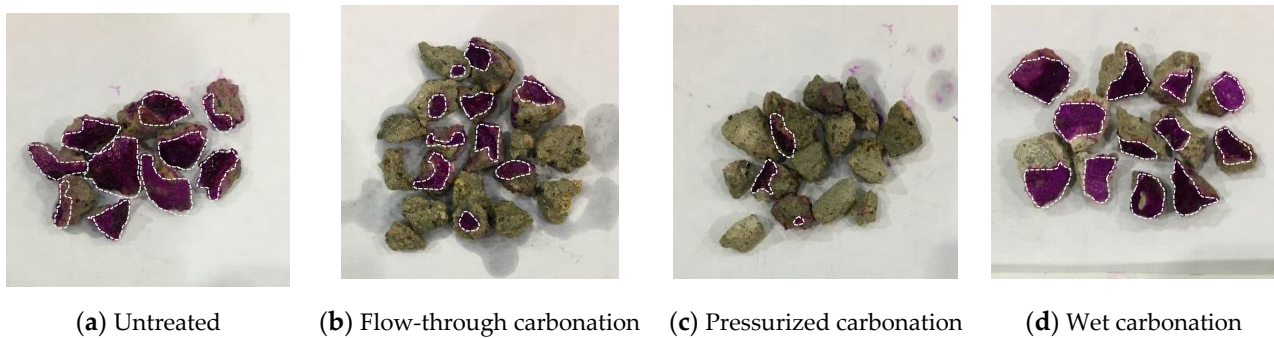


Figure 3. Untreated and carbonated RCAs after spraying phenolphthalein solution.

### 3.2. Density of Hardened Concrete

The densities of the seven groups of new concrete prepared are shown in Figure 4. The results showed that the density of NAC was 5.8% higher than that of RAC prepared with the untreated RCA. That is because the density of NCA was higher than that of RCA. After using the treatments methods, the density of RAC was slightly increased. However, the magnitudes of the increase were very small (<1.0%).

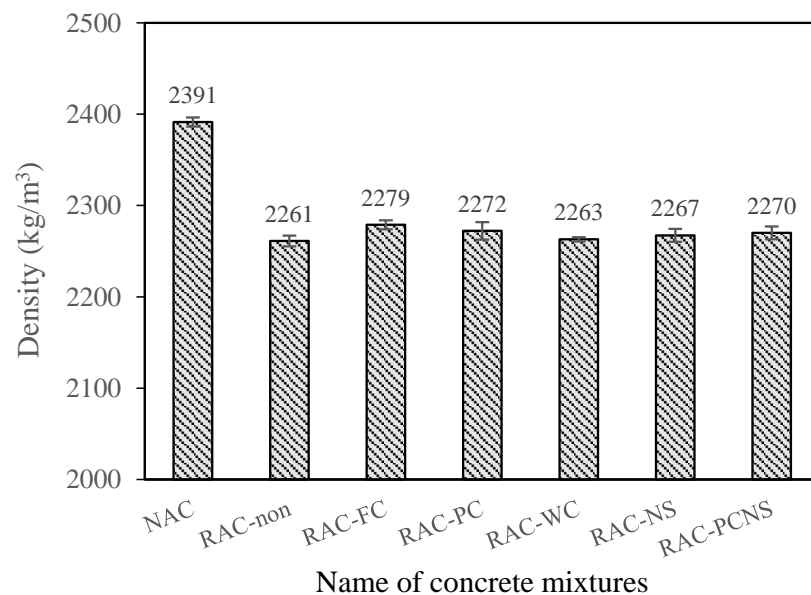


Figure 4. Densities of hardened concretes.

### 3.3. Stress–Strain Curve of Concrete

An example of stress–strain curve of concrete is shown in Figure 5. The peak stress is the maximum stress of the stress–strain curve. The peak strain is defined as the strain corresponding to the peak stress. The ultimate strain is defined as the strain corresponding to the stress at which 50% of the peak strain at the descending part of stress–strain curve is attained [19]. Toughness is an index to represent the energy absorption capacity of a

material, which is often defined as the area under the stress–strain curve. In this study, toughness of the concrete is determined as the area under the stress–strain curve up to the peak stress of the concrete specimens [36]. The elastic modulus ( $E_c$ ) is determined from the stress–strain curve using the following equation

$$E_c = \frac{\sigma_1 - \sigma_2}{\varepsilon_1 - \varepsilon_2} \quad (1)$$

where,  $\sigma_1$  and  $\sigma_2$  are the stresses corresponding to 5% and 1/3 of the peak stress, respectively;  $\varepsilon_1$  and  $\varepsilon_2$  are the strain values at the stress level  $\sigma_1$  and  $\sigma_2$ , respectively.

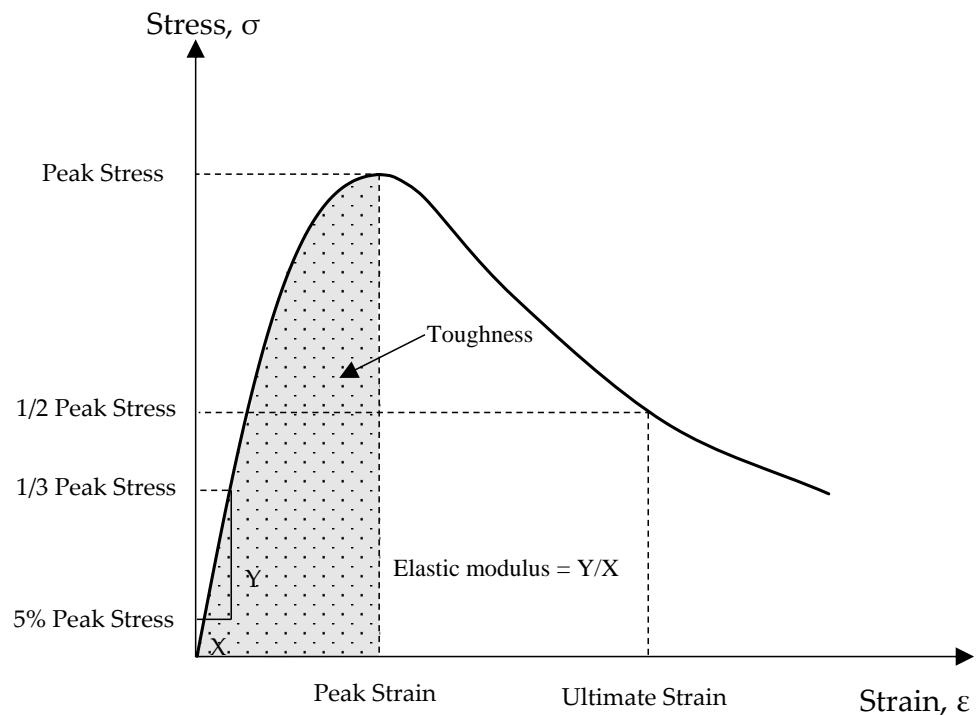


**Figure 5.** An example of stress–strain curve of concrete.

### 3.3.1. Peak Stress

The peak stresses of seven groups of concrete after subjecting to the compressive load test are shown in Figure 6. The peak stress of NAC was 44.7% higher than that of RAC-non. After using the RCA treatment techniques, the peak stresses of the RAC were increased. The increment by using the pressurized carbonation was higher than that of flow-through carbonation and wet carbonation. That is because when using the pressurized carbonation, the carbonation degree of RCA was higher than using other two carbonation techniques, leading to a better enhancement of RCA. The NS pre-spraying technique caused a slightly better improvement in peak stress than using the three types of carbonation techniques. That is because the ITZ between RCA and new mortar was enhanced after using NS pre-spraying, which may be more efficient to improve peak stress than the enhancement of RCA. When using the combined pressurized carbonation with NS pre-spraying technique, the peak stress exhibited the highest increase (17.1%) than the RAC-non because both the new ITZ and the RCA were enhanced. However, it was still significantly lower than that of NAC.

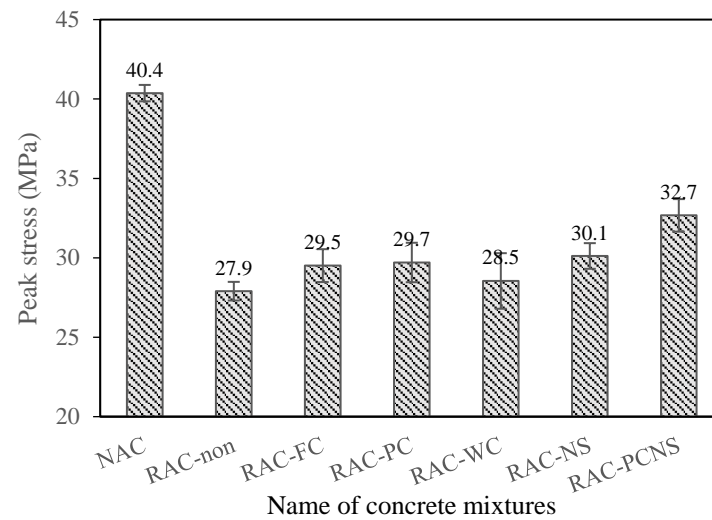


**Figure 6.** Peak stress of hardened concretes.

### 3.3.2. Elastic Modulus

The elastic modulus values of the studied concrete are shown in Figure 7. The elastic modulus of NAC was 30.3% higher than that of RAC-non. However, the elastic modulus of RAC was increased after using the treatment techniques. After using the three carbonation techniques, the increases were less than 3%. The NS pre-spraying technique induced a larger increase (7.6%). It indicates that the enhancement of the new ITZ might be more efficient in improving the elastic modulus of RAC than the enhancement of RCA. After using the combined pressurized carbonation and NS pre-spraying, the elastic modulus exhibited the highest increase (10.0%). However, the magnitude of increase in elastic modulus of RAC was much lower than that of the compressive strength, indicating that the influence of the carbonation treatments and NS pre-spraying treatments on elastic modulus of RAC was less obvious than that on compressive strength.

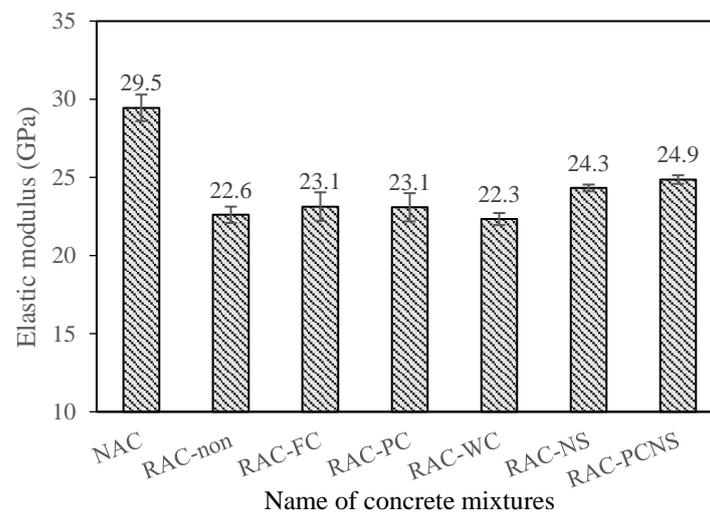


**Figure 7.** Elastic modulus of hardened concretes.

### 3.3.3. Peak Strain

The peak strains of the studied concrete are shown in Figure 8. It showed that the peak strain of NAC was slightly lower (1.2%) than that of RAC, and it did not show significantly changes after using the RCA treatment techniques although some variations were observed.

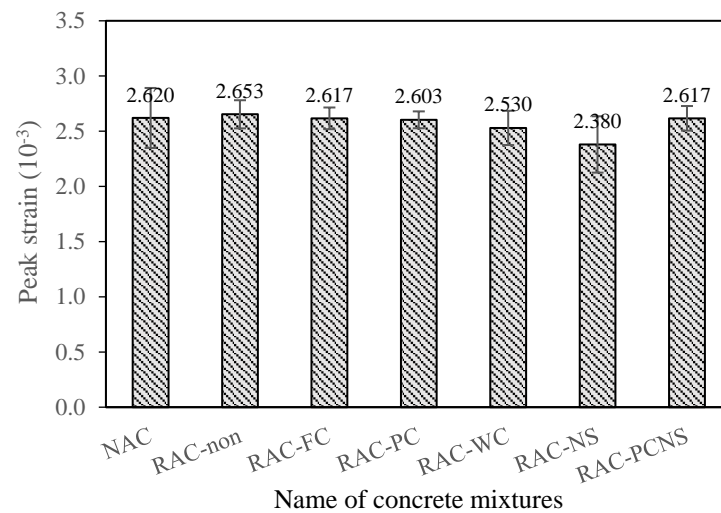


**Figure 8.** Peak strain of hardened concretes.

### 3.3.4. Ultimate Strain

The ultimate strain values of all the concrete specimens are shown in Figure 9. Similar to the peak strain, the ultimate strain of NAC was slightly lower (1.5%) than that of RAC-non. Meanwhile, after using these RCA treatment techniques, the ultimate strain of RAC were all reduced.

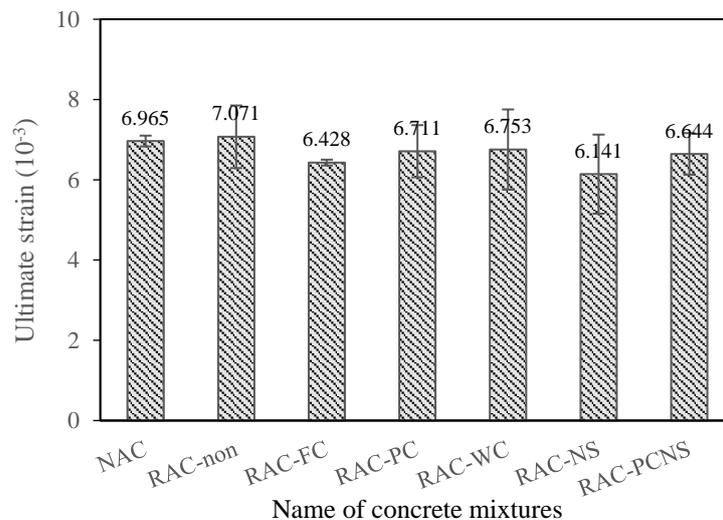


**Figure 9.** Ultimate strain of hardened concretes.

The ratio of ultimate strain to peak strain ( $\epsilon_{cu}/\epsilon_{c,r}$ ) is a parameter used to describe the trend of the descending part of stress–strain curve. A higher  $\epsilon_{cu}/\epsilon_{c,r}$  means that the stress decreases faster with the increase in strain at the descending part of stress–strain curve and the material is more brittle. The average  $\epsilon_{cu}/\epsilon_{c,r}$  values of the NAC, RAC-non, RAC-FC, RAC-PC, RAC-WC, RAC-NS and RAC-PCNS were 2.52, 2.66, 2.46, 2.54, 2.66, 2.57, 2.54. After using the RCA treatment techniques, the  $\epsilon_{cu}/\epsilon_{c,r}$  values were all reduced slightly, indicating that the stress decreased faster with the increase in strain at the descending part of stress–strain curve which also mean the concrete has become more brittle.

### 3.3.5. Toughness

The toughness values of all concrete specimens are shown in Figure 10. It shows that the toughness of NAC was 37.8% higher than that of RAC-non. After using the flow-through carbonation and pressurized carbonation, the toughness of RAC increased

slightly (2.7% and 2.6%, respectively) because of the increased peak stress and elastic modulus. However, the toughness of RAC decreased slightly (5.7% and 5.6%, respectively) when using the wet carbonation and NS pre-spraying techniques. It may be related to the decreased peak strain. After using the combined pressurized carbonation with NS pre-spraying technique, the toughness of RAC showed much a larger increase, which was 13.1%.

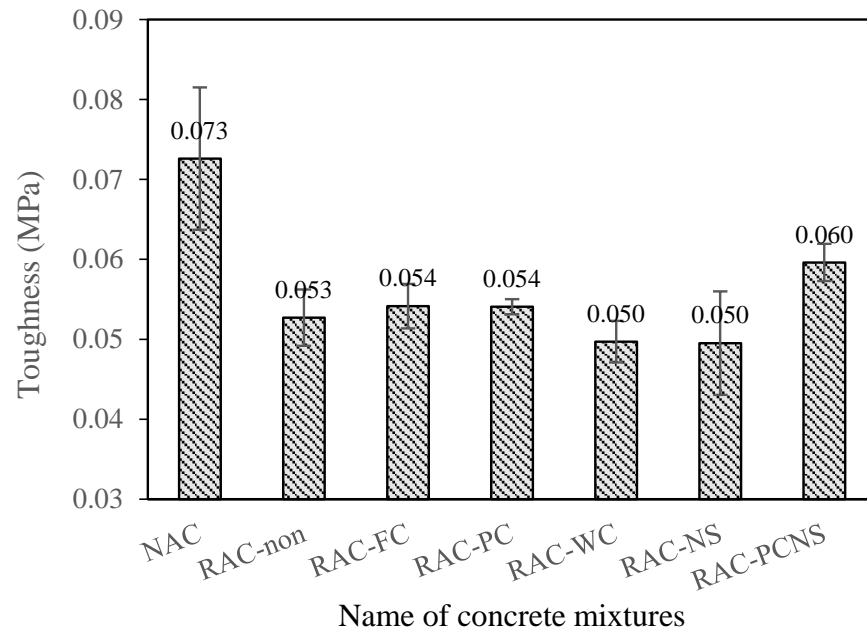


Figure 10. Toughness of hardened concretes.

### 3.3.6. Theoretical Model of Stress–Strain Curve

The theoretical model for stress–strain curve of NAC in the Chinese standard (GB50010-2010) was used to analyse the test results in this study. In the standard, the uni-axial compressive stress–strain curve is determined as

$$\sigma = (1 - d_c)E_c\varepsilon \tag{2}$$

$$d_c = \begin{cases} 1 - \frac{\rho_c n}{n-1+x^n} & x \leq 1 \\ 1 - \frac{\rho_c}{\alpha_c(x-1)^2+x} & x > 1 \end{cases} \tag{3}$$

$$n = \frac{E_c \varepsilon_{c,r}}{E_c \varepsilon_{c,r} - f_{c,r}} \tag{4}$$

$$\rho_c = \frac{f_{c,r}}{E_c \varepsilon_{c,r}} \tag{5}$$

$$x = \frac{\varepsilon}{\varepsilon_{c,r}} \tag{6}$$

where,  $\sigma$  and  $\varepsilon$  are the stress and the strain of concrete, respectively,  $d_c$  is a parameter for damage evolution;  $f_{c,r}$  is the representative value of compressive strength of concrete, it was taken as the peak stress in this study;  $\varepsilon_{c,r}$  is peak strain of concrete;  $E_c$  is elastic modulus of concrete.  $\alpha_c$  is a parameter for the descending part of stress–strain curve, which is related to the value of  $\varepsilon_{cu}/\varepsilon_{c,r}$ . Based on the Chinese standard GB50010-2010,  $\alpha_c$  was taken as 0.74, 1.06, 1.36 and 1.65 when the value of  $\varepsilon_{cu}/\varepsilon_{c,r}$  was 3.0, 2.6, 2.3 and 2.1, respectively. When the  $\varepsilon_{cu}/\varepsilon_{c,r}$  was between the above values (3.0, 2.6, 2.3 and 2.1), the value of  $\alpha_c$  was determined by linear interpolation method.

For each type of concrete, a typical experimental stress–strain curve was compared with the calculated one based on the above equations, as shown in Figure 11. It was

observed that the experimental stress–strain curves of all concrete specimens matched well the calculated stress–strain curves. Therefore, it is suggested that the uni-axial compressive stress–strain curve of concrete given in the Chinese code (GB50010-2010) are also suitable to the RACs with untreated RCA and treated RCA by using the studied RCA treatment techniques.

### 3.4. Carbonation Resistance of Concrete

The carbonation depth of concrete is an indicator to assess its carbonation resistance. A lower carbonation depth means better carbonation resistance. The 7-day and 28-day carbonation depths of the seven groups of concrete are shown in Figure 12. The 7-day and 28-day carbonation depths of RAC-non were much higher than that of NAC. After using the flow-through carbonation, pressurized carbonation and combined pressurized carbonation with NS pre-spraying, the 7-day carbonation depths of the corresponding RACs were even larger than that of RAC-non. However, the 28-day carbonation depths of these RACs were lower than that of RAC-non. That is because the carbonated RCAs influenced the carbonation depth of RAC in two ways. On one hand, the carbonated RCA was more densified than that of non-treated RCA, which reduced the penetration rate of  $\text{CO}_2$  and thus caused a reduction of carbonation depth. On the other hand, the carbonated RCA itself influenced the measurement of average carbonation depth, leading to an increase in carbonation depth of RAC. When the carbonation depth of RAC was small, the influence of carbonated RCA on the measurement carbonation depth was more significant. On the contrary, the influence of the carbonated RCA on the  $\text{CO}_2$  penetration rate played a more important role when the carbonation depth became larger. It could be anticipated that when the carbonation resistant test duration was longer, the adverse effect of the carbonated RCA could be reduced.

In contrast, the 7-day and 28-day carbonation depths of RAC-WC were both reduced compared to RAC-non. That is because only the surface layer of the RCA was carbonated after using the wet carbonation. At the same time, more nano- $\text{CaCO}_3$  particles were formed on the surface of RCA, which would densify the new ITZ [37]. As a result, the penetration rate of  $\text{CO}_2$  was reduced. This is similar to the NS pre-spraying method, in which the new ITZ could be significantly enhanced by the NS particles [35]. That is why the 7-day and 28-day carbonation depths of RAC-NS were similar to that of RAC-WC.

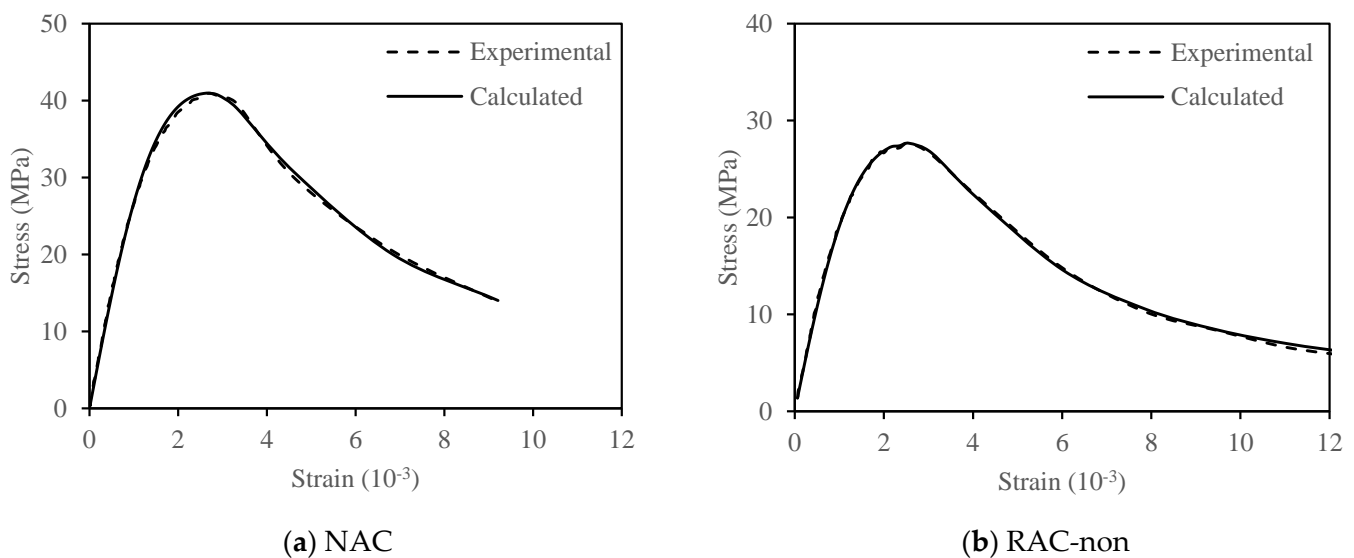
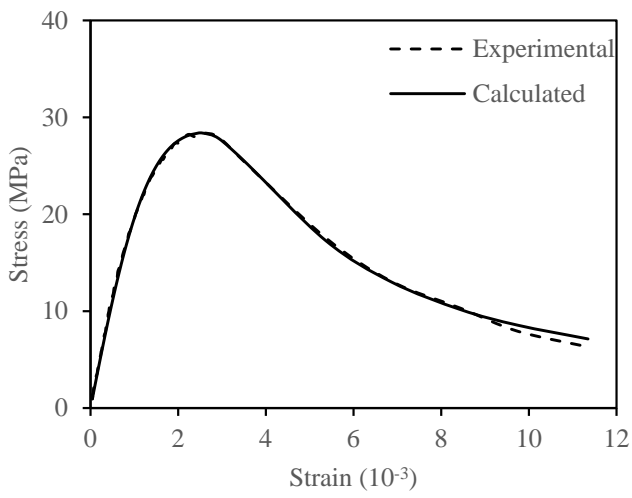
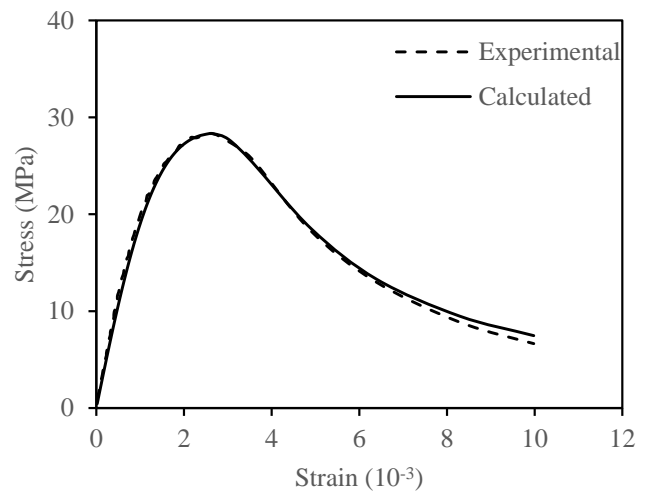


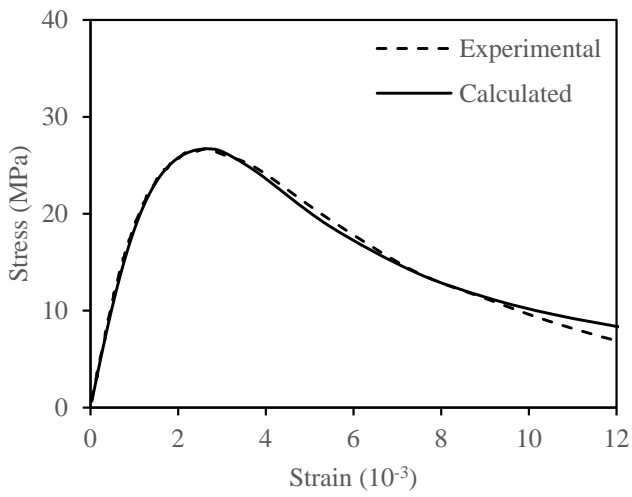
Figure 11. Cont.



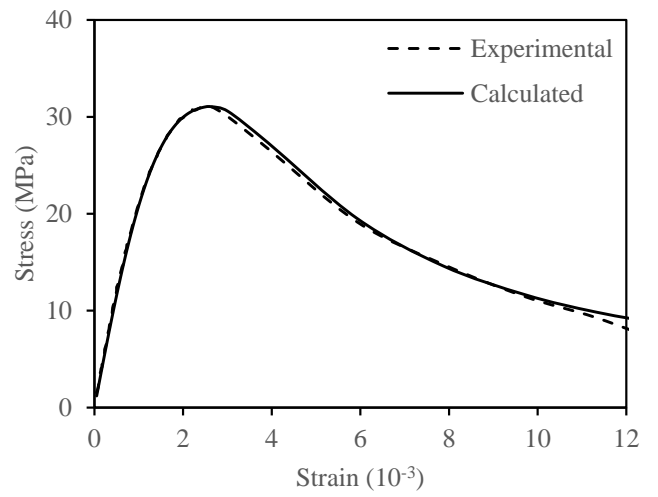
(c) RAC-FC



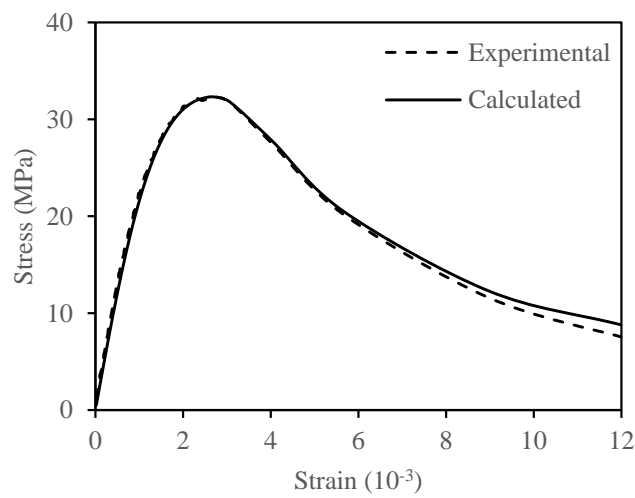
(d) RAC-PC



(e) RAC-WC



(f) RAC-NS



(g) RAC-PCNS

Figure 11. Experimental and calculated stress–strain curve.

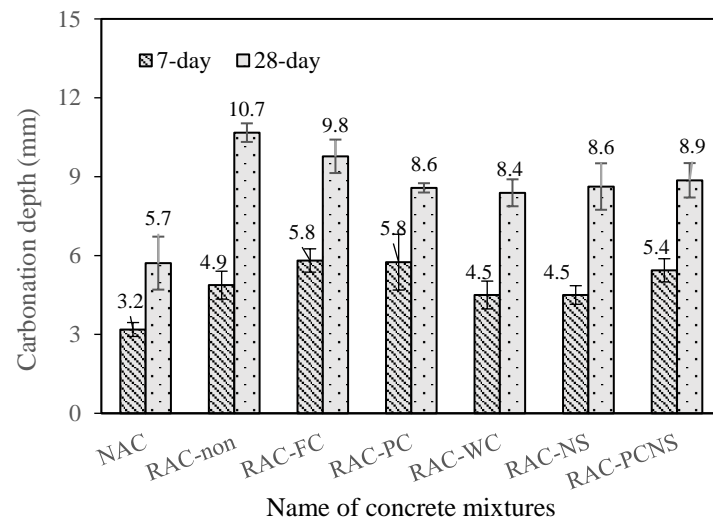


**Figure 12.** Carbonation depth of hardened concrete.

#### 4. Conclusions

In this study, the stress–strain curves and carbonation resistance of recycled aggregate concrete (RAC) after using different recycled coarse aggregate (RCA) treatment techniques were investigated, namely flow-through carbonation, pressurized carbonation, wet carbonation, nano silica (NS) pre-spraying and combined pressurized carbonation with NS pre-spraying. Based on the testing results, the main findings can be summarized below.

- (1) The theoretical model for stress–strain curve of natural aggregate concrete was also suitable to RAC after subjecting to the RCA treatment techniques. For all the studied RCA treatment techniques, the peak stress and elastic modulus of RAC were enhanced, but the peak strain did not show significant changes while the ultimate strain exhibited some reduction.
- (2) The 7-day carbonation depths of RAC after using flow-through carbonation, pressurized carbonation and combined pressurized carbonation with NS pre-spraying were larger than that of RAC using untreated RCA because of the negative effect of the carbonated RCA. However, the 28-day carbonation depth of RAC was reduced after using all the studied RCA treatment techniques. In other words, the carbonation resistance of RAC could be enhanced by using these techniques.
- (3) Comparing the efficiency of different RCA treatment techniques in enhancement of the peak stress and elastic modulus, the combined pressurized carbonation with NS pre-spraying was the best because both the RA and the new ITZ between RA and the new mortar was enhanced, followed by NS pre-spraying, pressurized carbonation and flow-through carbonation, and the worst was the wet carbonation because only the surface layer of RA was carbonated. The combined pressurized carbonation with NS pre-spraying can significantly improve the performance of RAC, which was better than the other four techniques. Thus, this technique has potential to be used in practical applications.

**Author Contributions:** Conceptualization, L.L., D.X. and C.S.P.; methodology, L.L., D.X. and C.S.P.; software, L.L.; validation, L.L.; formal analysis, L.L.; investigation, L.L.; resources, L.L. and C.S.P.; data curation, L.L.; writing—original draft preparation, L.L.; writing—review and editing, D.X. and C.S.P.; visualization, L.L.; supervision, D.X. and C.S.P.; project administration, D.X. and C.S.P.; funding acquisition, C.S.P. All authors have read and agreed to the published version of the manuscript.

**Funding:** This work was supported by Construction Industry Council (Hong Kong): CICR/03/19.

**Institutional Review Board Statement:** Not applicable.

**Informed Consent Statement:** Not applicable.

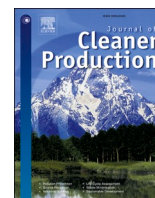
**Acknowledgments:** The authors wish to thank the Hong Kong Construction Industry Council (CIC) for financial support.

**Conflicts of Interest:** The authors declare no conflict of interest.

## References

1. Poon, C.S.; Shui, Z.H.; Lam, L. Effect of microstructure of ITZ on compressive strength of concrete prepared with recycled aggregates. *Constr. Build. Mater.* **2004**, *18*, 461–468. [[CrossRef](#)]
2. Xuan, D.; Zhan, B.; Poon, C.S. Durability of recycled aggregate concrete prepared with carbonated recycled concrete aggregates. *Cem. Concr. Compos.* **2017**, *84*, 214–221. [[CrossRef](#)]
3. Xuan, D.X.; Zhan, B.J.; Poon, C.S. Assessment of mechanical properties of concrete incorporating carbonated recycled concrete aggregates. *Cem. Concr. Compos.* **2016**, *65*, 67–74. [[CrossRef](#)]
4. Li, L.; Xiao, J.; Xuan, D.X.; Poon, C.S. Effect of carbonation of modeled recycled coarse aggregate on the mechanical properties of modeled recycled aggregate concrete. *Cem. Concr. Compos.* **2018**, *89*, 169–180. [[CrossRef](#)]
5. Xiao, J.Z.; Li, J.B.; Zhang, C. Mechanical properties of recycled aggregate concrete under uniaxial loading. *Cem. Concr. Res.* **2005**, *35*, 1187–1194. [[CrossRef](#)]
6. Ryu, J.S. An experimental study on the effect of recycled aggregate on concrete properties. *Mag. Concr. Res.* **2002**, *54*, 7–12. [[CrossRef](#)]
7. Topçu, I.B.; Sengel, S. Properties of concretes produced with waste concrete aggregate. *Cem. Concr. Res.* **2004**, *34*, 1307–1312. [[CrossRef](#)]
8. Etxeberria, M.; Vázquez, E.; Mari, A.; Barra, M. Influence of amount of recycled coarse aggregates and production process on properties of recycled aggregate concrete. *Cem. Concr. Res.* **2007**, *37*, 735–742. [[CrossRef](#)]
9. Xuan, D.; Molenaar, A.A.A.; Houben, L.J.M. Compressive and indirect tensile strengths of cement-treated mix granulates with recycled masonry and concrete aggregates. *J. Mater. Civ. Eng.* **2012**, *24*, 577–585. [[CrossRef](#)]
10. Ke, X.; Xu, D.; Cai, M. Experimental and numerical study on the eccentric compressive performance of RAC-encased RACFST composite columns. *Eng. Struct.* **2020**, *224*, 111227. [[CrossRef](#)]
11. Quattrone, M.; Angulo, S.C.; John, V.M. Energy and CO<sub>2</sub> from high performance recycled aggregate production. *Resour. Conserv. Recycl.* **2014**, *90*, 21–33. [[CrossRef](#)]
12. Nagataki, S.; Gokce, A.; Saeki, T.; Hisada, M. Assessment of recycling process induced damage sensitivity of recycled concrete aggregates. *Cem. Concr. Res.* **2004**, *34*, 965–971. [[CrossRef](#)]
13. Bru, K.; Touze, S.; Bourgeois, F.; Lippiatt, N.; Menard, Y. Assessment of a microwave-assisted recycling process for the recovery of high-quality aggregates from concrete waste. *Int. J. Miner. Process.* **2014**, *126*, 90–98. [[CrossRef](#)]
14. Akbarnezhad, A.; Ong, K.C.G.; Zhang, M.H.; Tam, C.T.; Foo, T.W.J. Microwave assisted beneficiation of recycled concrete aggregates. *Constr. Build. Mater.* **2011**, *25*, 3469–3479. [[CrossRef](#)]
15. Katz, A. Treatments for the improvement of recycled aggregate. *J. Mater. Civ. Eng.* **2004**, *16*, 597–603. [[CrossRef](#)]
16. Tam, V.W.Y.; Tam, C.M.; Le, K.N. Removal of cement mortar remains from recycled aggregate using pre-soaking approaches. *Resour. Conserv. Recycl.* **2007**, *50*, 82–101. [[CrossRef](#)]
17. Zhan, B.J.; Poon, C.S.; Liu, Q.; Kou, S.C.; Shi, C.J. Experimental study on CO<sub>2</sub> curing for enhancement of recycled aggregate properties. *Constr. Build. Mater.* **2014**, *67*, 3–7. [[CrossRef](#)]
18. Kou, S.C.; Zhan, B.J.; Poon, C.S. Use of a CO<sub>2</sub> curing step to improve the properties of concrete prepared with recycled aggregates. *Cem. Concr. Compos.* **2014**, *45*, 22–28. [[CrossRef](#)]
19. Li, L.; Poon, C.S.; Xiao, J.; Xuan, D.X. Effect of carbonated recycled coarse aggregate on the dynamic compressive behavior of recycled aggregate concrete. *Constr. Build. Mater.* **2017**, *151*, 52–62. [[CrossRef](#)]
20. Zhang, J.K.; Shi, C.J.; Li, Y.K.; Pan, X.Y.; Poon, C.S. Performance enhancement of recycled concrete aggregates through carbonation. *J. Mater. Civ. Eng.* **2015**, *27*, 04015029. [[CrossRef](#)]
21. Grabiec, A.M.; Klama, J.; Zawal, D.; Krupa, D. Modification of recycled concrete aggregate by calcium carbonate bio deposition. *Constr. Build. Mater.* **2012**, *34*, 145–150. [[CrossRef](#)]
22. Cheng, H.L.; Wang, C.Y. The influence of sodium silicate on the properties of recycled aggregate. *Gypsum Cem. Build.* **2005**, *12*, 12–14.
23. Kou, S.C.; Poon, C.S. Properties of concrete prepared with PVA-impregnated recycled concrete aggregates. *Cem. Concr. Compos.* **2010**, *32*, 649–654. [[CrossRef](#)]
24. Mansur, A.; Santos, D.; Mansur, H. A microstructural approach to adherence mechanism of poly (vinyl alcohol) modified cement systems to ceramic tiles. *Cem. Concr. Res.* **2007**, *37*, 270–282. [[CrossRef](#)]
25. Tam, V.W.Y.; Gao, X.F.; Tam, C.M. Microstructural analysis of recycled aggregate concrete produced from two-stage mixing approach. *Cem. Concr. Res.* **2005**, *35*, 1195–1203. [[CrossRef](#)]
26. Li, J.; Xiao, H.; Zhou, Y. Influence of coating recycled aggregate surface with pozzolanic powder on properties of recycled aggregate concrete. *Constr. Build. Mater.* **2009**, *23*, 1287–1291. [[CrossRef](#)]
27. Zhang, H.; Zhao, Y.; Meng, T.; Shah, S.P. Surface treatment on recycled coarse aggregates with nanomaterials. *J. Mater. Civ. Eng.* **2015**, *28*, 04015094. [[CrossRef](#)]

28. Zeng, W.; Zhao, Y.; Zheng, H.; Poon, C.S. Improvement in corrosion resistance of recycled aggregate concrete by nano silica suspension modification on recycled aggregates. *Cem. Concr. Compos.* **2020**, *106*, 103476. [[CrossRef](#)]
29. Liang, C.; Pan, B.; Ma, Z.; He, Z.; Duan, Z. Utilization of CO<sub>2</sub> curing to enhance the properties of recycled aggregate and prepared concrete: A review. *Cem. Concr. Compos.* **2020**, *105*, 103446. [[CrossRef](#)]
30. Shi, C.J.; Wu, Z.M.; Cao, Z.J.; Ling, T.C.; Zheng, J.L. Performance of mortar prepared with recycled concrete aggregate enhanced by CO<sub>2</sub> and pozzolan slurry. *Cem. Concr. Compos.* **2018**, *86*, 130–138. [[CrossRef](#)]
31. Kashef-Haghighi, S.; Ghoshal, S. CO<sub>2</sub> sequestration in concrete through accelerated carbonation curing in a flow-through reactor. *Ind. Eng. Chem. Res.* **2009**, *49*, 1143–1149. [[CrossRef](#)]
32. Maciej, Z.; Jørgen, S.; Jan, S.; Pawel, D.; Frank, B.; Mohsen, B.H. Phase assemblage and microstructure of cement paste subjected to enforced, wet carbonation. *Cem. Concr. Res.* **2020**, *130*, 105990.
33. Bertos, M.F.; Simons, S.J.R.; Hills, C.D.; Carey, P.J. A review of accelerated carbonation technology in the treatment of cement-based materials and sequestration of CO<sub>2</sub>. *J. Hazard Mater.* **2004**, *112*, 193–205.
34. Faiz, S.; Vimal, C.; Najj, M. Effect of mixing methods of nano silica on properties of recycled aggregate concrete. *Struct. Concr.* **2018**, *19*, 387–399.
35. Li, L.; Xuan, D.X.; Sojobi, A.O.; Liu, S.; Chu, S.H.; Poon, C.S. Development of nano-silica treatment methods to enhance recycled aggregate concrete. *Cem. Concr. Compos.* **2021**, *118*, 103963. [[CrossRef](#)]
36. Kazmi, S.M.S.; Munir, M.J.; Wu, Y.F.; Patnaikuni, I.; Zhou, Y.; Xing, F. Influence of different treatment methods on the mechanical behavior of recycled aggregate concrete: A comparative study. *Cem. Concr. Compos.* **2019**, *104*, 103398. [[CrossRef](#)]
37. Zhan, B.J.; Xuan, D.X.; Poon, C.S.; Scrivener, K.L. Characterization of interfacial transition zone in concrete prepared with carbonated modeled recycled concrete aggregates. *Cem. Concr. Res.* **2020**, *136*, 106175. [[CrossRef](#)]



# Fast enhancement of recycled fine aggregates properties by wet carbonation

Xiaoliang Fang, Dongxing Xuan, Peiliang Shen, Chi Sun Poon\*

Department of Civil and Environmental Engineering, The Hong Kong Polytechnic University, Hung Hom, Kowloon, Hong Kong

## ARTICLE INFO

Handling editor: Prof. Jiri Jaromir Klemes

### Keywords:

Wet carbonation  
Recycled concrete aggregate  
Upcycling  
Fine aggregate

## ABSTRACT

Accelerated carbonation for recycled concrete aggregate (RCA) was one of the effective and economic solutions for improving the quality of RCA and its concrete products. Previously, a fast wet carbonation method was developed and proved to be effective for property enhancement of the coarse fraction of RCA by transforming the carbonation reaction from a gas-solid phase to a liquid-solid phase. Fast carbonation is essential for providing a cost effective and practical method of enhancing the properties of recycled aggregates by waste CO<sub>2</sub>. In order to investigate the feasibility and effectiveness of the wet carbonation for fine RCA (i.e. < 5 mm), this study presents the results of an experimental investigation by using both laboratory-prepared well-hydrated cement paste particles (RCP) and a real fine RCA derived from demolished concrete. The test results of RCP revealed that a quick 10-min wet carbonation densified the surface layer of the particles, significantly reduced the volumes of the pores less than 10 nm, and increased the carbonation products by 2.6–3.5%. Moreover, the mortar specimens prepared by the carbonated fine RCA showed a 32.6% increase in compressive strength and a 6.4% reduction in drying shrinkage. Replacing 50% river sand by the carbonated fine RCA in the new mortar would not result in significant property deterioration.

## 1. Introduction

Accelerated carbonation, regarded as one of the effective and economic approaches for improving the quality of recycled concrete aggregate (RCA), was commonly carried out by either pressurized carbonation or flow-through carbonation in a gas-solid state (Liang et al., 2020; Luo et al., 2021; Zhang et al., 2017). However, normally a relatively long carbonation time (hours to days) is required (Fang et al., 2017; Luo et al., 2021; Pan et al., 2017; Siriruang et al., 2016; Thiery et al., 2013). Therefore, attempts have been made to improve the efficiency and effectiveness of accelerated carbonation for RCA recently, such as utilizing Ca<sup>2+</sup>-rich wastewater, Ca(OH)<sub>2</sub> solution, limewater as pre-treatment methods coupled with accelerated carbonation to enhance its efficiency (Fang et al., 2020b; Pan et al., 2017; Zhan et al., 2018).

Also, the majority of the RCA related application uses coarse RCA while the recycling and reuse of the fine portion of RCA are limited (Evangelista and De Brito, 2014). Khatib (2005) utilized < 5 mm RCA in concrete to replace natural fine aggregates and reported a reduction of compressive strength but a higher strength development after 28 days,

and higher shrinkage when compared with conventional concrete. Deteriorations in properties including water absorption, resistance to chloride-ion penetration, water sorptivity, water penetration under pressure were reported (Mardani-Aghabaglou et al., 2015; Sim and Park, 2011). Hence, the applications of fine RCA in concrete were usually limited to low-graded products. For example, incorporating fine RCA in the controlled low strength materials (CLSM) is one of the applications due to its low strength requirement (Crouch et al., 1998; Fang et al., 2019; Zhang et al., 2018).

Thereby, attempts have been made to improve the recycling and reuse of the fine RCA. A study introduced extra grinding and sieving to produce RCA powder (RCCF) which would be able to replace up to 25% Portland cement without altering the properties of the mortars (Okri-Nelfia et al., 2016). Some studies introduced additional additives into the concrete mixtures to compensate for the negative effects induced by the fine RCA and/or utilized various methods to enhance the properties of the fine RCA (Anastasiou et al., 2014; Cuenca-Moyano et al., 2014; Pan et al., 2017).

Due to the advantages of using carbonation in coarse RCA enhancement, it had been used for fine RCA as well (Shi et al., 2016;

\* Corresponding author.

E-mail addresses: [17901090r@connect.polyu.hk](mailto:17901090r@connect.polyu.hk) (X. Fang), [cecspon@polyu.edu.hk](mailto:cecspon@polyu.edu.hk) (C.S. Poon).

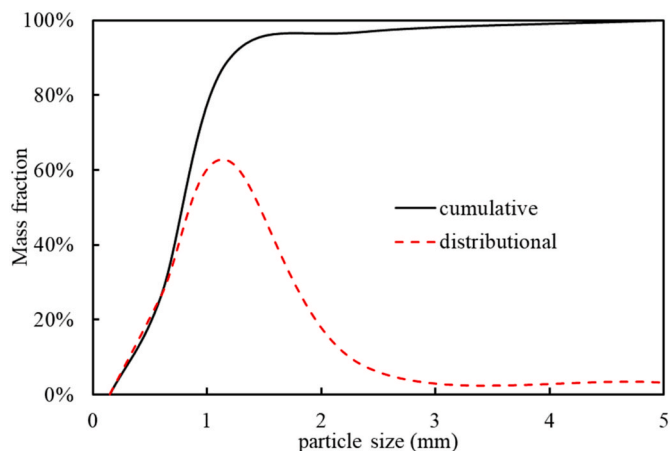


Fig. 1. Grading of the river sand.

Zhan et al., 2019). Zhang et al. (2015) treated the collected fine RCA < 2.5 mm in a carbonation chamber and used it to prepare recycled aggregate mortar afterward (Zhang et al., 2015). The study reported improved properties of the treated fine RCA in density, water absorption, and crushing value as well as the enhanced performance of the mortar in drying shrinkage, flowability, and compressive strength. Pan et al. (2017) pre-soaked the fine RCA in a calcium solution before using gas-solid carbonation in order to improve its effectiveness (Pan et al., 2017). The treated fine RCA exhibited excellent properties including crushing value, water absorption, powder content, and mortar strength. Li et al. (2018) prepared a modeled idealized RCA <5 mm and carbonated by an accelerated gas-solid carbonation process (Li et al., 2018). The study reported a higher micro-hardness in both the old interfacial transition zone (ITZ) and the old mortar. Furthermore, the compressive strength and modulus of the concrete prepared by the carbonated RCA were also significantly improved.

The gas-solid pressurized carbonation process usually requires special equipment, a long carbonation time, and externally applied pressure. The flow-through gas-solid carbonation process had been found to be less efficient due to the low partial pressure (Kashef-Haghighi and Ghoshal, 2010). Recently, new wet carbonation methods have been developed (Fang et al., 2020a, 2021a, 2020a; Liu et al., 2021; Zajac et al., 2020b). Instead of direct gas-solid carbonation, these studies proposed the injection of gaseous CO<sub>2</sub> into a liquid to facilitate the carbonation reaction. The encouraging outcomes such as high carbonation efficiency and low energy consumption render wet carbonation a promising alternative carbonation method for enhancing the quality of fine RCA (Liu et al., 2021).

But all previous studies on wet carbonation focused on carbonating the coarse fraction of RCA while relatively little attention was paid on the fine RCA. This study aimed to investigate the effect of the wet carbonation method on the fine fraction RCA with the aim of exploring the possibility of using the carbonated RCA to replace natural fine aggregates. Besides, efficiency of the wet carbonation was compared with the conventional gas-solid phase carbonation methods in terms of CO<sub>2</sub> uptake. The changes in porosity and carbonation products were analyzed. Moreover, the compressive strength and drying shrinkage of mortar specimens prepared by the raw RCA, carbonated RCA, and river sand were compared.

## 2. Experimental program

### 2.1. Recycled fine aggregate

For assessing the effect of carbonation on the properties of the fine RCA, as the compositions of real RCA varied randomly a pure cement paste was used to simulate the fine RCA as its the primary active

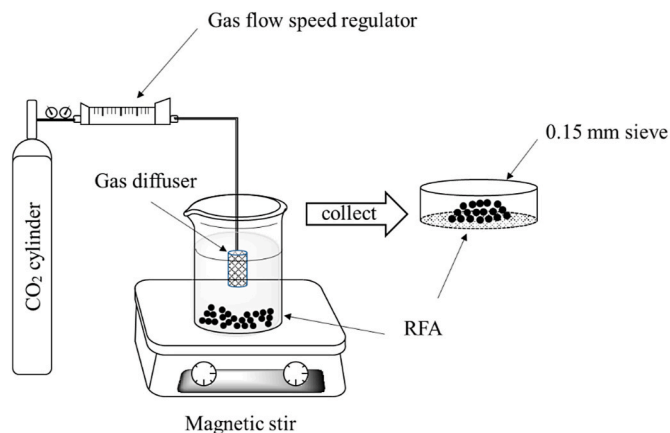


Fig. 2. Wet carbonation setup.

component in the RCA. A well-hydrated cement paste (2-year storage in air-tight bags) originally prepared with a w/c ratio of 0.4 using CEM1 OPC was crushed and ground by a planetary grinder and sieved into two particle size categories to produce the fine aggregate (RCP): 0.15–2.36 mm and 2.36–5 mm. The fine powdery fraction was removed. For the porosity and carbonation products tests, the 0.15–2.36 mm RCP was further divided into three size ranges: 0.15–0.6 mm, 0.6–1.18 mm, 1.18–2.36 mm.

For preparing the mortar specimens, a real recycled fine aggregate (RFA) with a size range of 0.15–5 mm was used and it was derived from a batch of designed concrete which was cast by a local concrete plant with a known mix proportion (Xuan et al., 2017). The concrete was crushed and processed to different size ranges. The cement paste content of the RFA with a size range of 0.15–2.36 mm and 2.36–5 mm was 29.3% and 26.0% respectively measured by a HCl solution dissolution method described in a previous study (Fang et al., 2017). The RFA was used to partially or fully replace river sand in the cement mortar after subjecting to wet carbonation. The particle grading of RFA was prepared according to that of the river sand (Fig. 1).

### 2.2. Carbonation methods

The setup of the laboratory wet carbonation method is shown in Fig. 2. The CO<sub>2</sub> (>98% purity) gas was injected at a rate of 0.2 L/min/g<sub>RFA</sub> for 10 min as a previous study pointed out it was the optimal duration for wet carbonation (Liu et al., 2021). The magnetic stirring speed was set at 200 rpm. After wet carbonation, the RFA was collected by a 0.15 mm sieve. The carbonated RCP and RFA were oven-dried at 105 °C for 24h before test. Moreover, the 2.36–5 mm RFA were

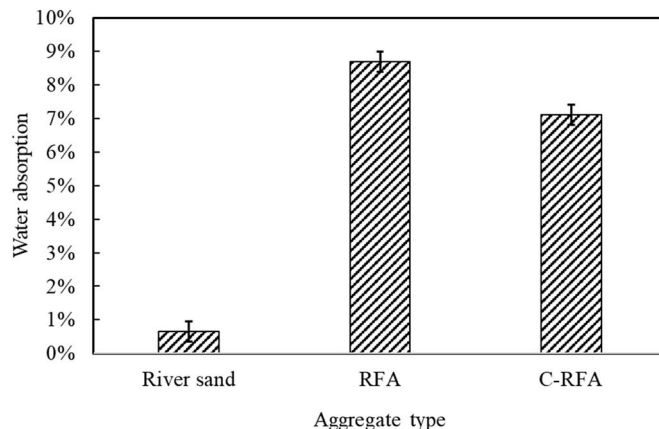


Fig. 3. Water absorption values.

**Table 1**  
Mixture designs of mortar specimens ( $\text{kg}/\text{m}^3$ ).

Replacement ratio	River sand	Carbonated RFA	Raw RFA	Water	Cement	Flowability (ASTM C1437-01, 2001)	Adjusted water
0%	1800	0		300	600	$200 \pm 20$ mm	11.5
50%	900	900		300	600		69.7
50%	900		900	300	600		84.1
100%	0	1800		300	600		127.8
100%	0		1800	300	600		156.6

subjected to 2 min, 10 min, and 1h wet carbonation under the same condition for microscopic analysis, and 10 min pressurized carbonation (0.1 bar) and flow-through carbonation (same flow rate as wet carbonation) respectively to compare the  $\text{CO}_2$  uptake by three different carbonation methods. The methodologies used for the pressurized and flow-through gas-solid carbonation processes have been reported previously (Fang et al, 2020b, 2021b, 2020b).

### 2.3. Mortar specimens

To compare and evaluate the effects of replacing river sand with the raw RFA and carbonated RFA on the mechanical properties, mortar specimens were prepared to test for drying shrinkage (ASTM C1148-92a, 2014) and compressive strength (ASTM C349-08, 2008). The cement to aggregate ratio and effective water to cement ratio of the mortar was 1:3 and 0.5 respectively. The water absorption values of the three types of aggregates and the mixture designs are listed in Fig. 3 and Table 1 respectively. It should be noted that water adjustments were done to take into account the water absorption values of the aggregates. For the rest mixtures, water was adjusted in order to reach the same flowability (ASTM C1437).

For each group of mortar mixture, three  $25 \text{ mm} \times 25 \text{ mm} \times 280 \text{ mm}$  specimens and three  $40 \text{ mm} \times 40 \text{ mm} \times 40 \text{ mm}$  cubes for drying shrinkage test and compressive strength test were prepared respectively.

### 2.4. Testing apparatus

#### 2.4.1. Water absorption, drying shrinkage, and compressive strength

The water absorption values of the RFA were determined according to BS EN 1097 (2013). The drying shrinkage and the compressive strength of the mortar specimens were tested according to ASTM C1148 and ASTM C349 (ASTM C1148-92a, 2014; ASTM C349-08, 2008).

#### 2.4.2. Brunauer-Emmett-Teller (BET)

The BET test was utilized to measure the porosity of three RFA size categories: 0.15–0.6 mm, 0.6–1.18 mm, 1.18–2.36 mm by a Micromeritics RSAP 2020 plus BET apparatus.

#### 2.4.3. Mercury intrusion porosimetry (MIP)

The porosity of RFA with the particle size of 2.36–5 mm was analyzed by MIP because it was too large for BET while the other three categories were too small for the MIP test. A Micromeritics AutoPore IV 9500 was used for testing the porosity of RFA particles. The samples were pre-dried for 48 h ( $-85^\circ\text{C}$  and a vacuum of 0.133 mBar) using a freeze dryer (Labconco FreeZone 2.5Plus).

#### 2.4.4. Thermal gravimetric analysis (TGA)

TGA of the RFA particles was performed in order to obtain the profiles of  $\text{Ca}(\text{OH})_2$  (CH) and calcium carbonate contents. The samples were dried at  $60^\circ\text{C}$  for 24h and ground into fine powders. The fractions passing through a  $75\text{-}\mu\text{m}$  sieve were collected for TGA. 10 mg powder sample was heated from 50 to  $1050^\circ\text{C}$  at a heating rate of  $10^\circ\text{C min}^{-1}$  with an Ar stripping gas (Rigaku, Thermo plus EVO2). The mass loss between 550 and  $800^\circ\text{C}$  represents the decomposition of  $\text{CaCO}_3$  (CC) (Alarcon-Ruiz et al., 2005). The content of CC can be calculated based on the ratio of mass loss and the ignited mass at  $1050^\circ\text{C}$ . The  $\text{CO}_2$  uptake was the increase of the mass loss values between 550 and  $800^\circ\text{C}$  of the samples after wet carbonation.

#### 2.4.5. Powdered X-ray diffraction (XRD)

XRD was performed by a Rigaku Smart-Lab apparatus with Cu-K $\alpha$  radiation ( $\lambda = 1.54 \text{ \AA}$ ) at 45 kV and 200 mA, to determine and analyze crystalline compositions. The dry samples were ground into fine powders passing through a  $75\text{-}\mu\text{m}$  sieve and mixed with an AR grade corundum ( $\text{Al}_2\text{O}_3$ , 99.99%, Aladdin) with a mass ratio of 9:1 for semi-quantitatively analysis of the carbonation products using the reference intensity ratio (RIR) method.

#### 2.4.6. Scanning electron microscopy (SEM)

The SEM analysis was conducted on gold coated fractured surfaces of the samples using a Tescan VEGA 3 apparatus (HV: 20 kV, working distance: 15 mm, magnitude: 3000–9000  $\times$ ).

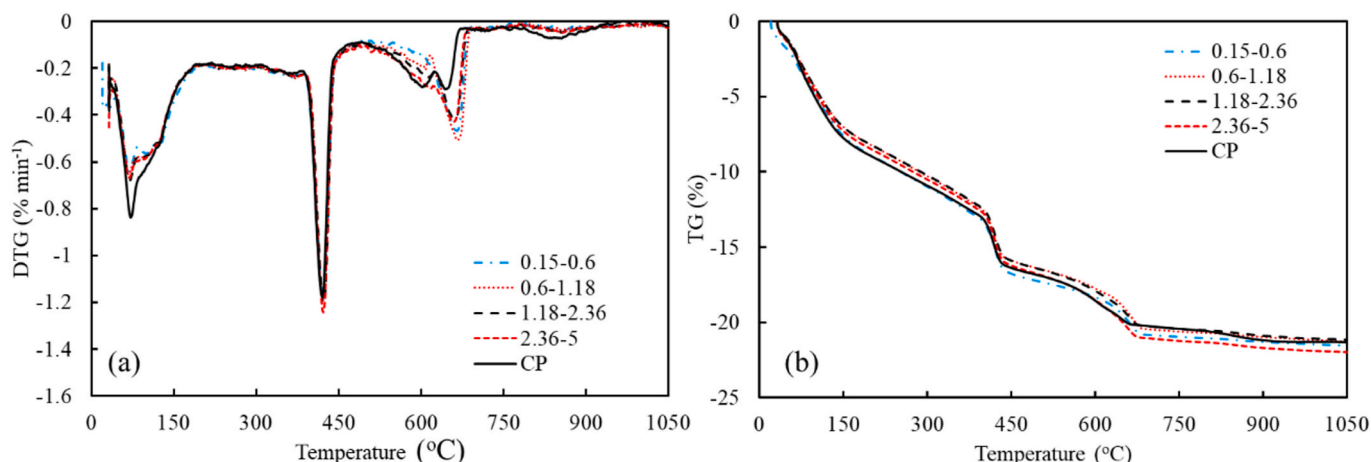


**Fig. 4.** The (a) DTG and (b) TG results of wet carbonation on RCP with different size range.

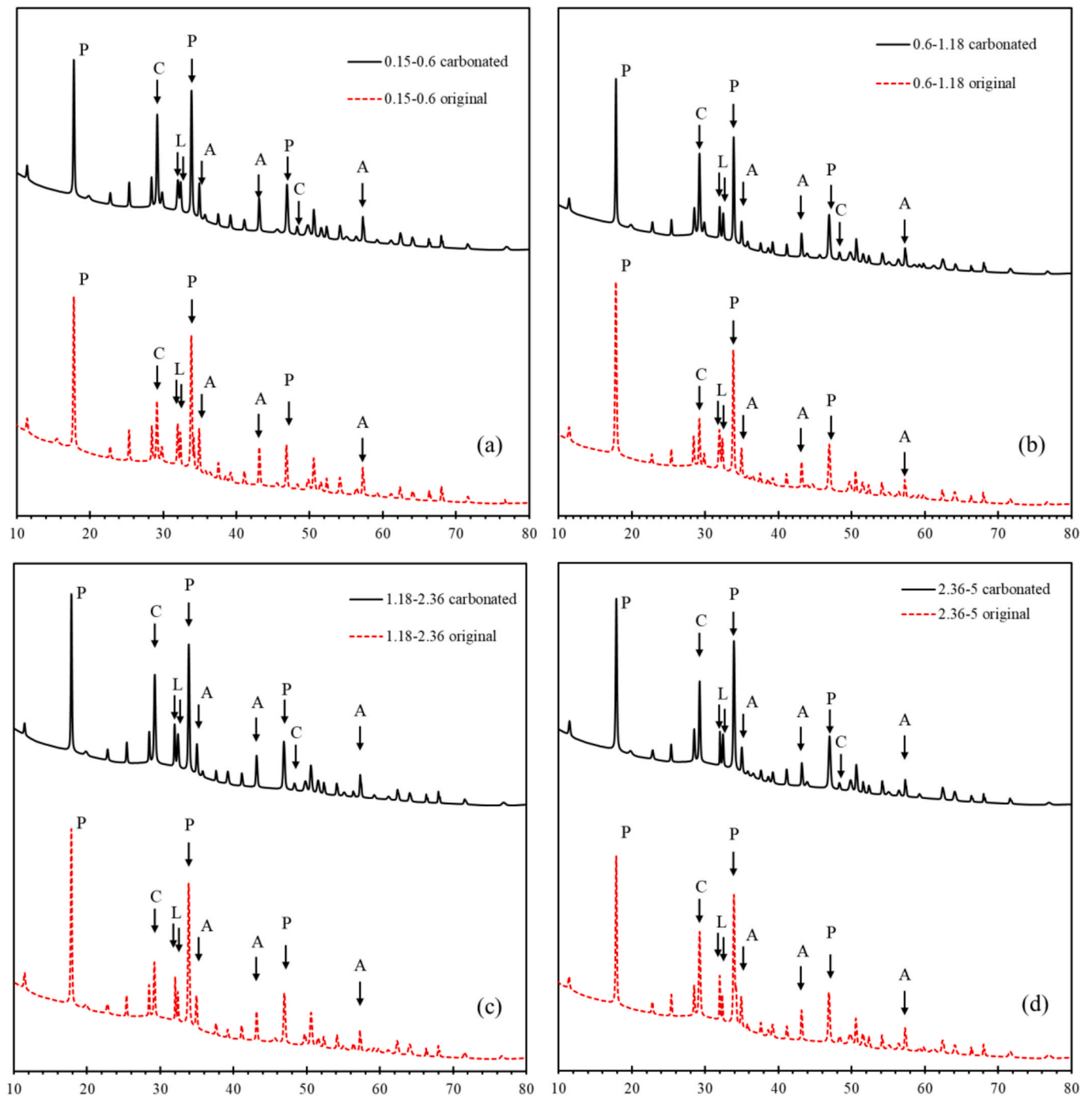


Fig. 5. The XRD patterns of RCP: (a) 0.15–0.6 mm; (b) 0.6–1.18 mm; (c) 1.18–2.36 mm; (d) 2.36–5 mm. (P = portlandite C = calcite, L = dicalcium silicate, A = corundum) X-axis:  $\text{CuK}\alpha$ ,  $2\theta$  (degree).

Table 2  
QXRD results of RCP.

		CH wt%	CC wt%
0.15–0.6 mm	Original	15.4	11.2
0.15–0.6 mm	Carbonated	14.9	14.7
0.6–1.18 mm	Original	15.4	10.3
0.6–1.18 mm	Carbonated	14.1	13.6
1.18–2.36 mm	Original	16.2	10.8
1.18–2.36 mm	Carbonated	14.4	13.6
2.36–5 mm	Original	15.0	13.6
2.36–5 mm	Carbonated	14.1	16.2

### 3. Results and discussion

#### 3.1. Carbonation products

##### 3.1.1. Comparison of carbonation effect in terms of TGA

Fig. 4 presents the comparison of the effect of wet carbonation on RCP with different particle sizes with the original RCP by TGA results. Fig. 4(a) shows that the wet carbonated RCP had a substantial increase in mass loss between 550 and 800 °C comparing to the original RCP, indicating that the wet carbonation effectively increased the amount of carbonation products formed. Fig. 4(b) shows the total mass loss of the wet carbonated RCP was higher than that of the original RCP. By

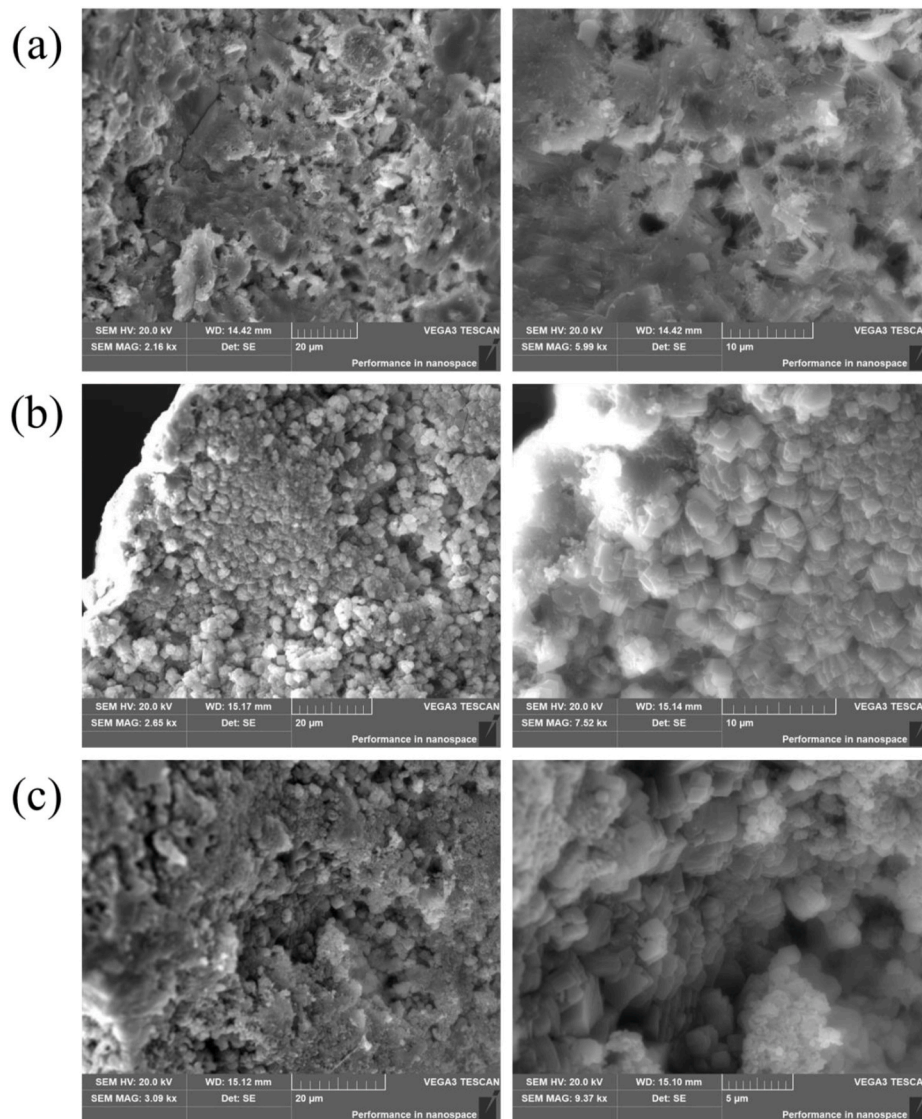


Fig. 6. SEM image of 2.36–5 mm particles subjected to wet carbonation: (a) 2 min, (b) 10 min, (c) 1h.

comparison, the  $\text{CO}_2$  uptake was increased by over 10% after wet carbonation and the mass fraction of carbonation products was increased up to 8.7%. It is also noticeable that the effect of particle size on the carbonation products was limited as both DTG and TG data showed marginal variation (0.1% and 1.1% respectively) among the carbonated RCP samples. This finding suggested that the 10-min carbonation was equally effective for RCP ranging from 0.15 to 5 mm. The reason is probably due to a short carbonation time of 10 min and the evenly distributed  $\text{CO}_2$  during the wet carbonation (Liu et al., 2021).

### 3.1.2. XRD results of wet carbonation

Fig. 5 shows the XRD patterns of the RCP samples and Table 2 lists the QXRD data. All four types of RCP showed similar XRD patterns. The crystalline phase of portlandite, externally added corundum, and calcite was detected from the original RCP. Comparing with the original RCP, an increase in the peak intensity of calcite was noticed from the carbonated RCP. And after the wet carbonation, the mass fraction of portlandite, ranging from 14.1 wt% to 14.9%, was still significant in all RCP samples. The QXRD data further presents the mass fraction changes of the CH and CC in RCP samples before and after carbonation. The reduction of the CH was from 0.5 wt% to 1.8 wt% and the increase of the CC was from 2.6 wt% to 3.5 wt%, indicating that the hydration products

other than CH were also carbonated. The wet carbonation increased the content of CC as the carbonation product which is believed to be able to fill the pores of RCP and therefore improve its quality (Papadakis et al., 1992; Thiery et al., 2013). As a result of the pore-filling effect of the carbonation products, the water absorption of the RFA was reduced by about 2% after the wet carbonation (Fig. 3). Due to the short carbonation duration, the decrease of CH content was not significant. Nevertheless, the wet carbonation still effectively increased the amount of carbonation products formed in the RCP.

## 3.2. Microscopic analysis

### 3.2.1. Effect of carbonation time

Fig. 6 shows the SEM images of the sections of the 2.36–5 mm RCP particles. Judging from the image, the carbonation products (mainly calcite) increased at the edge of the RCP particles as the wet carbonation time increased. After 2 min, there were hardly any carbonation products being noticed in SEM images. After 10 min, some carbonation products were noticed scattering across the section. After 1h, a lot of carbonation products were observed on the surface layers of the RCP particle.

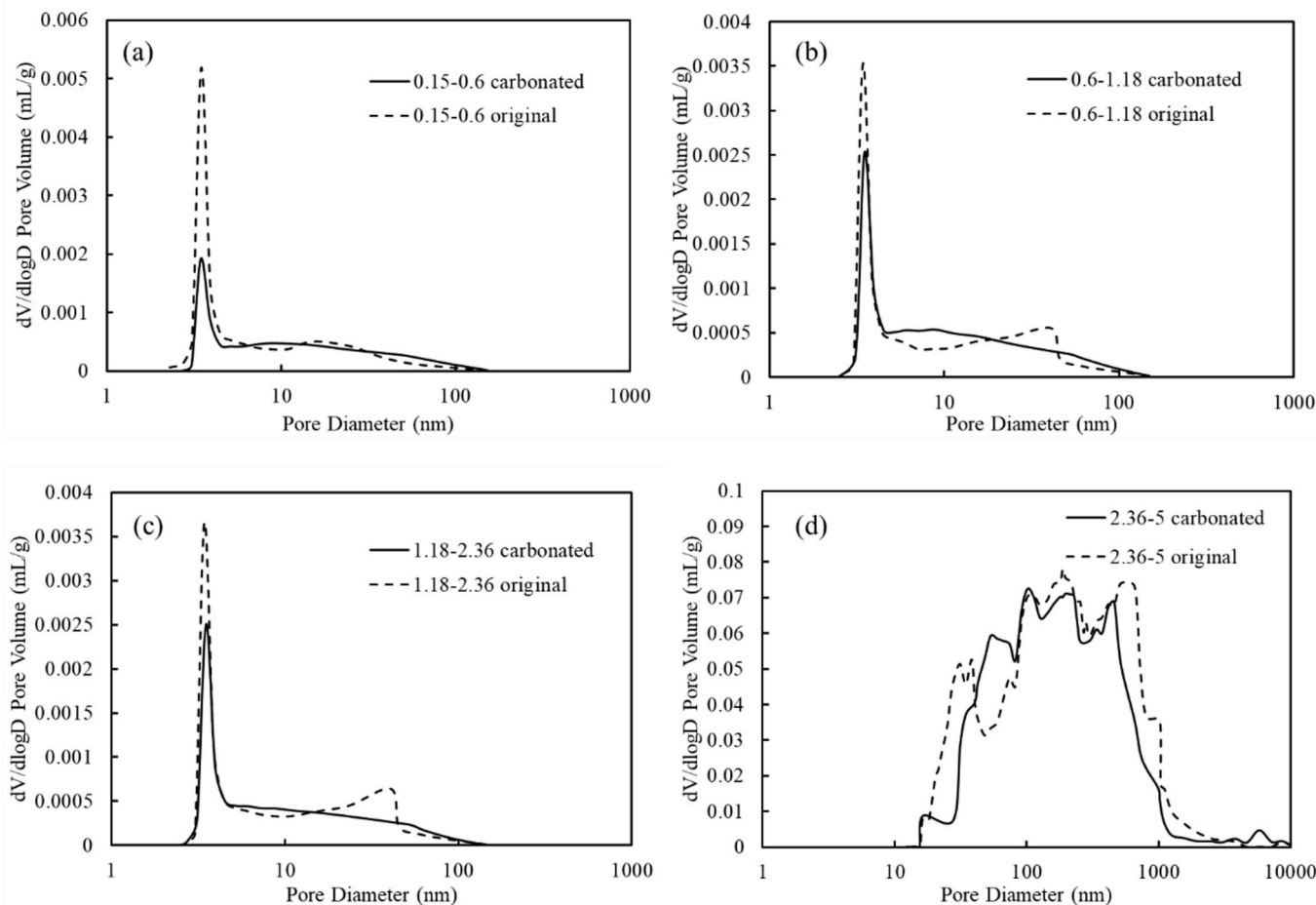


Fig. 7. Pore volume distribution of RCP: (a) 0.15–0.6 mm; (b) 0.6–1.18 mm; (c) 1.18–2.36 mm; (d) 2.36–5 mm.

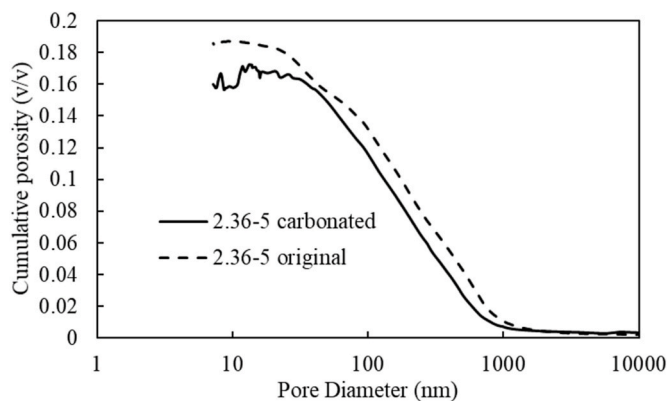


Fig. 8. Cumulative porosity of 2.36–5 mm RCP.

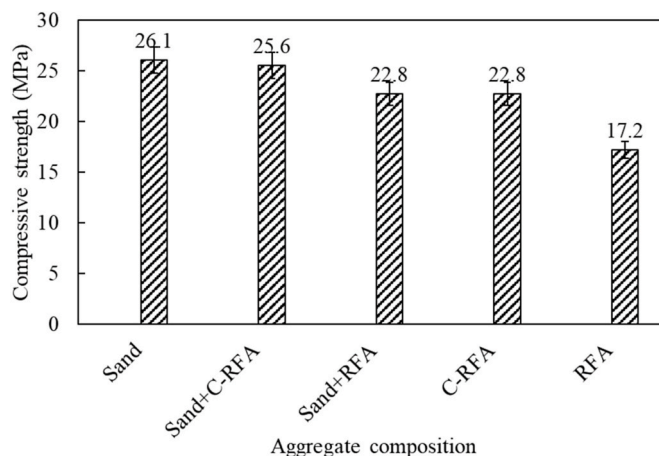


Fig. 9. Compressive strength values of mortar specimens.

### 3.2.2. Changes in the pore volume of RCP by wet carbonation

Due to the small particle size, the pore volumes of RCP with 0.15–0.6 mm, 0.6–1.18 mm, and 1.18–2.36 mm particle sizes were measured by BET and the results are shown in Fig. 7 (a), (b), and (c). While the pore volume of RCP with 2.36–5 mm particle size was measured by MIP (Figs. 7(d) and 8). Fig. 7(a), (b), and (c) showed reduced pore volume distributions of RCP after carbonation, especially for pores smaller than 10 nm. Meanwhile, the carbonation of 2.36–5 mm RCP transformed large pores into smaller pores as shown in Fig. 7(d). Also, Fig. 8 reveals that the wet-carbonation reduced the total porosity of the 2.36–5 mm RCP. These results suggested that the wet carbonated generated nano-

size carbonation products which significantly reduced the volume of gel pores of the RCP.

### 3.3. Effect on mortar specimens

The comparison of 28-day compressive strength and drying shrinkage of the mortar prepared with different types of fine aggregates are shown in Fig. 9 and Fig. 10 respectively. For ease of description, raw RFA and carbonated RFA were annotated as RFA and C-RFA

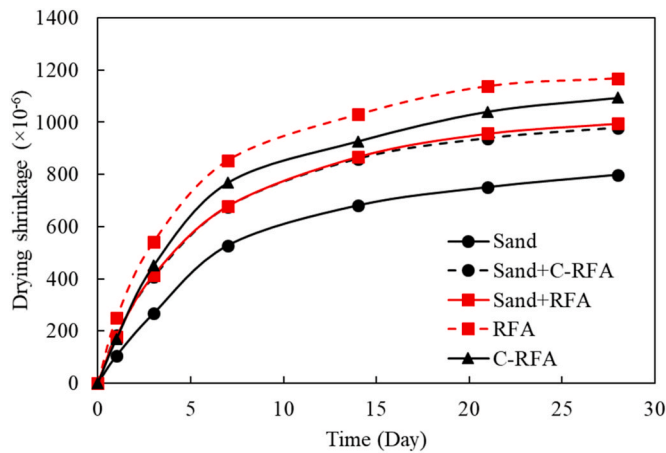


Fig. 10. Drying shrinkage of mortar specimens.

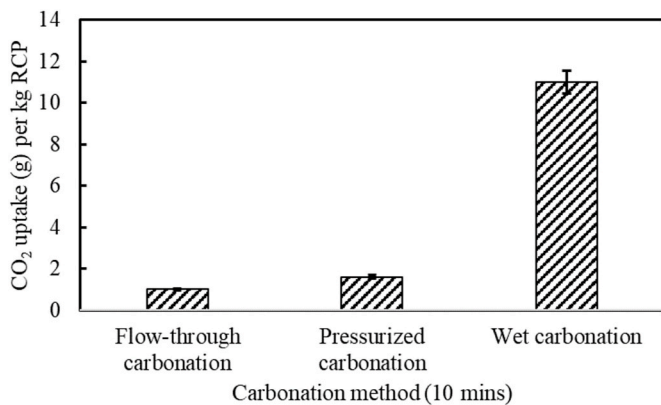


Fig. 11. CO<sub>2</sub> uptake comparison between three different carbonation methods.

respectively.

### 3.3.1. Compressive strength

As Fig. 9 shows, the 100% sand mortar mixture achieved the highest strength while the 100% RFA mixture attained the lowest strength. The specimens prepared with 50% sand replaced by C-RFA showed similar strength to the 100% sand mixture. But replacing 50% sand by RFA resulted in a noticeable strength reduction. On the other hand, the specimens prepared with 100% C-RFA showed a significant strength increase compared with those prepared with 100% RFA, suggesting that wet carbonation was able to enhance the quality of RFA and therefore improve the mechanical performance of mortar specimens. The carbonation products which were mainly formed on the surface of the

RFA particles as revealed by SEM, improved the properties of RFA by increasing its density and reducing its water absorption. This eventually led to the improvement of the compressive strength of the produced new mortars. This is consistent with the results of Liu et al. (2021) who pointed out the produced carbonation products would benefit the interface between C-RFA and the cement paste.

### 3.3.2. Drying shrinkage

As Fig. 10 shows, the 100% sand specimens showed the lowest shrinkage values while the 100% RFA specimens had the highest. The 100% C-RFA specimens showed a lower shrinkage value than the 100% RFA specimens, indicating the beneficial property improvement for RFA after wet carbonation. There was no significant difference in shrinkage value between the specimens prepared with replacing 50% sand by C-RFA or RFA.

### 3.4. Comparison between different carbonation methods

Fig. 11 compares the CO<sub>2</sub> uptake by three different carbonation methods after the first 10 min. The CO<sub>2</sub> uptake was calculated by TGA results. The flow-through carbonation, pressurized carbonation, and wet carbonation resulted in a 10-min CO<sub>2</sub> uptake of 0.1 wt%, 0.16 wt%, and 1.1 wt% respectively. The reason is that the wet carbonation transformed a gas-solid reaction into a liquid-solid reaction and therefore enhanced the chemical reaction rate (Zajac et al., 2020; Liu et al., 2021; Papadakis et al., 1992; Zajac et al., 2020). Moreover, the effect of wet carbonation would be more effective for RFA with different particle gradings and the water used of the wet carbonation process can be recycled.

The mortar specimens prepared by C-RFA showed a 30.8% increase in compressive strength compared to RFA specimens. It was due to the densified surface layer evenly formed during the wet carbonation which was beneficial for bonding with the new cement paste (Xiao et al., 2018; Zajac et al., 2020). As a result, replacing 50% sand with C-RFA in the mixture design only led to a strength reduction of less than 2% of the mortar specimens. As Table 3 shows, the wet carbonation method was superior in enhancing the compressive strength of new concrete/mortar samples prepared with treated RCA than those reported in the selected previous studies.

## 4. Conclusion

This paper presented the experimental research results of applying the wet carbonation method to improve the quality of RFA with particle size ranging from 0.15 to 5 mm. The RCP and the RFA were soaked in water and subjected to wet carbonation. The properties of both RFA and its mortar specimens were analyzed and compared.

The wet carbonation was effective in improving the properties of RFA as evident in the pore volume reduction.

The 10 min wet carbonation was found to be the optimal in this study

Table 3  
Comparison of carbonation treatment in studies.

Source(s)	Type of treatment	Specimen type	Particle size of RCA	Replacement ratio	Strength comparing with control specimen	Strength comparing to untreated RCA specimen	Suggested replacement ratio
Zhang et al. (2015)	CO <sub>2</sub> chamber with +0.4 MPa for 4h	Mortar	0.16–2.5 mm	100%	–10% (G-RCA)–5% (C-RCA)	+12% (G-RCA)+6% (C-RCA)	N/A
Xuan et al., (2017)	Pressurized carbonation with +0.1/5 bar for 24h	Concrete	5–10 mm10–20 mm	100%	–9.6%	+22.6%	Up to 60%
Tam et al., (2016)	Carbonation chamber with varying pressure (0–150 kPa) and time (0–90 min)	Concrete	10 mm20 mm	30%100%	+0.7%–14.8%	–3.3% + 6.5%	30%
Fang et al., (2021b)	Wastewater spray with 24h flow-through carbonation	Concrete	5–10 mm	100%	+1.3%	+14.1%	N/A
Current study	10-min wet carbonation	Mortar	0.15–5 mm	50%100%	–1.9%–12.6%	+12.3% + 32.6%	50%

as either increasing or reducing the carbonation time would lead to a looser microstructure.

The application of wet carbonation on RFA resulted in a 30.8% increase in compressive strength and noticeable enhancements in the drying shrinkage performance of the new mortar specimens. Replacing 50% river sand by carbonated RFA would result in a similar compressive strength and in significant deterioration in drying shrinkage.

#### CRedit authorship contribution statement

**Xiaoliang Fang:** Conceptualization, Methodology, Investigation, Data Formal analysis, Writing – original draft, Writing – review & editing. **Chi Sun Poon:** Conceptualization, Supervision, Methodology, Writing – review&finalizing.

#### Declaration of competing interest

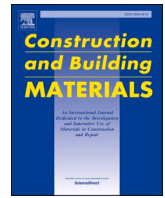
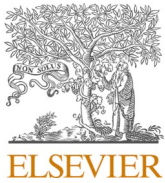
The authors declare that they have no known competing financial interests or personal relationships that could have appeared to influence the work reported in this paper.

#### Acknowledgment

The authors wish to acknowledge the financial support of the Research Grants Council General Research Fund (PolyU 152144/17E), the Construction Industry Council Research Fund, and the Strategic Public Policy Research Funding Scheme.

#### References

- Anastasiou, E., Georgiadis Filikas, K., Stefanidou, M., 2014. Utilization of fine recycled aggregates in concrete with fly ash and steel slag. *Construct. Build. Mater.* 50, 154–161. <https://doi.org/10.1016/j.conbuildmat.2013.09.037>.
- ASTM C1148-92a, 2014. Standard Test Method for Measuring the Drying Shrinkage of Masonry Mortar. *ASTM Stand. B. i*, pp. 2–4. <https://doi.org/10.1520/C1148-92AR14.2>.
- ASTM C1437-01, 2001. Standard Test Method for Flow of Hydraulic Cement Mortar: C1437-01. <https://doi.org/10.1520/C1437-20.2>. Standard 7–8.
- ASTM C349-08, 2008. Standard Test Method for Compressive Strength of Hydraulic-Cement Mortars (Using Portions of Prisms Broken in Flexure). <https://doi.org/10.1520/C0349-18.2>. ASTM International 1–4.
- BS EN 1097, 2013. Tests for Mechanical and Physical Properties of Aggregates, Part 6: Determination of Particle Density and Water Absorption.
- Crouch, L.K., Gamble, R., Brogdon, J.F., Tucker, C.J., 1998. Use of high-fines limestone screenings as aggregate for controlled low-strength material (CLSM). In: *The Design and Application of Controlled Low-Strength Materials (Flowable Fill)*. ASTM International.
- Cuenca-Moyano, G.M., Martín-Morales, M., Valverde-Palacios, I., Valverde-Espinosa, I., Zamorano, M., 2014. Influence of pre-soaked recycled fine aggregate on the properties of masonry mortar. *Construct. Build. Mater.* 70, 71–79. <https://doi.org/10.1016/j.conbuildmat.2014.07.098>.
- Evangelista, L., De Brito, J., 2014. Concrete with fine recycled aggregates: a review. *Eur. J. Environ. Civ. Eng.* 18, 129–172. <https://doi.org/10.1080/19648189.2013.851038>.
- Fang, X., Wang, L., Poon, C.S., Baek, K., Tsang, D.C.W., Kwok, S.K., 2019. Transforming waterworks sludge into controlled low-strength material: bench-scale optimization and field test validation. *J. Environ. Manag.* 232, 254–263. <https://doi.org/10.1016/j.jenvman.2018.11.091>.
- Fang, X., Xuan, D., Poon, C.S., 2017. Empirical modelling of CO<sub>2</sub> uptake by recycled concrete aggregates under accelerated carbonation conditions. *Mater. Struct.* 50 <https://doi.org/10.1617/s11527-017-1066-y>.
- Fang, X., Xuan, D., Zhan, B., Li, W., Poon, C.S., 2020a. A novel upcycling technique of recycled cement paste powder by a two-step carbonation process. *J. Clean. Prod.*
- Fang, X., Xuan, D., Zhan, B., Li, W., Sun, C., 2021a. Characterization and optimization of a two-step carbonation process for valorization of recycled cement paste fine powder. *Construct. Build. Mater.* 278, 122343. <https://doi.org/10.1016/j.conbuildmat.2021.122343>.
- Fang, X., Zhan, B., Poon, C.S., 2021b. Enhancement of recycled aggregates and concrete by combined treatment of spraying Ca<sup>2+</sup> rich wastewater and flow-through carbonation. *Construct. Build. Mater.* 277, 122202. <https://doi.org/10.1016/j.conbuildmat.2020.122202>.
- Fang, X., Zhan, B., Poon, C.S., 2020b. Enhancing the accelerated carbonation of recycled concrete aggregates by using reclaimed wastewater from concrete batching plants. *Construct. Build. Mater.* 239, 117810. <https://doi.org/10.1016/j.conbuildmat.2019.117810>.
- Kashef-Haghighi, S., Ghoshal, S., 2010. CO<sub>2</sub> sequestration in concrete through accelerated carbonation curing in a flow-through reactor. *Ind. Eng. Chem. Res.* 49, 1143–1149. <https://doi.org/10.1021/ie900703d>.
- Khatib, J.M., 2005. Properties of concrete incorporating fine recycled aggregate. *Cement Concr. Res.* 35, 763–769. <https://doi.org/10.1016/j.cemconres.2004.06.017>.
- Li, L., Xiao, J., Xuan, D., Poon, C.S., 2018. Effect of carbonation of modeled recycled coarse aggregate on the mechanical properties of modeled recycled aggregate concrete. *Cement Concr. Compos.* 89, 169–180. <https://doi.org/10.1016/j.cemconcomp.2018.02.018>.
- Liang, C., Pan, B., Ma, Z., He, Z., Duan, Z., 2020. Utilization of CO<sub>2</sub> curing to enhance the properties of recycled aggregate and prepared concrete: a review. *Cement Concr. Compos.* 105, 103446. <https://doi.org/10.1016/j.cemconcomp.2019.103446>.
- Liu, S., Shen, P., Xuan, D., Li, L., Sojebi, A., Zhan, B., 2021. A comparison of liquid-solid and gas-solid accelerated carbonation for enhancement of recycled concrete aggregate. *Cement Concr. Compos.* 118, 103988. <https://doi.org/10.1016/j.cemconcomp.2021.103988>.
- Luo, Z., Li, W., Wang, K., Castel, A., Shah, S.P., 2021. Cement and Concrete Research Comparison on the properties of ITZs in fly ash-based geopolymers and Portland cement concretes with equivalent flowability. *Cement Concr. Res.* 143, 106392. <https://doi.org/10.1016/j.cemconres.2021.106392>.
- Mardani-Aghabaglou, A., Tuyan, M., Ramyar, K., 2015. Mechanical and durability performance of concrete incorporating fine recycled concrete and glass aggregates. *Mater. Struct. Constr.* 48, 2629–2640. <https://doi.org/10.1617/s11527-014-0342-3>.
- Oksri-Nelfia, L., Mahieux, P.Y., Amiri, O., Turcry, P., Lux, J., 2016. Reuse of recycled crushed concrete fines as mineral addition in cementitious materials. *Mater. Struct. Constr.* 49, 3239–3251. <https://doi.org/10.1617/s11527-015-0716-1>.
- Pan, G., Zhan, M., Fu, M., Wang, Y., Lu, X., 2017a. Effect of CO<sub>2</sub> curing on demolition recycled fine aggregates enhanced by calcium hydroxide pre-soaking. *Construct. Build. Mater.* 154, 810–818. <https://doi.org/10.1016/j.conbuildmat.2017.07.079>.
- Papadakis, V.G., Fardis, M.N., Vayenas, C.G., 1992. Hydration and carbonation of pozzolanic cements. *ACI Mater. J.* 89.
- Shi, C., Li, Y., Zhang, J., Li, W., Chong, L., Xie, Z., 2016. Performance enhancement of recycled concrete aggregate – a review. *J. Clean. Prod.* 112, 466–472. <https://doi.org/10.1016/j.jclepro.2015.08.057>.
- Sim, J., Park, C., 2011. Compressive strength and resistance to chloride ion penetration and carbonation of recycled aggregate concrete with varying amount of fly ash and fine recycled aggregate. *Waste Manag.* 31, 2352–2360. <https://doi.org/10.1016/j.wasman.2011.06.014>.
- Siriruang, C., Toochinda, P., Julnipitawong, P., Tangtermsirikul, S., 2016. CO<sub>2</sub> capture using fly ash from coal fired power plant and applications of CO<sub>2</sub>-captured fly ash as a mineral admixture for concrete. *J. Environ. Manag.* 170, 70–78. <https://doi.org/10.1016/j.jenvman.2016.01.010>.
- Tam, V.W.Y., Butera, A., Le, K.N., 2016. Carbon-conditioned recycled aggregate in concrete production. *J. Clean. Prod.* 133, 672–680. <https://doi.org/10.1016/j.jclepro.2016.06.007>.
- Thiery, M., Dangla, P., Belin, P., Habert, G., Roussel, N., 2013. Carbonation kinetics of a bed of recycled concrete aggregates: a laboratory study on model materials. *Cement Concr. Res.* 46, 50–65.
- Xuan, D., Zhan, B., Poon, C.S., 2017. Durability of recycled aggregate concrete prepared with carbonated recycled concrete aggregates. *Cement Concr. Compos.* 84, 214–221. <https://doi.org/10.1016/j.cemconcomp.2017.09.015>.
- Zajac, M., Skibsted, J., Durdzinski, P., Bullerjahn, F., Skocek, J., Ben Haha, M., 2020a. Kinetics of enforced carbonation of cement paste. *Cement Concr. Res.* 131, 106013. <https://doi.org/10.1016/j.cemconres.2020.106013>.
- Zajac, M., Skibsted, J., Skocek, J., Durdzinski, P., Bullerjahn, F., Ben, M., 2020b. Cement and Concrete Research Phase assemblage and microstructure of cement paste subjected to enforced , wet carbonation. *Cement Concr. Res.* 130, 105990. <https://doi.org/10.1016/j.cemconres.2020.105990>.
- Zajac, M., Skocek, J., Durdzinski, P., Bullerjahn, F., Skibsted, J., Ben Haha, M., 2020c. Effect of carbonated cement paste on composite cement hydration and performance. *Cement Concr. Res.* 134, 106090. <https://doi.org/10.1016/j.cemconres.2020.106090>.
- Zhan, B.J., Xuan, D.X., Poon, C.S., 2018. Enhancement of recycled aggregate properties by accelerated CO<sub>2</sub> curing coupled with limewater soaking process. *Cement Concr. Compos.* 89, 230–237. <https://doi.org/10.1016/j.cemconcomp.2018.03.011>.
- Zhan, B.J., Xuan, D.X., Zeng, W., Poon, C.S., 2019. Carbonation treatment of recycled concrete aggregate: effect on transport properties and steel corrosion of recycled aggregate concrete. *Cement Concr. Compos.* 104, 103360. <https://doi.org/10.1016/j.cemconcomp.2019.103360>.
- Zhang, D., Ghoulah, Z., Shao, Y., 2017. Review on carbonation curing of cement-based materials. *J. CO<sub>2</sub> Util.* 21, 119–131. <https://doi.org/10.1016/j.jcou.2017.07.003>.
- Zhang, J., Shi, C., Li, Y., Pan, X., Poon, C.-S., Xie, Z., 2015. Performance enhancement of recycled concrete aggregates through carbonation. *J. Mater. Civ. Eng.* 4015029.
- Zhang, J., Wang, J., Li, X., Zhou, T., Guo, Y., 2018. Rapid-hardening controlled low strength materials made of recycled fine aggregate from construction and demolition waste. *Construct. Build. Mater.* 173, 81–89. <https://doi.org/10.1016/j.conbuildmat.2018.04.023>.



# Efficiencies of carbonation and nano silica treatment methods in enhancing the performance of recycled aggregate concrete

Long Li<sup>a</sup>, Dongxing Xuan<sup>a</sup>, A.O. Sojobi<sup>a,b</sup>, Songhui Liu<sup>a,c</sup>, Chi Sun Poon<sup>a,\*</sup>

<sup>a</sup> Department of Civil and Environmental Engineering, The Hong Kong Polytechnic University, Hung Hom, Hong Kong, PR China

<sup>b</sup> Department of Building and Real Estate, The Hong Kong Polytechnic University, Hung Hom, Hong Kong, PR China

<sup>c</sup> School of Materials Science and Engineering, Henan Polytechnic University, Henan, PR China

## ARTICLE INFO

### Keywords:

Recycled coarse aggregate  
Carbonation  
Nano silica  
Mechanical property  
Durability  
Microhardness

## ABSTRACT

This study compared the efficiencies of five recycled aggregate treatment methods (pressurized gas–solid carbonation (PC), flow-through gas–solid carbonation (FC), wet carbonation (WC), nano-silica (NS) spraying and combined PC with NS spraying (PCNS)) in enhancing the performance of recycled aggregate concrete (RAC). Mechanical properties, durability and microhardness of RACs were evaluated. The results showed that PC method recorded higher enhancing efficiency than both FC and WC method. NS spraying method caused higher improvement in mechanical properties of RAC than three carbonation methods. Because of the synergistic effect of enhanced old mortar and new ITZ, PCNS method recorded the highest efficiency.

## 1. Introduction

Large amount of construction and demolition (C&D) waste is being generated all over the world. Owing to the disposal problem of C&D wastes, recycling of waste concrete in form of recycled coarse aggregate (RCA) as partial or full replacements of natural coarse aggregate (NCA) to produce recycled aggregate concrete (RAC) has been proposed as an effective solution [1]. Moreover, it can conserve natural resources that is required for producing natural aggregate. Therefore, recent studies [2,3] advocate aggressive and integrated strategies to promote RCA applications in construction. However, because of lower mechanical properties and durability of RAC compared with natural aggregate concrete (NAC) [4,5,6,7,8,9], it is still not commonly used in structural engineering up to now. Previous studies [10,11,12,13] have attributed to the inferior mechanical properties and durability of RAC to larger water absorption, higher porosity and lower density of RCA than NCA.

To widen scope of utilization of RAC in real construction applications, many methods have been proposed to improve the properties of RAC in recent decades [14]. Proposed methods are classified into four types: (1) Removal of attached old mortar from RCA using techniques such as mechanical grinding [15], microwave heating [16,17], ultrasonic cleaning [18], and acidic presoaking [15,19]; (2) Enhancement of old mortar of RCA which includes techniques such as accelerated carbonation [20,21,22], microbial carbonate precipitation [23] and

polyvinyl alcohol presoaking [24]; (3) Enhancement of new interface transition zone (ITZ) between RCA and new mortar with surface coating techniques by using the materials such as cement slurry [25], pozzolan slurries [26] and nanoparticles [27,28]; (4) Enhancement of new mortar by adding some supplementary cementitious materials [29,30] or nanoparticles [31,32] in concrete. The first three methods belong to RCA pretreatment methods. Among them, the old mortar or new ITZ enhancing techniques should be more practical and economical by avoiding secondary pollution associated with the removal of old mortar and the use of other chemicals.

Among the methods to enhance old mortar of RCA, accelerated carbonation has attracted most attention. When using accelerated carbonation method, CO<sub>2</sub> penetrates into RCA and reacts with calcium hydroxide, calcium silicate hydrate (C-S-H) and un-hydrated cement clinkers, generating calcium carbonate and silica gel which results in densified RCA [33]. Four accelerated carbonation methods are identified in literature [33]: (1) Standard gas–solid carbonation method, of which the condition is similar to that for testing the carbonation resistance of concrete [34,35,36]; (2) Pressurized gas–solid carbonation (PC) method [20,21], which can accelerate the penetration rate into RCA by applying a high CO<sub>2</sub> pressure. (3) Flow-through gas–solid carbonation (FC) method [37], of which CO<sub>2</sub> is injected into carbonation chamber from one side at ambient pressure, allowed to pass through RCA samples and discharged from the opposite side, (4) Wet carbonation (WC)

\* Corresponding author.

E-mail address: [cecsphoon@polyu.edu.hk](mailto:cecsphoon@polyu.edu.hk) (C.S. Poon).

method [38,39], of which RCA is placed in water while CO<sub>2</sub> is injected into the water. All these carbonation treatments can improve physical properties of RCA and performance of RAC. However, the practicality and efficiency of these methods could be different. Therefore, it is imperative to make a comparison on the efficiencies of different carbonation methods systematically.

Separately, among the methods to enhance new ITZ in RAC, pre-soaking RCA in nano silica (NS) suspension has attracted a lot of research interests. Some studies [27,28,40] reported that NS pre-soaking method could enhance physical properties of RCA and performance of RAC. However, porous RCA could absorb NS suspension after pre-soaking and a thick layer of NS suspension would attach on the RCA's surface. As a result, it requires a high amount of expensive NS suspension, and thus this method may have a lower feasibility economically. To avoid this shortcoming, a recent study [41] proposed a new method by spraying NS suspension on RCA's surface, which requires much less NS to achieve similar or even better performance than pre-soaking method. However, it is unknown which is better to enhance RAC's performance when compared this type of new ITZ strengthening method with carbonation methods.

Therefore, the objective of this study is to compare the efficiency of the NS spraying method mentioned above with three types of carbonation methods (namely PC, FC and WC methods) in improving the mechanical properties and durability of RACs prepared with the treated RCAs. Moreover, to explore the possible synergistic effect of carbonation methods and the NS spraying method for enhancing the properties of RAC, a combined pressurized gas–solid carbonation with NS spraying (PCNS) method was also adopted. In addition, to explore the possible mechanisms of these RCA treatment methods in improving the performance of RAC, microhardness of RACs were measured and morphologies the surface of RCA after using different treatments were observed using a scanning electron microscope (SEM).

## 2. Materials and methods

### 2.1. Materials

A type of Portland cement CEM I 52.5 N was used as binder. River sand, which was cleaned with tap water and then oven-dried for 1 day at 105°C, was used as fine aggregate. Grading curve of the river sand is shown in Fig. 1. The river sand satisfied grading requirement of fine aggregate used for concrete according to the standard ASTM C33/C33M. A batch of demolition waste concrete, collected from a local demolition site, was used for RCA production. Due to good site management of the demolition project, besides old concrete, other impurities were rarely found in the collected waste concrete. The demolition waste concrete was crushed in laboratory and then sieved to produce RCA with two size

ranges (10–20 mm and 5–10 mm). Particles less than 5 mm or higher than 20 mm were not used in the experiment. NCA used was a crushed granite, which had similar size ranges to the RCA after sieving. The gradings of both RCA and NCA for concrete were controlled in this study. The mass ratio of the smaller coarse aggregate (5–10 mm) to the larger one (10–20 mm) was 1:4. The physical properties of coarse aggregate and fine aggregate are shown in Table 1. A water based commercially available nano silica (NS) suspension with average particle size of 106 nm and milk white color was used in spraying RCA. The chemical compositions of the NS suspension were measured by an X-ray fluorescence analyzer, as shown in Table 2. The pH value of the NS suspension was 10.0, while its density was 1.205 g/cm<sup>3</sup>.

### 2.2. Procedures of RCA treatment methods

(1) FC method. First, RCA was placed in an environmental chamber at 25 °C and 50% relative humidity for one day. Next, in every carbonation process, about 5.0 kg RCA was spread on some wire mesh containers with size of about 150 × 100 × 30 mm to ensure uniform carbonation and these containers were placed on a plastic plate, and the plate was horizontally placed inside a cylindrical chamber with dimension of Φ200 × 800 mm. Finally, CO<sub>2</sub> gas (>99% purity) with a flow rate of 1.0 L/min was injected from a plastic pipe (Φ8 mm) at one side and emitted from another one at the other side. The setup was introduced in previous study [42]. Duration of the carbonation was 24 h.

(2) PC method. Carbonation chamber with a volume of about 33 L that had been presented in some previous studies [13,21] was utilized. Before carbonation, RCA was placed in an environmental chamber at 25 °C and 50% relative humidity for one day. After placing RCA with about 20 kg in mass in carbonation chamber, CO<sub>2</sub> gas (>99% purity) was injected into the chamber at a constant pressure of + 1.0 Bar with aid of a gas regulator. Duration of the carbonation was 24 h.

(3) WC method. About 20 kg RCA was placed in mesh containers with dimension of 300 × 400 × 100 mm and soaked in water in a big plastic box (about 40L in volume) . The water was mixed by a mechanical device at a speed of 200 rpm. Subsequently, CO<sub>2</sub> gas (>99% purity) with a flow rate of 2 L/min was injected into the water through a fine-bubble generation diffuser for 6 h.

(4) NS spraying method. RCA was air-dried before treatment and the NS suspension was sprayed on RCA's surface with a handheld spraying bottle while RCA (about 5.0 kg each time) was being rotated in an inclined disc granulator with dimension of Φ500mm × 170 mm at 10 rpm. Schematic of the NS spraying method is shown in Fig. 2. The NS suspension that sprayed on RCA was 3% of RCA by mass.

(5) PCNS method. First, pre-conditioned RCA was treated similar to the PC method as mentioned above. Subsequently, the already carbonated RCA was stored in an environmental chamber at 25 °C and 50% relative humidity for one day. Finally, the carbonated RCA were treated by using the NS spraying method above.

After using the above five treatment methods, the corresponding treated RCAs, which were successively labeled as RCA-FC, RCA-PC, RCA-WC, RCA-NS and RCA-PCNS, were placed in an environmental chamber with a relative humidity of 50% at 25°C for several days for air-drying before they were used for casting new concrete.

### 2.3. Mix proportions

Seven groups of concrete were casted using NCA, untreated RCA and treated RCAs. The mix proportions are presented in Table 3. The effective water to cement (W/C) ratio was maintained at 0.6 by adding additional water, which was determined by considering water absorption and moisture content of NCA and RCAs.

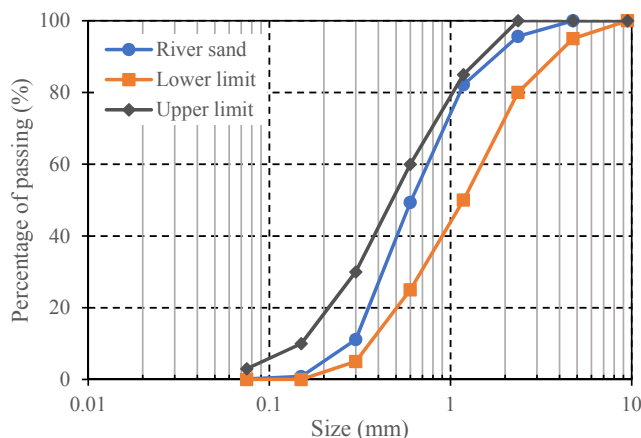


Fig. 1. Grading curve of river sand.

**Table 1**  
Physical properties of coarse aggregate and fine aggregate.

Aggregate type	Water absorption(%)	Moisture content(%)	Crushing value	Bulk density(kg/m <sup>3</sup> )	Particle density on an oven-dry basis(kg/m <sup>3</sup> )
River sand	0.42	0	–	1521	2670
RCA (5–10 mm)	7.80	1.91	–	1121	2204
RCA (10–20 mm)	6.70	1.75	29.7	1150	2234
NCA (5–10 mm)	0.69	0.20	–	1452	2634
NCA (10–20 mm)	0.57	0.20	24.1	1490	2602

**Table 2**  
Chemical compositions of NS suspension.

Percentage (%)	Chemical compositions					
	SiO <sub>2</sub>	H <sub>2</sub> O	K <sub>2</sub> O	Al <sub>2</sub> O <sub>3</sub>	Fe <sub>2</sub> O <sub>3</sub>	Ag <sub>2</sub> O
	34.280	65.558	0.055	0.049	0.018	0.041

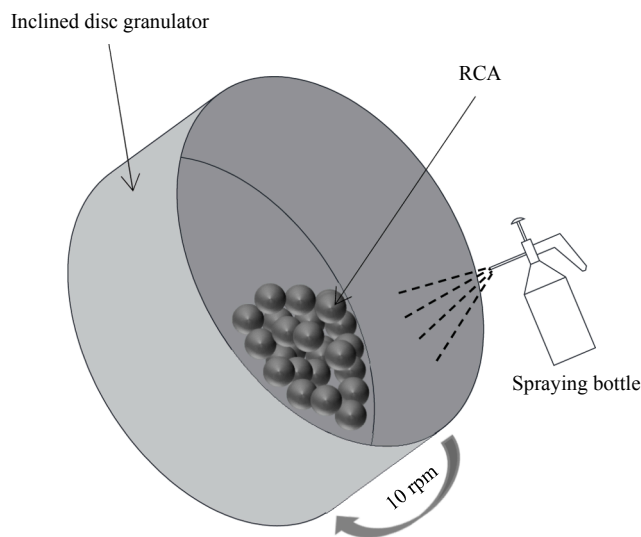


**Fig. 2.** Schematic of the NS spraying method.

## 2.4. Testing methods

### 2.4.1. Measurement of physical properties of aggregates

Water absorption, bulk density and particle density of NCA and RCAs were measured by following the procedures in BS 812–2. In the standard, there are three types of particle densities, namely particle density on an oven dried basis, apparent particle density and particle density on a saturated and surface-dried basis. The first type was used in this study. To eliminate influence of discreteness of the aggregate itself, for each treatment method, same batch of RCA was utilized for measuring its water absorption and particle density before and after treatment. The crushing value of NAC and untreated RCA were measured according to the standard BS 812–110.

**Table 3**  
Mix proportions of concrete.

Mixture	Aggregate type	W/C ratio	Water(kg/m <sup>3</sup> )	Additional water (kg/m <sup>3</sup> )	Cement(kg/m <sup>3</sup> )	Sand(kg/m <sup>3</sup> )	Coarse aggregate(5–10 mm) (kg/m <sup>3</sup> )	Coarse aggregate(10–20 mm) (kg/m <sup>3</sup> )
NAC	NCA	0.60	195	4.5	325	752	282	846
RAC-non	Untreated RCA	0.60	195	58.9	325	752	282	846
RAC-FC	RCA-FC	0.60	195	53.7	325	752	282	846
RAC-PC	RCA-PC	0.60	195	53.9	325	752	282	846
RAC-WC	RCA-WC	0.60	195	59.7	325	752	282	846
RAC-NS	RCA-NS	0.60	195	60.1	325	752	282	846
RAC-PCNS	RCA-PCNS	0.60	195	51.5	325	752	282	846

### 2.4.2. Measurement of compressive strength

Three cubic specimens (100 × 100 × 100 mm) in each type of concrete were prepared for measurement of compressive strength at age of 28 days. According to BS EN 12390–3, the loading rate in the compressive strength testing was selected as 0.6 MPa/s.

### 2.4.3. Measurement of secant modulus of elasticity

For each group of concrete, three cylindrical specimens (Φ100 × 200 mm) were prepared for measurement of secant modulus of elasticity at age of 28 days. Based on BS EN 12390–13, the loading rate was set as 0.6 MPa/s. The secant modulus of elasticity was determined as the secant slope of stress–strain curve between 5% and 1/3 of peak stress.

### 2.4.4. Measurement of sorptivity

Sorptivity, which is rate of absorption of water, is an important index of concrete durability. For each group of concrete, three cylindrical specimens (Φ100 × 50 mm), which were obtained by cutting from a bigger cylinder specimen (Φ100 × 200 mm), were prepared for measurement of sorptivity of concrete in line with ASTM C1585–13. Both initial rate of absorption and secondary rate of absorption were measured in this study.

### 2.4.5. Measurement of chloride penetration

Resistance of concrete to chloride penetration is also an important durability index. For each group of concrete, three cylindrical specimens similar with those used in sorptivity testing were prepared for measurement of chloride penetration resistance. According to ASTM C1202–19, each specimen was fixed between two cells, which were filled separately with 3% NaCl solution and 0.3 N NaOH solution. Charge passed through each specimen was measured as the indicator of chloride penetration resistance.

### 2.4.6. Measurement of microhardness

For each group of concrete, two samples with about 20 × 20 × 15 mm in size, which had been obtained from a cylindrical concrete specimen by cutting, were prepared to measure microhardness. The detailed procedures for preparing samples has been given in previous study [41]. Microhardness testing was conducted on polished surface of samples by a Vickers micro-hardness tester (HVX-1000A). For each group of concrete, three areas near the RCA-new mortar interface were selected from two samples for microhardness testing. A typical area and the distribution of the points for microhardness testing are presented in Fig. 3. RCA-new mortar interface was herein set as the origin of

coordinates, while the distance of the points in RCA region from interface was considered as negative and those in new mortar region as positive. For old mortar, the points for testing were located from  $-80\ \mu\text{m}$  to  $-40\ \mu\text{m}$ . For new ITZ, the measured distance was about  $10\ \mu\text{m}$ . For new mortar, the points for testing were evenly spaced at distance from  $40\ \mu\text{m}$  to  $200\ \mu\text{m}$ . At least four points were tested at each distance to obtain the average and standard deviation.

### 3. Testing results

#### 3.1. Physical properties of RCA after treatments

Table 4 shows the physical properties of RCA before and after subjecting to five treatment methods. After using these treatment methods, water absorption and moisture content of RCAs decreased, while particle density increased. Comparing different carbonation methods, PC method had highest efficiency in reducing water absorption and increasing particle density, FC method was in the second place while the WC method recorded the least efficiency. The sequence was similar to the corresponding carbonation degrees of RCA, which were reported in a previous study by authors [43]. It indicates that enhancement of physical properties of RCA by carbonation was dependent on its carbonation degree. However, NS spraying method only induced a slight decrease in water absorption of RCA because the NS suspension only penetrated into the surface layer of RCA and reacted with calcium hydroxide to form C-S-H, leading to densified surface layer of RCA. The PCNS method brought about the highest reduction in water absorption of RCA because PC method and NS spraying method worked together.

#### 3.2. Slump of fresh concrete

Fig. 4 shows the slump values of seven groups of concrete. The slump of all RACs was lower than that of NAC. This phenomenon has also been reported by Kebaïli et.al [44] and explained from two aspects. First, replacement of NCA by RCA with same mass led to the volume increase in concrete, which was equivalent to a reduction of water content or cement paste per unit volume. Second, angular shape and rough surface of RCA also contributes to slump reduction of RAC. In addition, Yang et. al [45] reported that generation of fine particles due to the weaker particles of RCA is another reason for slump reduction of RAC. When RCAs were treated by the five treatment methods, the slumps of all the corresponding RACs were lower than that of RAC-non. That was because the water absorption of untreated RCA was higher than that of treated RCAs, resulting in a relatively higher total water content in the corresponding RAC-non. When measuring slump, RCA was not able to absorb

all the additional water, leading to a higher water content in the matrix of RAC-non.

#### 3.3. Compressive strength of hardened concrete

28-day compressive strengths results are presented in Fig. 5. It showed that compressive strength of RAC-non was reduced by 28.2% when compared with NAC. This was a generally accepted tendency. Bai et.al [46] found that there was a 95% probability that compressive strength of RAC with 100% RCA reduced by 23.4% than that of NAC. After using RCA treatments methods, compressive strength of RAC were increased by different extents. Among different types of carbonation methods, PC method ranked best in enhancing compressive strength (9.1%), followed by FC method (3.9%) and WC method (3.3%). Observed efficiency trend was similar to the influences on physical properties of RCA. When using NS spraying method, although physical properties of RCA were less enhanced than using three carbonation methods, compressive strength of the corresponding RAC-NS showed a larger increase (10.2%). It indicates that the increased compressive strength by NS spraying method is due to enhancement of new ITZ rather than enhancement of RCA. The use of PCNS method attained an improvement of 20.7%, which was even higher than the total of that using PC method and NS spraying method separately. These results indicate that enhancements of new ITZ and RCA have synergetic effect in improving compressive strength of RAC.

#### 3.4. Secant modulus of elasticity of hardened concrete

Secant modulus of elasticity results are reported in Fig. 6. Secant modulus of elasticity of RAC-non was significantly reduced by 30.9% when compared with that of NAC. The reduction rate is within normal range. The study by Xiao et.al [47] showed that the modulus of elasticity of RAC with 100%RCA was about 15–45% lower than that of NAC, depending on the quality of RCA. Secant modulus of elasticity only slightly increased (less than 3%) with application of three carbonation treatment methods. The enhancement of modulus of elasticity was lower than that of strength, and it can be attributed to weak ITZs which neutralizes the contribution of aggregate enhancement [48]. When using NS spraying method, secant modulus of elasticity of the corresponding RAC-NS increased by 7.6%. It is due to enhancement of new ITZ, which had significant influence on modulus of elasticity of concrete [48]. PCNS method recorded 10.0% increase in secant modulus of elasticity, which was even higher than the total of that using PC method and NS spraying method separately. It should be noted that the improvement in secant modulus of elasticity was much lower than that of compressive strength.

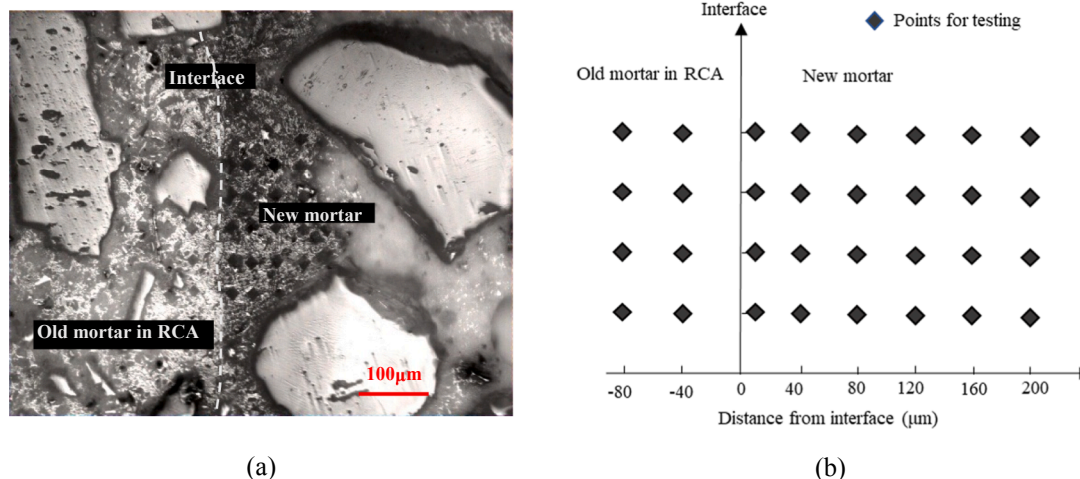


Fig. 3. A typical area (a) and distribution of the points (b) for microhardness testing.

**Table 4**  
Physical properties of RCA before and after treatments.

RCA treatment methods	Size of RCA (mm)	Water absorption of RCA(%)			Particle density of RCA(g/cm <sup>3</sup> )			Moisture content of RCA(%)		
		Before treatment	After treatment	Rate of reduction	Before treatment	After treatment	Rate of reduction	Before treatment	After treatment	Rate of reduction
FC method	5–10	7.71	7.02	8.9%	2.190	2.219	1.3%	2.02	1.91	5.4%
	10–20	6.82	6.39	6.3%	2.216	2.233	0.8%	1.67	1.75	−4.8%
PC method	5–10	7.76	6.64	14.4%	2.207	2.257	2.3%	2.02	1.40	30.7%
	10–20	6.40	5.64	11.9%	2.252	2.292	1.8%	1.67	1.01	39.5%
WC method	5–10	7.83	7.41	5.3%	2.192	2.203	0.5%	2.02	1.77	12.4%
	10–20	6.99	6.70	4.1%	2.216	2.228	0.5%	1.67	1.52	9.0%
NS method	5–10	7.83	7.54	3.6%	2.192	2.215	1.0%	2.02	1.80	10.9%
	10–20	6.99	6.79	2.8%	2.215	2.234	0.9%	1.67	1.60	4.2%
PCNS method	5–10	7.76	6.45	16.8%	2.207	2.254	2.1%	2.02	1.42	29.7%
	10–20	6.40	5.48	14.4%	2.252	2.293	1.8%	1.67	1.07	35.9%

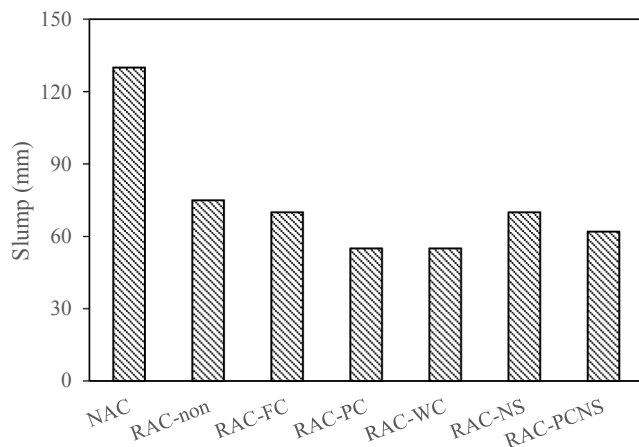


Fig. 4. Slump of fresh concretes.

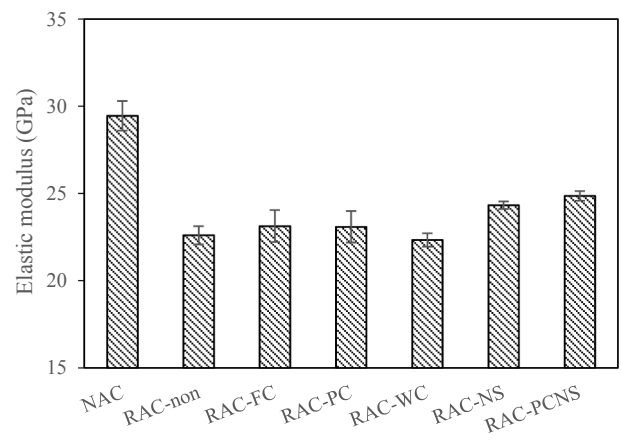


Fig. 6. Secant modulus of elasticity of hardened concretes.

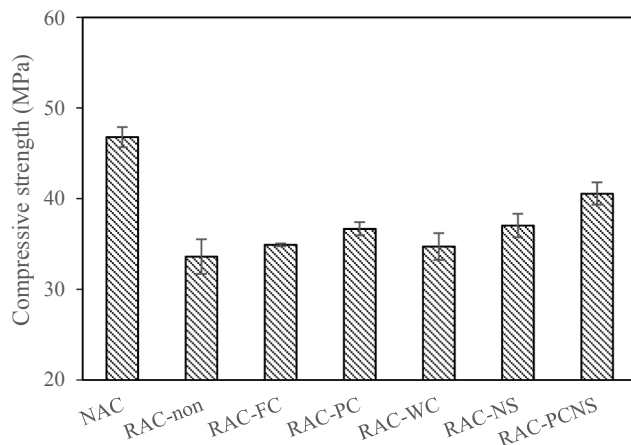


Fig. 5. Compressive strengths of hardened concretes.

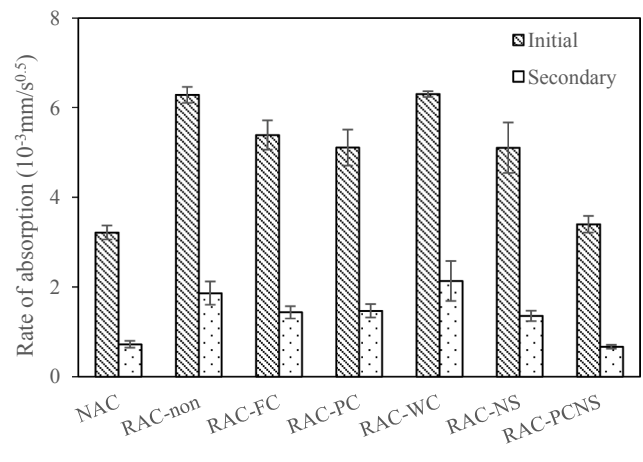


Fig. 7. Sorptivity of hardened concretes.

3.5. Sorptivity of hardened concrete

The sorptivity results including initial and secondary rates of absorption are presented in Fig. 7. It showed that the rate of absorption of RAC-non was much higher than NAC. The initial and secondary rate of absorption of NAC decreased by 48.9% and 61.1% when compared with RAC-non. That is because the use of RCA increased overall porosity of concrete. However, rate of absorption was obviously reduced after using RCA treatment methods. That is because enhancement of RCA after treatment can reduce porosity of RAC, while enhancement of new ITZ after treatment can influence the seepage path of water, leading to more water going around RCA instead of penetrating RCA. Among three

carbonation methods, PC method caused the largest reduction, FC method was second while WC method led to the lowest reduction. It indicates that reduction in sorptivity of RAC by carbonation methods is also dependent on carbonation degree of RCA. After using NS spraying method, rate of absorption of the corresponding RAC-NS showed a similar reduction with RAC-PC due to enhancement of new ITZ. When PCNS method was adopted, rate of absorption was significantly reduced to a level close to that of NAC because of enhancement of both RCA and new ITZ.

### 3.6. Chloride penetration resistance of hardened concrete

Chloride penetration resistance of concrete, which is reflected by value of charge passed, is shown in Fig. 8. It could be found that the charge passed of RAC-non was 30.5% higher than that of NAC. After using these RCA treatment methods, the charge passed of the corresponding RACs was reduced to different degree. The reasons are similar to that of sorptivity as stated above. Among three carbonation treatment methods, FC and PC method were better in improving chloride penetration resistance of RAC. When using NS spraying method, charge passed of RAC decreased by 3.8%. When PCNS method was used, the decrease in charge passed of RAC was 24.4%, which was even larger than the total of that using PC method and NS spraying method. It indicates that enhancement of new ITZ and RCA have synergistic effect in improving durability of RAC.

### 3.7. Microhardness of hardened concrete

Microhardness values of concrete at zones near the interface between RCA/NCA and new mortar are shown in Fig. 9. The indentation points was located at distance of  $-80 \mu\text{m}$  to  $200 \mu\text{m}$  from interface (as shown in Fig. 3), which covered old mortar, new ITZ and new mortar. It showed that old mortar exhibited larger microhardness values than new mortar in all RACs. In RAC-non, microhardness at distance of  $10 \mu\text{m}$  was slightly lower, and it fluctuated along the increasing distance after  $40 \mu\text{m}$ . Therefore, the value at distance of  $10 \mu\text{m}$  was considered as the microhardness of new ITZ. After using these RCA treatment methods, microhardness of new ITZ and old mortar showed obvious changes, while the change in microhardness of new mortar was not significant. The detailed influences of five RCA treatment methods on average microhardness of old mortar, new ITZ and new mortar were introduced below.

Microhardness values of new mortar at distances of  $40 \sim 200 \mu\text{m}$  from interface in different types of concrete are shown in Fig. 10. The microhardness of new mortar in RAC-non was lower than that of NAC. The possible reason is that real W/C ratio of new mortar in RAC was higher than that of NAC because of water bleeding from RCA when casting concrete [49]. However, the microhardness of new mortar did not show obvious change after using these RCA treatment methods. It implies that the influences of these RCA treatment methods on new mortar are not significant.

Microhardness values of new ITZs at  $10 \mu\text{m}$  from interface in seven groups of concrete are presented in Fig. 11. The microhardness of new ITZ in RAC-non was lower than that of NAC. The reason was similar to the corresponding new mortar as stated above. The microhardness of new ITZ increased by 20.4% and 17.5% respectively after using FC or PC method. WC method recorded 36.5% increase in microhardness of new ITZ, which was larger than that both FC and PC method. NS spraying

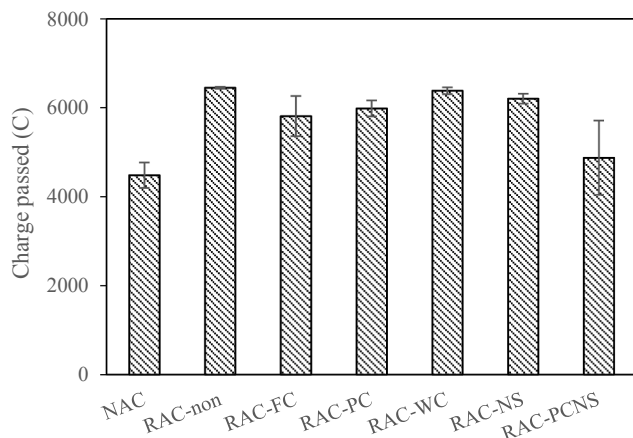


Fig. 8. Chloride penetration resistance of hardened concretes.

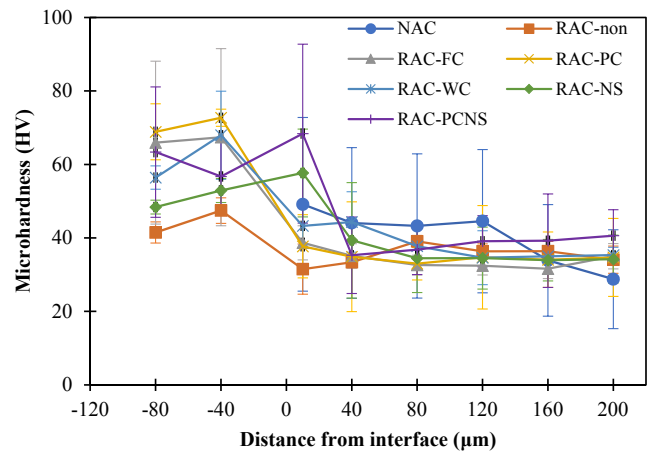


Fig. 9. Microhardness of hardened concretes.

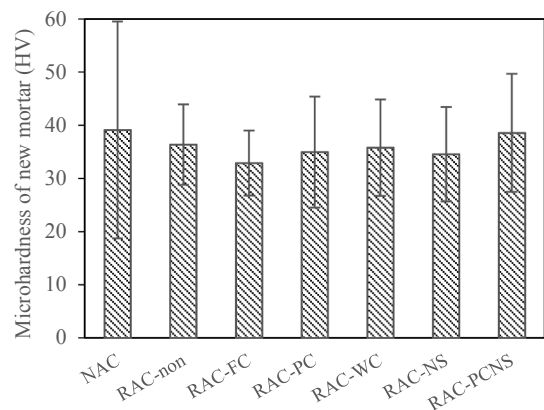


Fig. 10. Microhardness of new mortar in concretes.

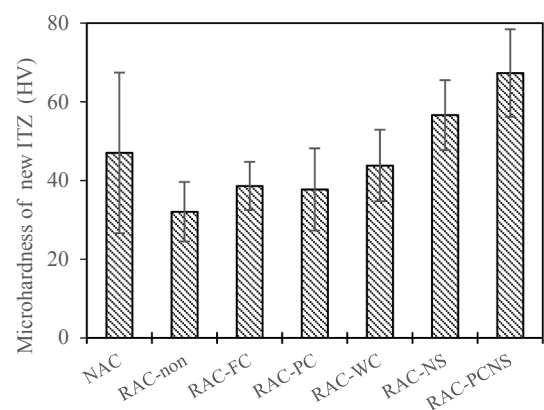


Fig. 11. Microhardness of new ITZ in concretes.

method resulted in 76.4% increase in microhardness of new ITZ, which was higher than that three carbonation treatments. The microhardness of new ITZ showed the highest improvement (109.7%) when PCNS method was used. The reasons for them will be discussed in the next section.

The microhardness results of old mortar in RACs are reported in Fig. 12. It showed that the microhardness values of old mortar in RAC were increased after using all the RCA treatment methods. Among them, NS spraying exhibited a much smaller enhancement, which was due to the reaction between nano silica and calcium hydroxide in RCA [28].

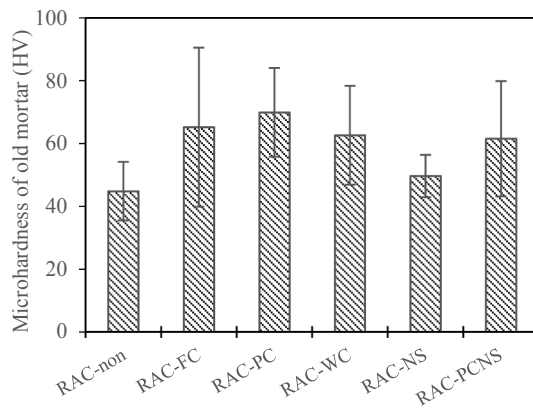


Fig. 12. Microhardness of old mortars in RCA.

When using three carbonation treatment methods and PCNS method, the microhardness values of old mortars were all significantly enhanced because the carbonation of cement hydration products (calcium hydroxide and C-S-H) and un-hydrated cement clinkers in RCA [33] can make it more densified.

## 4. Discussion

### 4.1. Mechanism of the RCA treatment methods

According to the test results, all of RCA treatment methods in this study could enhance RCA's performance. The mechanisms are discussed below:

A three-phase model of RAC-non, which comprises of untreated RCA, new mortar and new ITZ, is shown in Fig. 13(a). By applying PC method, the majority of RCA were carbonated, which was confirmed by spraying phenolphthalein indicator on the fractured section of RCA. The old mortar in carbonated layer of RCA was significantly enhanced, as evidenced by microhardness results. That is because  $\text{CO}_2$  reacted with hydration products of cement (calcium hydroxide and C-S-H) and un-hydrated clinkers in RCA and formed  $\text{CaCO}_3$  and silica gel [33], enhancing the microstructure of old mortar in RCA. Moreover, based on SEM observations of RCA before and after different treatments as shown in Fig. 14, many  $\text{CaCO}_3$  particles with size of about  $1 \mu\text{m}$  were formed on the surface of RCA after using PC method. It promoted the formation of C-S-H in new ITZ due to the nucleation effect, which also contributed to the enhancement of new ITZ [50]. This is the reason for the increase in microhardness of new ITZ after using PC method. Because of the enhanced carbonated RCA layer and new ITZ, the performance of RAC-PC was improved when compared with RAC-non. The schematic of RAC-PC was shown in Fig. 13(c).

After using FC method, the situation was similar to that of PC method. However, thickness of the carbonated layer for FC method was smaller. That was because  $\text{CO}_2$  would not be able to penetrate RCA effectively without applying pressure, and this led to less enhancement in physical properties of RCA-FC than RCA-PC. As a result, FC method induced a relatively smaller improvement in performance of RAC. The schematic of RAC-FC is shown in Fig. 13(b).

By using WC method, new ITZ was better enhanced than that of FC and PC method, as evidenced by microhardness result. That might be because many small  $\text{SiO}_2$  particles, which was confirmed by EDS, were formed on the surface of RCA due to fast wet carbonation, as shown in Fig. 14(c). These nano-sized  $\text{SiO}_2$  particles exerted filling effect and promoted formation of additional C-S-H in new ITZ because of nucleation and pozzolanic reactions [51], and it is more effective to enhance new ITZ than  $\text{CaCO}_3$  particles that formed after using PC or FC methods. However, as only surface layer of RCA was carbonated, which was confirmed by spraying phenolphthalein indicator on the fractured

section of RCA, WC method only slightly enhanced physical properties of RCA. It might be due to dense layer of carbonation product formed on the surface of RCA which prevented inner part of RCA from participating in carbonation reaction. It indicates that enhanced new ITZ was the main factor responsible for the improved performance of RAC-WC. But because the enhancement of new ITZ by WC method was still limited, the improvement in mechanical properties and durability was relatively lower than other two carbonation treatment methods. The schematic of RAC-WC is shown in Fig. 12(d).

When NS spraying method was adopted, NS particles on the surface of RCA (as presented in Fig. 14(d)) can react with calcium hydroxide in cement paste of new mortar to form a layer of C-S-H with low Ca/Si ratio [52]. As a result, new ITZ of RAC-NS was significantly densified, as evidenced by microhardness results. Generally, the mechanical properties such as strength and elastic modulus and durability of RCA can be improved as a result of enhancement of new ITZs [25,26,27,53]. Therefore, significantly enhanced new ITZ should be the key to enhanced performance of RAC-NS, although old mortar in surface layer of RCA was also slightly enhanced due to the pozzolanic effect of NS [41]. Compared with WC method, the amount of NS particles on RCA after spraying NS suspension was much larger, and thus new ITZ was enhanced much more significantly, as confirmed by microhardness results. Because of the significantly enhanced new ITZ, the improvement in mechanical properties of RAC after using NS spraying method was even higher than using PC method. The schematic of RAC-NS is shown in Fig. 13(e).

Based on the mechanism of PC method and NS spraying method as mentioned above, both the majority of RCA and new ITZ could be obviously enhanced by using PCNS method. The schematic of RAC-PCNS is displayed in Fig. 13 (f). Interestingly, when PCNS method was adopted, the increase in mechanical properties and durability of RCA was even larger than total improvement obtained using PC method and NS spraying method separately. These results imply that enhancements of RCA and new ITZ had synergistic effect in improving the performance of RAC.

### 4.2. Economic efficiency

Carbonation treatment requires the use of designated treatment plants. But as decarbonization is a global issue, if RCA can be used to sequester waste  $\text{CO}_2$  by using the carbonation treatment, the economic benefit can be used to offset the cost of treatment.

Regarding NS spraying method, it only involves a simple spraying process and the production line is easy to build. Based on the experimental test results, a 3% NS suspension is needed while the price of NS suspension in China is about US\$400/t. Therefore, the material cost for NS spraying treatment would be about US\$13 per cubic metre of RAC that contains 100% RCA, which is about 21.7% of the cost of commercial C40 concrete in China. However, there are environmental and cost benefits associated with the recycling of construction wastes, including avoidance of exploitation of natural aggregates and landfilling. A previous study by our group has quantified the life cycle environmental benefits of recycling of RAC [53]. More detailed life cycle cost analysis is needed to quantify the economic benefits.

## 5. Conclusions

In this study, the efficiencies of five types of recycled coarse aggregate (RCA) treatment methods, namely flow-through gas–solid carbonation (FC), pressurized gas–solid carbonation (PC), wet carbonation (WC), nano silica (NS) spraying and combined pressurized gas–solid carbonation with NS spraying (PCNS) method, in enhancing the performance of recycled aggregate concrete (RAC) were investigated. The following findings are summarized.

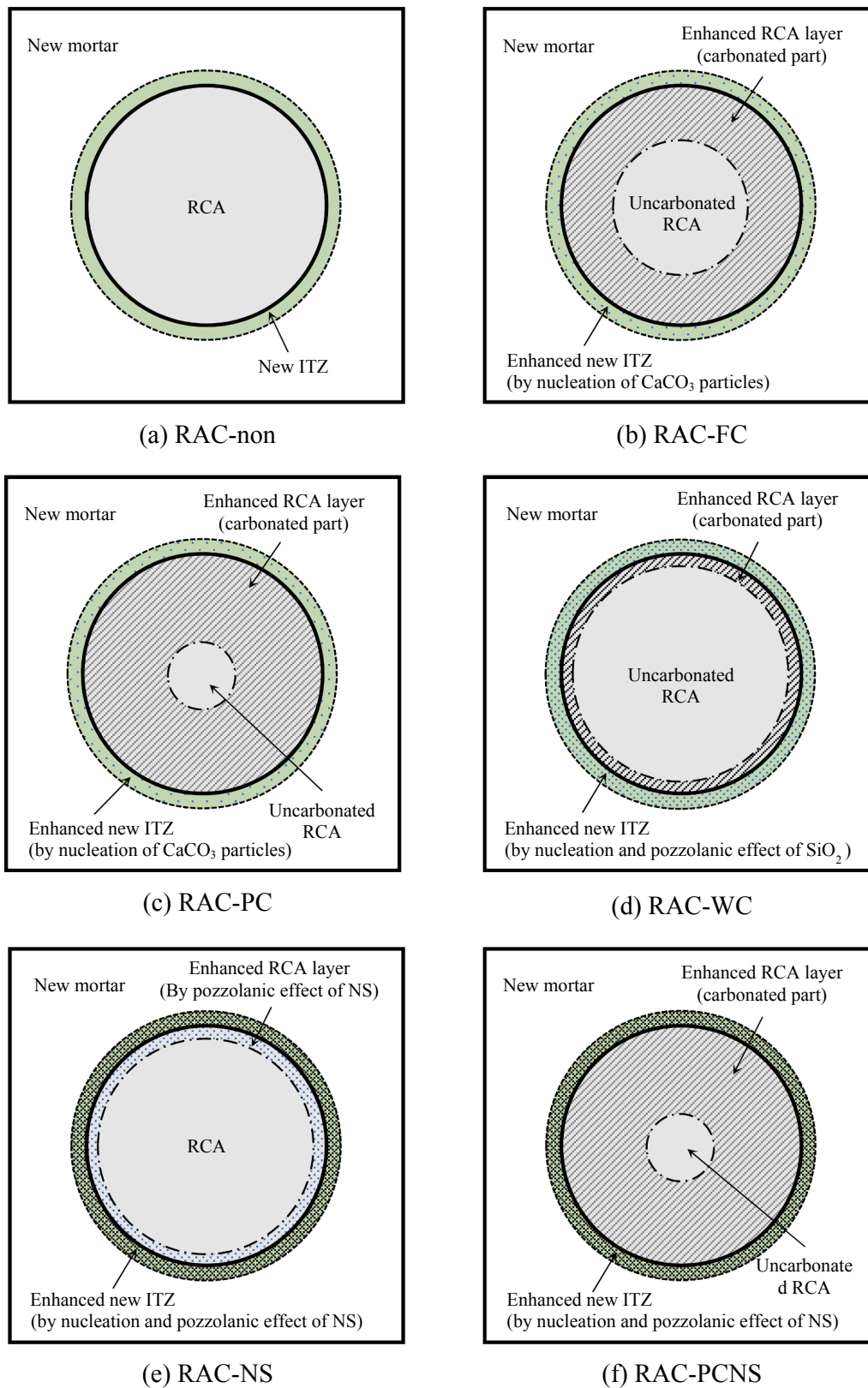


Fig. 13. Schematics of RACs with different RCA treatment methods.

- (1) Mechanical properties and durability of RAC can be improved by using the five RCA treatment methods.
- (2) Among three carbonation treatment methods, PC method recorded highest efficiency in improving physical properties of RCA, mechanical properties and durability of RAC. Compared with PC

- method, NS spraying method had a higher efficiency in enhancing mechanical properties of RAC.
- (3) PCNS method had a highest efficiency in enhancing the performance of RAC, which was even higher than the total of that using PC method and NS spraying method individually. Using this

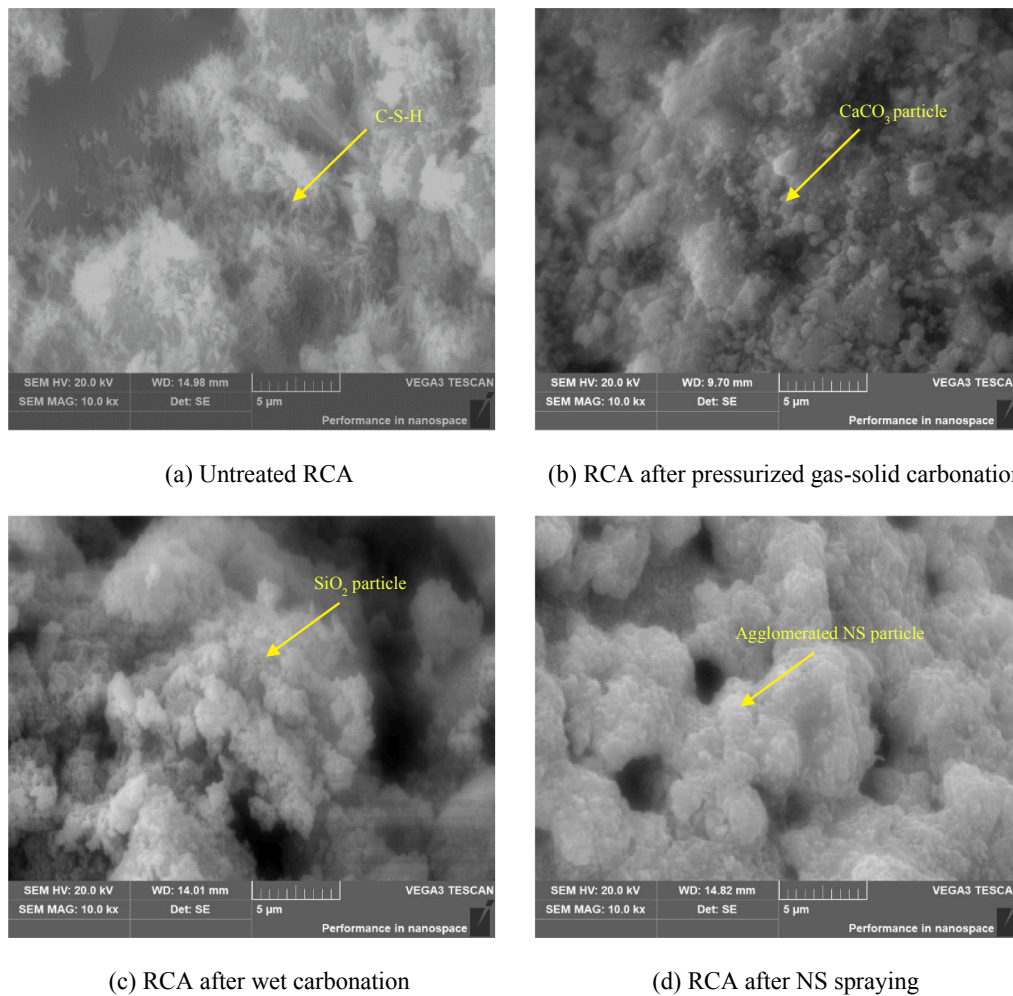


Fig. 14. Microstructures of RCA before and after different treatments by SEM.

combined treatment, compressive strength of RAC increased by 20.7% and sorptivity of RAC was close to that of NAC.

- (4) When using FC or PC method, both the enhanced old mortar of RCA and new ITZ contributed to improving performance of RAC. Regarding WC and NS spraying method, the significantly enhanced new ITZ was the main factor for improving performance of RAC. For PCNS method, both old mortar and new ITZ were significantly improved, leading to a synergistic effect in enhancing mechanical properties and durability of RAC.

#### CRediT authorship contribution statement

**Long Li:** Conceptualization, Methodology, Investigation, Writing - original draft, Validation. **Dongxing Xuan:** Conceptualization, Writing - review & editing. **A.O. Sojobi:** Investigation, Writing - review & editing. **Songhui Liu:** Investigation, Writing - review & editing. **Chi Sun Poon:** Conceptualization, Writing - review & editing, Supervision, Funding acquisition.

#### Declaration of Competing Interest

The authors declare that they have no known competing financial interests or personal relationships that could have appeared to influence the work reported in this paper.

#### Acknowledgements

The authors are thankful to financial support by Construction Industry Council (CICR/03/19) and Research Grants Council GRF (PolyU 152144/17E).

#### References

- [1] A.O. Sojobi, D. Xuan, L. Li, S. Liu, C.S. Poon, Optimization of gas-solid carbonation conditions of recycled aggregates using a linear weighted sum method, *Developments in the Built Environment* 7 (2021) 100053.
- [2] L.W. Zhang, A.O. Sojobi, K.M. Liew, Sustainable CFRP-reinforced recycled concrete for cleaner eco-friendly construction, *J. Cleaner Prod.* 233 (2019) 56–75.
- [3] M.S. Aslam, B. Huang, L. Cui, Review of construction and demolition waste management in China and USA, *J. Environ. Manage.* 264 (2020), 110445.
- [4] B.o. Wang, L. Yan, Q. Fu, B. Kasal, A Comprehensive Review on Recycled Aggregate and Recycled Aggregate Concrete, *Resour. Conserv. Recycl.* 171 (2021) 105565, <https://doi.org/10.1016/j.resconrec.2021.105565>.
- [5] J. Xiao, W. Li, Y. Fan, X. Huang, An overview of study on recycled aggregate concrete in China (1996–2011), *Constr. Build. Mater.* 31 (2012) (2012) 364–383.
- [6] M. Upshaw, C. S. Cai, Critical Review of Recycled Aggregate Concrete Properties, Improvements, and Numerical Models. *Journal of Materials in Civil Engineering*, 32(11)(2020) 03120005.
- [7] M. Etxebarria, E. Vázquez, A. Marí, M. Barra, Influence of amount of recycled coarse aggregates and production process on properties of recycled aggregate concrete, *Cem. Concr. Res.* 37 (5) (2007) 735–742.
- [8] J. Xiao, L. Li, L. Shen, J. Yuan, Effects of strain rate on mechanical behavior of modeled recycled aggregate concrete under uniaxial compression, *Constr. Build. Mater.* 93 (2015) 214–222.
- [9] Z.H. Duan, C.S. Poon, Properties of recycled aggregate concrete made with recycled aggregates with different amounts of old adhered mortars, *Mater. Des.* 58 (2014) 19–29.

- [10] F. Théréné, E. Keitaa, J. Naël-Redolfib, P. Boustingorryb, L. Bonafousb, N. Roussela, Water absorption of recycled aggregates: Measurements, influence of temperature and practical consequences, *Cem. Concr. Res.* 137 (2020), 106196.
- [11] C. Shi, Y. Li, J. Zhang, W. Li, L. Chong, Z. Xie, Performance enhancement of recycled concrete aggregate – A review, *J. Cleaner Prod.* 112 (2016) 466–472.
- [12] D.X. Xuan, B.J. Zhan, C.S. Poon, Assessment of mechanical properties of concrete incorporating carbonated recycled concrete aggregates, *Cem. Concr. Compos.* 65 (2016) 67–74.
- [13] L. Li, J. Xiao, D.X. Xuan, C.S. Poon, Effect of carbonation of modeled recycled coarse aggregate on the mechanical properties of modeled recycled aggregate concrete, *Cem. Concr. Compos.* 89 (2018) 169–180.
- [14] K. Ouyang, C. Shi, H. Chu, et al., An overview on the efficiency of different pretreatment techniques for recycled concrete aggregate, *J. Cleaner Prod.* 263 (2020), 121264.
- [15] A. Verma, V.S. Babu, S. Arunachalam, Characterization of recycled aggregate by the combined method: Acid soaking and mechanical grinding technique, *Mater. Today.. Proc.* (2021).
- [16] H. Choi, M. Lim, H. Choi, R. Kitagaki, T. Noguchi, Using Microwave Heating to Completely Recycle Concrete, *Journal of Environmental Protection* 05 (07) (2014) 583–596.
- [17] A. Akbarnezhad, K.C.G. Ong, M.H. Zhang, C.T. Tam, T.W.J. Foo, Microwave assisted beneficiation of recycled concrete aggregates, *Constr. Build. Mater.* 25 (8) (2011) 3469–3479.
- [18] A. Katz, Treatments for the improvement of recycled aggregate, *J. Mater. Civ. Eng.* 16 (6) (2004) 597–603.
- [19] V.W.Y. Tam, C.M. Tam, K.N. Le, Removal of cement mortar remains from recycled aggregate using pre-soaking approaches, *Resour. Conserv. Recycl.* 50 (1) (2007) 82–101.
- [20] B. Zhan, C.S. Poon, Q. Liu, S. Kou, C. Shi, Experimental study on CO<sub>2</sub> curing for enhancement of recycled aggregate properties, *Constr. Build. Mater.* 67 (2014) 3–7.
- [21] L. Li, C.S. Poon, J. Xiao, D.X. Xuan, Effect of carbonated recycled coarse aggregate on the dynamic compressive behavior of recycled aggregate concrete, *Constr. Build. Mater.* 151 (2017) 52–62.
- [22] J. Zhang, C. Shi, Y. Li, X. Pan, C.S. Poon, Z. Xie, Performance enhancement of recycled concrete aggregates through carbonation, *J. Mater. Civ. Eng.* 27 (11) (2015) 04015029, [https://doi.org/10.1061/\(ASCE\)MT.1943-5533.0001296](https://doi.org/10.1061/(ASCE)MT.1943-5533.0001296).
- [23] A.M. Grabić, J. Klama, D. Zawal, et al., Modification of recycled concrete aggregate by calcium carbonate bio deposition, *Constr. Build. Mater.* 34 (2012) 145–150.
- [24] A.A.P. Mansur, D.B. Santos, H.S. Mansur, A microstructural approach to adherence mechanism of poly (vinyl alcohol) modified cement systems to ceramic tiles, *Cem. Concr. Res.* 37 (2) (2007) 270–282.
- [25] V.W.Y. Tam, X.F. Gao, C.M. Tam, Microstructural analysis of recycled aggregate concrete produced from two-stage mixing approach, *Cem. Concr. Res.* 35 (6) (2005) 1195–1203.
- [26] J. Li, H. Xiao, Y. Zhou, Influence of coating recycled aggregate surface with pozzolanic powder on properties of recycled aggregate concrete, *Constr. Build. Mater.* 23 (3) (2009) 1287–1291.
- [27] H. Zhang, Y. Zhao, T. Meng, S.P. Shah, Surface treatment on recycled coarse aggregates with nanomaterials, *J. Mater. Civ. Eng.* 28 (2) (2016) 04015094, [https://doi.org/10.1061/\(ASCE\)MT.1943-5533.0001368](https://doi.org/10.1061/(ASCE)MT.1943-5533.0001368).
- [28] W. Zeng, Y. Zhao, H. Zheng, C.S. Poon, Improvement in corrosion resistance of recycled aggregate concrete by nano silica suspension modification on recycled aggregates, *Cem. Concr. Compos.* 106 (2020), 103476.
- [29] S.C. Kou, C.S. Poon, Long-term mechanical and durability properties of recycle aggregate concrete prepared with the incorporation of fly ash, *Cem. Concr. Compos.* 37 (2013) 12–19.
- [30] V. Corinaldesi, G. Moriconi, Influence of mineral additions on the performance of 100% recycled aggregate concrete, *Constr. Build. Mater.* 23 (2009) 2869–2876.
- [31] W. Li, C. Long, V.W.Y. Tam, C.S. Poon, W.H. Duan, Effects of nano-particles on failure process and microstructural properties of recycled aggregate concrete, *Constr. Build. Mater.* 142 (2017) 42–50.
- [32] B.B. Mukharjee, S.V. Barai, Influence of Nano-Silica on the properties of recycled aggregate concrete, *Constr. Build. Mater.* 55 (2014) 29–37.
- [33] C. Liang, B. Pan, Z. Ma, Z. He, Z. Duan, Utilization of CO<sub>2</sub> curing to enhance the properties of recycled aggregate and prepared concrete: A review, *Cem. Concr. Compos.* 105 (2020) 103446, <https://doi.org/10.1016/j.cemconcomp.2019.103446>.
- [34] C.J. Shi, Z.M. Wu, Z.J. Cao, T.C. Ling, J.L. Zheng, Performance of mortar prepared with recycled concrete aggregate enhanced by CO<sub>2</sub> and pozzolan slurry, *Cem. Concr. Compos.* 86 (2018) 130–138.
- [35] C. Liang N.a. Lu H. Ma Z. Ma Z. Duan 39 2020 101185 10.1016/j.jcou.2020.101185.
- [36] C. Liang, H. Ma, Y. Pan, Z. Ma, Z. Duan, Z. He, Chloride permeability and the caused steel corrosion in the concrete with carbonated recycled aggregate, *Constr. Build. Mater.* 218 (2019) 506–518.
- [37] S. Kashef-Haghighi, S. Ghoshal, CO<sub>2</sub> sequestration in concrete through accelerated carbonation curing in a flow-through reactor, *Ind. Eng. Chem. Res.* 49 (3) (2010) 1143–1149.
- [38] Z. Maciej, S. Jørgen, S. Jan, D. Pawel, B. Frank, B.H. Mohsen, Phase assemblage and microstructure of cement paste subjected to enforced, wet carbonation, *Cem. Concr. Res.* 130 (2020), 105990.
- [39] S.H. Liu, P.L. Shen, D.X. Xuan, L. Li, A.O. Sojobi, B.J. Zhan, C.S. Poon, A comparison of liquid-solid and gas-solid accelerated carbonation for enhancement of recycled concrete aggregate, *Cem. Concr. Compos.* 118 (2021), 103988.
- [40] F. Shaikh, V. Chavda, N. Minhaj, H.S. Arel, Effect of mixing methods of nano silica on properties of recycled aggregate concrete, *Structural Concrete* 19 (2) (2018) 387–399.
- [41] L. Li, D.X. Xuan, A.O. Sojobi, S. Liu, S.H. Chu, C.S. Poon, Development of nano-silica treatment methods to enhance recycled aggregate concrete, *Cem. Concr. Compos.* 118 (2021), 103963.
- [42] X. Fang, B. Zhan, C.S. Poon, Enhancement of recycled aggregates and concrete by combined treatment of spraying Ca<sup>2+</sup> rich wastewater and flow-through carbonation, *Constr. Build. Mater.* 277 (2021), 122202.
- [43] L. Li, D. Xuan, C.S. Poon, Stress-Strain Curve and Carbonation Resistance of Recycled Aggregate Concrete after Using Different RCA Treatment Techniques, *Applied Sciences* 11 (9) (2021) 4283.
- [44] O. Kebaili, M. Mouret, N. Arabi, F. Cassagnabere, Adverse effect of the mass substitution of natural aggregates by air-dried recycled concrete aggregates on the self-compacting ability of concrete: evidence and analysis through an example, *J. Cleaner Prod.* 87 (2015) 752–761.
- [45] J. Yang, Q. Du, Y. Bao, Concrete with recycled concrete aggregate and crushed clay bricks, *Constr. Build. Mater.* 25 (4) (2011) 1935–1945.
- [46] G. Bai, C. Zhu, C. Liu, B. Liu, An evaluation of the recycled aggregate characteristics and the recycled aggregate concrete mechanical properties, *Constr. Build. Mater.* 240 (2020), 117978.
- [47] J. Xiao, W. Li, Y. Fan, X. Huang, An overview of study on recycled aggregate concrete in China (1996–2011), *Constr. Build. Mater.* 31 (1) (2012) 364–383.
- [48] C. Zhou, K. Li, F.u. Ma, Numerical and statistical analysis of elastic modulus of concrete as a three-phase heterogeneous composite, *Comput. Struct.* 139 (2014) 33–42.
- [49] C.S. Poon, Z.H. Shui, L. Lam, Effect of microstructure of ITZ on compressive strength of concrete prepared with recycled aggregates, *Constr. Build. Mater.* 18 (6) (2004) 461–468.
- [50] B.J. Zhan, D.X. Xuan, C.S. Poon, K.L. Scrivener, Characterization of interfacial transition zone in concrete prepared with carbonated modeled recycled concrete aggregates, *Cem. Concr. Res.* 136 (2020), 106175.
- [51] L.P. Singh, S.R. Karade, S.K. Bhattacharyya, M.M. Yousuf, S. Ahalawat, Beneficial role of nanosilica in cement based materials – A review, *Constr. Build. Mater.* 47 (2013) 1069–1077.
- [52] L. Li, D. Xuan, S.H. Chu, J.X. Lu, C.S. Poon, Efficiency and mechanism of nano-silica pre-spraying treatment in performance enhancement of recycled aggregate concrete, *Constr. Build. Mater.* 301 (2021), 124093.
- [53] M.U. Hossain, C.S. Poon, I.M.C. Lo, J.C.P. Chen, Comparative environmental evaluation of aggregate production from recycled waste materials and virgin sources by LCA, *Resour. Conserv. Recycl.* 109 (2016) 67–77.



# Modification of recycled aggregate by spraying colloidal nano silica and silica fume

Long Li · Dongxing Xuan · S. H. Chu · Chi Sun Poon

Received: 8 June 2021 / Accepted: 1 November 2021 / Published online: 16 November 2021  
© RILEM 2021

**Abstract** In this study, modification methods of recycled coarse aggregate (RCA), namely spraying colloidal nano silica (NS) and silica fume (SF) on the surface of RCA, were adopted to enhance the performance of recycled aggregate concrete (RAC). In the RCA modification methods, colloidal NS with different particle sizes (12 nm, 54 nm and 106 nm) and colloidal SF with a particle size of 420 nm were considered. To understand the effectiveness of silica with different particle sizes, mechanical properties and durability of RAC prepared with the modified RCA were evaluated. Microhardness and scanning electron microscopy (SEM) tests were conducted to investigate the microstructural properties. Test results showed that the mechanical properties and durability of RAC were enhanced remarkably after spraying colloidal NS and SF on the surface of RCA, whilst the performance enhancement was larger at a larger particle size of NS. Moreover, it was found that spraying colloidal SF on RCA enhanced both the new mortar and the new interfacial transition zone (ITZ) in RAC, while

spraying colloidal NS only enhanced the new ITZ, as evidenced by microhardness investigations. This study deepens the understanding of enhancing the performance of RAC to approach that of natural aggregate concrete.

**Keywords** Nano silica · Silica fume · Microhardness · Strength · Durability · Recycled coarse aggregate (RCA)

## 1 Introduction

The continuous urbanization worldwide yields a huge amount of construction and demolition waste, particularly in developing countries, worsening the environment and occupying the limited landfill. To solve this problem, the re-utilization of waste concrete as recycled coarse aggregate (RCA) for concrete production is a promising solution. The production of recycled aggregate concrete (RAC) not only consumes construction and demolition waste but also conserves natural resources. However, RAC is generally inferior to natural aggregate concrete (NAC) in terms of mechanical properties and durability [1–5] and thus it is not widely applied in structural engineering so far. Previous studies concluded that the main reasons for the inferior performance of RAC are the higher water absorption, higher porosity and lower density of RCA in comparison with natural aggregates [6–9].

---

L. Li · D. Xuan · S. H. Chu · C. S. Poon (✉)  
Department of Civil and Environmental Engineering, The  
Hong Kong Polytechnic University, Kowloon, Hong  
Kong  
e-mail: cecspoon@polyu.edu.hk

C. S. Poon  
Research Centre for Resources Engineering towards  
Carbon Neutrality (RCRE), The Hong Kong Polytechnic  
University, Kowloon, Hong Kong



To improve the properties of RAC, many RCA modification methods have been proposed [10]. In general, these RCA modification methods belong to three categories [11]. First, removing the old mortar attached on RCA by mechanical grinding [12, 13], microwave heating [14, 15], ultrasonic cleaning in water [16], pre-soaking in acid solutions [17], and so on. Second, enhancing the old mortar with techniques such as accelerated carbonation [18–21], microbial carbonate precipitation [22], sodium silicate solution pre-soaking [23], and polyvinyl alcohol pre-soaking [24]. Third, enhancing the new interface transition zone (ITZ) by coating RCA with cement slurry [25], geopolymer slurry [26], pozzolan slurries [27], silica fume slurry [28], or nanoparticles [29, 30], etc. Apart from these RCA modification methods, another way is enhancing the new mortar in RAC by incorporating supplementary cementitious materials such as fly ash/silica fume [31, 32] and nanoparticles [33, 34] in the concrete mixture.

Nanoparticles have been utilized to enhance the performance of RAC. Among various nanoparticle technologies, pre-soaking RCA in colloidal nano silica (NS) and directly mixing NS in concrete mixture have attracted increasing attention [35]. It was reported that these NS treatment methods can improve the mechanical properties [29, 30, 36–38] and durability of RAC [29, 30, 38]. However, pre-soaking RCA in colloidal NS consumes a large amount of colloidal NS as water absorption of RCA is high and thus exhibits inadequate economic feasibility, while directly mixing NS in concrete leads to a reduction of workability.

A previous study by the authors [39] adopted a new RCA modification method by spraying colloidal NS on RCA which consumed less NS than the pre-soaking method. Moreover, this RCA modification method had no obvious negative influence on the workability of RAC and contributed to improved mechanical properties and durability over that of the NS pre-soaking method. It has been reported [40–42] that the particle size of NS influences the performance of cement paste. Thus, the particle size of NS may also influence the efficiency of NS spraying treatment in enhancing the performance of RAC, which is not well understood so far. To fill this research gap, this study investigates the effect of using different particle sizes of colloidal NS for spraying RCA on the performance of RAC. To facilitate comparison, a type of colloidal silica fume

(SF), considered as a larger size silica, was also used to modify RCA.

## 2 Materials and methods

### 2.1 Materials

Ordinary Portland cement CEM I 52.5N was used. The fine aggregate was a river sand with a fineness modulus of 2.6. A batch of RCA was collected from a local construction waste recycling company. After crushing and sieving, two size fractions of RCA were obtained, namely 10–20 mm and 5–10 mm. To maintain consistency, natural coarse aggregate (NCA) was also sieved into these two size fractions. Three types of commercial colloidal NS were used to pretreat RCA. The SiO<sub>2</sub> contents were about 30% in each. A type of solid SF in gray color was mixed with water by 3:7 to produce the colloidal SF. The chemical compositions of the solid SF and cement are reported in Table 1. The particle size distributions of the three types of NS and the SF were determined by a Particle Size and Zeta Potential Analyzer (Zetasizer Nano ZS90), as shown in Fig. 1. Their average particle sizes were 12 nm, 54 nm, 106 nm and 420 nm which are labelled as NS12, NS54, NS106 and SF420, respectively.

### 2.2 Spraying colloidal NS and SF on RCA

The colloidal NS and SF were sprayed on the surface of air-dried RCA by a handheld spraying device. To ensure a uniform spraying process, each batch of 5.0 kg RCA was put into a rotating inclined mixer ( $\Phi 500 \times 170$  mm) at a rotation speed of 10 rev/min when colloidal NS and SF were applied [39]. The amount of colloidal NS and SF for spraying was fixed at 3% of RCA by mass consistently, which was an optimal amount determined in the previous study [39]. Then, the treated RCA was stored in an environmental chamber (relative humidity of 50% at 25 °C) for 4 days prior to concrete production.

### 2.3 Mix proportions of concrete

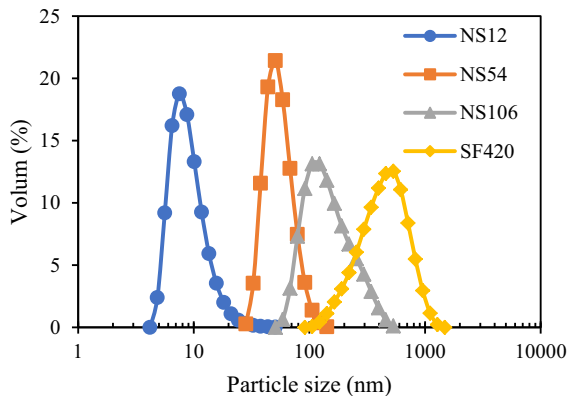
A total of 6 concrete mixtures were prepared by using NCA, untreated RCA, and RCAs treated by spraying NS12, NS54, NS106 and SF420. The corresponding



**Table 1** Chemical compositions of cement and SF

Material	Chemical compositions (% by mass)								
	MgO	Al <sub>2</sub> O <sub>3</sub>	SiO <sub>2</sub>	P <sub>2</sub> O <sub>5</sub>	SO <sub>3</sub>	K <sub>2</sub> O	CaO	TiO <sub>2</sub>	Fe <sub>2</sub> O <sub>3</sub>
Cement	0.92 (0.25)	5.28 (0.78)	18.69 (0.26)	0.11 (0.07)	4.09 (0.58)	0.78 (0.12)	66.67 (0.16)	0.19 (0.13)	3.02 (0.19)
SF	0.27 (0.08)	0.06 (0.08)	95.93 (0.05)	0.12 (0.02)	2.92 (0.15)	0.41 (0.01)	0.16 (0.01)	0 (0)	0.11 (0.02)

The value in the brackets are standard deviations

**Fig. 1** Particle size distributions of NS and SF

concrete mixtures were labeled as NAC, RAC-non, RAC-NS12, RAC-NS54, RAC-NS106 and RAC-SF420, respectively. The mix proportions are given in Table 2. To take the water absorption of the NCA and RCAs into consideration, additional water was added to keep a consistent effective water to cement (W/C) ratio for all the mixtures. The mass of additional water was equal to the mass of coarse aggregate multiplied by the value of water absorption

of coarse aggregate minus its moisture content. Because the water absorptions of RCAs before and after spraying colloidal NS or SF were similar, the same amount of additional water was used in RACs prepared with untreated RCA and treated RCAs.

## 2.4 Test methods

### 2.4.1 Determination of physical properties of aggregate and concrete

The water absorption and particle density of coarse aggregate were measured according to BS 812-2. The particle density was calculated on an oven-dry basis. In the NCA and RCA samples, the mass ratio of 10–20 mm to 5–10 mm particles under air-dry state was 2:1, which was consistent with the ratio used for producing the concrete mixes.

The density of hardened concrete was measured according to BS EN 12390-7. In this study, the mass of hardened concrete was measured on a basis of a water-saturated state. The volume of hardened concrete was obtained by water displacement.

**Table 2** Mix proportions of concrete

Concrete mixtures	Type of coarse aggregate	W/C ratio	Effective water (kg/m <sup>3</sup> )	Additional water (kg/m <sup>3</sup> )	Cement (kg/m <sup>3</sup> )	Sand (kg/m <sup>3</sup> )	Coarse aggregate (5–10 mm) (kg/m <sup>3</sup> )	Coarse aggregate (10–20 mm) (kg/m <sup>3</sup> )
NAC	NCA	0.60	195	4.5	325	752	376	752
RAC-non	Untreated RCA	0.60	195	36	325	752	376	752
RAC-NS12	RCA by spraying NS12	0.60	195	36	325	752	376	752
RAC-NS54	RCA by spraying NS54	0.60	195	36	325	752	376	752
RAC-NS106	RCA by spraying NS106	0.60	195	36	325	752	376	752
RAC-SF420	RCA by spraying SF420	0.60	195	36	325	752	376	752

### 2.4.2 Exploration of microstructure of coarse aggregate and concrete

The microstructures of RCAs before and after spraying different colloidal NS or SF were observed using a scanning electron microscope (SEM) (Tescan VEGA3) under the secondary electron mode. Before testing, the treated RCA was dried in a vacuum chamber at 40 °C and then the surfaces of the samples were sputter-coated with a conductive golden layer.

The microstructure of RACs near the new interface between RCA and new mortar was observed under a backscattered electron (BSE) mode in the SEM and the equipped energy-dispersive spectrometer (EDS) was used to determine the chemical composition of the new ITZ. The samples used in microhardness testing as introduced below were utilized for the BSE testing.

### 2.4.3 Determination of microhardness of concrete

For each type of concrete, two samples with size of  $\sim 20 \times 20 \times 15$  mm were obtained by cutting from a cylindrical specimen ( $\Phi 100 \times 200$  mm) to measure the microhardness. The samples were vacuum-dried at 40 °C for 24 h before impregnated with epoxy resin in a cylindrical container ( $\Phi 30 \times 30$  mm). Then, one surface of each sample was polished using Buehler AutoMet 250. Lastly, the samples were placed in a vacuum chamber at 40 °C until testing.

Vickers micro-hardness tester (HVX-1000A) was utilized in this study. The load was controlled as 0.098 N. For each group of concrete, three zones were randomly selected within two samples for microhardness testing. A typical zone in RACs for microhardness testing and the layout of the testing points are depicted in Fig. 2. The interface between old mortar and new mortar was defined as the reference line. The region with negative values refers to old mortar while the region with positive values refers to new ITZ and new mortar. The microhardness of old mortar was measured from  $-80$  to  $-40$   $\mu\text{m}$ . The microhardness of new ITZ was determined at the distance of 10  $\mu\text{m}$  from the interface. For new mortar, measurements were taken at a distance ranging from 40 to 160  $\mu\text{m}$ . At least 4 indentations were performed at each distance with an interval of 40  $\mu\text{m}$ .

### 2.4.4 Determination of mechanical properties of concrete

The compressive strength of concrete was determined according to BS EN 12390-3 at the age of 28 days. Three cubic specimens ( $100 \times 100 \times 100$  mm) were used for each group for obtaining the average strength. The loading rate was 0.6 MPa/s.

The tensile splitting strength of concrete at the age of 4 months was determined as per BS EN 12390-6 using three cubic specimens with a size of  $100 \times 100 \times 100$  mm. The loading rate was set as 0.05 MPa/s.

The secant modulus of elasticity was determined from three cylinders ( $\Phi 100 \times 200$  mm) as stipulated in BS EN 12390-13. The loading rate was set at 0.6 MPa/s for obtaining the stress–strain curves. The secant modulus of elasticity was defined as the slope of the secant line between 5% and 1/3 of peak stress at the ascending part of stress–strain curve.

### 2.4.5 Determination of durability of concrete

For each group of concrete, the rate of water absorption was determined as per ASTM C1585-13 using three cylindrical specimens ( $\Phi 100 \times 50$  mm), which were cut from a larger cylinder ( $\Phi 100 \times 200$  mm). After pre-conditioning, the specimens were placed in water with an immersion depth of about 2 mm and the mass of the specimens was measured at specific times within 8 days. Detailed procedures could be referred to the previous study [39]. The ratio of the change in mass to the product of the cross-section area of specimen and density of water is defined as the absorption. The slope of the fitting line for the absorption against the square root of time ( $s^{1/2}$ ) between 1 min and 6 h is defined as the initial rate of water absorption, and that between 1 and 8 days is defined as the secondary rate of water absorption.

The chloride penetration resistance of concrete was determined based on ASTM C1202-19. The specimens were the same as those used in the rate of water absorption testing. After pre-conditioning, the specimens were fixed between two applied voltage cells which were separately filled with 3% NaCl solution and 3 N NaOH solution, respectively. A voltage of 60 V was used after the cells linking to a data logger for a testing period of 6 h. The values of charge passed



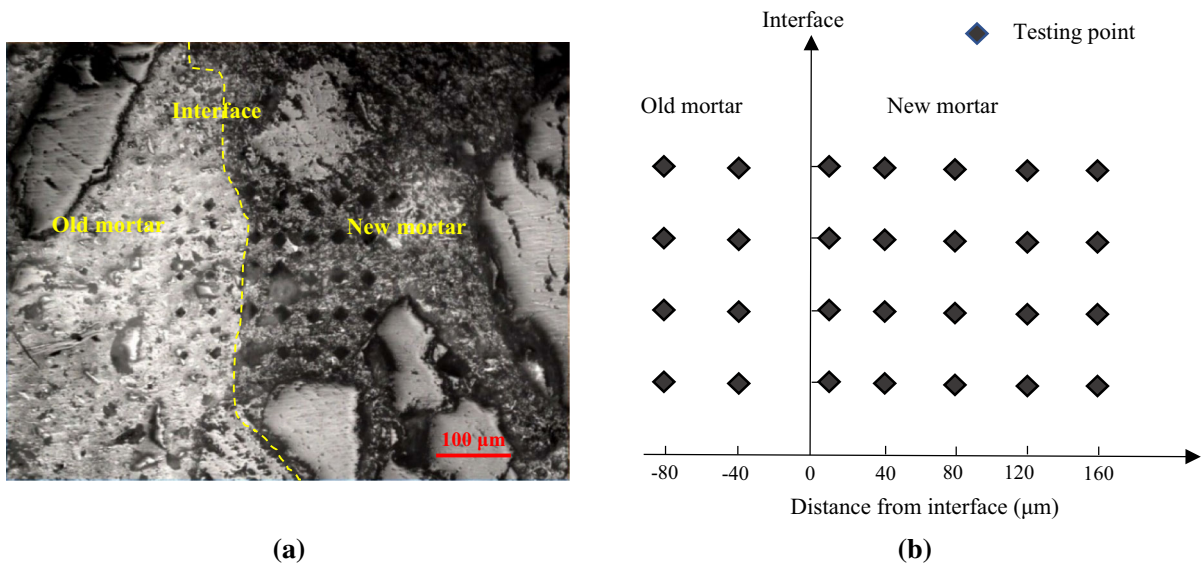


**Fig. 2** A typical zone in RACs for microhardness testing (a) and layout of indentation points (b)

were recorded once a minute to evaluate the chloride penetration.

Carbonation depth was measured using an accelerating carbonation method in BS EN 12390-12. Three cubes ( $100 \times 100 \times 100$  mm) were prepared for each concrete group. The specimens which were water-cured for 28 days were placed in the laboratory for 14 days for pre-conditioning and then put in a carbonation chamber for 28 days. The concentration of  $\text{CO}_2$  in the chamber was 3.5%, the temperature was  $20^\circ\text{C}$ , and the relative humidity was 57%. After carbonation, the specimens were split by machine and phenolphthalein solution indicator was sprayed on the cross section. The average distance from the edge of the zone in pink color to the surface of specimen is defined as the carbonation depth.

### 3 Test results and discussions

#### 3.1 Physical properties of coarse aggregate and concrete

The physical properties of NCA, untreated RCA and treated RCA by spraying NS or SF are shown in Table 3. After spraying different types of NS or SF, the water absorption and particle density of RCA changed little, implying that the NS and SF spraying treatment did not enhance the physical properties of RCA. It is

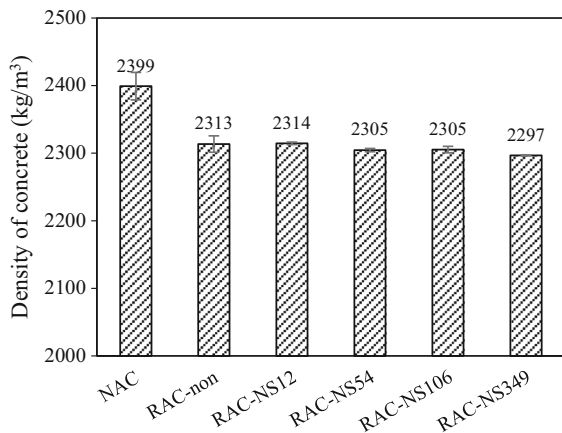
different from the results of using another traditional NS modification method, namely pre-soaking RCA in NS suspension. It was reported that the water absorption of RCA was decreased by 10.2% by pre-soaking RCA in NS suspension [30]. That is because compared to the NS spraying method in this study, much more NS suspension was absorbed by RCA when using NS pre-soaking method. The results also indicate that the enhancement of mechanical properties and durability of RAC by using NS spraying method is not due to the enhancement of RCA.

The densities of the hardened concretes are reported in Fig. 3. As expected, NAC exhibited a higher (3.7%) density than RAC-non. With the use of the treated RCAs, the density of RACs did not show significant changes. That is because the density of RAC was strongly related to the density of RCA, which was not significantly influenced by the different NS and SF spraying. This is different from the results when NS was used to replace the same amount of cement in RAC. It was reported that the density of RAC was significantly enhanced when 3% of cement was replaced by NS due to the filling to voids in old mortar and new mortar [36]. The results indicate that enhancement of old mortar and new mortar are not the main reason for the performance enhancement of RAC by using NS spraying method.

**Table 3** Physical properties of NCA and RCAs

Type of RCA	Water absorption (%)	Particle density (kg/m <sup>3</sup> )
NCA	0.63 (0.09)	2618 (23)
Untreated RCA	4.43 (0.29)	2369 (27)
RCA after spraying NS12	4.64 (0.03)	2355 (9)
RCA after spraying NS54	4.38 (0.04)	2371 (9)
RCA after spraying NS106	4.35 (0.03)	2369 (0)
RCA after spraying SF420	4.56 (0.07)	2363 (5)

The values inside brackets are standard deviations

**Fig. 3** Densities of hardened concretes

### 3.2 Microstructures of coarse aggregate and concrete

The microstructures of the surface of RCAs before and after NS or SF treatments under SEM are shown in Fig. 4. The surface layer of the untreated RCA was porous, which was assigned as calcium silicate hydrates (C–S–H), as shown in Fig. 4a. After spraying three types of colloidal NS (NS12, NS54 and NS106) on the surface of RCA and air-drying, a thin layer of silica gel was identified on the surface of RCA, which is caused by the dehydration of the colloidal NS. Above the silica gel layer, certain amounts of agglomerated NS particles could be found, as shown in Fig. 4b–d. By contrast, after spraying colloidal SF on RCA and air-dried, no silica gel was observed while the amount of agglomerated SF particles was much larger than the previous case, as shown in Fig. 4e. In addition, some cracks were observed in the silica gel layer after spraying colloidal NS on the surface of RCA due to the drying process. It was reported that cracks frequently occur in the colloidal films,

especially for those made from nanoparticle suspension [43, 44].

BSE images of RAC at the zone near the interface between RCA and new mortar are shown in Fig. 5. As shown in Fig. 5a, there were a lot of pores in the area close to the interface (namely new ITZ) in RAC-non. However, from Fig. 5b–e, it can be observed that a densified layer about 10–40 μm in thickness was formed in the new ITZ of RACs after using NS or SF spraying. Based on the results of EDS, the main elemental compositions of the densified layer were Ca, Si and O. The Ca/Si ratios of the densified layer in RAC-NS12, RAC-NS54, RAC-NS106 and RAC-SF420 were about 0.43, 0.56, 0.32 and 0.40, respectively. The values were much lower than the Ca/Si ratio of the C–S–H in ordinary Portland cement paste, which was about 1.75 [45]. This indicates that the densified layers were C–S–H with a lower Ca/Si ratio. Furthermore, it was observed from Fig. 5 that in RACs after using NS spraying treatments, the amount of pores in the new cement paste close to the densified layer was less than that in RAC-non. These features show the new ITZ of RAC was enhanced after using NS or SF spraying. In addition, some cracks were observed in the densified C–S–H layer in RAC prepared with NS/SF modified RCA. In fact, there were also some cracks in old mortar and new mortar. It is possible that these cracks were formed due to the loss of water when the samples for SEM microstructural testing were placed in vacuum-dry chamber for drying, rather than really existed. Otherwise, those cracks in new ITZ of RAC prepared with NS/SF modified RCA would result in lower performance especially durability, but it was not consistent with the test results.

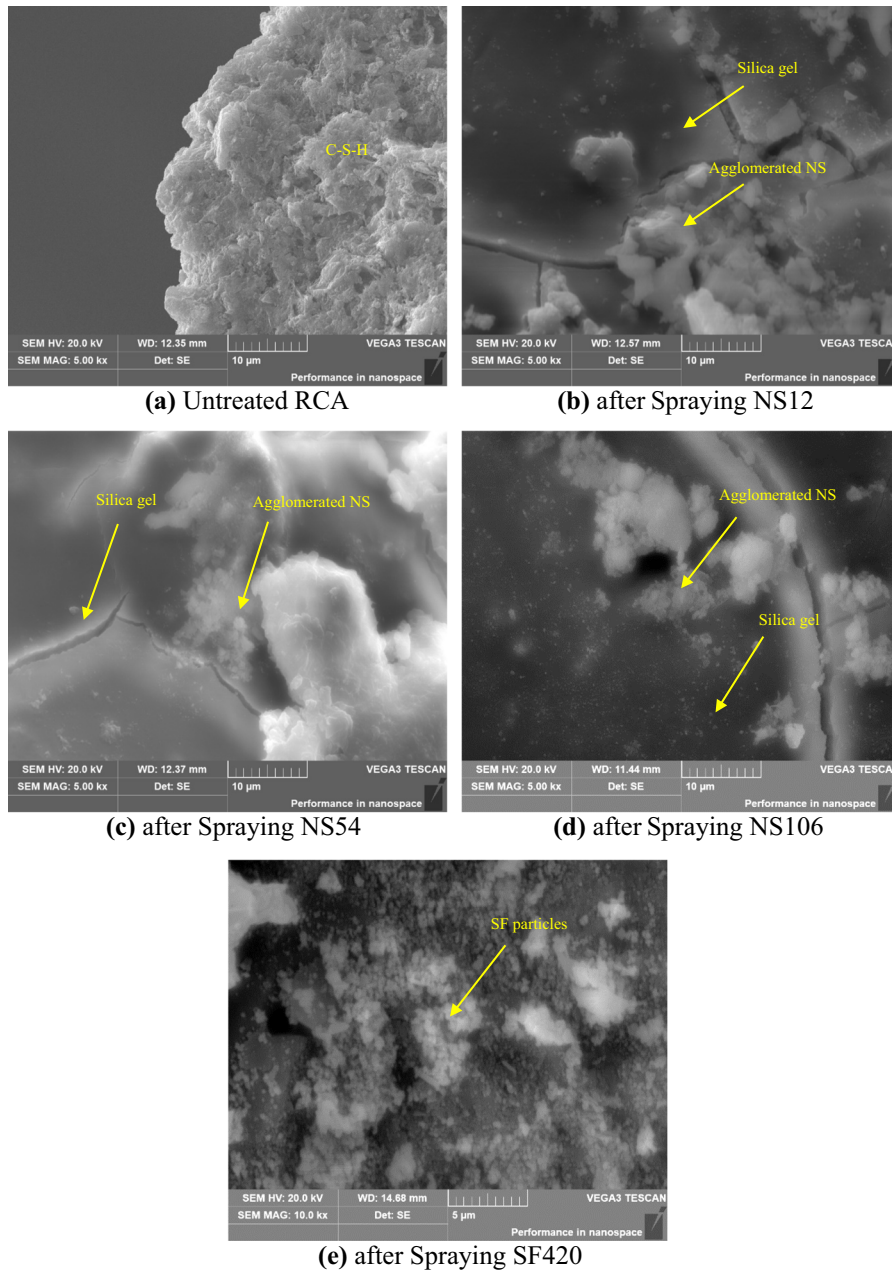


**Fig. 4** Microstructure of the surface of RCAs before and after NS treatment

### 3.3 Microhardness of concrete

The microhardness results at the interface between RCA and new mortar are reported in Fig. 6. Generally, higher microhardness value corresponds to smaller size of indent mark under same loading, which indicates that the material at the indent point is more densified. It can be found that the old mortar in RACs

demonstrated a higher microhardness than the new mortar. In addition, no obvious difference was found at different distances from the measurement point to the interface, for both old and new mortar. Moreover, no obvious difference was observed from the microhardness of the new mortar in RAC-non and NAC. After applying the NS spraying, the microhardness of the new ITZ in some indentation zones showed

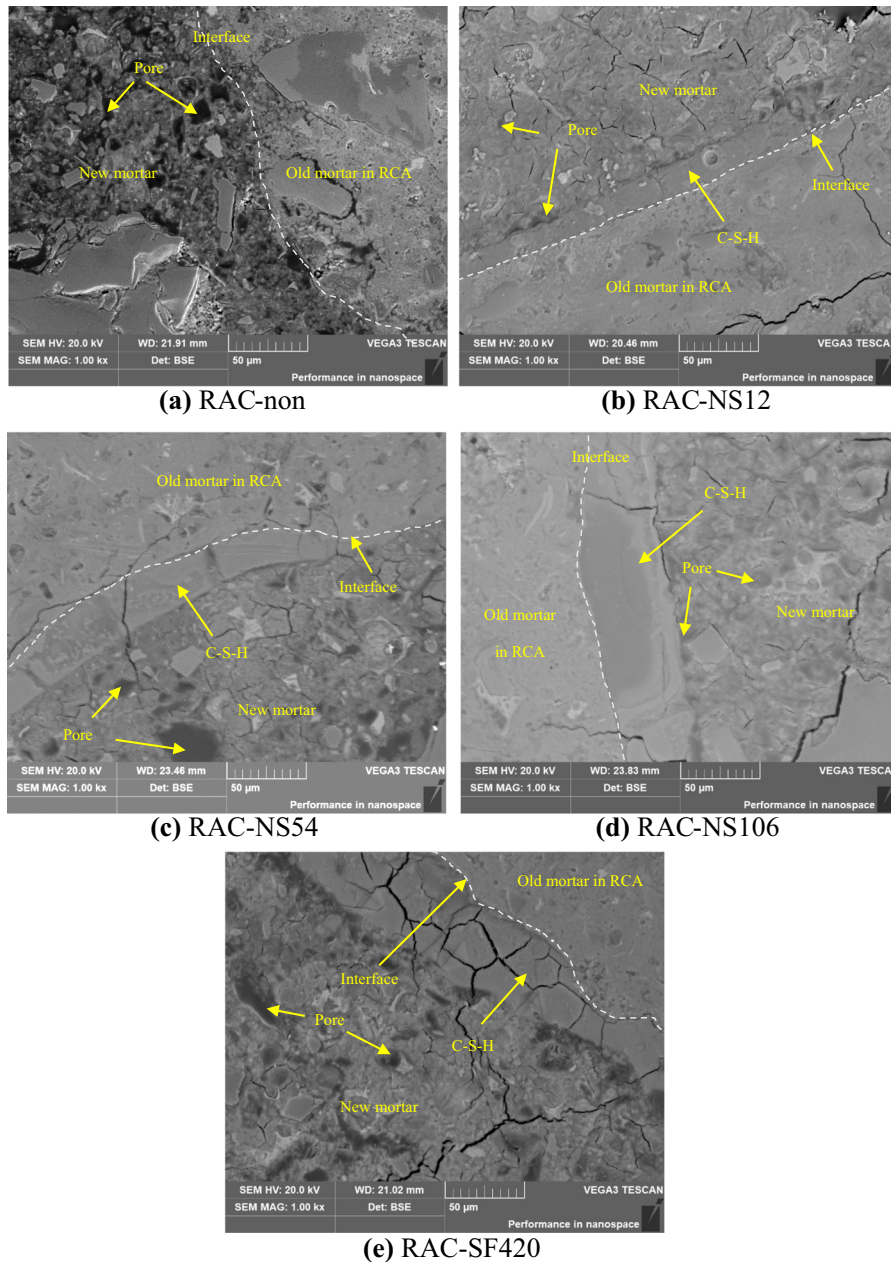


**Fig. 5** BSE images of RAC at the zones near the interface between RCA and new mortar

significant enhancements. That is because the calcium hydroxide produced from cement hydration in new mortar reacted with the silica gel left on the surface of RCA, forming a densified layer of C-S-H with a low Ca/Si ratio around the RCA. In RAC-SF420, not only the microhardness of new ITZ, but also the new mortar in some indentation zones was improved significantly. The reasons are discussed as follows. According to

SEM results, after spraying colloidal SF, a lot of agglomerated SF particles were left on the surface of RCA without the formation of a silica gel layer. After mixing the colloidal SF modified RCA with cement, a layer of C-S-H was also formed around RCA because of the reaction between the SF particles and calcium hydroxide, leading to the enhancement of new ITZ. It is similar to the case of using NS. But the difference

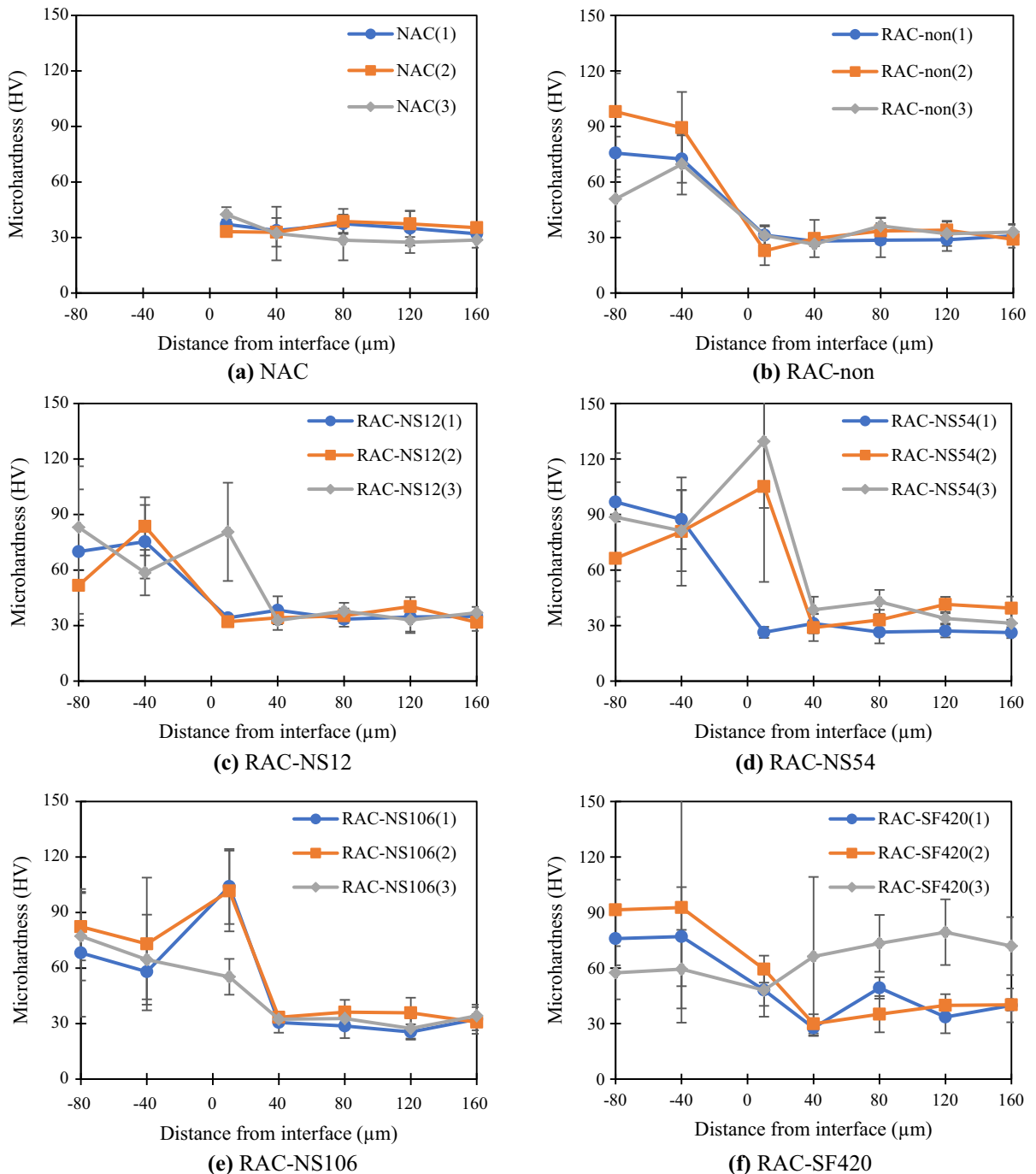


**Fig. 6** Microhardness of concretes near the interface between RCA and new mortar

was that the SF particles, which remained on the surface of RCA without forming silica gel, were able to involve into new mortar and promoted the hydration of cement to form additional C–S–H because of

nucleation effect and pozzolanic effect [46]. As a result, the new mortar was also enhanced.

The average microhardness of the old mortar, new ITZ and new mortar are analyzed in Fig. 7. The



average microhardness of RAC-NS12, RAC-NS54 and RAC-NS106 were slightly higher than that of RAC-non for the new mortar, but the average microhardness of RAC-SF420 increased by 58.6%, as shown in Fig. 7a. It implies that spraying the colloidal SF on the surface of RCA contributed to a significant enhancement of the new mortar, but the colloidal NS had only slight influences. From Fig. 7b, it can be observed that after spraying the different colloidal NS and SF on RCA, the microhardness of the new ITZ in RAC was significantly improved and the increment was higher when using the colloidal NS. It implies that the C–S–H layer (mentioned in Sect. 3.2) around the RCA produced by the reaction between the silica gel and calcium hydroxide was more densified than that produced by the reaction between the silica fume particles and calcium hydroxide. In addition, as shown

in Fig. 7c, the microhardness of the old mortar did not show significant changes after spraying the different colloidal NS and SF, which is consistent with the results in Sect. 3.1 that the physical properties of RCA had no obvious change. In summary, spraying the colloidal NS on RCA contributed to significant enhancements in the new ITZ of RAC, while spraying the colloidal SF caused enhancement of both the new ITZ and new mortar of RAC.

### 3.4 Mechanical properties of concrete

The main mechanical performance indexes of concrete are shown in Table 4. The compressive strength of NAC was 17.8% higher than RAC-non. After spraying colloidal NS/SF on RCA, the compressive strength of RAC increased. Moreover, the

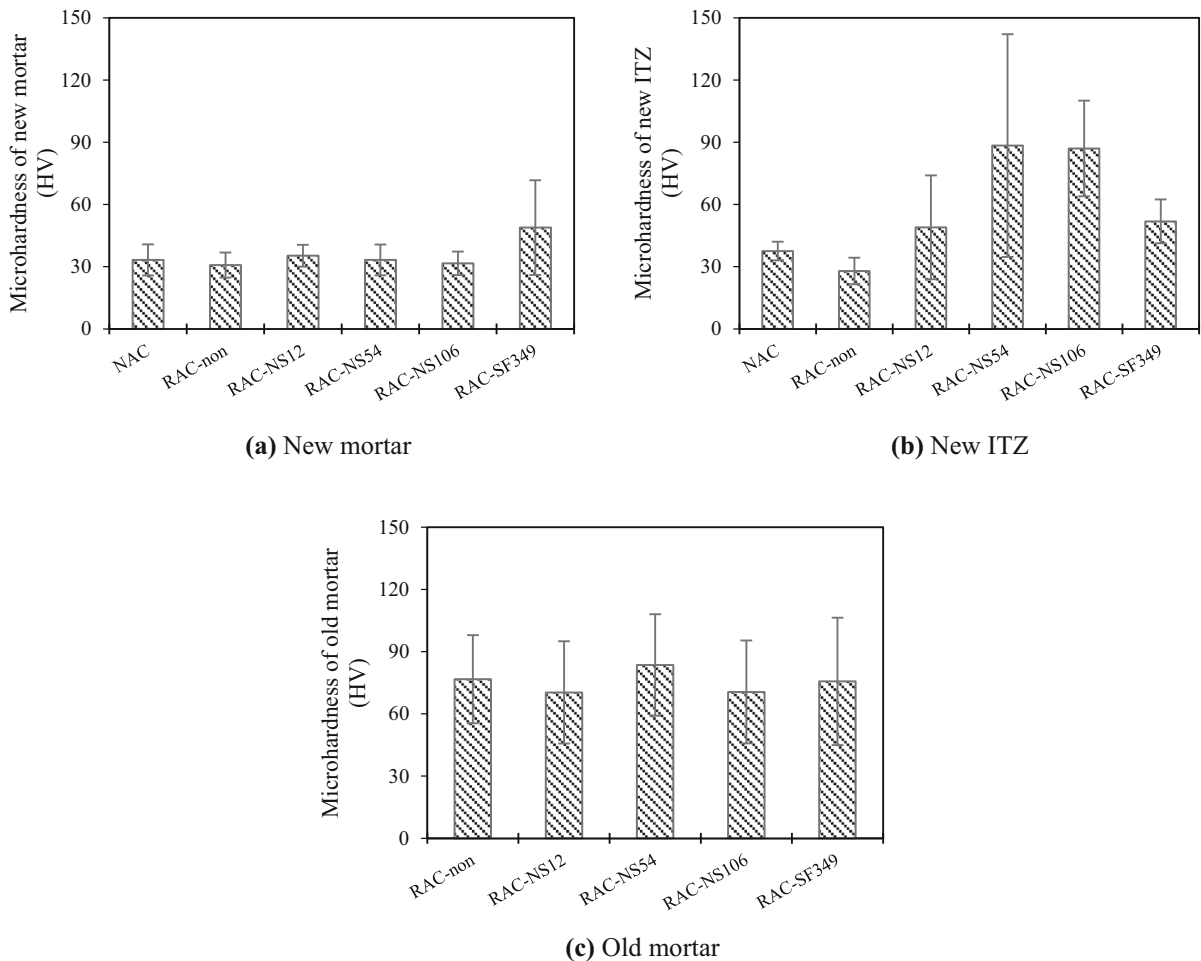


**Fig. 7** Average microhardness values of new mortar, new ITZ and old mortar in concretes



**Table 4** Mechanical performance indexes of concrete

Specimens	Cubic compressive strength (MPa)	Tensile split strength (MPa)	Peak stress (MPa)	Peak strain ( $\mu\epsilon$ )	Secant modulus of elasticity (GPa)
NAC	49.6 (0.6)	4.46 (0.27)	40.2 (0.41)	2327 (93)	30.5 (1.04)
RAC-non	42.1 (1.2)	4.14 (0.38)	34.9 (1.12)	2323 (208)	26.6 (1.56)
RAC-NS12	44.0 (1.0)	4.15 (0.16)	35.2 (0.88)	2413 (142)	28.2 (0.92)
RAC-NS54	44.5 (1.5)	3.98 (0.07)	36.9 (0.43)	2437 (110)	28.1 (1.39)
RAC-NS106	45.0 (1.0)	4.42 (0.07)	36.7 (0.96)	2183 (133)	28.4 (1.26)
RAC-SF420	46.0 (1.4)	3.95 (0.26)	37.8 (1.09)	2183 (168)	29.7 (0.61)

The values in the brackets are standard deviations

compressive strength increased with the use of NS with a larger particle size. This trend is similar to the case of using different particle sizes of NS to replace cement in cement mortar/paste. It was reported that the compressive strength of cement paste/mortar increased when larger particles size of NS was used to replace cement [41, 42]. When RCA was modified by spraying colloidal SF, the corresponding mix RAC-SF420 showed the largest increase (9.2%) in the compressive strength.

From the Table 4, it can be seen that the tensile splitting strength of NAC was 7.8% higher than that of RAC-non. After spraying NS or SF, the tensile splitting strength of RAC showed unobvious trends. Such an obscure trend may be caused by the large variations in the measured tensile splitting strength, which outshined the influence of the NS or SF spraying treatment.

The stress–strain curves of concrete under uniaxial compressive loading are shown in Fig. 8. It showed that the ascending parts of three stress–strain curves in each group of concrete were close, while the descending parts had some difference. The main parameters of the stress–strain curves of concrete, namely peak stress, peak strain and second modulus of elasticity, are also shown in Table 4. It was observed that the peak stress of RAC-non was lower than NAC, while the peak stress of RAC generally increased with the increase of NS particle size. This tendency was similar to that of cubic compressive strength. The peak strain of RAC did not show a clear trend after using colloidal NS to modify RCA. The secant modulus of elasticity of NAC was 14.9% higher than that of RAC-non. After spraying NS or SF, the secant modulus of elasticity of RAC was improved. Similar to the compressive

strength results, the increase in secant modulus of elasticity became larger with the increase of NS particle size.

To sum up, the mechanical properties of RAC were enhanced after using colloidal NS to modify RCA. It was due to the enhanced new ITZ in RAC when colloidal NS was used, as evidenced by the microhardness results. Moreover, the use of larger size NS led to better mechanical properties of RAC. That may be because the colloidal NS with larger particle size was more difficult to penetrate into RCA, and thus more silica gel and agglomerated NS particles remained on the surface of RCA, which contributed to more significant enhancement of new ITZ. In addition, the use of colloidal SF had given rise to largest enhancement of mechanical properties of RAC. That is because both new ITZ and new mortar were enhanced after spraying colloidal SF on RCA although new ITZ showed less enhancement, as confirmed by microhardness results.

### 3.5 Durability of concrete

The rate of water absorption is an important aspect of the durability, as it may impair the quality of concrete. Figure 9 reports the initial and secondary rates of water absorption. Apparently, the initial and secondary rates of water absorption of NAC were 18.9% and 33.7% smaller than RAC-non, respectively. After NS spraying, the rate of water absorption of RAC decreased and the magnitude of the decrease generally exhibited an increasing trend with the increase of NS particle size. When SF420 was used, the initial and secondary rates of water absorption of the corresponding RAC (RAC-SF420) were 29.6% and 66.3% lower

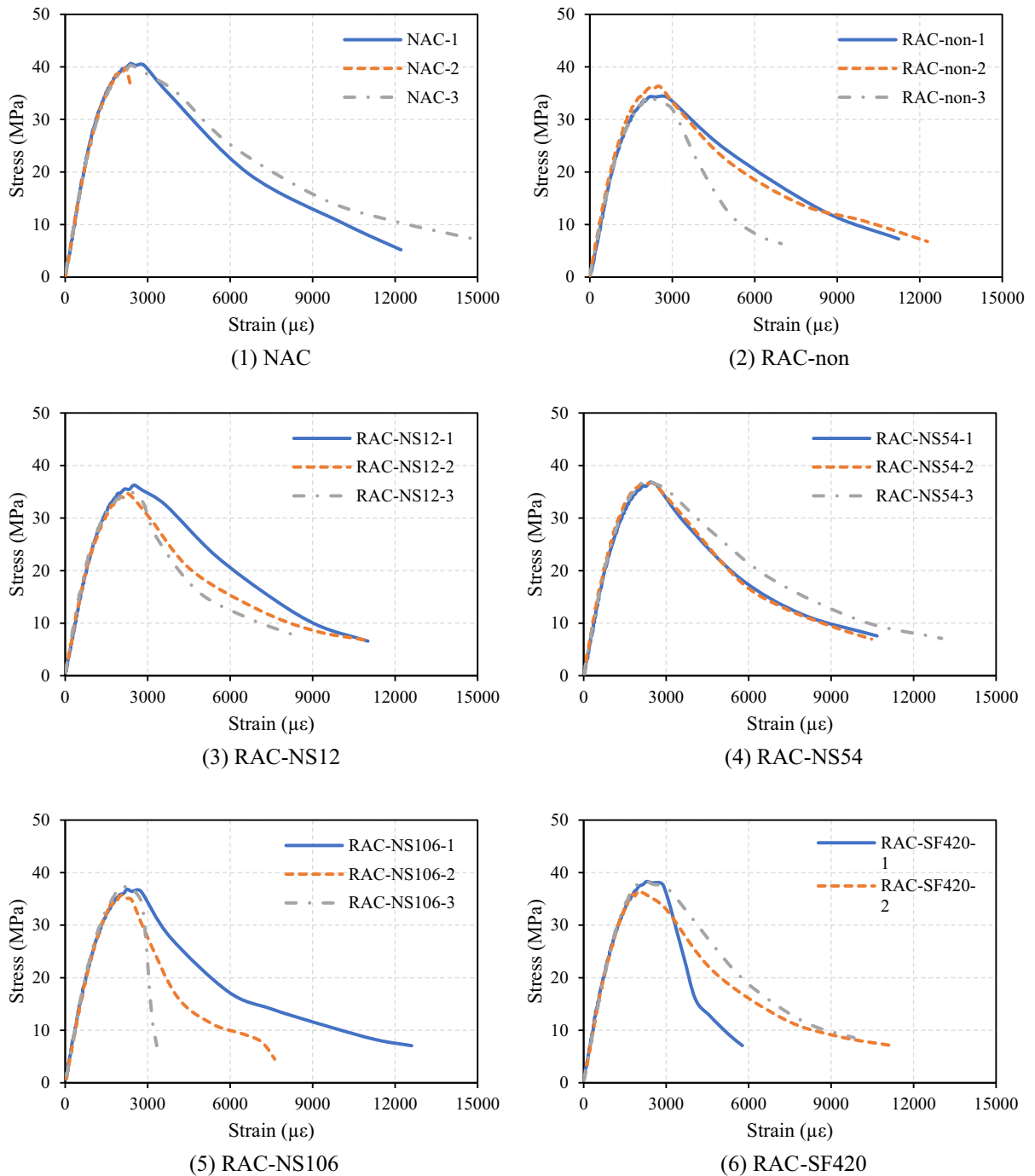


**Fig. 8** Stress–strain curves of hardened concrete

than RAC-non, and they were even lower than those of the NAC.

The charge passed of concrete reflects its chloride penetration resistance. In general, the charge passed

has a negative relation with the chloride penetration resistance. Figure 10 shows the results of the charge passed. From the figure, it can be seen that the use of untreated RCA induced a higher value of charge



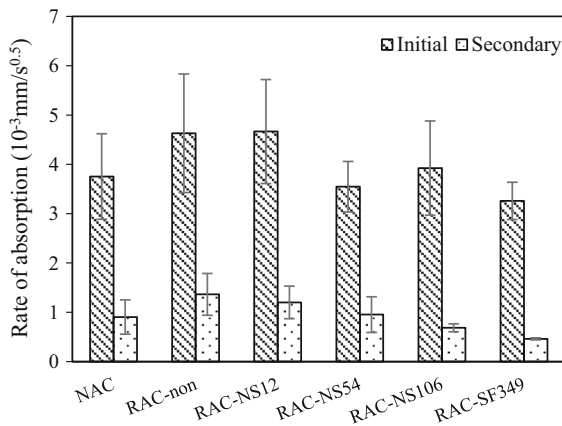


**Fig. 9** Rate of water absorption of hardened concretes

passed. However, after using NS or SF spraying treatment methods, the charge passed of RACs decreased and NS with a larger particle size gave rise to a lower charge passed. When spraying SF420 on RCA, the charge passed of RAC-SF420 was 46.1% lower than RAC-non, and it was even lower than that of NAC.

The carbonation depths of concrete, which have a negative relation with its carbonation resistance, are given in Fig. 11. The figure revealed that the 28-day carbonation depth of RAC-non was much higher than that of NAC. However, the carbonation depths of RACs decreased after using the NS or SF spraying treatment method. Moreover, the decrease level was generally higher when using the NS with a larger particle size. Compared with RAC-non, the carbonation depth of RAC-NS12, RAC-NS54, RAC-NS1106

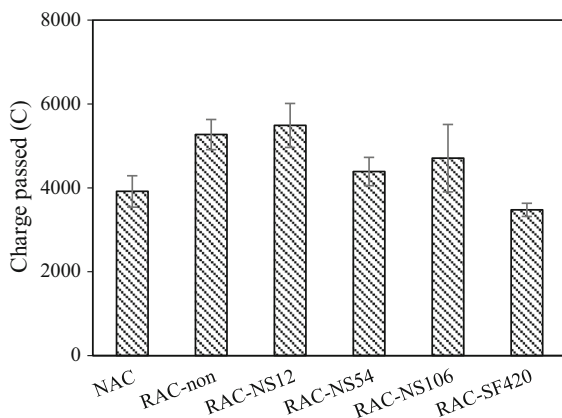


**Fig. 10** Chloride penetration resistance of hardened concretes

and RAC-SF420 decreased by 10.1%, 13.0% 30.5% and 28.4%, respectively.

To sum up, the durability of RAC was enhanced after using colloidal NS or SF to modify RCA, while larger size NS led to larger enhancement. Moreover, spraying colloidal SF brought in the largest enhancement. The reasons for these phenomena are similar to that for mechanical properties. However, the increase of durability was much higher than that of mechanical properties. In particular, the rate of water absorption, chloride penetration resistance and carbonation resistance of RAC prepared with colloidal SF modified RCA were even close to that of NAC. That is because the densified new ITZ changed the seepage path of water, chloride and CO<sub>2</sub> gas from “penetrating RA” to “going around the edge of RA”. As a result, the negative effect caused by weak RCA could be significantly reduced.

#### 4 Conclusions

In this study, different recycled coarse aggregate (RCA) modification methods, namely spraying colloidal nano silica (NS) with varying particle sizes and silica fume (SF) with a size of 420 nm on the surface of RCA, were utilized. Their efficiencies in enhancing the performance of recycled aggregate concrete (RAC) have been evaluated. Based on the results and discussions, key conclusions are given in the following.

- (1) Spraying colloidal NS/SF on RCA exerted little influence on the physical properties of RCA and

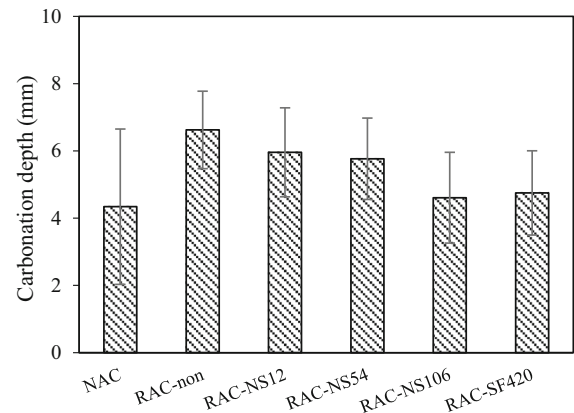


**Fig. 11** Carbonation resistance of hardened concretes

the density of RAC, while remarkably enhanced the mechanical properties such as compressive strength and elastic modulus and durability of RAC like water absorptivity, chloride penetration resistance and carbonation resistance.

- (2) Comparing the use of NS with different particles sizes namely 12 nm, 54 nm and 106 nm, a larger particle size of NS brought pronounced enhancement effect on the mechanical properties and durability of RAC. Moreover, the use of colloidal SF with average particle size of 420 nm yielded the largest enhancement effect. After using modified RCA by spraying colloidal SF, the compressive strength and elastic modulus of the corresponding RAC increased by 9.2% and 11.7%, respectively. Its durability was even close to that of natural aggregate concrete. In detail, the secondary rate of water absorption, charge passed value and carbonation depth decreased by 66.3%, 46.1% and 28.4%, respectively. Considering better enhancement in performance of RAC and lower cost of SF than NS, it is recommended to use colloidal SF to modify RCA.
- (3) Spraying colloidal NS on RCA contributed to a significantly enhanced new interface transition zone (ITZ) in RAC because the silica gel on the RCA reacted with calcium hydroxide in new mortar and formed a densified layer of C–S–H with low Ca/Si ratio. As a result, the mechanical properties and durability of RAC was improved. As for spraying colloidal SF on RCA, it resulted in enhancement of both new ITZ and new mortar in RAC. That is why the mechanical properties and durability of the corresponding RAC were the best.

**Funding** This study was funded by Hong Kong Construction Industry Council (CICR/03/19) and Research Grants Council GRF (PolyU 152144/17E).

#### Declarations

**Conflict of interest** The authors declare that they have no conflict of interest.

## References

1. Xiao J, Li L, Shen L, Yuan J (2015) Effects of strain rate on mechanical behavior of modeled recycled aggregate concrete under uniaxial compression. *Constr Build Mater* 93:214–222
2. Xiao J, Li W, Fan Y, Huang X (2012) An overview of study on recycled aggregate concrete in China (1996–2011). *Constr Build Mater* 31:364–383
3. Wang B, Yan L, Fu Q, Kasal B (2021) A comprehensive review on recycled aggregate and recycled aggregate concrete. *Resour Conserv Recycl* 171:105565
4. Upshaw M, Cai CJ (2020) Critical review of recycled aggregate concrete properties, improvements, and numerical models. *J Mater Civ Eng* 32(11):03120005
5. Zaben A, Maslehuddin M, Al-Amoudi OSB, Al-Dulaijan SU (2021) Influence of mix composition on the properties of recycled aggregate concrete. *Struct Concr* 22:1–13
6. Théréne F, Keitaa E, Naël-Redolfib J, Boustingorryb P, Bonafousb L, Roussela N (2020) Water absorption of recycled aggregates: measurements, influence of temperature and practical consequences. *Cement Concr Res* 137:106196
7. Xuan D, Houben LJM, Molenaar AAA, Shui Z (2010) Cement treated recycled demolition waste as a road base material. *J Wuhan Univ Technol Mater Sci Ed* 25(4):696–699
8. Li L, Xiao J, Xuan D, Poon CS (2018) Effect of carbonation of modeled recycled coarse aggregate on the mechanical properties of modeled recycled aggregate concrete. *Cement Concr Compos* 89:169–180
9. Tam VWY, Wattage H, Le KN, Buteraa A, Soomro M (2021) Methods to improve microstructural properties of recycled concrete aggregate: a critical review. *Constr Build Mater* 270:121490
10. Ouyang K, Shi C, Chu H et al (2020) An overview on the efficiency of different pretreatment techniques for recycled concrete aggregate. *J Clean Prod* 263:121264
11. Li L, Xuan D, Poon CS (2021) Stress–strain curve and carbonation resistance of recycled aggregate concrete after using different RCA treatment techniques. *Appl Sci* 11(9):4283
12. Verma A, Babu VS, Arunachalam S (2021) Characterization of recycled aggregate by the combined method: acid soaking and mechanical grinding technique. *Mater Today Proc*
13. Nagataki S, Gokce A, Saeki T, Hisada M (2004) Assessment of recycling process induced damage sensitivity of recycled concrete aggregates. *Cem Concr Res* 34(6):965–971
14. Choi H, Lim M, Choi H, Kitagaki R, Noguchi T (2014) Using microwave heating to completely recycle concrete. *J Environ Prot* 5:583–596
15. Akbarnezhad A, Ong KCG, Zhang MH, Tam CT, Foo TWJ (2011) Microwave assisted beneficiation of recycled concrete aggregates. *Constr Build Mater* 25(8):3469–3479
16. Katz A (2004) Treatments for the improvement of recycled aggregate. *J Mater Civ Eng* 16(6):597–603
17. Kim HS, Kim B, Kim KS, Kim JM (2017) Quality improvement of recycled aggregates using the acid



- treatment method and the strength characteristics of the resulting mortar. *J Mater Cycles Waste Manag* 19(2):968–976
18. Zhan B, Poon CS, Liu Q, Kou SC, Shi CJ (2014) Experimental study on CO<sub>2</sub> curing for enhancement of recycled aggregate properties. *Constr Build Mater* 67:3–7
  19. Kou SC, Zhan B, Poon CS (2014) Use of a CO<sub>2</sub> curing step to improve the properties of concrete prepared with recycled aggregates. *Cement Concr Compos* 45:22–28
  20. Li L, Poon CS, Xiao J, Xuan D (2017) Effect of carbonated recycled coarse aggregate on the dynamic compressive behavior of recycled aggregate concrete. *Constr Build Mater* 151:52–62
  21. Zhang JK, Shi CJ, Li YK, Pan XY, Poon CS (2015) Performance enhancement of recycled concrete aggregates through carbonation. *J Mater Civ Eng* 27(11):04015029
  22. Grabiec AM, Klama J, Zawal D et al (2012) Modification of recycled concrete aggregate by calcium carbonate bio deposition. *Constr Build Mater* 34:145–150
  23. Bui NK, Satomi T, Takahashi H (2018) Enhancement of recycled aggregate concrete properties by a new treatment method. *Int J GEOMATE* 14(41):68–76
  24. Kou SC, Poon CS (2010) Properties of concrete prepared with PVA-impregnated recycled concrete aggregates. *Cement Concr Compos* 32(8):649–654
  25. Tam VWY, Gao XF, Tam CM (2005) Microstructural analysis of recycled aggregate concrete produced from two-stage mixing approach. *Cem Concr Res* 35(6):1195–1203
  26. Junak J, Sicakova A (2017) Effect of surface modifications of recycled concrete aggregate on concrete properties. *Buildings Basel* 8(1):2
  27. Li J, Xiao H, Zhou Y (2009) Influence of coating recycled aggregate surface with pozzolanic powder on properties of recycled aggregate concrete. *Constr Build Mater* 23(3):1287–1291
  28. Sasanipour H, Aslani F, Taherinezhad J (2021) Chloride ion permeability improvement of recycled aggregate concrete using pretreated recycled aggregates by silica fume slurry. *Constr Build Mater* 270:121498
  29. Zhang H, Zhao Y, Meng T et al (2015) Surface treatment on recycled coarse aggregates with nanomaterials. *J Mater Civ Eng* 28(2):04015094
  30. Zeng W, Zhao Y, Zheng H, Poon CS (2020) Improvement in corrosion resistance of recycled aggregate concrete by nano silica suspension modification on recycled aggregates. *Cement Concr Compos* 106:103476
  31. Kou SC, Poon CS (2013) Long-term mechanical and durability properties of recycle aggregate concrete prepared with the incorporation of fly ash. *Cement Concr Compos* 37:12–19
  32. Corinaldesi V, Moriconi G (2009) Influence of mineral additions on the performance of 100% recycled aggregate concrete. *Constr Build Mater* 23:2869–2876
  33. Li W, Long C, Tam VWY, Poon CS, Duan WH (2017) Effects of nano-particles on failure process and microstructural properties of recycled aggregate concrete. *Constr Build Mater* 142:42–50
  34. Mukharjee BB, Barai SV (2014) Influence of nano-silica on the properties of recycled aggregate concrete. *Constr Build Mater* 55:29–37
  35. Luo Z, Li W, Tam VWY, Xiao J, Shah SP (2019) Current progress on nanotechnology application in recycled aggregate concrete. *J Sustain Cement Based Mater* 8(2):79–96
  36. Mukharjee BB, Barai SV (2015) Development of construction materials using nano-silica and aggregates recycled from construction and demolition waste. *Waste Manag Res* 33(6):515–523
  37. Younis KH, Mustafa SM (2018) Feasibility of using nanoparticles of SiO<sub>2</sub> to improve the performance of recycled aggregate concrete. *Adv Mater Sci Eng* 2018:1–11
  38. Shaikh F, Chavda V, Minhaj N, Arel HS (2018) Effect of mixing methods of nano silica on properties of recycled aggregate concrete. *Struct Concr* 19:387–399
  39. Li L, Xuan DX, Sojobi AO, Liu S, Chu SH, Poon CS (2021) Development of nano-silica treatment methods to enhance recycled aggregate concrete. *Cement Concr Compos* 118:103963
  40. Zhang X, Yang H, Yang Q, Du X, Li C, Cheng X (2019) Effects of particle size of colloidal nanosilica on hydration of Portland cement at early age. *Adv Mech Eng* 11(2):1–9
  41. Haruehansapong S, Pulngern T, Chucheeepsakul S (2014) Effect of the particle size of nanosilica on the compressive strength and the optimum replacement content of cement mortar containing nano-SiO<sub>2</sub>. *Constr Build Mater* 50:471–477
  42. Meng T, Ying K, Hong Y, Xu Q (2020) Effect of different particle sizes of nano-SiO<sub>2</sub> on the properties and microstructure of cement paste. *Nanotechnol Rev Berl* 9(1):833–842
  43. Kim JY, Cho K, Ryu S, Kim S, Weon BM (2015) Crack formation and prevention in colloidal drops. *Sci Rep* 5(1):13166–13166
  44. Liu T, Luo H, Ma J, Wang P, Wang L, Jing G (2014) Tuning crack pattern by phase separation in the drying of binary colloid-polymer suspension. *Phys Lett A* 378(16–17):1191–1199
  45. Richardson IG (1999) The nature of C–S–H in hardened cements. *Cem Concr Res* 29:1131–1147
  46. Singh LP, Karade SR, Bhattacharyya SK, Yousuf MM, Ahalawat S (2013) Beneficial role of nanosilica in cement based materials—a review. *Constr Build Mater* 47:1069–1077

**Publisher's Note** Springer Nature remains neutral with regard to jurisdictional claims in published maps and institutional affiliations.

